DISTRIBUTION STATEMENT A
Approved for Public Release
Distribution Unlimited

NLO 99

Contract F61775-99-WF080

NLO Materials Workshop

DERA Malvern UK

20-21 September 1999

**Reproduced From
Best Available Copy**

19991105 104

We wish to thank the following for their contribution to the success of this Conference:

European Office of Aerospace Research and Development

Air Force Office of Scientific Research

United States Air Force Research Laboratory

UK Ministry of Defence (International Research Collaboration Dept)

Defence Evaluation and Research Agency

DTIC QUALITY INSPECTED 4

AQF00-02-0422

REPORT DOCUMENTATION PAGE

Form Approved OMB No. 0704-0188

Public reporting burden for this collection of information is estimated to average 1 hour per response, including the time for reviewing instructions, searching existing data sources, gathering and maintaining the data needed, and completing and reviewing the collection of information. Send comments regarding this burden estimate or any other aspect of this collection of information, including suggestions for reducing this burden to Washington Headquarters Services, Directorate for Information Operations and Reports, 1215 Jefferson Davis Highway, Suite 1204, Arlington, VA 22202-4302, and to the Office of Management and Budget, Paperwork Reduction Project (0704-0188), Washington, DC 20503.

1. AGENCY USE ONLY (Leave blank)	2. REPORT DATE	3. REPORT TYPE AND DATES COVERED
	September 1999	Conference Proceedings

4. TITLE AND SUBTITLE

Workshop on Nonlinear Optical Materials

5. FUNDING NUMBERS

F61775-99-WF

6. AUTHOR(S)

Conference Committee

7. PERFORMING ORGANIZATION NAME(S) AND ADDRESS(ES)

DERA
St. Andrews Rd.,
Malvern WR14 3PS
England

8. PERFORMING ORGANIZATION REPORT NUMBER

N/A

9. SPONSORING/MONITORING AGENCY NAME(S) AND ADDRESS(ES)

EOARD
PSC 802 BOX 14
FPO 09499-0200

10. SPONSORING/MONITORING AGENCY REPORT NUMBER

CSP 99-5080

11. SUPPLEMENTARY NOTES

12a. DISTRIBUTION/AVAILABILITY STATEMENT

Approved for public release; distribution is unlimited.

12b. DISTRIBUTION CODE

A

13. ABSTRACT (Maximum 200 words)

The Final Proceedings for Workshop on Nonlinear Optical Materials, 20 September 1999 - 21 September 1999

This is an interdisciplinary conference. Topics include growth, characterization, and applications of chalcopyrites and other nonlinear optical materials for use in the mid-IR.

14. SUBJECT TERMS

EOARD, Chalcopyrite materials, Non-linear Optical Materials

15. NUMBER OF PAGES

Too many to count

16. PRICE CODE

N/A

17. SECURITY CLASSIFICATION OF REPORT	18. SECURITY CLASSIFICATION OF THIS PAGE	19, SECURITY CLASSIFICATION OF ABSTRACT	20. LIMITATION OF ABSTRACT
UNCLASSIFIED	UNCLASSIFIED	UNCLASSIFIED	UL

NLO Materials Workshop

Woodward Building, DERA Malvern
20-21 September 1999

Monday 20 September

09.15	Registration and Coffee
09.45	Introduction and Welcome Jayne Ackroyd Manager EOP Dept DERA
10.00	NLO Materials – Key Technical Issues A W Vere DERA
10.15	ZGP – The DERA Programme C J Flynn DERA
10.35	ZGP annealing studies L L Chng DSO Singapore
10.50	Non-linear absorption and damage measurements in chalcopyrite crystals Shekar Guha AFRL/MLPO
11.05	ZGP –crystals: homogeneity region, real defects and optical quality V Voevodin R&D Center 'ATOM Tomsk
11.25	Break
11.45	Secondary ion mass spectrometry analysis of $CdGeAs_2$ J Solomon University of Dayton
11.55	Refractive Index measurements and phase-matching calculations in chalcopyrites D Zelmon AFRL/MLPO
12.10	Analysis of CGA using Thermal admittance spectroscopy Steven Smith University of Dayton, Research Institute
12.15	High Frequency ZGP Tandem OPO J A C Terry DERA

We would like to thank the following for their contribution to the Workshop:
European Office of Aerospace Research and Development
Air Force Office of Scientific Research
United States Air Force Research Laboratory
UK Ministry of Defence (International Research Collaboration Dept)
Defence Evaluation and Research Agency

12.45	Buffet Lunch	
14.00	Recent Advances in chalcopyrites for mid to far IR frequency conversion	P Schunemann
14.20	NLO materials at IOM A Gribenyukov. Institute of Optical Monitoring Tomsk	
14.35	ZGP Growth and thermal treatment G Verozubova IOM Tomsk Russia	
14.50	Optical and electron transport properties of $ZnGeP_2$ and$CdGeAs_2$ B Bairamov Ioffe Institute St Petersburg Russia	
15.20	Tea	
15.50	Identification of defects in ZGP by EPR/ENDOR L Halliburton University of West Virginia	
16.10	Theory of defects in chalcopyrites R Pandey University of Michigan	
16.40	Defect energy and band structure of ZGP Keith Nash / Mike Fearn DERA Malvern	
16.50	Tellurium-selenium alloys M Ohmer Materials Labs WPAFB Dayton Ohio	
17.00	Discussion – Calcopyrites II	
19.30	**Workshop Dinner**	

(coach collection from hotels at approx 19.00)

Tuesday 21 September

09.00	Non-linear Optical Crystal development at AFRL materials directorate N Fernelius AFRL/MLPO
09.30	Non-linear crystals for IR region in DTIM L. Isaenko Institute of Monocrystals Novosibirsk
10.00	Spectroscopic properties of Pure and Rare-Earth-ion-doped Non-linear Crystals for the mid IR A Elisseev Institute of Monocrystals Novosibirsk
10.15	$LiNbO_3$ H Gallagher U. of Strathclyde
10.30	Growth and Characterisation of photorefractive materials C Finnan University of Strathclyde
10.45	Coffee
11.00	Laboratory visits (or free discussion period)
12.30	Lunch
13.30	Developments in PPLN fabrication P Smith University of Southampton
13.50	Growth of phosphates and arsenates for periodic poling R Ward/K Hutton University of Oxford
14.10	Tunable quasi-phase-matched SHG of a CO_2 laser in GaAs Shekar Guha AFRL/MLPO
14.30	Periodically –poled $BaTiO_3$ P Schunemann Lockheed Martin, Nashua
14.50	Panel discussion - Quasi-phase matching
15.20	Tea and informal discussion session on issues arising from he workshop and debate on future research
16.00	Workshop closes. (The room will be available for informal discussion groups until 17.00)

Title	FirstName	LastName	Company/University	Country	WorkPhone	FaxNumber	EmailAddress
Prof	Bakhych	Bairamov	A I Ioffe Physico-Techical Intitute	Russia	+7 (812) 247-9140	+7 (812) 247-1017	bairamov@bahish.ioffe.rssi.ru
Dr	David	Burlage	Cleveland Crystals	USA	+1-216-486-6100 x3026	+1-216-486-6103	db@clevelandcrystals.com
Dr	David	Titterton	DERA Farnborough	UK	+44(0)1252-393264	+44(0)1252-392007	
Ms	Jayne	Ackroyd	DERA Malvern	UK	+44(0)1684-896607	+44(0)1684-896715	
Dr	Doug	Burgess	DERA Malvern	UK	+44(0)1684-895177	+44(0)1684-895603	
	Ian	Elder	DERA Malvern	UK	+44(0)1684-896139	+44(0)1684-896270	
Dr	Mike	Fearn	DERA Malvern	UK	+44(0)1684-895371	+44(0)1684-894428	
Mr	Colin	Flynn	DERA Malvern	UK	+44-(0)1684-894360	+44(0)1684-894311	cjflynn@dera.gov.uk
Mr	Mike	Harris	DERA Malvern	UK	+44(0)1684-894099	+44(0)1684-894428	
Dr	Keith	Nash	DERA Malvern	UK	+44(0)1684-894746	+44(0)1684-896150	
	David	Orchard	DERA Malvern	UK	+44(0)1684-895377		
	John	Payne	DERA Malvern	UK	+44(0)1684-895766	+44(0)1684-896270	
Mr	Phil	Smith	DERA Malvern	UK	+44(0)1684-894243	+44(0)1684-894311	
Dr	Phil	Soan	DERA Malvern	UK	+44(0)1684-896336	+44(0)1684-896270	
Ms	Lesley	Taylor	DERA Malvern	UK	+44(0)1684-894231	+44(0)1684-894311	lltaylor@dera.gov.uk
	Johnny	Terry	DERA Malvern	UK	+44(0)1684-896295	+44(0)1684-896270	
Dr	Tony	Vere	DERA Malvern	UK	+44(0)1684-894583	+44(0)1684-894311	awvere@dera.gov.uk
Prof	Ludmila	Isaenko	Design & Technolocial Inst of Monocrystals	Russia	+7-3832-333-843	+7-3832-333-843	lisa@lea.nsk.su
Dr	Leng Leng	Chng	DSO National Labs	Singapore	c/o DERA Malvern		clenglen@dso.org.sg
Mr	Jim	Telfer	Hilger Crystals	UK	+44(0)1843-231166 x100	+44(0)1843-290310	jim@hilger-crystals.co.uk
Mr	John	Ingleby	Ingcrys Laser Systems Ltd	UK	+44(0)1494-482541	+44(0)1494-2873	jingleby@netcomuk.co.uk
Dr	Alexander	Elisseev	Institute of Mineralogy & Petrography	Russia	+7-3832-332-409	+7-3832-333-843	alex@elis.nsk.ru
Dr	Alexander	Gribenyukov	Institute of Optical Monitoring	Russia	+7-3822-259589	+7-3822-258950	alexandre@losiom.tomsk.ru
Dr	Galina	Verozubova	Institute of Optical Monitoring	Russia	+7-3822-259589	+7-3822-258950	galina@losiom.tomsk.ru
Dr	Tom	Pollak	Lockheed Martin	USA	+1-603-885-4405	+1-603-885-0207	thomas.m.pollak@lmco.com
Dr	Pete	Schunemann	Lockheed Martin	USA	+1-603-885-5401	+1-603-885-0207	peter.g.schunemann@lmco.com
Dr	Ravi	Pandey	Michigan Tech University	USA	+1-906-487-2831	+1-906-487-2933	pandey@mtu.edu
Dr	Valeri	Voevodin	R&D Centre "ATOM"	Russia	+7-3822-413636	+7-3822-413636	voevodin@elefot.tsu.ru
Dr	James	Solomon	University of Dayton	USA	+1-937-656-5712	+1-937-656-7788	james.solomon@ml.afrl.af.mil
Dr	Keith	Hutton	University of Oxford	UK	+44(0)1865-272223	+44(0)1865-272400	k.hutton1@physics.ox.ac.uk
Dr	Roger	Ward	University of Oxford	UK	+44(0)1865-272355	+44(0)1865-272400	r.ward2@physics.ox.ac.uk
Dr	Peter	Smith	University of Southampton	UK	+44(0)1703-592809	+44(0)1703-593149	pgrs@orc.soton.ac.uk
Mr	Craig	Finnan	University of Strathclyde	UK	+44(0)141-548-3165	+44(0)141-553-4162	craig.j.finnan@strath.ac.uk
Mr	Hugh	Gallagher	University of Strathclyde	UK	+44(0)141-548-4015	+44(0)141-552-2891	h.g.gallagher@strath.ac.uk
Dr	Larry	Halliburton	University of West Virginia	USA	+1-304-2933422 x1442	+1-304-293-5732	lhallibu@wvu.edu
Dr	Nils	Fernelius	Wright Patterson AFB	USA	+1-937-255-4474 x3217	+1-937-255-4913	nils.fernelius@ml.afrl.af.mil
Dr	Shekhar	Guha	Wright Patterson AFB	USA	+1-937-252-3132 x3022	+1-937-252-0418	shekhar.guha@afrl.af.mil
Dr	Melvin	Ohmer	Wright Patterson AFB	USA	+1-937-255-4474 x3233	+1-937-255-4913	melvin.ohmer@ml.afrl.af.mil
Dr	Steven	Smith	Wright Patterson AFB	USA	+1-937-255-4474,x3221	+1-937-255-4913	steven.smith@afrl.af.mil
Dr	David	Zelmon	Wright Patterson AFB	USA	+1-937-255-4474 x3231	+1-937-255-4913	david.zelmon@afrl.af.mil
Dr	Martin	Stickley	EOARD, London		+44(0)171-514-4354	+44(0)171-514-4960	mstickley@eoard.af.mil

Bulk Optical Materials at DERA Malvern

- 1965 Laser materials $CaWO_4$ Ruby YAG
- 1966 NLO Materials $LiNbO_3$ $LiTaO_3$
- 1967 New NLO programme -wide materials survey

  tungsten bronzes BSN SBN, KLN and others

  Chalcogenides Ag_3AsS_3 $AgGaSe_2$ $AgGaS_2$
- 1970's Expanding programme

  Solution growth KDP, KTN

  Bulk growth (CZ and Bridgman) CdTe CdSeTe

DERA

Notes

Welcome

To the

Non-linear Optical Materials Workshop

DERA Malvern
20 September 1999

Jayne Ackroyd
Business Group Manager EO Protection

DERA

Workshop Benefits

- Collaboration
- Ideas Exchange
- Best use of funding and resources

Enjoy!

DERA

What is DERA?

- The largest Research and Technology organisation of its kind in Europe
- £1 billion turnover
- Owned by the UK Government
- Our mission is:
  - to be the main advisor to the UK Government on technology issues
  - to create wealth by technology transfer to industry

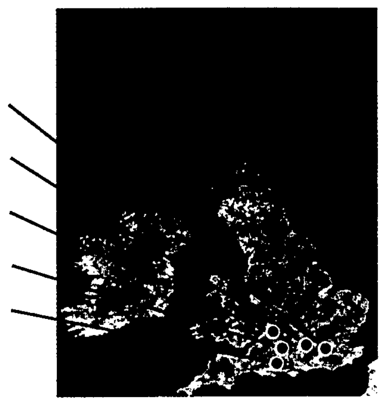

May 1999

DERA

DERA Evolution

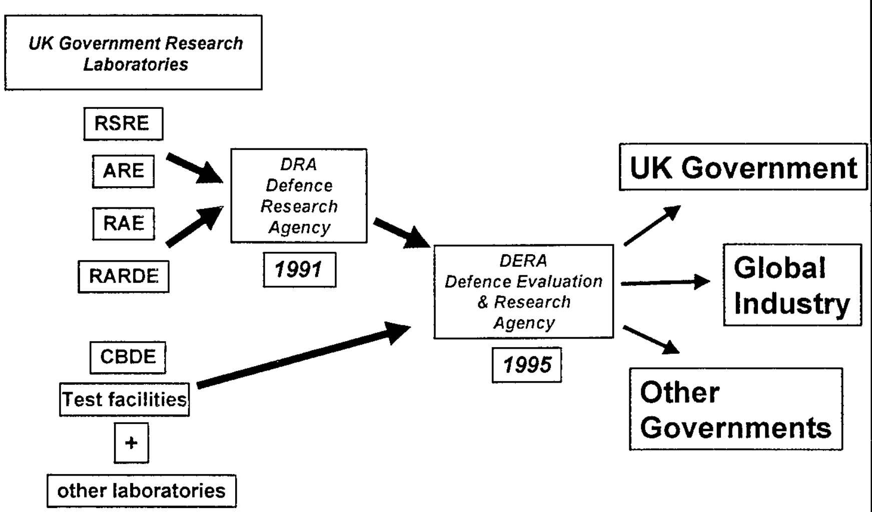

May 1999

DERA

Bulk Optical Materials at DERA Malvern

- 1985-90 Slow contraction of programmes
  Laser growth concentrated on eye-safe lasers
  YLF and related materials
  Alternatives to YAG e.g YAP

- 1985-90 Declining interest in NLO Materials
  Too difficult and limited markets

- 1992 Improved growth technology and emergence of ZGP, $AgGaSe_2$ as potential high power OPO and SHG materials reinvigorates NLO programme

DERA

NLO Materials - What Next?

- A short Introduction to the range, content and key issues for discussion at the Workshop and beyond

A W Vere
DERA Malvern

NLO Materials

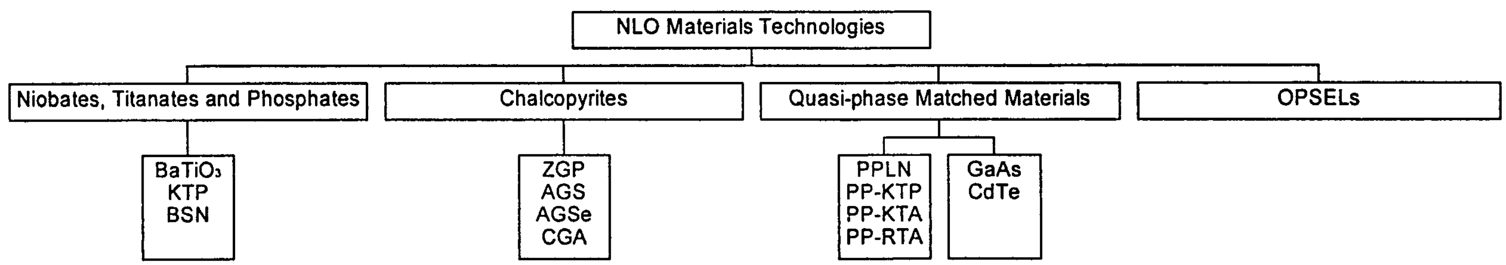

VG1

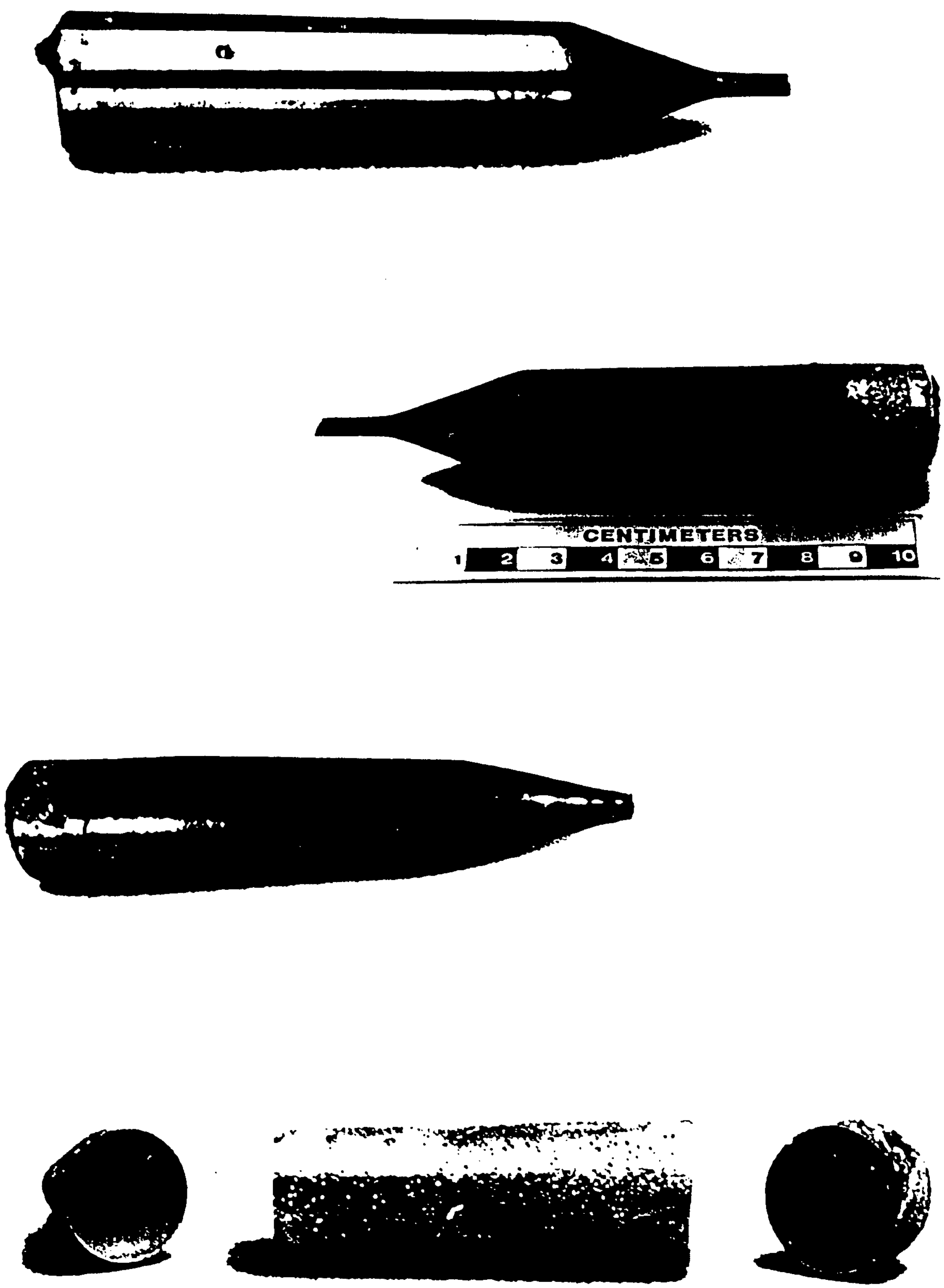

DERA

2 micron absorbance

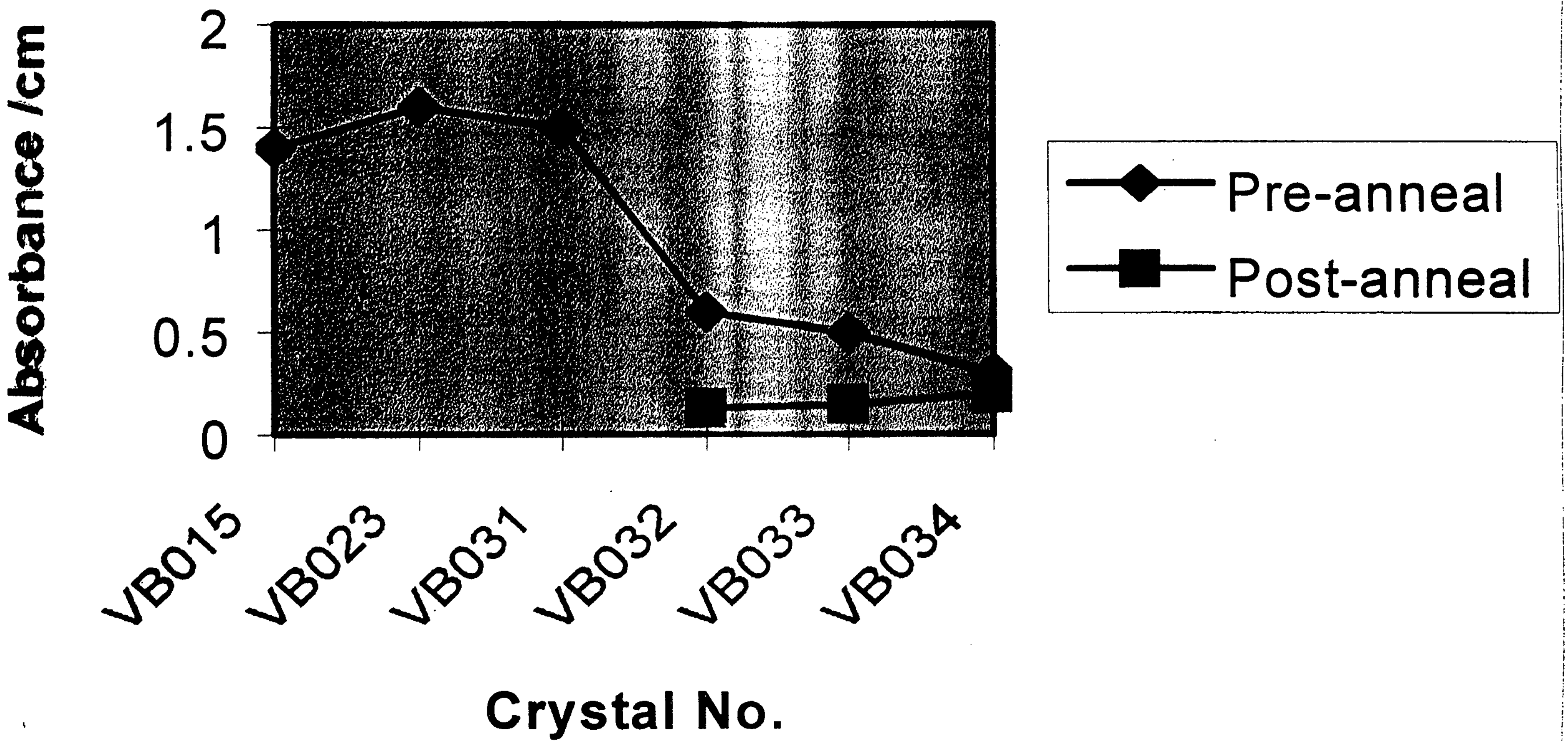

DERA

2 micron absorption in ZGP

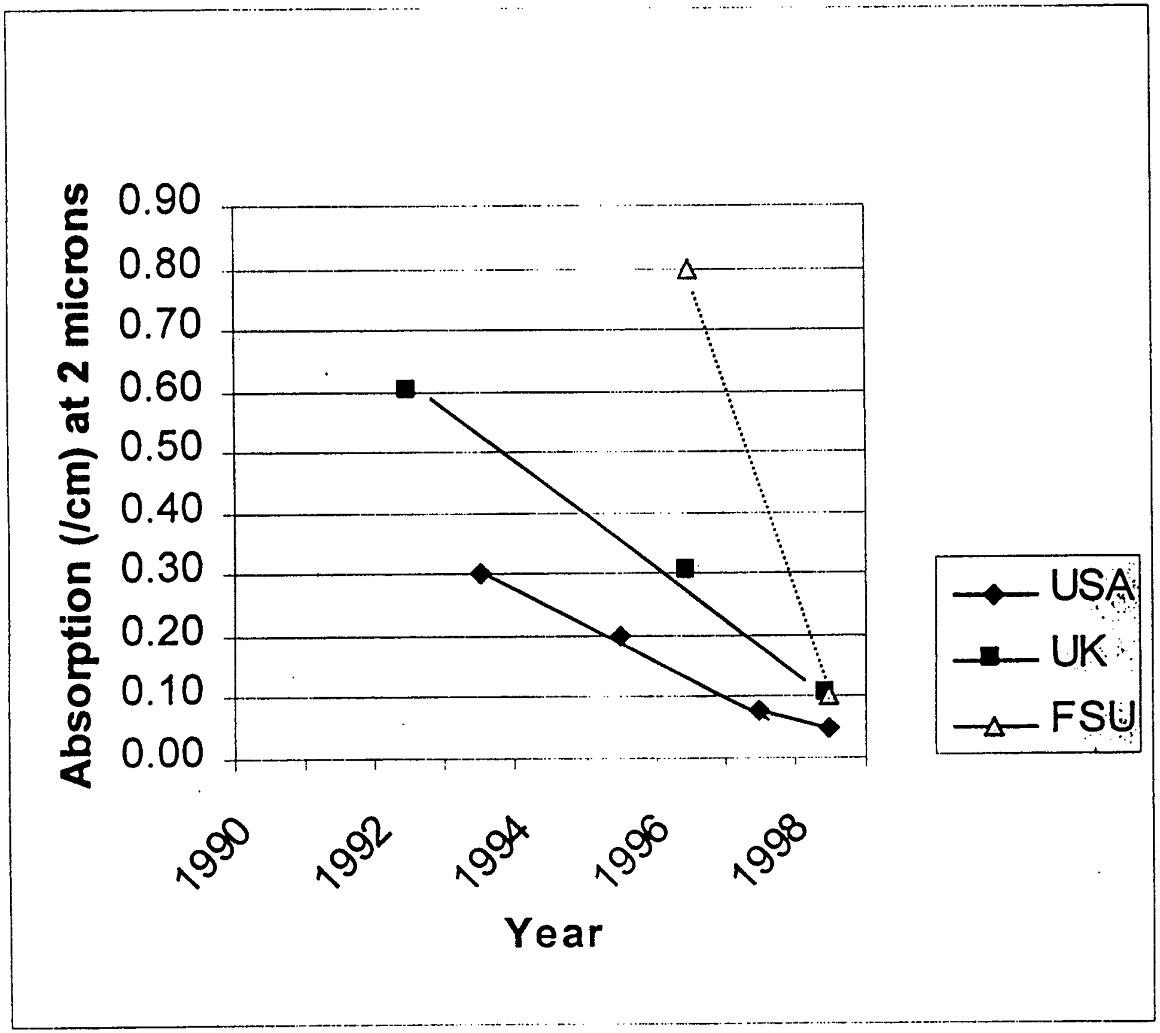

8

8

Variation of Absorbance and Carrier Concentration with Stoichiometry

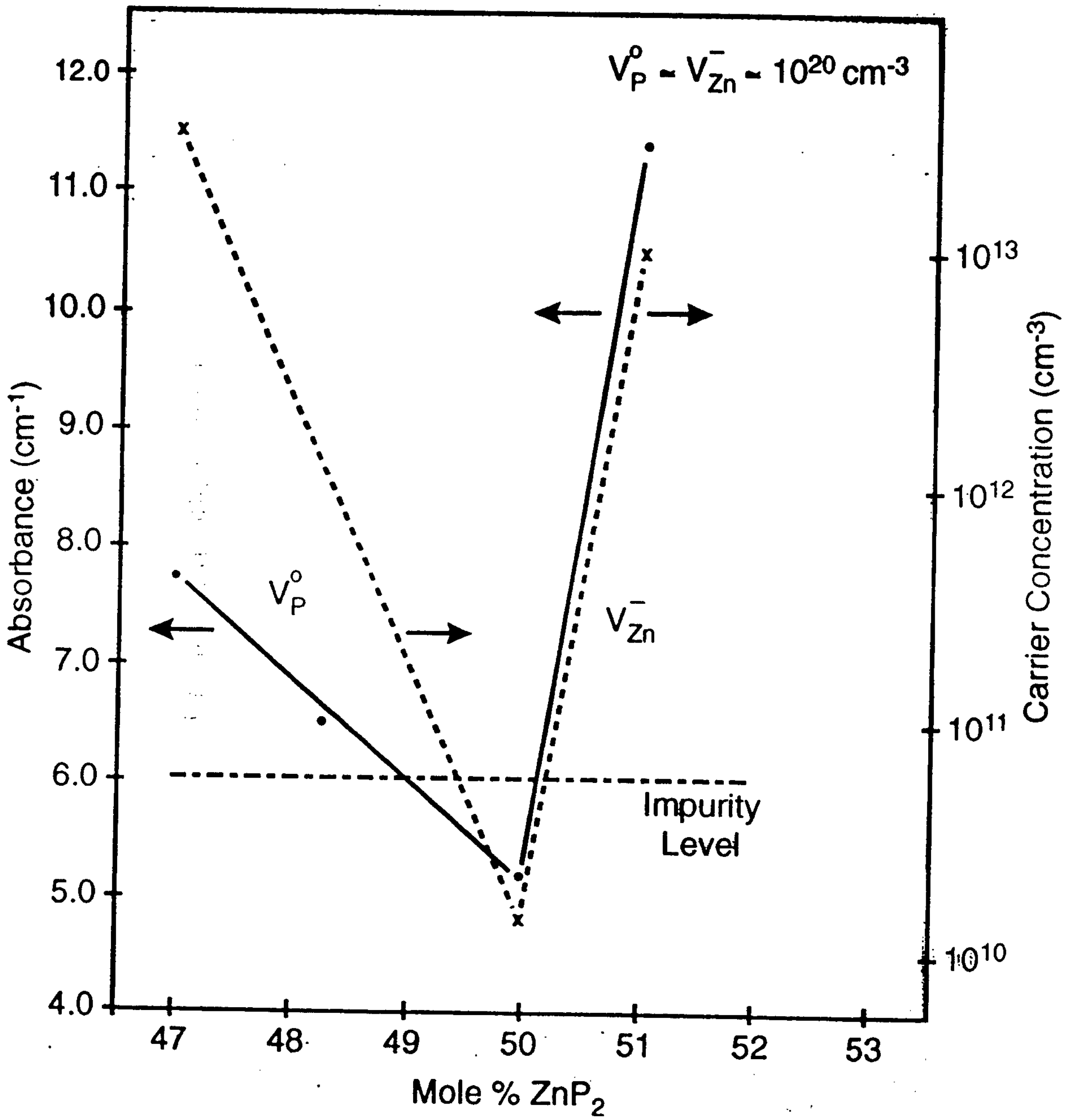

•——• P G Schunemann, Control of Stoichiometry in Semiconductor Heterostructures (Workshop – Bad Suhl, Germany, 1995)

x- - - -x V S Grigor'eva et al, Sov Tech Phys Lett 1 No 2 (1975) 61

— — — Impurity Level (Hypothetical)

DERA

ZnGeP2: DERA Malvern Programme

Tony Vere, Colin Flynn, Phil Smith
DERA Malvern

DERA

Key Properties of $ZnGeP_2$

- High vapour pressure ($P_{P_2} \sim 10^{10}$ over melt)
- High melting point (1028 ^{o}C)
- Brittle fracture mode
- Thermal expansion coefficient (5.0^{-6} $\|c$, 7.8^{-6} $\perp c$)
- Potential precipitation problems
- Band edge optical absorption tail

DERA

Growth programme: OBJECTIVE

- Grow single crystal ZGP
- Low absorption ($< 0.1 cm^{-1}$ at $2.128 \mu m$)
- Understand optical absorption/scattering mechanisms
- Fabricate optical parametric oscillator (OPO) element for use in mid IR.

DERA

Growth programme: HISTORY

- Initially, starting material produced by Wafer Tech
- Vertical Bridgman (VB) & Horizontal Bridgman (HB) produced crystals with mosaic cracking for a few years
- VB now producing good single crystal (PBN crucibles, [016] seed, insulation around seed holder)
- HB improving but abandoned due to VB success
- Collaboration with Institute of Optical Monitoring (IOM), Tomsk
- Starting material now obtained from IOM

DERA

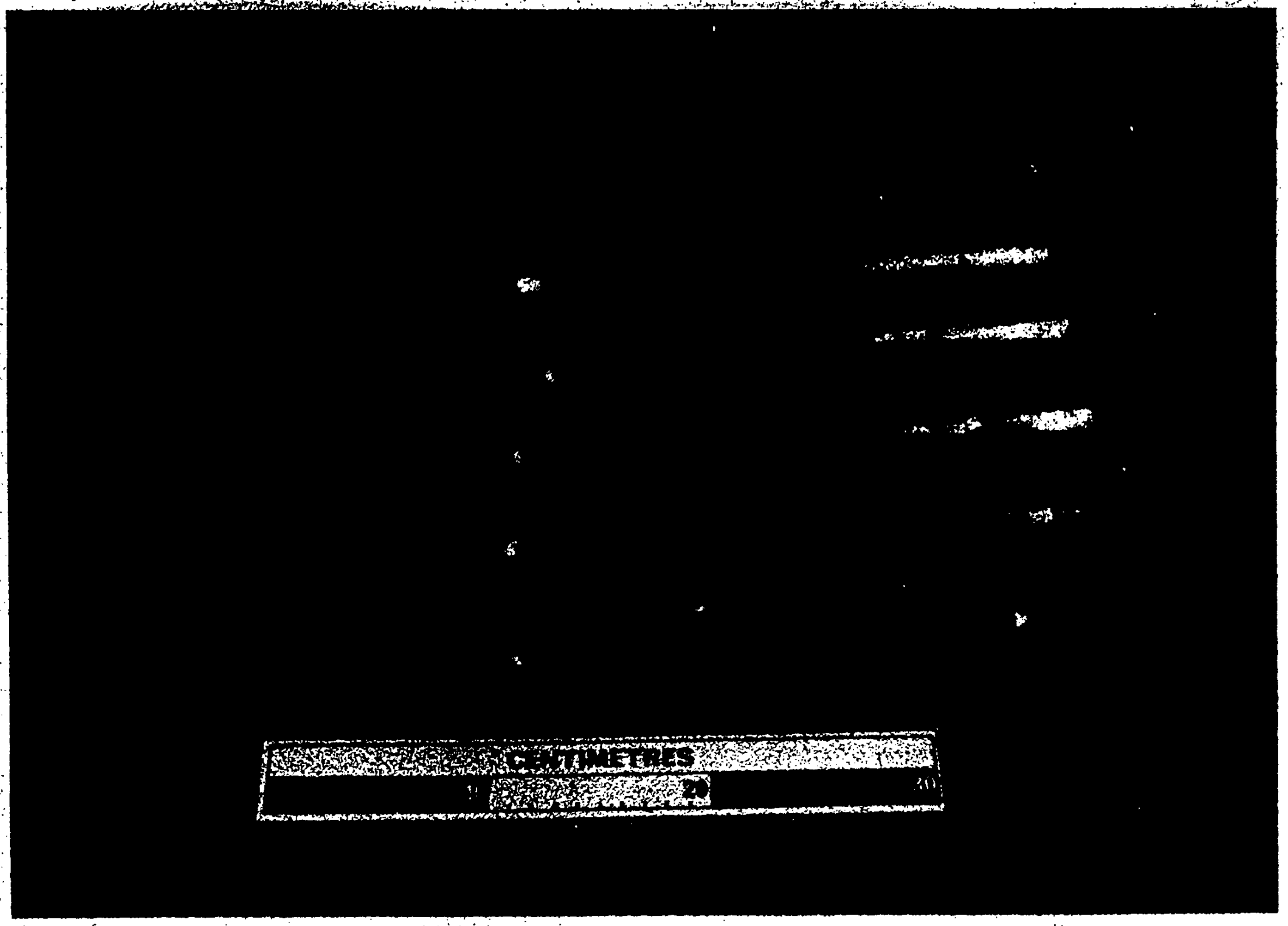

DRA

Comparison of starting materials

- Glow Discharge Mass Spectrometry (GDMS) data for IOM and Wafer Tech starting material.

	ppb by atom	
Element	IOM	Wafer Tech
S	120	<20
Mn	29	200
Fe	24	280

DERA

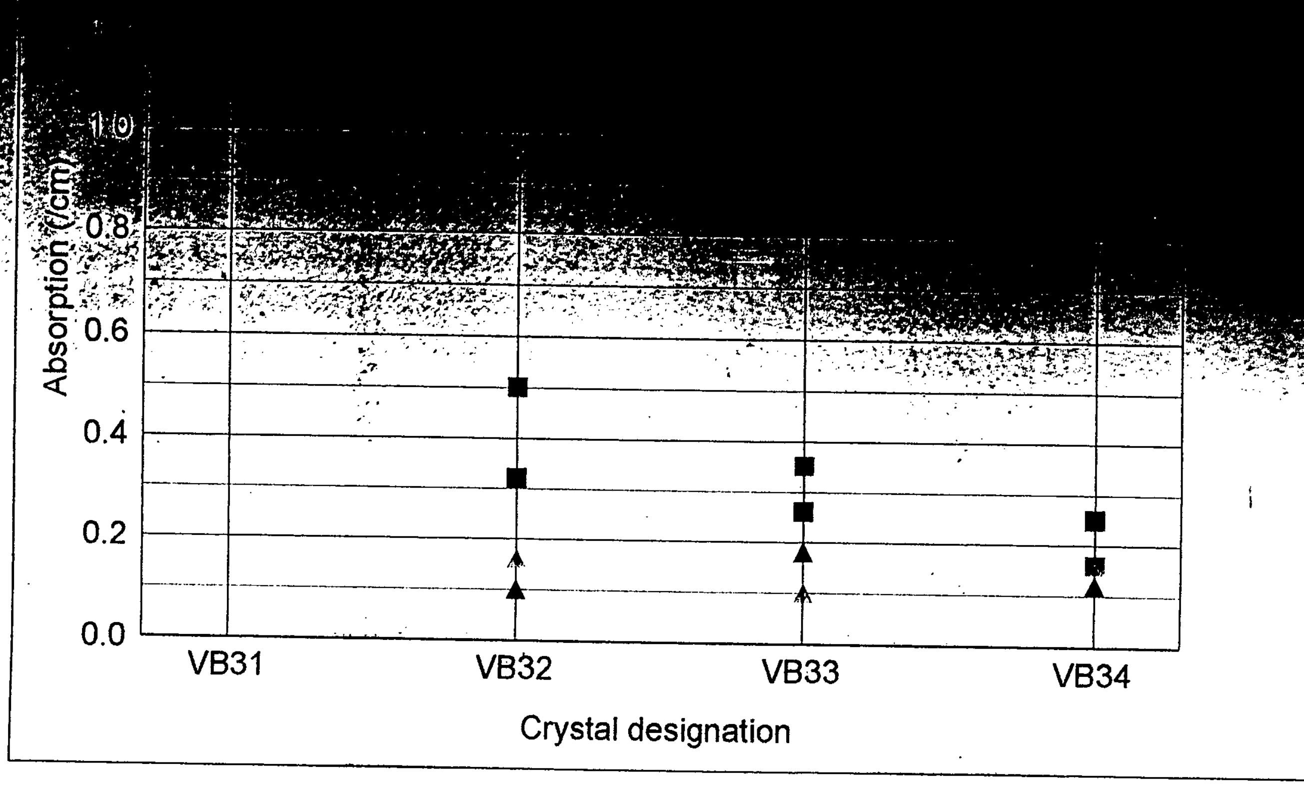
1.0
0.8
0.6
0.4
0.2
0.0
Absorption (/cm)
VB31
VB32
VB33
VB34
Crystal designation

DERA

Variation of absorption coefficient with annealing time

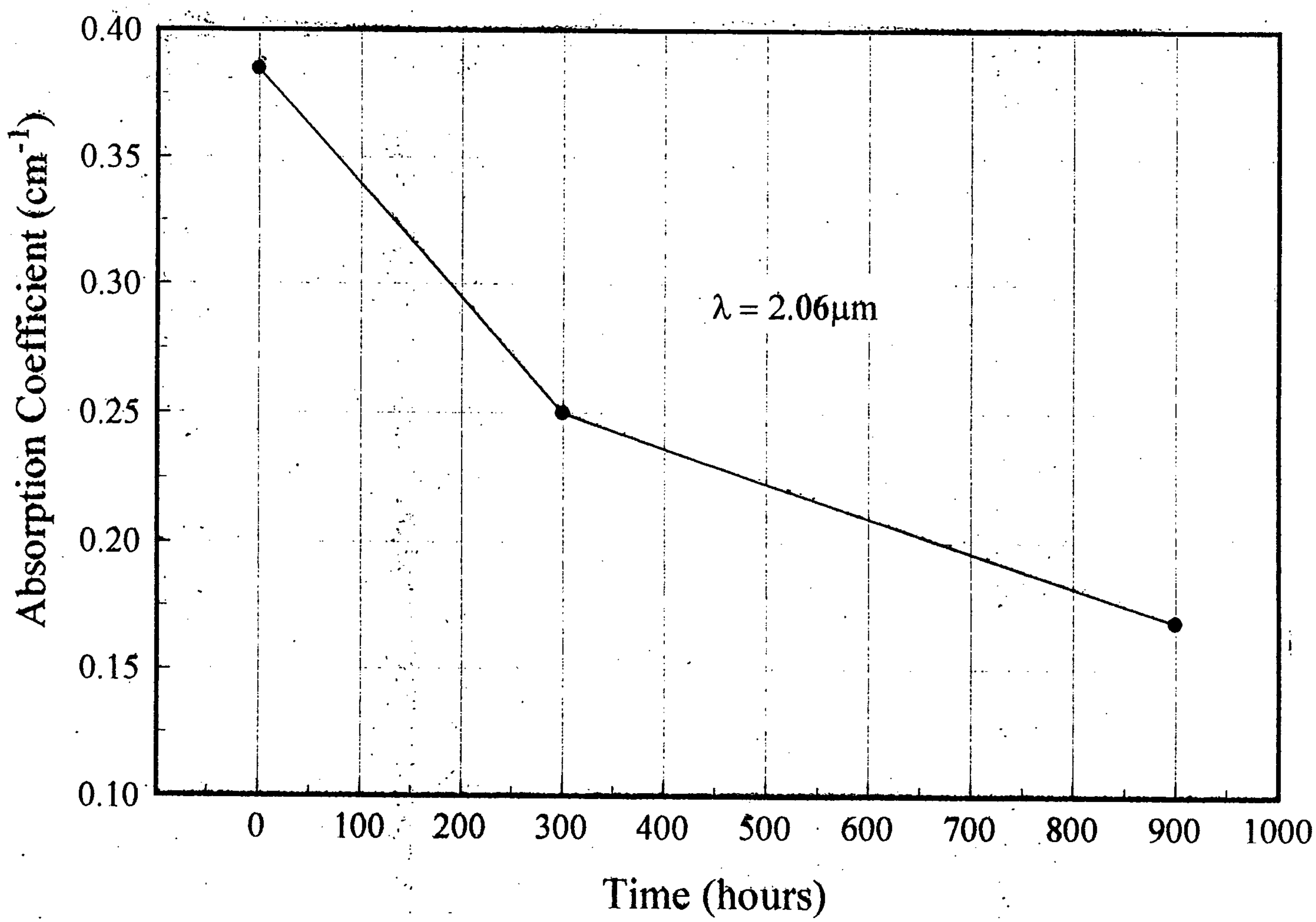

DERA

Effect of annealing on the transmission of ZGP

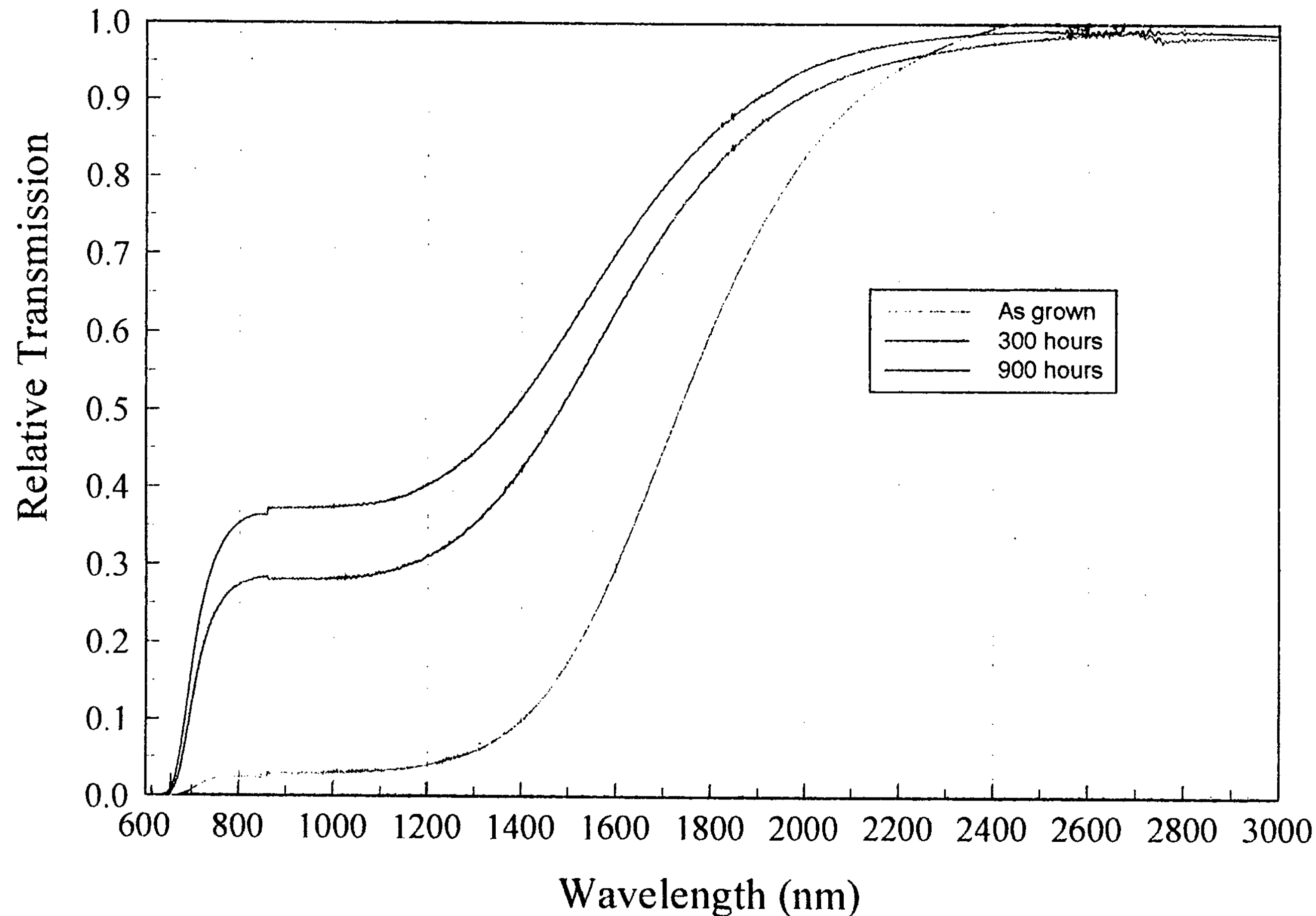

DERA

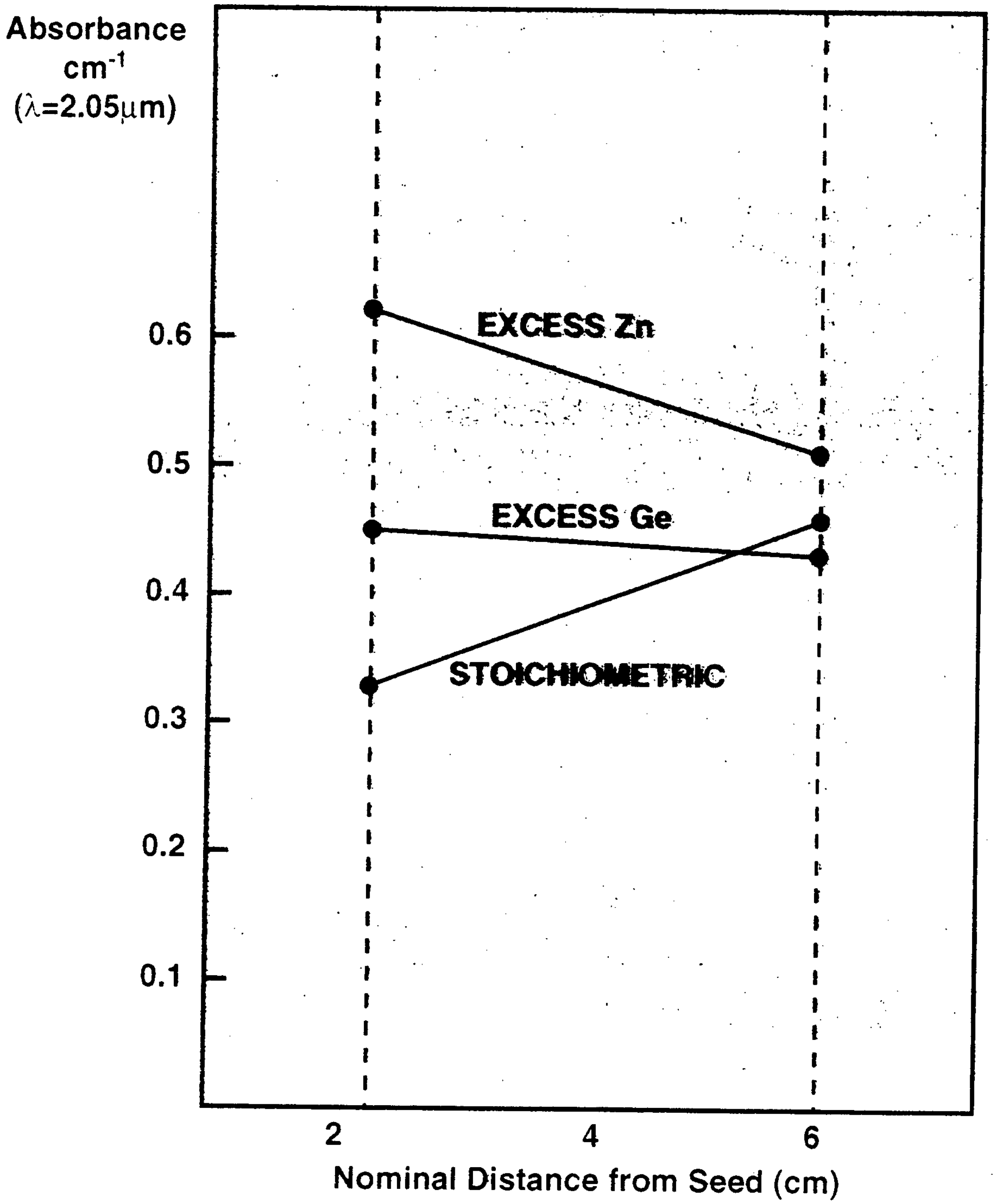

Absorbance
cm^{-1}
(λ=2.05μm)
0.6
0.5
0.4
0.3
0.2
0.1
EXCESS Zn
EXCESS Ge
STOICHIOMETRIC
2
4
6
Nominal Distance from Seed (cm)

DERA

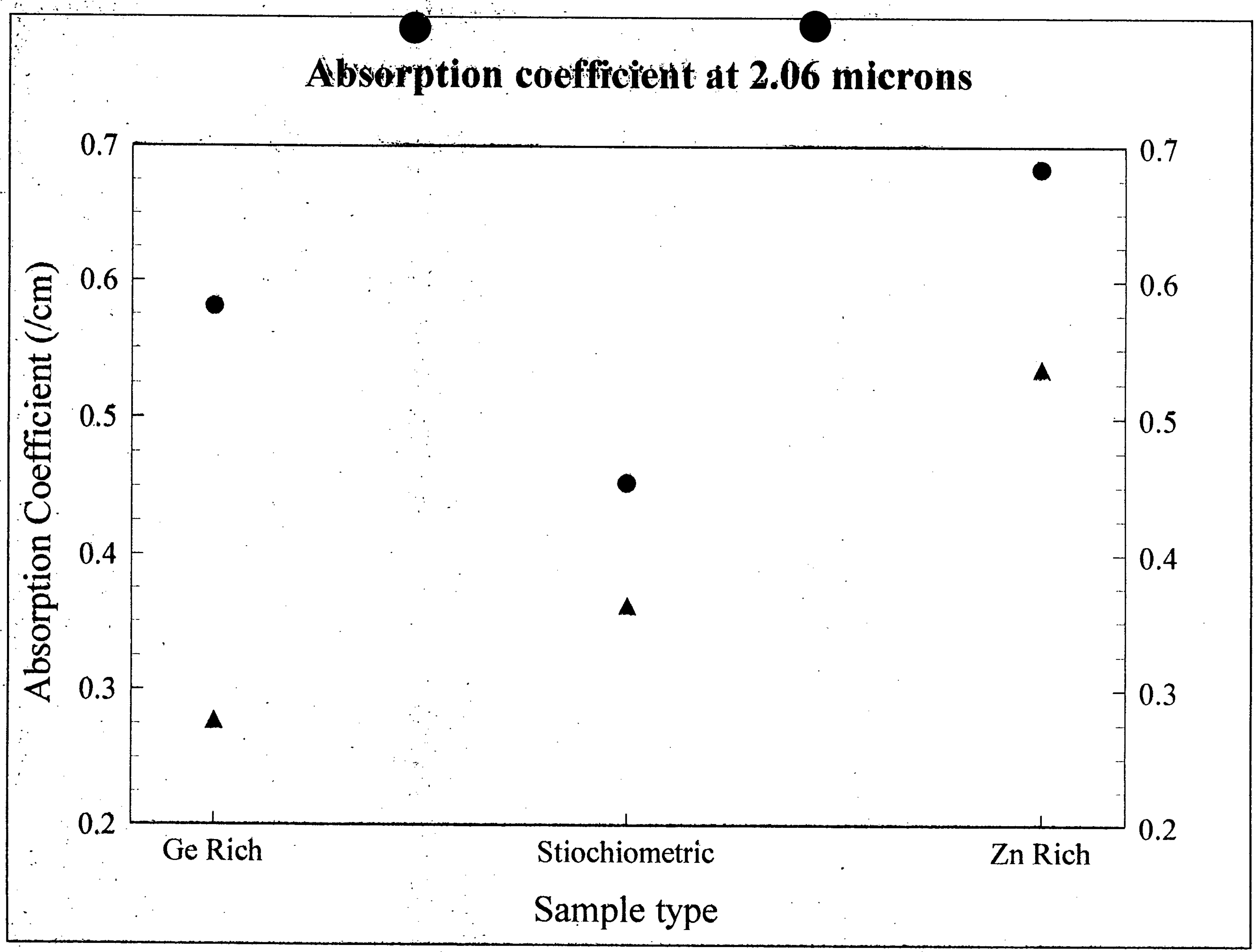

Absorption coefficient at 2.06 microns
Absorption Coefficient (/cm)
0.7
0.6
0.5
0.4
0.3
0.2
Ge Rich
Stiochiometric
Zn Rich
Sample type

Lattice parameter for <001> direction
in first-to-freeze, c-axis slices

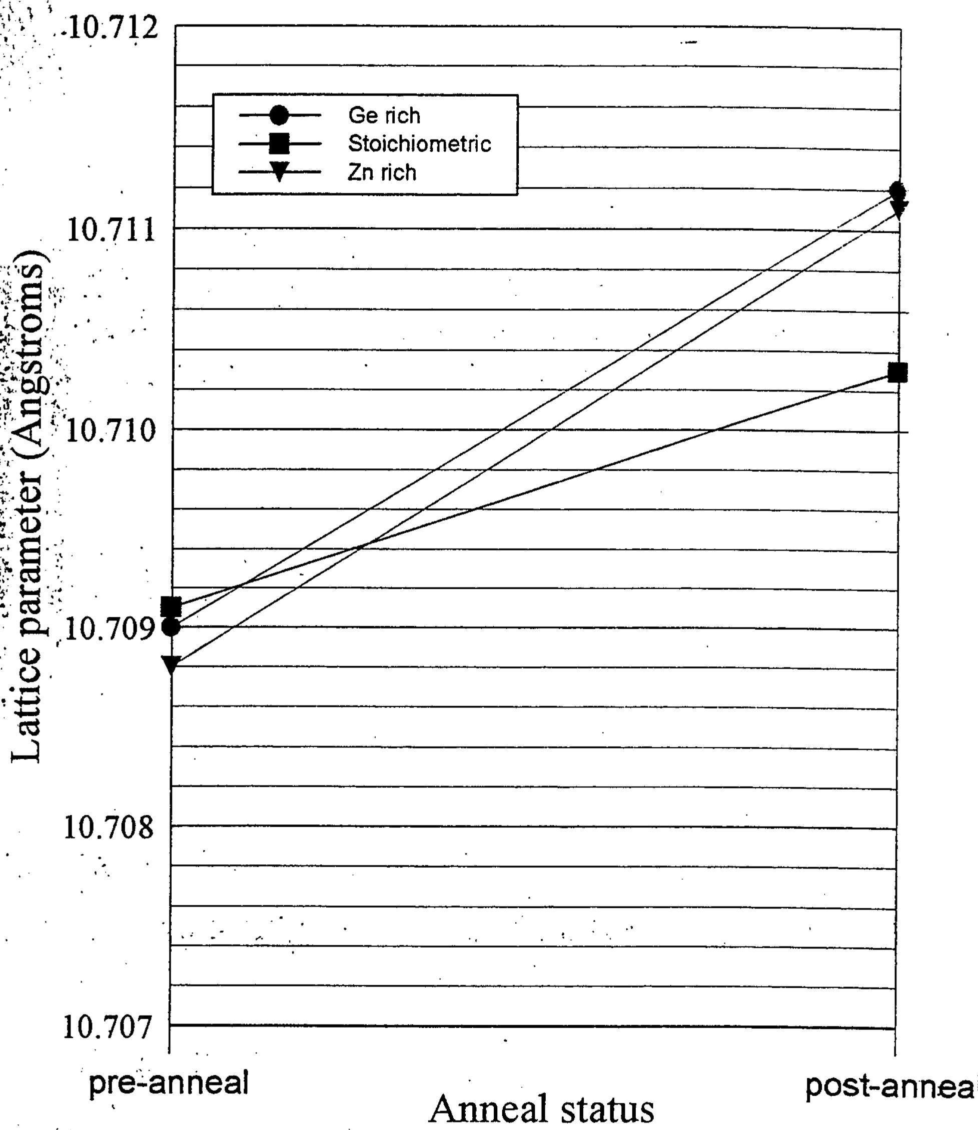

DERA

Lattice parameter for <100> & <010> directions
in first-to-freeze, c-axis slices

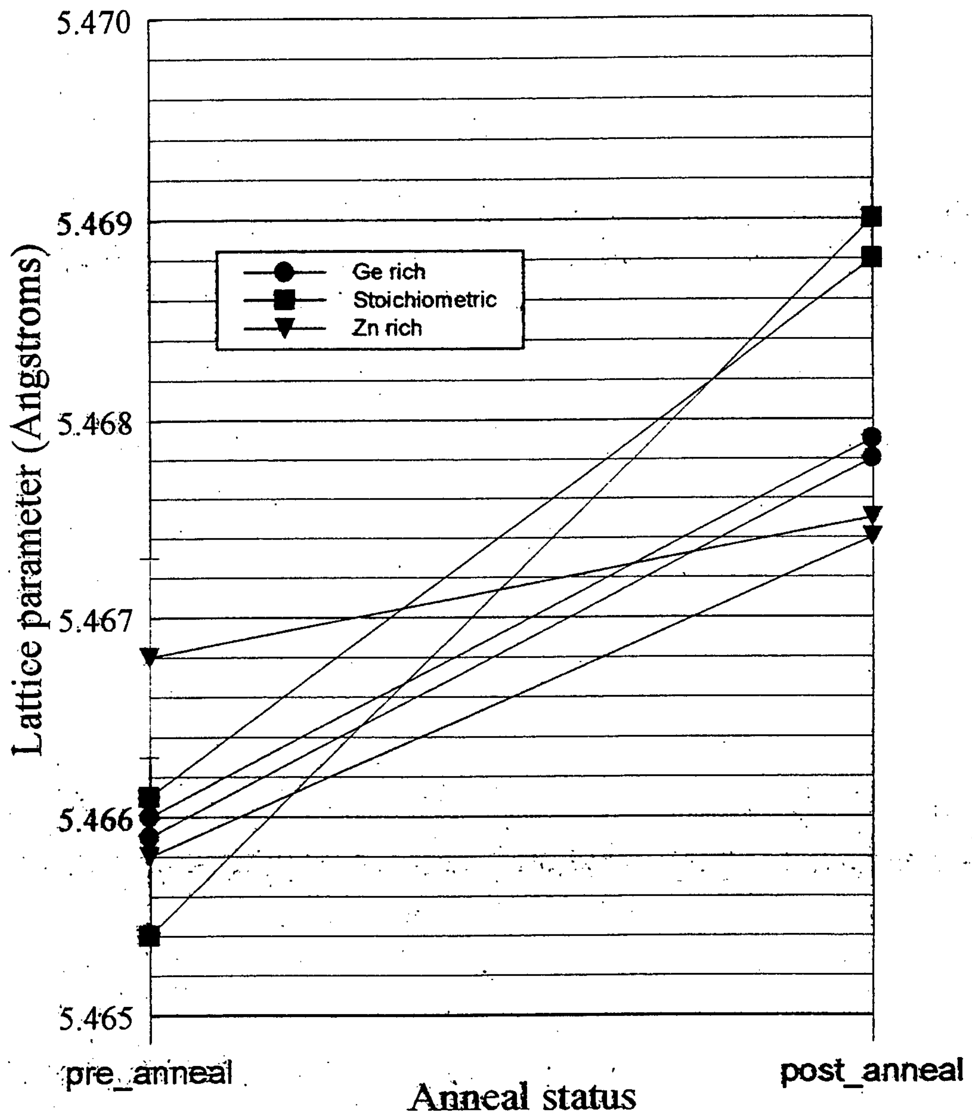

DERA

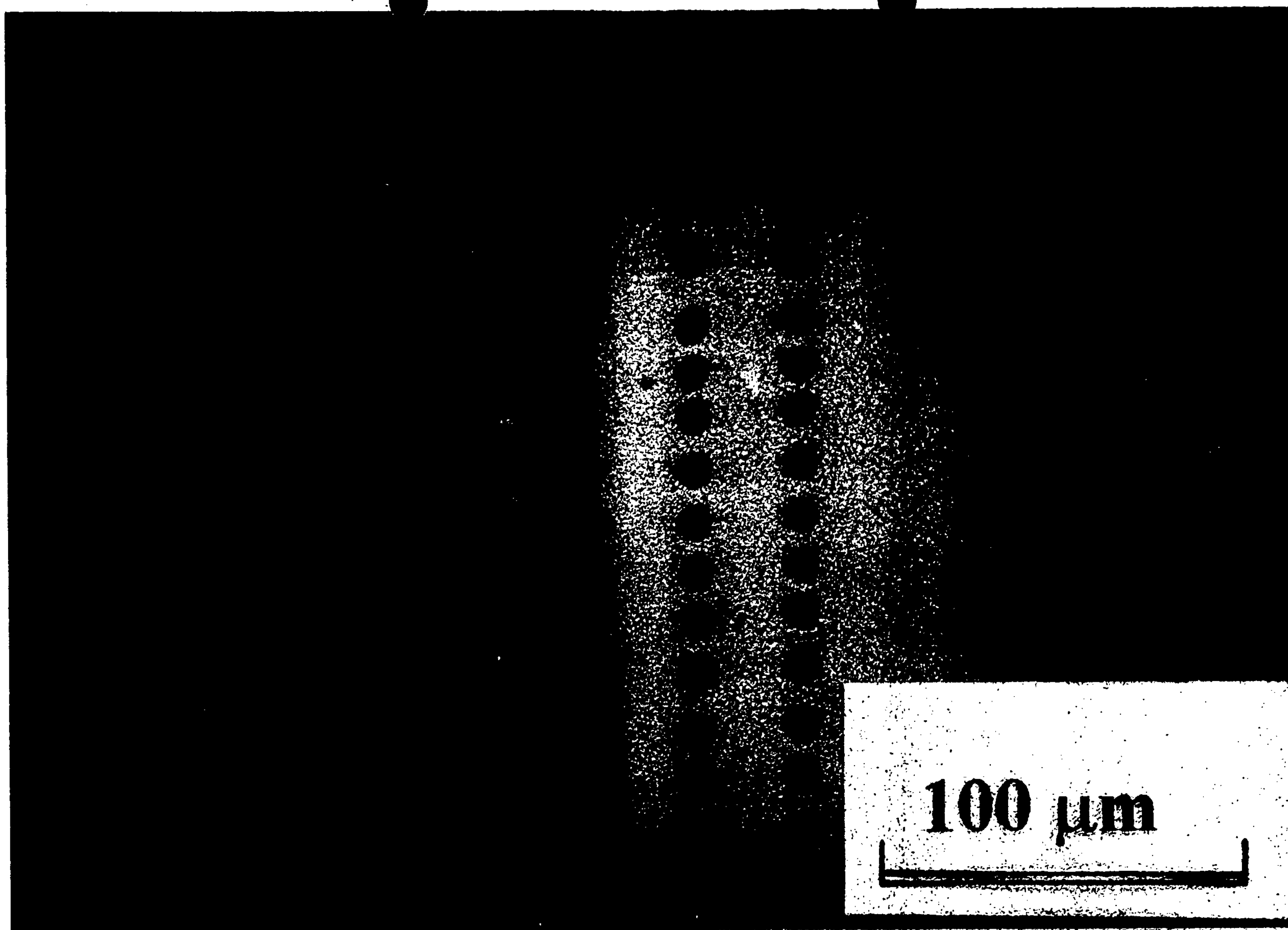
100 µm

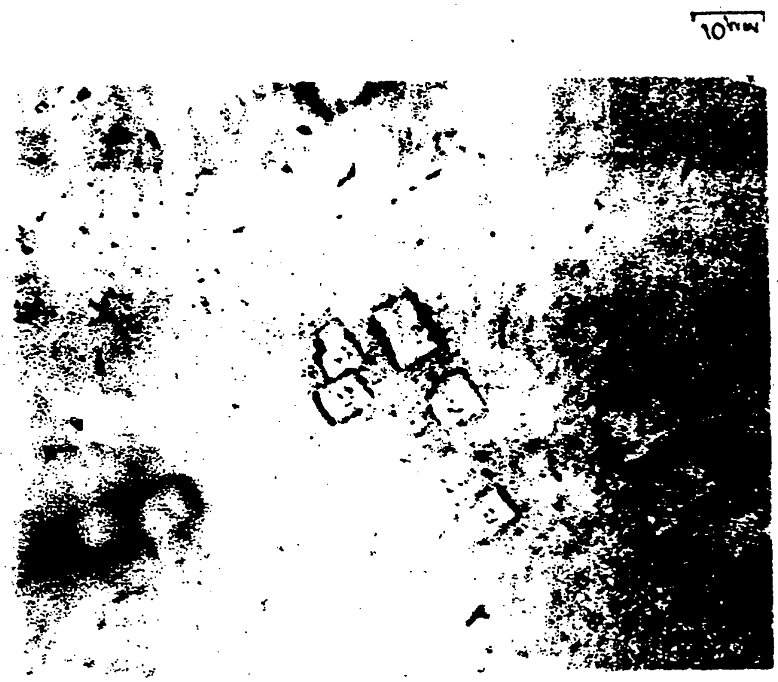

Summary

- Growing good quality single crystal ZGP
- Need to control stoichiometry of starting charge to avoid precipitation
- Absorption coefficient ‘bottoming out’ but still worthwhile pursuing annealing studies
- Now need to concentrate programme on identifying causes of absorption

DERA

ZGP Annealing Studies

L L Chng, Y-W Lee and H-G Ang

DSO National Laboratories, Singapore

C J Flynn, P C Smith and A W Vere

DERA Malvern UK

DSO NATIONAL LABORATORIES

Effect of Annealing Temperature on the Optical Absorption of IAO Zinc Germanium Phosphide Samples

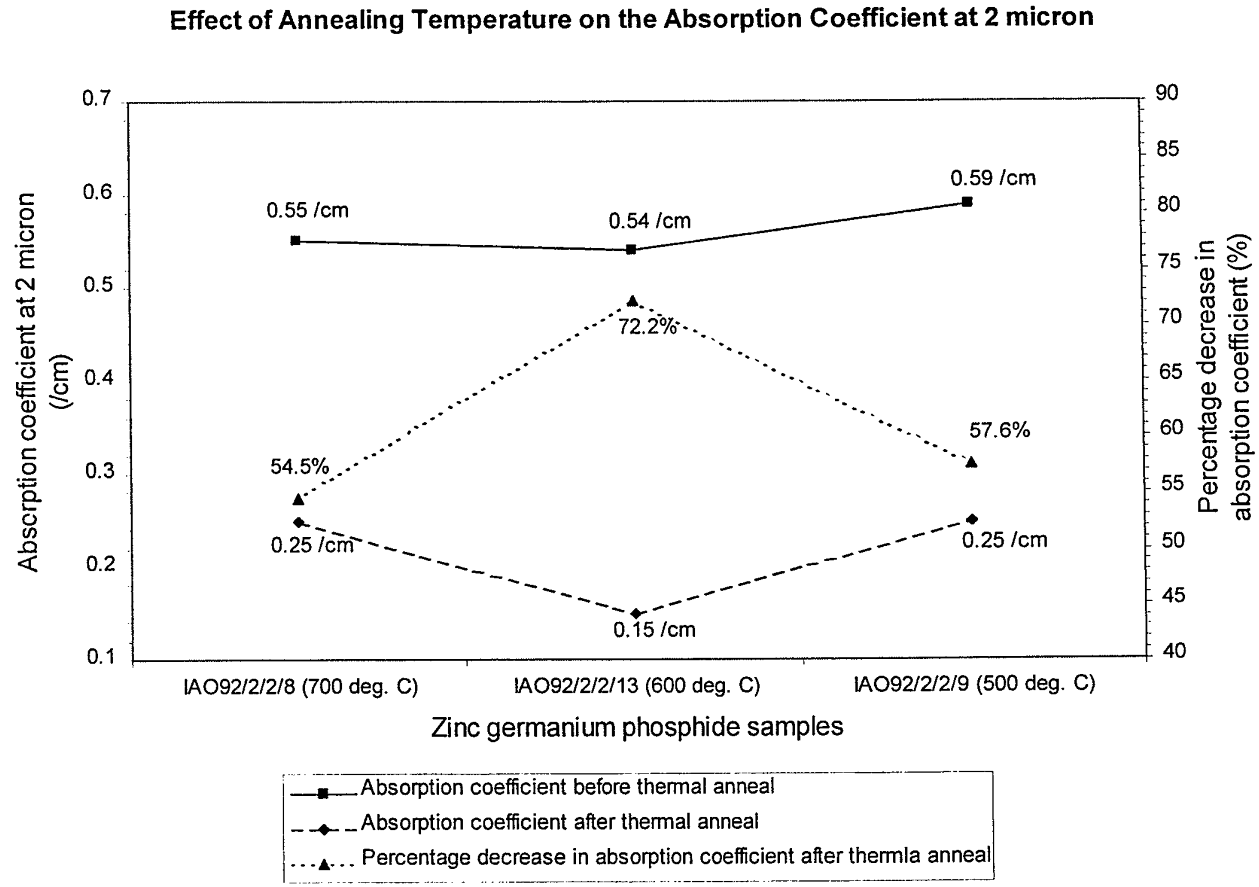

DSO NATIONAL LABORATORIES

Effect of Annealing Time on the Optical Absorption of IAO Zinc Germanium Phosphide Samples

Effect of Annealing Time on the Absorption Coefficient at 2 micron

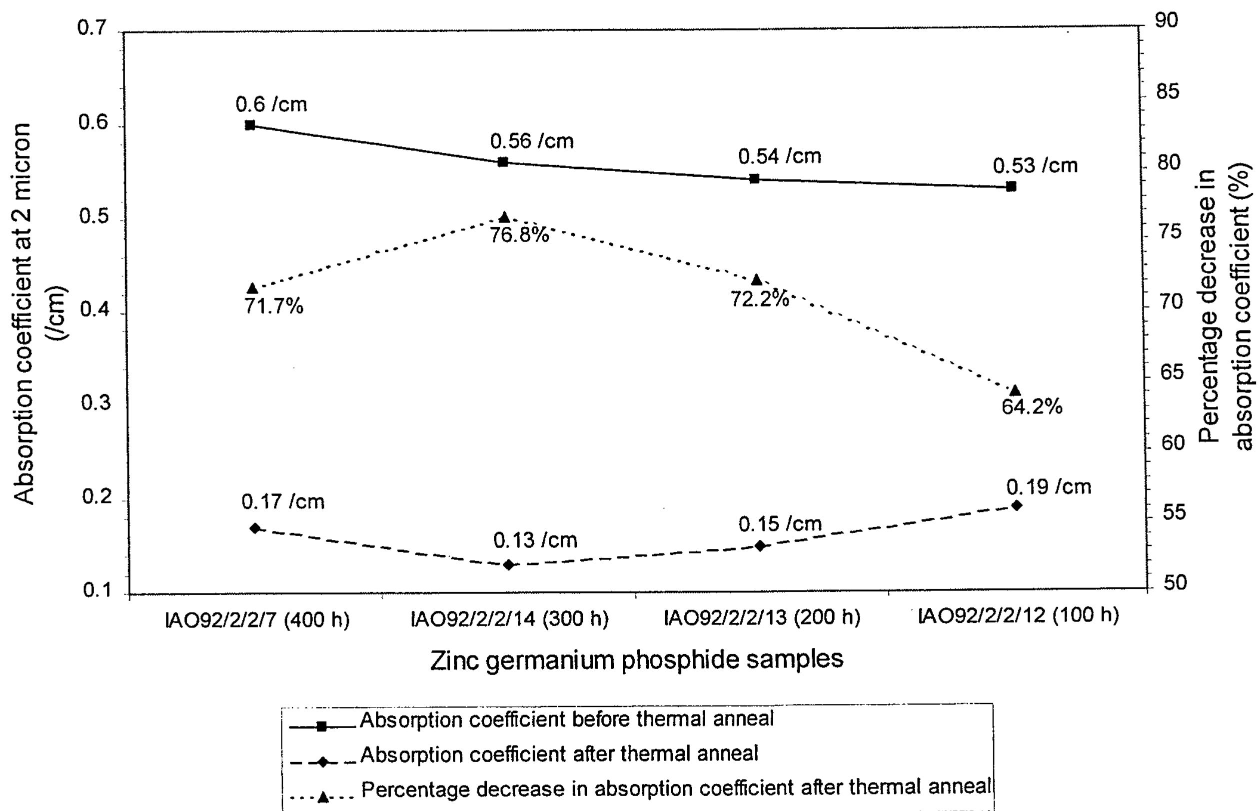

DSO NATIONAL LABORATORIES

Effect of Annealing Vapour Pressure on the Optical Absorption of IAO Zinc Germanium Phosphide Samples

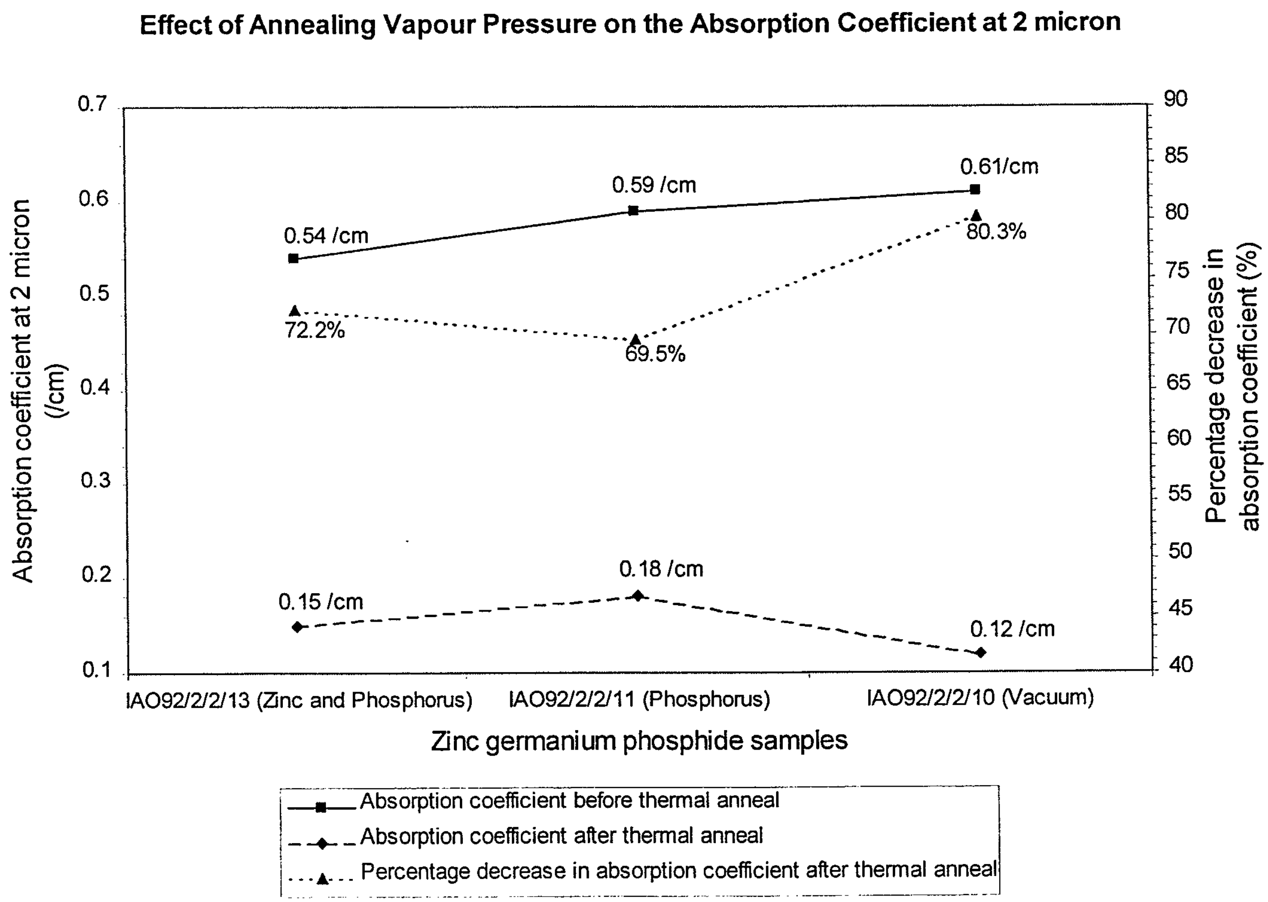

DSO NATIONAL LABORATORIES

Effect of Annealing Heating/Cooling Rate on the Optical Absorption of IAO Zinc Germanium Phosphide Samples

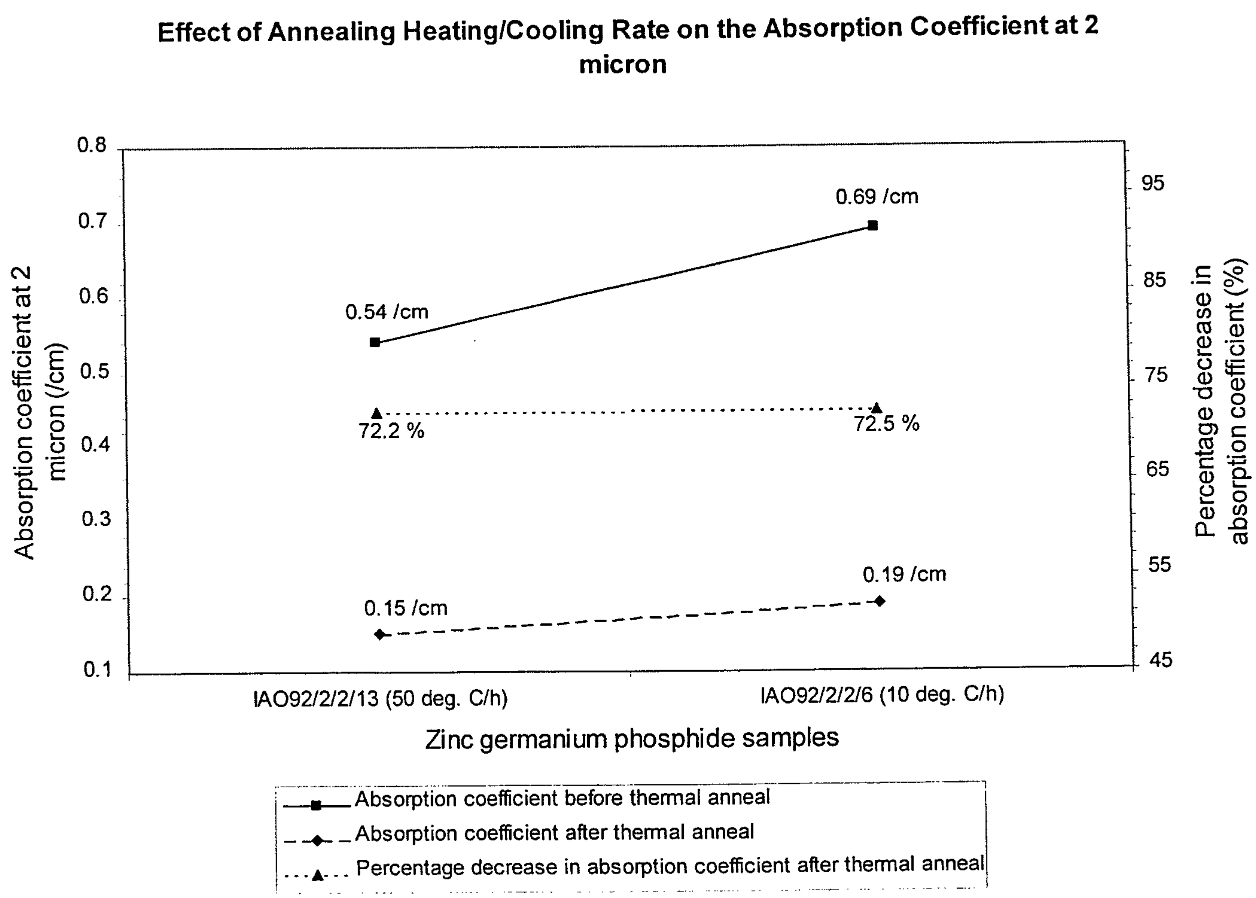

DSO NATIONAL LABORATORIES

Effect of Re-Annealing on the Optical Absorption of IAO Zinc Germanium Phosphide Samples

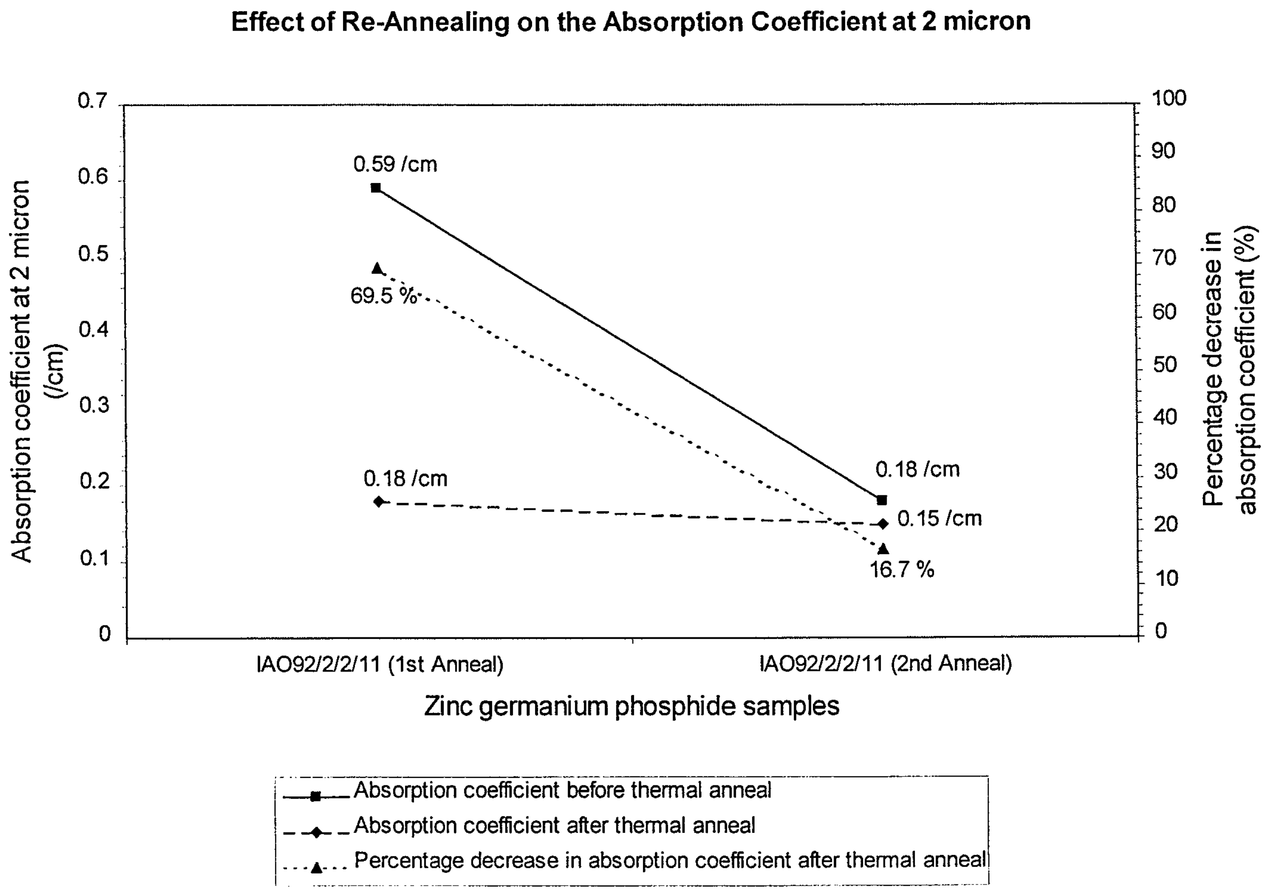

DSO NATIONAL LABORATORIES

Reduction of the Near-Infrared Absorption of Zinc Germanium Phosphide Through Post-Growth Annealing Treatment

- Optimal annealing temperature of ZGP is 600°C.
- Optimal annealing time should be 200 - 400 h.
- Optimal annealing atmosphere is vacuum.
- Thermal annealing of zinc germanium phosphide decreased the 2-μm optical absorption by at least 50%.
- Rate of heating and cooling ZGP did not affect the percentage decrease in the 2 μm absorption coefficient.
- Re-annealing ZGP reduced further the 2 μm absorption coefficient.

DSO NATIONAL LABORATORIES

Shekhar Guha, Michael Eaton, F. Ken Hopkins and Melvin C. Ohmer
AFRL/MLP
Wright Patterson Air Force Base, OH 45433-7702

shekhar.guha@afrl.af.mil

NLO99 Workshop, DERA, Malvern, UK, 20 - 21 September, 1999

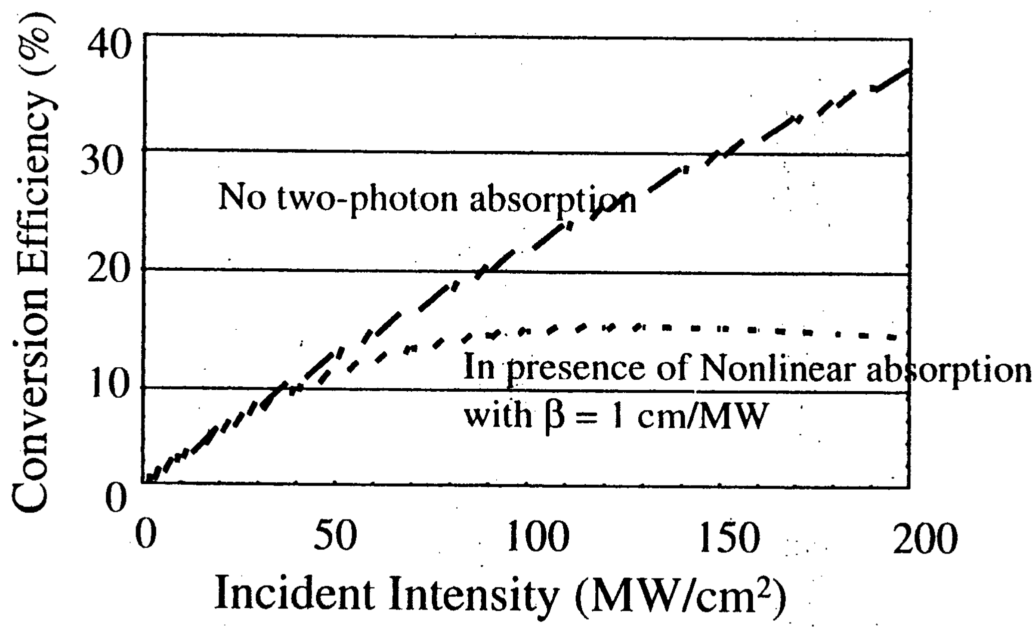

$$\frac{dA_1}{dz} = -i\kappa A_1^* A_2$$

$$\frac{dA_2}{dz} = -i\kappa A_1^2 - \beta(A_2 A_2^*) A_2$$

Presence of two-photon absorption limits high power generation

Sample name	Sample thickness (μm)	Carrier concentration (10^{16} cm^{-3})	Absorption coefficient (cm^{-1})			
			300 K		90 K	
			$\parallel$	$\perp$	$\parallel$	$\perp$
2G	974	0.4	2.5	2.8	0.6	0.1
4Q	912	4.9	19	9	8.5	4.2
4M	934	6.9	22	9	11	0.6
4O	957	7.8	32	18	10	0.6

Sample size: ~ 1 cm x 1 cm x 1 mm
c axis in the polished face

CGA (S 106)

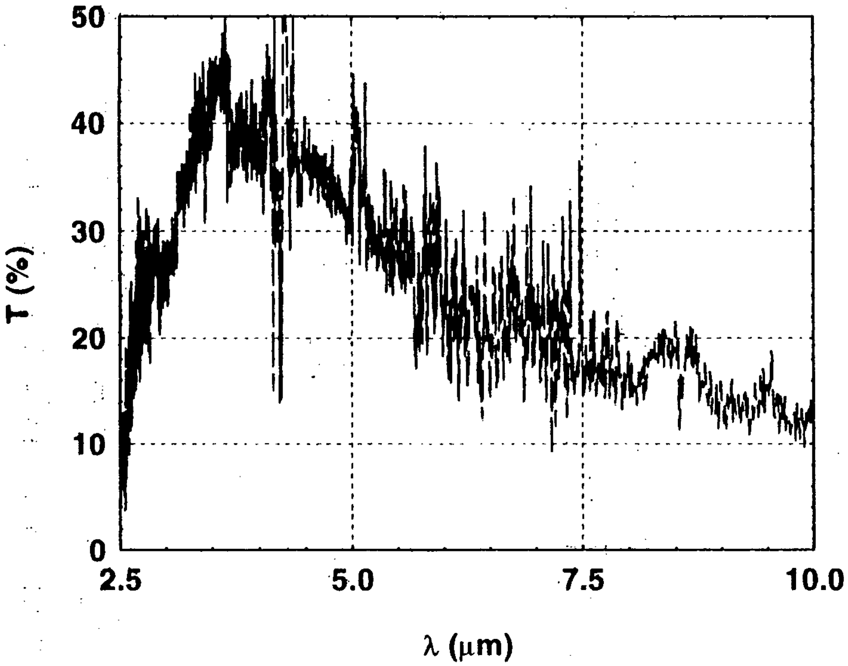

CdGeAs2 sample 2

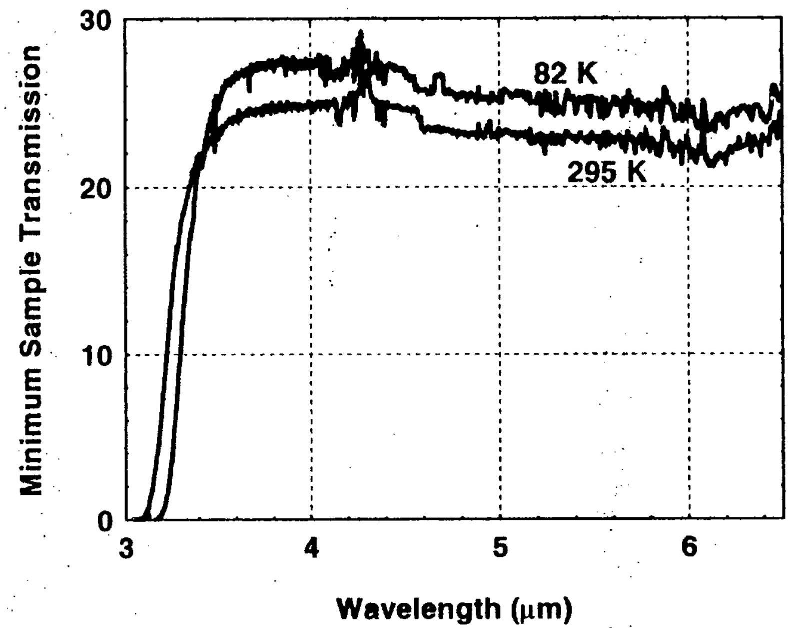

Bandgap of CGA increases with temperature increase

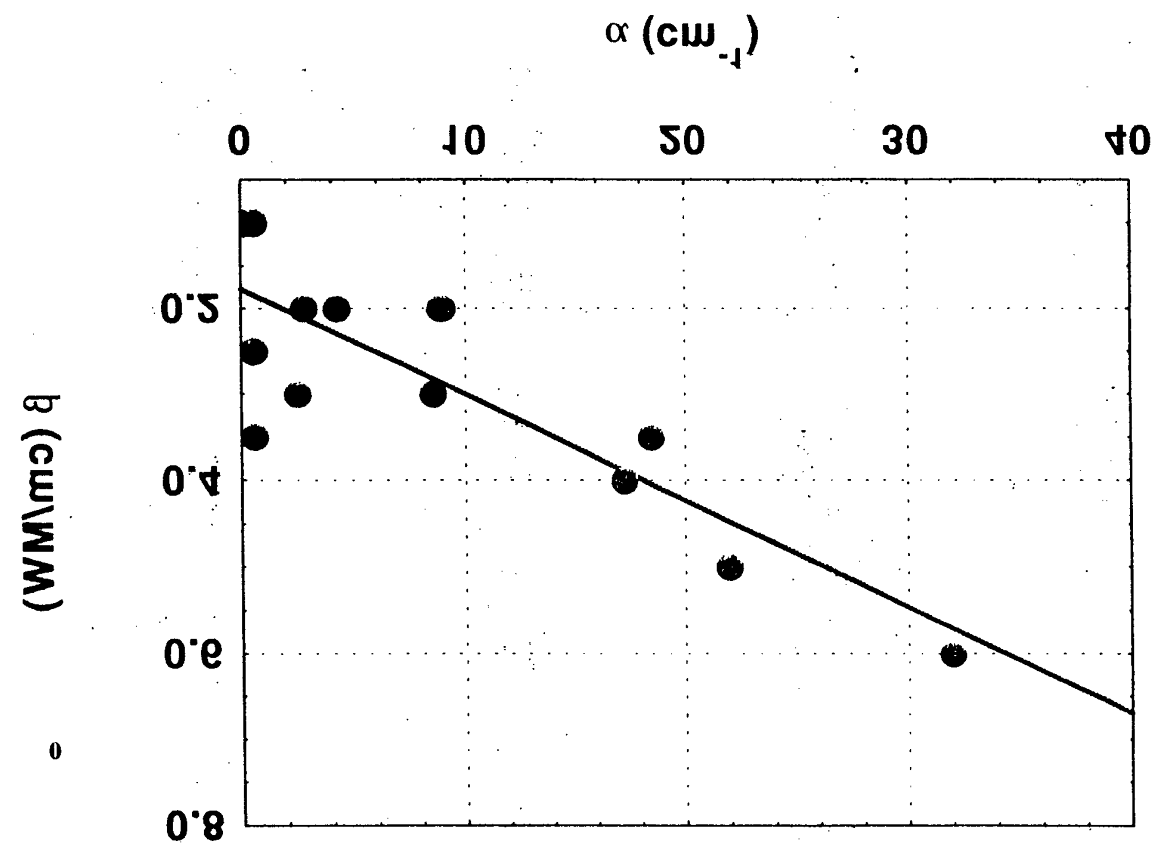
α (cm⁻¹)
0
10
20
30
40
β (cm/MW)
0.2
0.4
0.6
0.8

β (cm/MW)

Sample	300 K		90 K	
	∥	⊥	∥	⊥
2G	0.3	0.2	0.25	0.1
4Q	0.35	0.2	0.2	0.3
4M	0.5	0.2	1.5	0.1
4O	0.6	0.4	1	0.35

- Anisotropy
- Temperature Dependence

2.09 μm

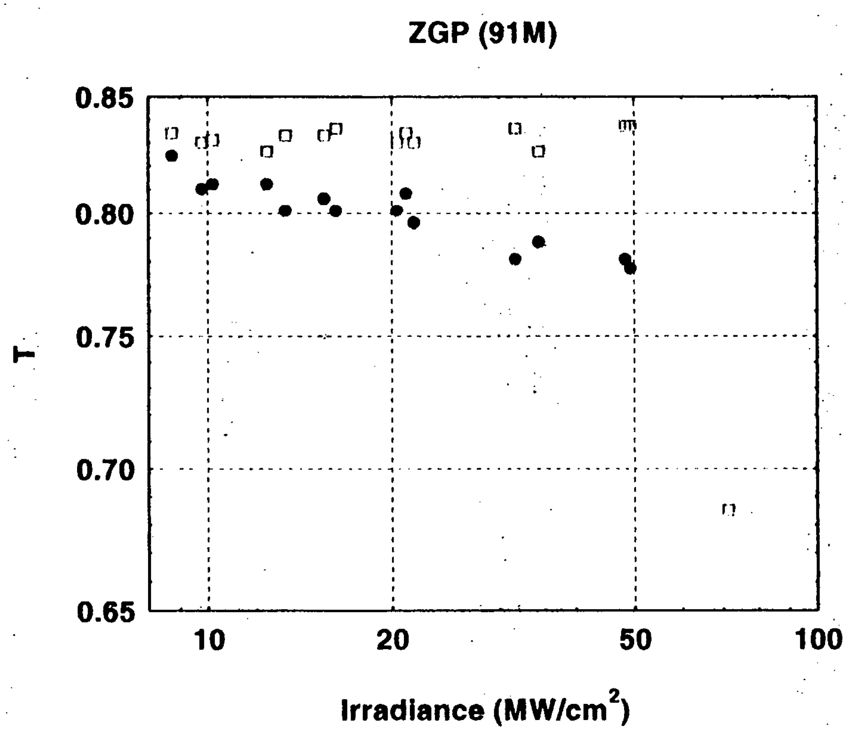

2.94 μm

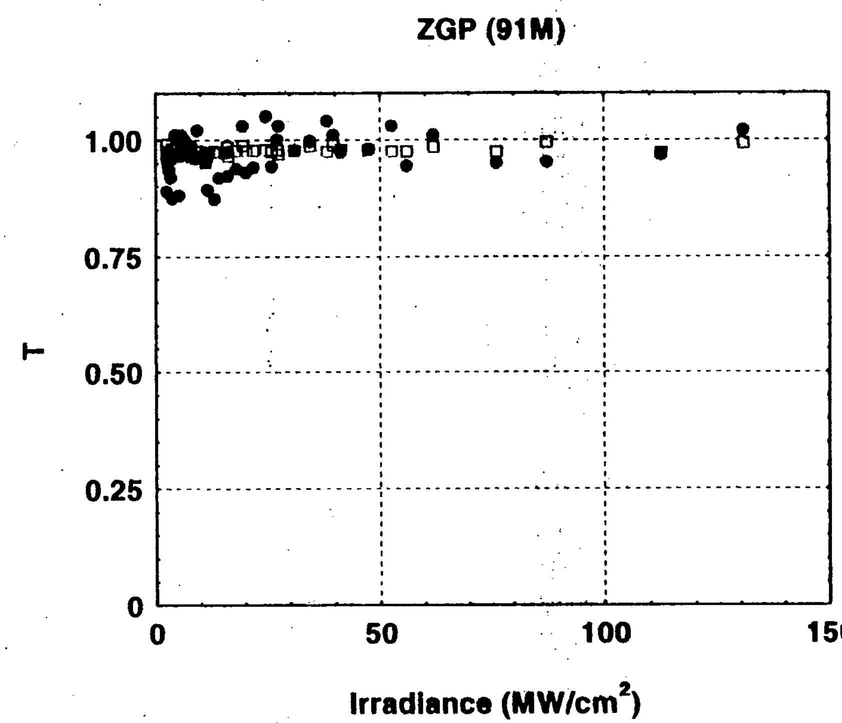

Nonlinearity and damage in $ZnGeP_2$ observed at 2.09 μm but not at 2.94 μm

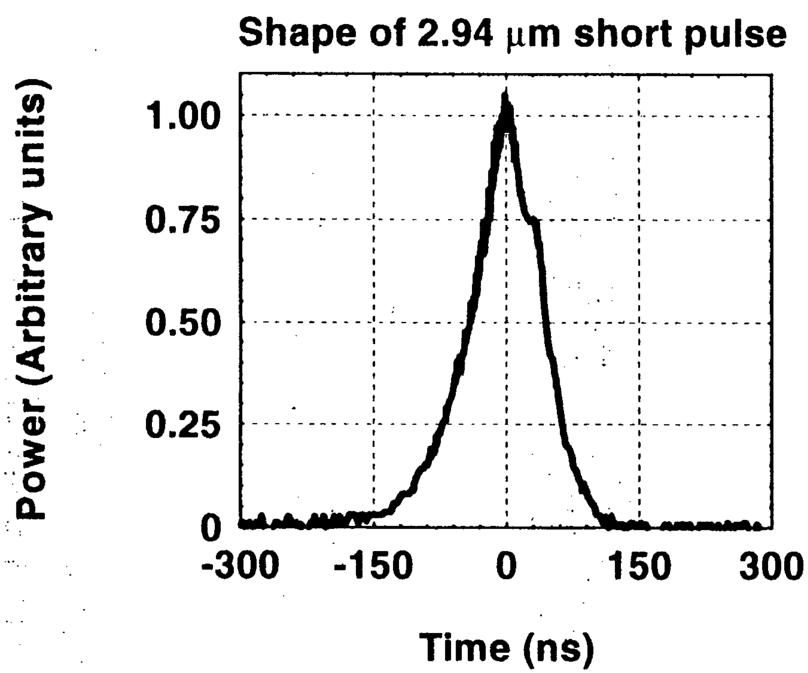

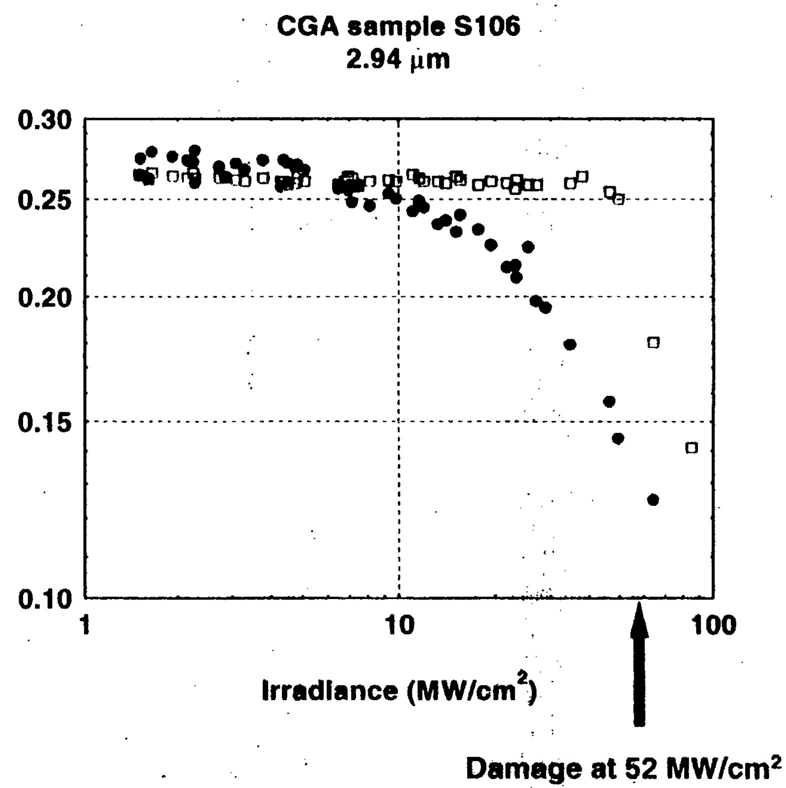

Effective Nonlinearity < 0.05 cm/MW

Sample Number ~~(cm/MW)~~	Coating status	Linear Absorption (cm-1)		Nonlinear Absorption cm/MW	
		Ordinary	Extraordinary	Ordinary	Extraordinary
92H	Uncoated	0.29	1.04	0.04	0.12
92N	Standard AR	0.33	0.70	0.08	0.35
92P	Standard AR	0.32	0.69	0.06	0.20
92Q	ARDO52x98	0.30	0.75	0.12	0.25

Strong anisotropy in the NLA of $ZnGeP_2$ is observed

ZGP - crystals:
homogeneity region, real defects and optical quality

R@D Center ATOM
(Advanced Technologies for Optical Materials)

Semiconductor Material Science Laboratory
Siberian Physico-Technical Institute at Tomsk State University

Crystals	**GaSe**	**$ZnGeP_2$**	**$CdGeAs_2$**	**Tl_3AsSe_3**
Transparency region, μm	0.7-16	2.1 2.5-8 10	2.5-16	2-17
Optical losses in transparency region, cm^{-1}	< 0.1	< 0.2< 0.1 0.2	< 0.2	< 0.1
Monocrystals size				
diameter, mm	30	30	20	40
length, mm	100	80	50	80
Nonlinear elements size, mm×mm×mm	≤ 20×20×20	≤ 15×15×25	≤ 10×10×15	-

MOLTECH Corp. (USA), EKSMA (Lithuania), ELAN (St.-Petersburg, Russia) and other.

Chronology of $ZnGeP_2$ researches in Siberian Physico-Technical Institute

1973 - 1975 - Coping the $ZnGeP_2$ technology developed in Ioffe PTI

1978 - beginning the works on development new technology of $ZnGeP_2$ growing (V.G. Voevodin)

1980 - producing large $ZnGeP_2$ single-crystal ingots of high optical quality ($\alpha < 0.1$ cm^{-1} @ 2.5 - 8.5 mkm)

1982 - 1986 - the cycle of main publications on PFC in $ZnGeP_2$ (SPTI, IAO, IGP, IAP)

1986 - 1988 transfer the $ZnGeP_2$ technology to SDB "Optika" (now IOM) together with the equipment and part of servicing staff

1990 - present - together with R&D Centre "ATOM" team-work on the solving of the following problems:
- thermodynamical calculations of $ZnGeP_2$ homogeneity region;
- clearing up the nature of defects in $ZnGeP_2$;
- search the reliable ways of reduce the optical losses in the range $\lambda < 2.5$ mkm

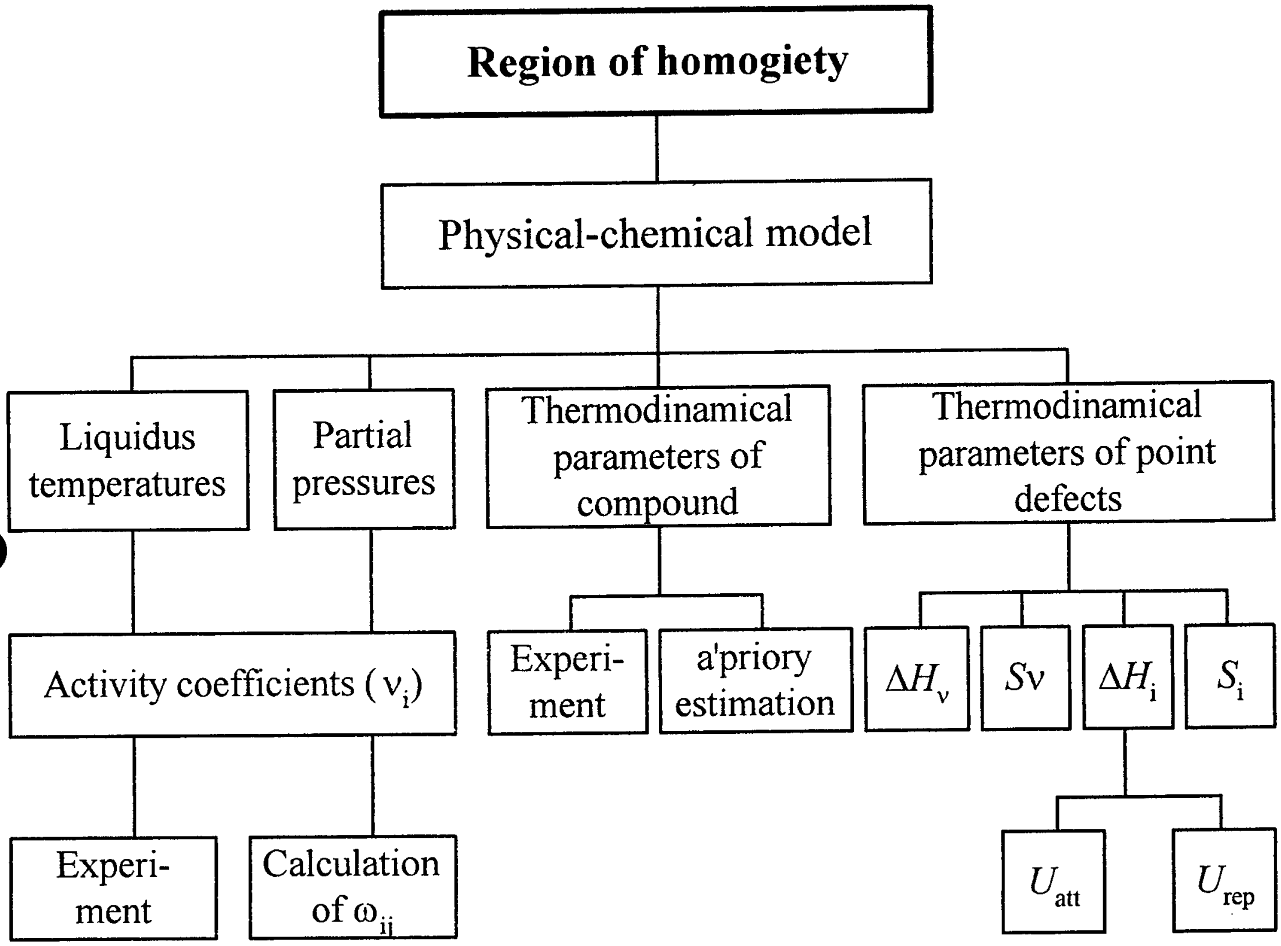
Region of homogiety
Physical-chemical model
Liquidus temperatures
Partial pressures
Thermodinamical parameters of compound
Thermodinamical parameters of point defects
Activity coefficients (ν_i)
Experi-ment
a'priory estimation
ΔH_v
$S\nu$
ΔH_i
S_i
Experi-ment
Calculation of ω_{ij}
U_{att}
U_{rep}

Table II.Entropies and enthalpies of neutral vacancies in $ZnGeP_2$

Element	Zn	Ge	P
Entropy in J/(mol K)	41.6	54.4	52.4
Enthalpy in kJ/mol	18.3	28.9	16.8

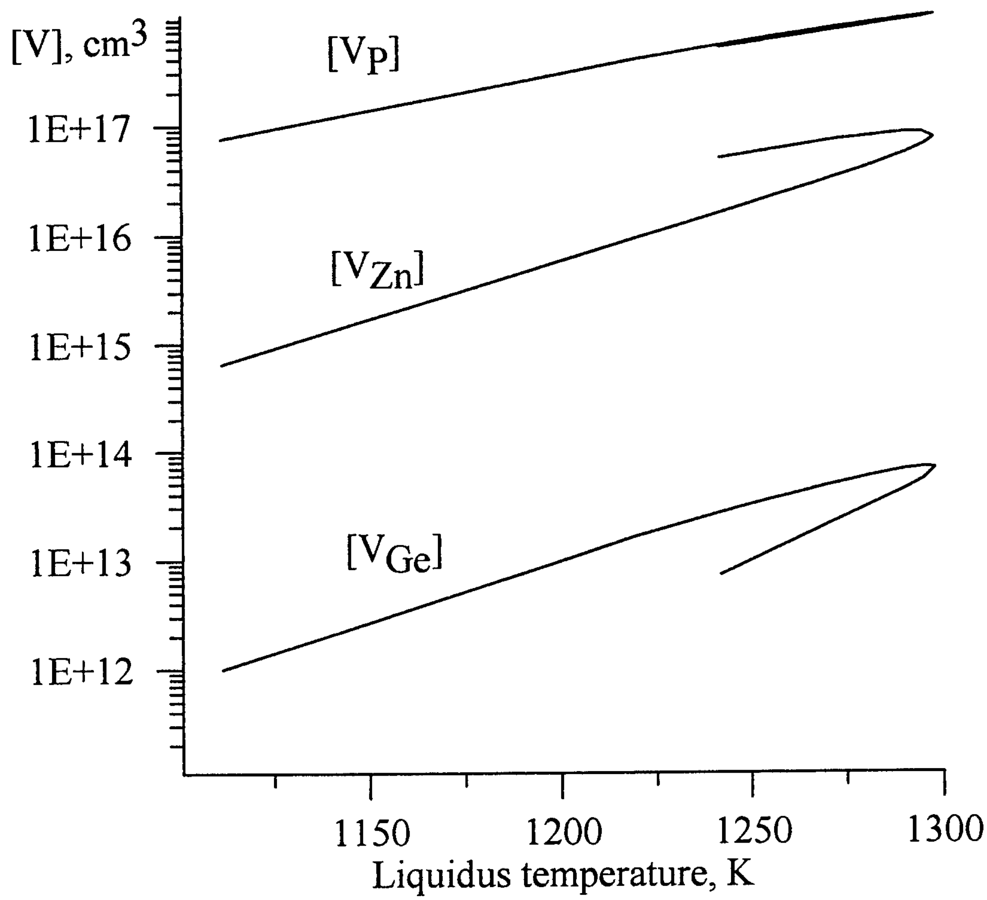

Fig. 3. The neutral vacancies concentration in $ZnGeP_2$ as a function of liquidus temperature; cut Ge - ZnP_2 .

The ionised vacancies concentrations in $ZnGeP_2$

Ionisation energy $E_{tM} = I_M(m^*/m)(z/\varepsilon + 5C/6)^2$, $C = 1/\varepsilon_0 - 1/\varepsilon$ (11)

where I_M is first ionisation potential of atom M, z is effective charge, ε is static dielectric constant, ε_0 is high-frequency dielectric constant.

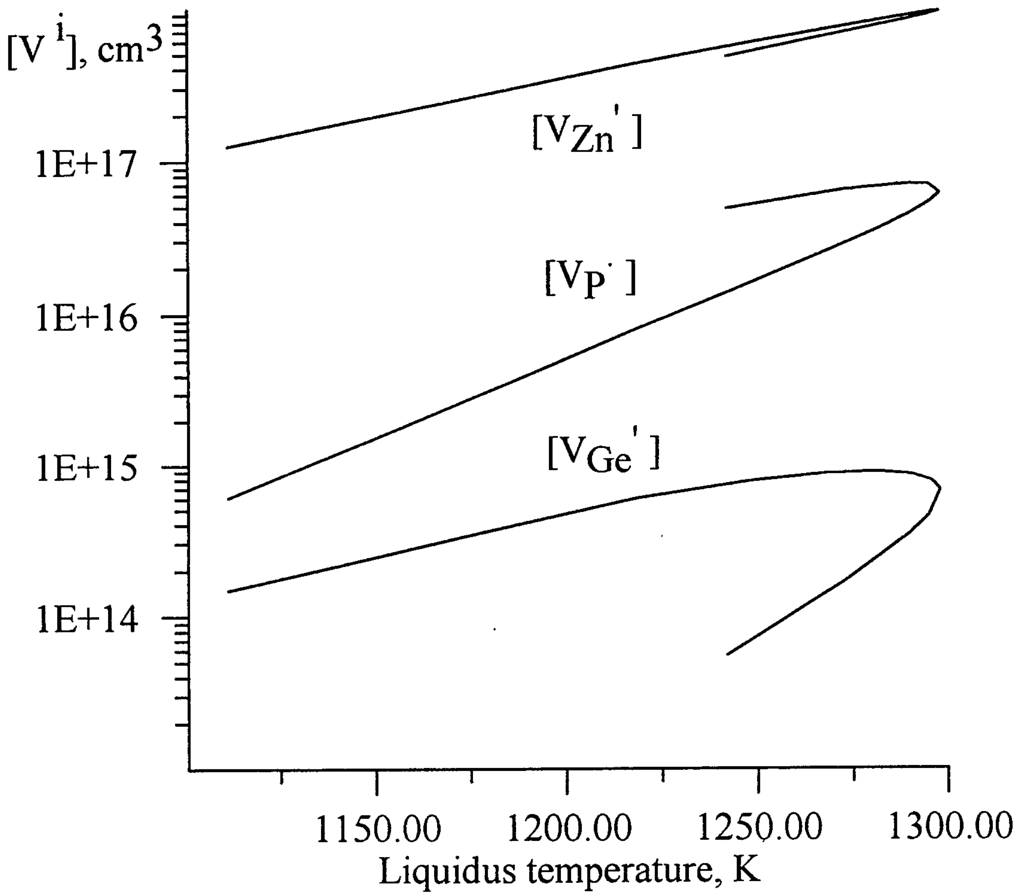

Fig. 4. The ionised vacancies concentration in $ZnGeP_2$ as a function of liquidus temperature; cut Ge - ZnP_2 .

9

Results of estimation of interstitials concentrations

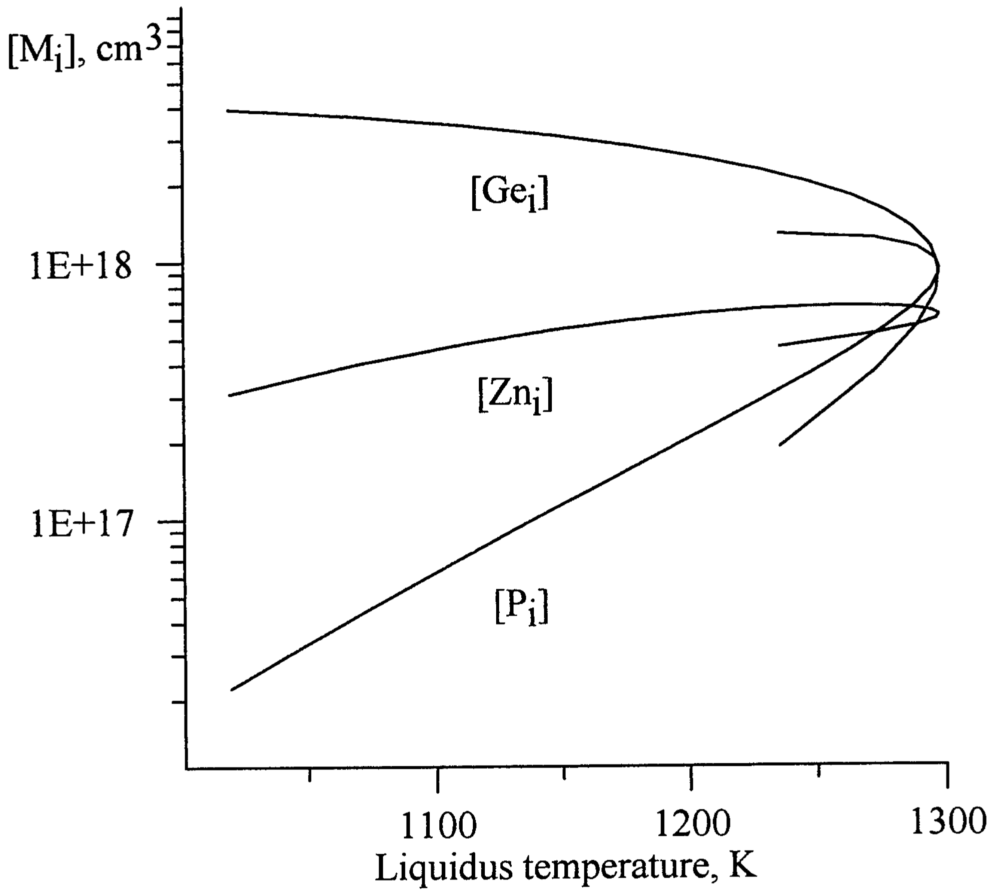

Fig. 5 Interstitials concentration in $ZnGeP_2$ as a function of liquidus temperature; Ge - ZnP_2 - cut

Results of simulation of the region of homodienity formation

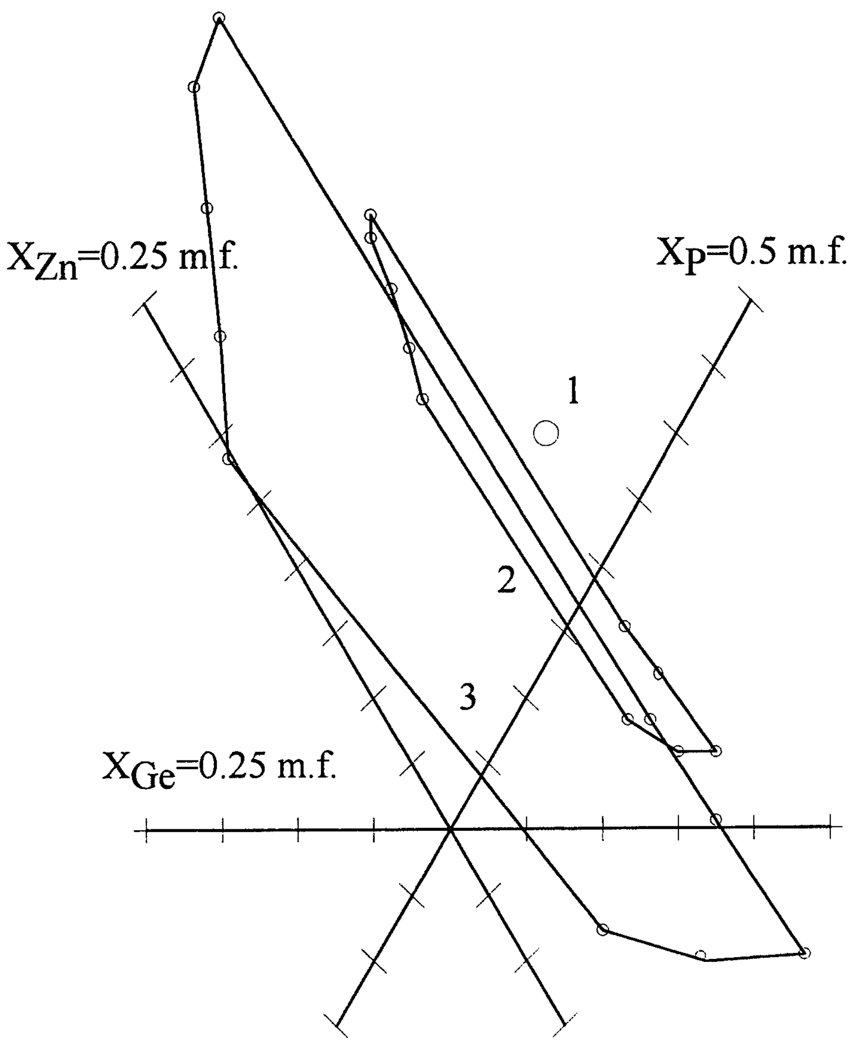

Fig. 6. $ZnGeP_2$ region of homogietity, estimated as deviation of corresponding concentrations of point defects.

T, K: 1 - 1298; 2 - 1270; 3 - 1210.

Axes correspond to
X_{Zn}=0.25 mol fractions, X_{Ge}=0.25 mol fractions, X_P=0.5 mol fractions.

Value of scale deviation is 0.0003 mol %.

Optical losses in ZGP at $\lambda < 2.5\ \mu$

Versions of main reason for the losses	A: photoionization of deep acceptors (V_{zn}?) [Brudnyi ao] B: light scattering by microinclusions of Zn and Ge [Voevodin ao] C: light scattering by β-ZGP clusters or photoionization of Zn_{Ge}-Ge_{Zn} antisite pairs [Shimony ao, J. Cryst. Growth, 198/199 (1999) 583-587

Post-growth treatment of ZGP for losses decreasing

1.	Annealing at 500-550°C	[Rud' ao]	A. B?
2.	Electron (e-) irradiation	[Brudnyi ao]	C?
3.	Laser & 1.06 μ annealing	[Voevodin ao]	B.
4.	γ-irradiation	[Shuneman ao]	A. B?
5.	Ultrasonic treatment	[Voevodin ao]	B. C?

LT-annealing of ZGP crystals

Sample #	As-grown α, cm^{-1} (λ=2.5 μ)	As-grown α, cm^{-1} (λ=5 μ)	As-grown N_d, cm^{-2}	Condition of LTA	Annealed α, cm^{-1} (λ=2.5 μ)	Annealed α, cm^{-1} (λ=5 μ)	Annealed N_d, cm^{-2}
187	0.5	0.3	10^6	550°C 150 h ZGP powder	0.2	0.01	$3\cdot10^5$
165	1.0	0.7	$5\cdot10^4$	550°C 150 h 2 at P_4	0.3	0.07	10^5
282	0.8	0.3	10^5	550°C 150 h 1.3 at P_4	0.3	0.1	$8\cdot10^4$
273	1.8	1.8	$5\cdot10^4$	550°C 150 h 2 at P_4	0.05	0.04	$3\cdot10^4$

Ultrasonic treatment of ZGP crystals

Sample #	As-grown α, cm^{-1} (λ=2.5 μ)	As-grown α, cm^{-1} (λ=5 μ)	As-grown N_d, cm^{-2}	As-grown N_i, cm^{-2}	After treatment α, cm^{-1} (λ=2.5 μ)	After treatment α, cm^{-1} (λ=5 μ)	After treatment N_d, cm^{-2}	After treatment N_i, cm^{-2}
188	1.8	1.8	10^5	$2\cdot10^2$	1.3	1.3	$7\cdot10^4$	10^2
306	0.8	0.6	$6\cdot10^4$	$2\cdot10^3$	0.5	0.4	$4\cdot10^4$	10^3

Absorption coefficient of $ZnGeP_2$ at wavelength $\lambda = 1.06$ mcm versus energy density of pulsed laser radiation ($\tau = 1$ ms)

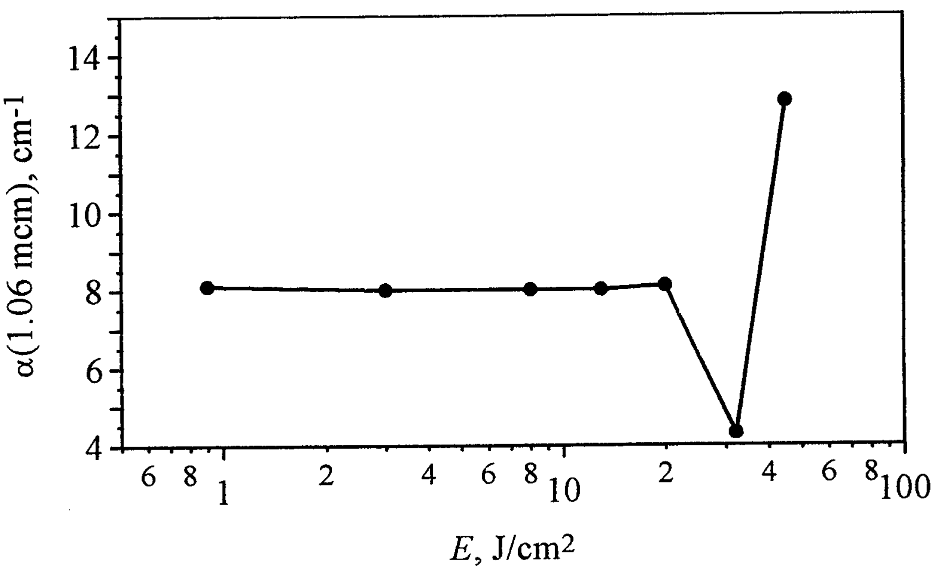

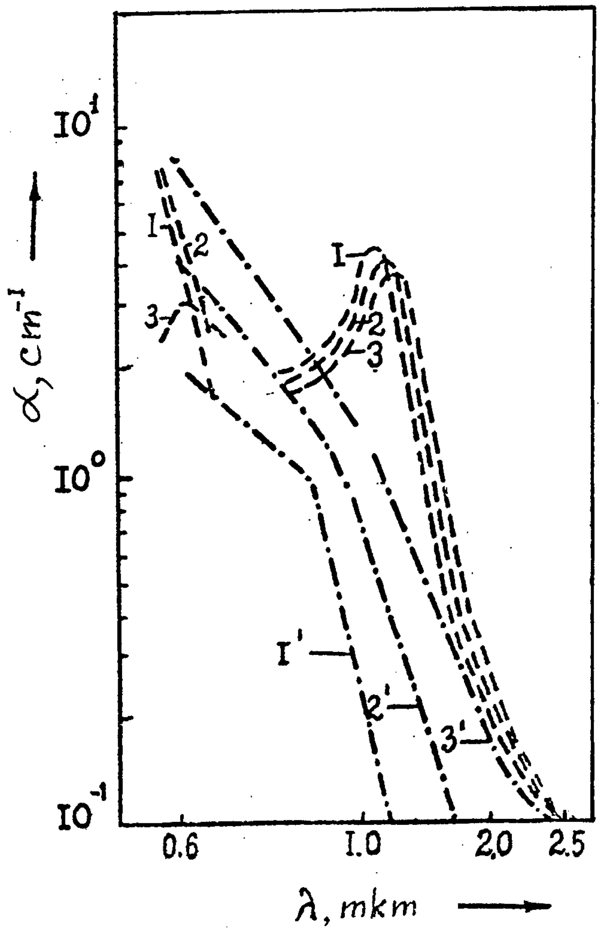

Calculated spectra of light losses in $ZnGeP_2$ with microinclusions of Zn (1-3) and Ge (1'-3').

Diameter of inclusions is : 1, 1' - 200 Å; 2, 2' - 400 Å; 3, 3' - 600 Å; Volume fraction is $C=10^{-6}$

LASER@1.06μ ANNEALING MODEL

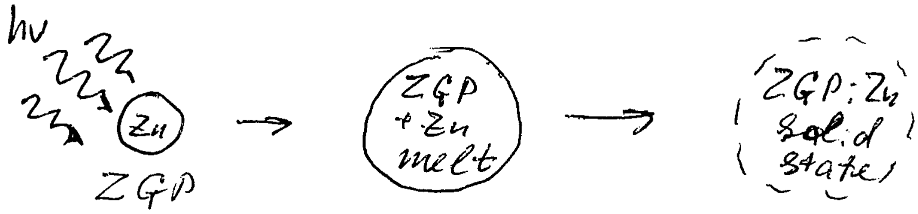

LT(550°C)-ANNEALING MODEL

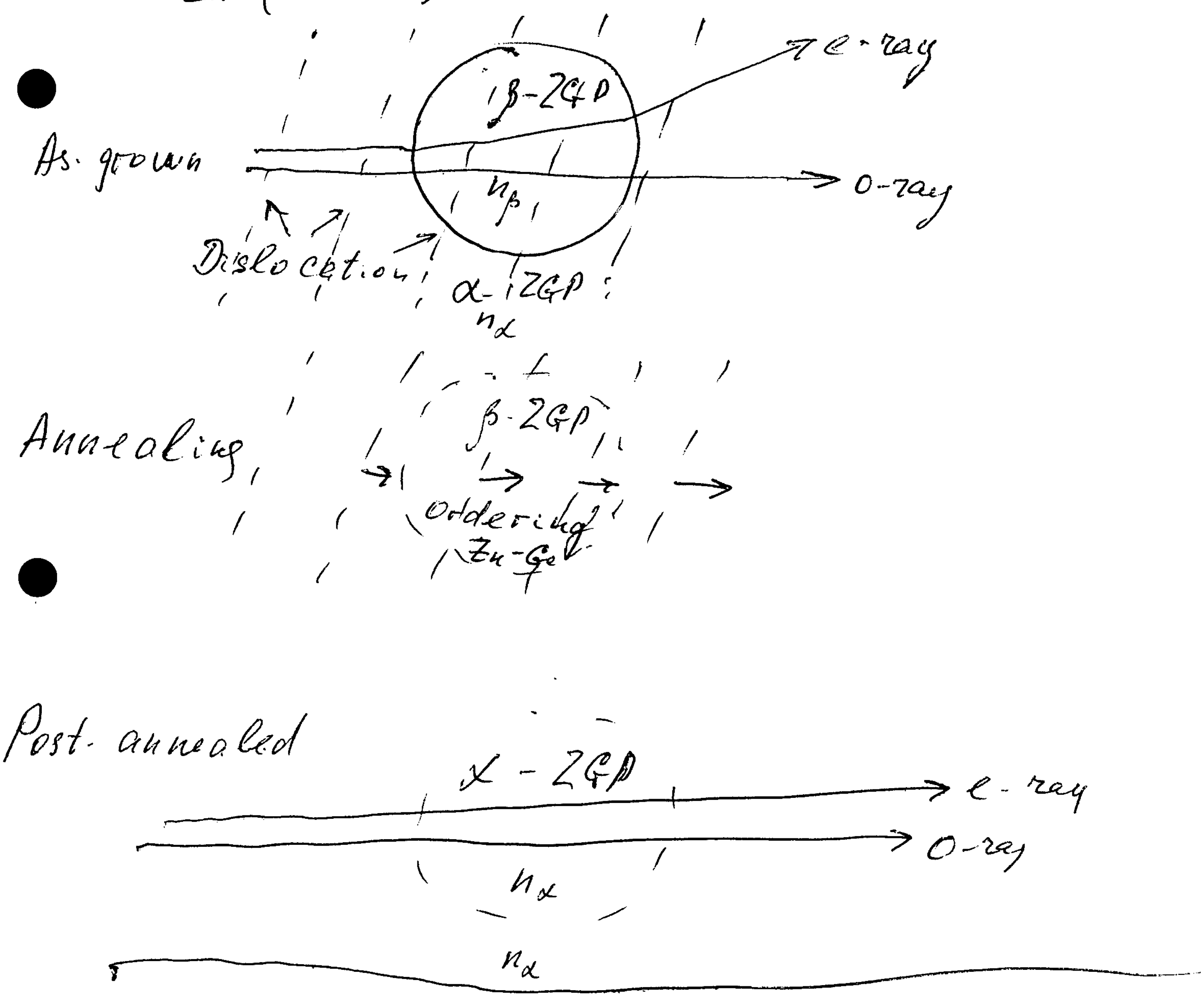

C-LINE #62013
CLEAR TOPPER

SIMS Analysis of $CdGeAs_2$

J. S. Solomon*
University of Dayton Research Institute
Dayton, OH 45469-0167
USA

* Work supported by the Materials and Manufacturing Directorate
Air Force Research Laboratory, United States Air Force

UDRI
UNIVERSITY of DAYTON

C-LINE #62013
CLEAR TOPPER

Main Features of SIMS

POSITIVE:

- Information depth in the "monolayer range"
- Detection of all elements and isotopes
- Extremely high elemental sensitivity for many elements
- Quantitative (with standards)

NEGATIVE:

- Large differences in sensitivity for many elements
- No unified model to explain process.
- Process highly dependent on
  - Instrumental Parameters
  - Matrix composition
- Quantification difficult in mixed matrixes
- Destructive

UDRI
UNIVERSITY of DAYTON

10 keV $O_2 \rightarrow CdGeAs_2$

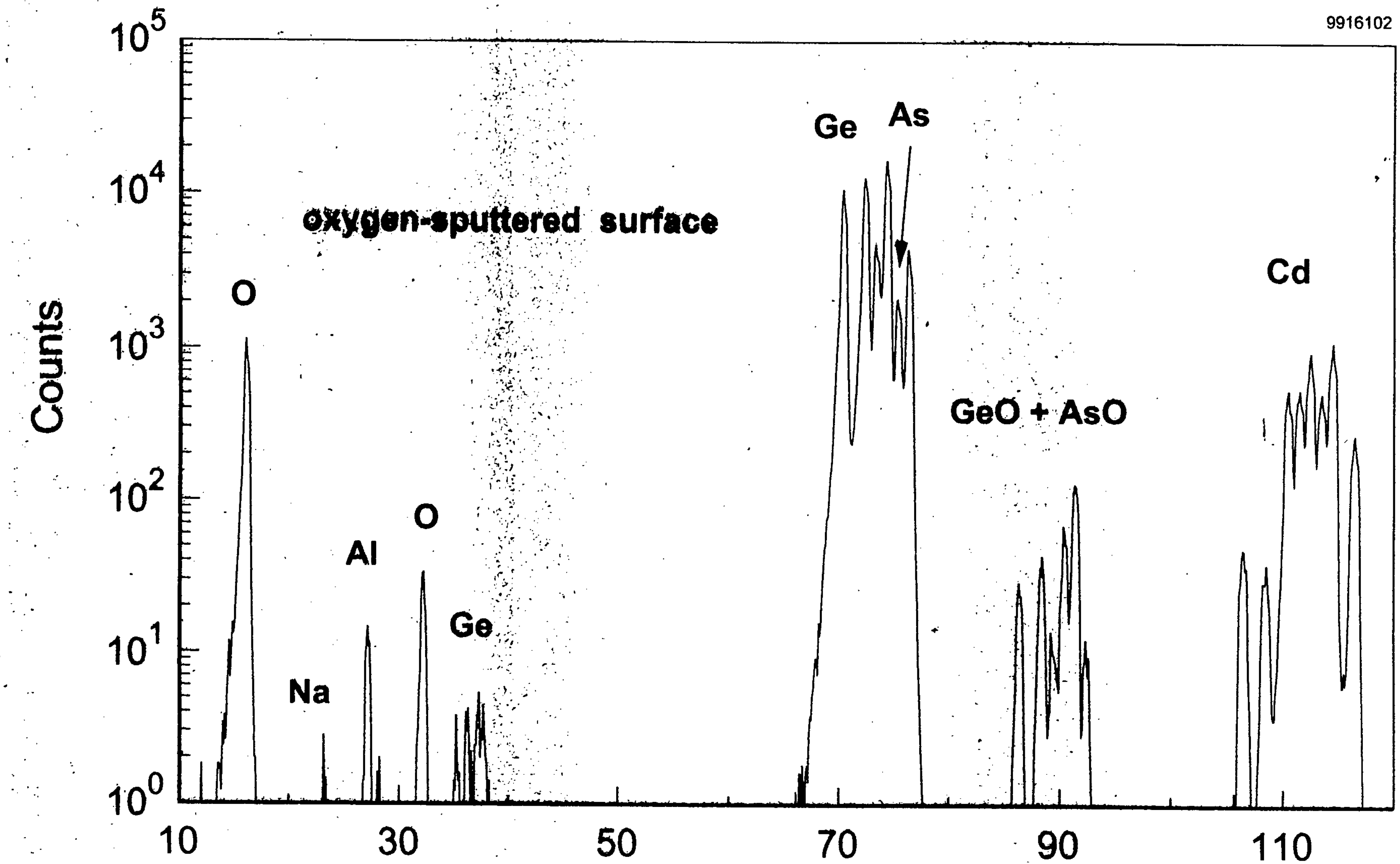

SIMS Analysis of ZnO

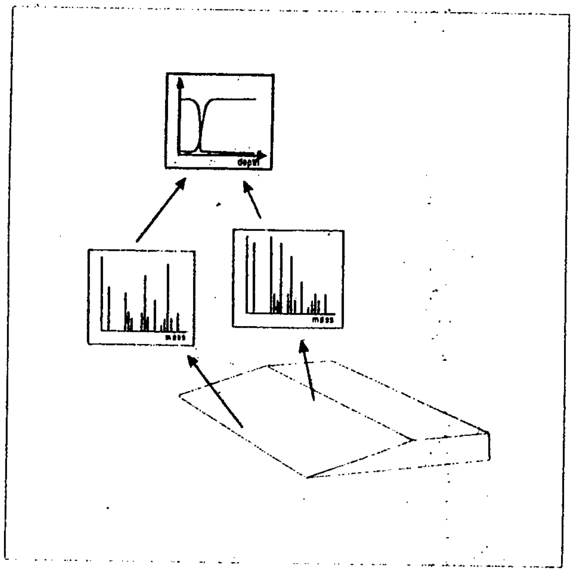

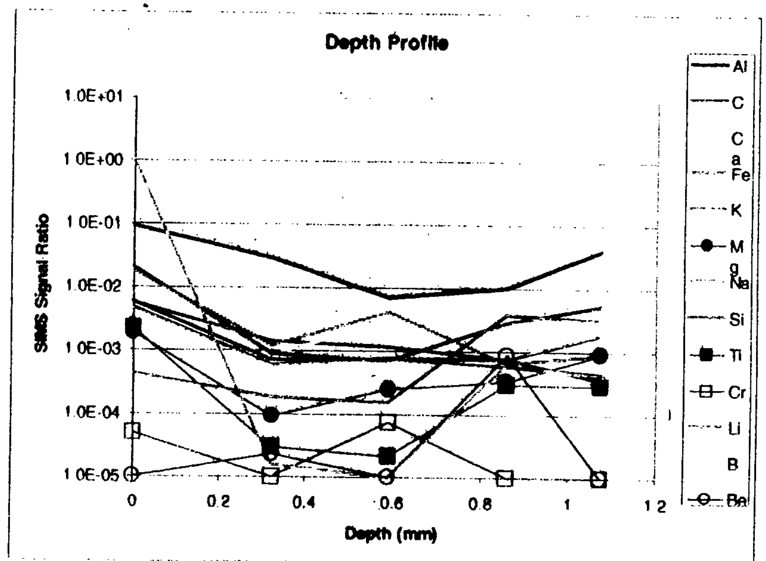

UDRI UNIVERSITY of DAYTON RESEARCH INSTITUTE

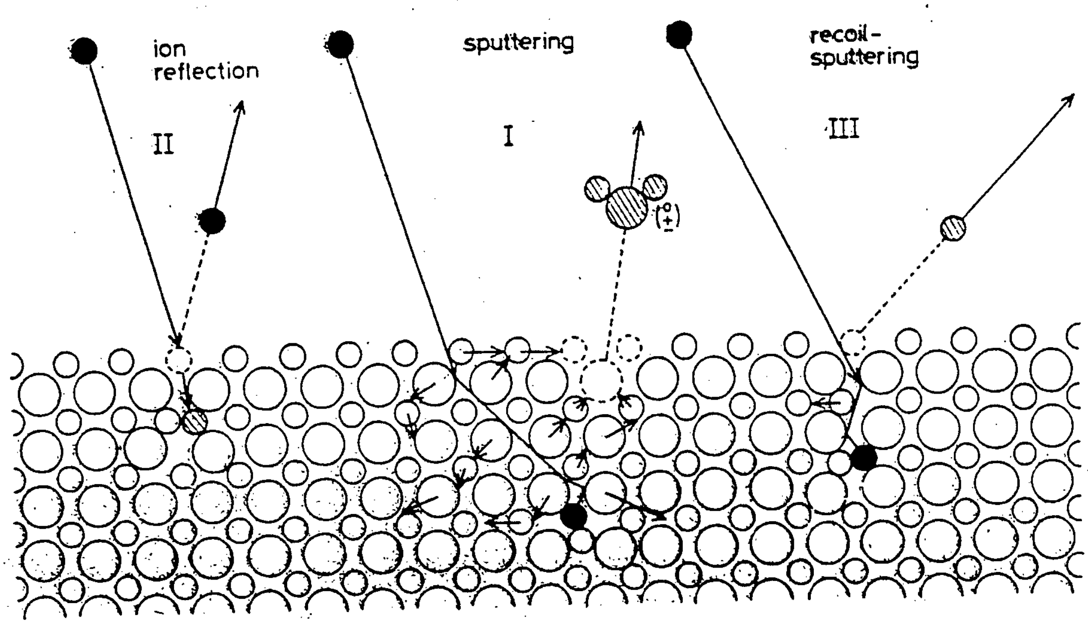

C-LINE #62013
CLEAR TOPPER

Materials and Manufacturing Directorate
Sensor Materials Branch *AFRL/MLPO*

Refractive Indices of Zinc Germanium Phosphide from 2-9 Microns and Implications for Phase Matching in Optical Parametric Oscillators

David E. Zelmon, David L .Small, and

Peter G. Schunemann

Refractive Indices-ZGP
DAve S + me-9/9/99

y = sqrt(m1+m2*m0^ 2/(m0^ 2-...		
ne	Value	Error
m1	6.33463522	3.42104
m2	3.61682203	3.41727
m3	0.21868451	0.1938097
m4	0.416037956	0.07730434
m5	288.432653	35.65936
Chisq	3.16616005e-07	NA
R	0.999954035	NA

y = sqrt(m1+m2*m0^ 2/(m0^ 2-...		
no	Value	Error
m1	6.16504	5.270687
m2	3.55150249	5.265372
m3	0.206686029	0.2885603
m4	0.496664015	0.1568017
m5	314.934657	69.0479
Chisq	1.24995736e-06	NA
R	0.999829382	NA

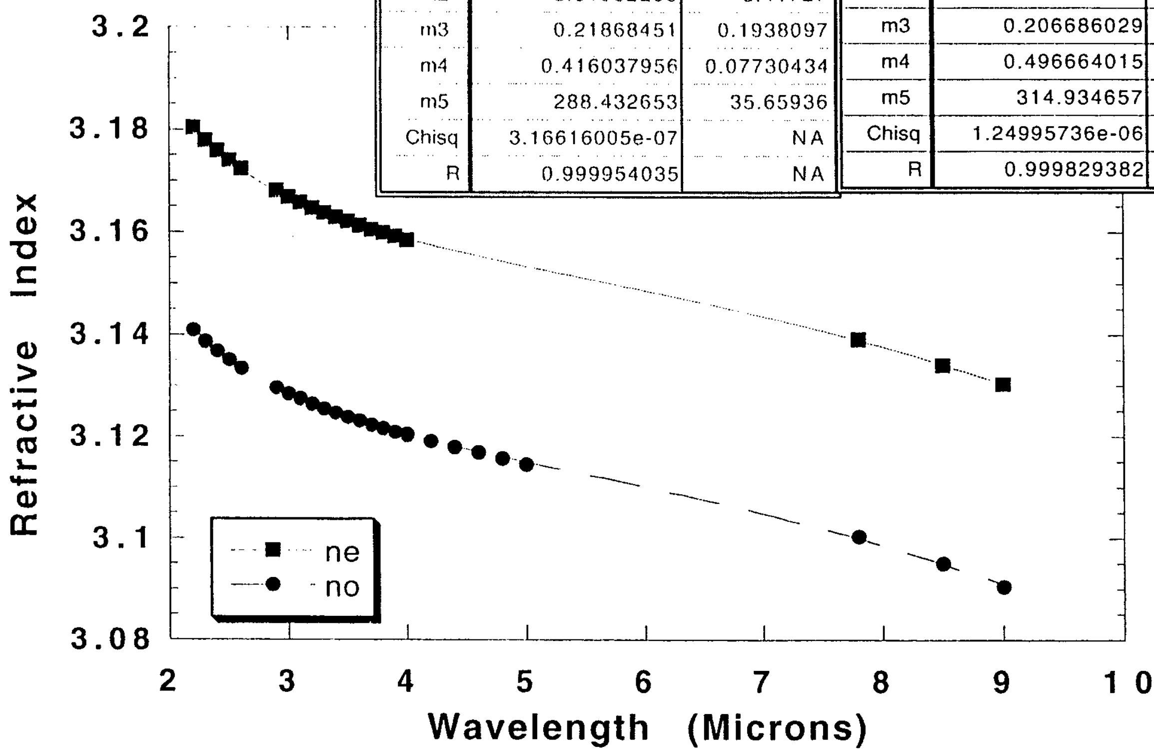

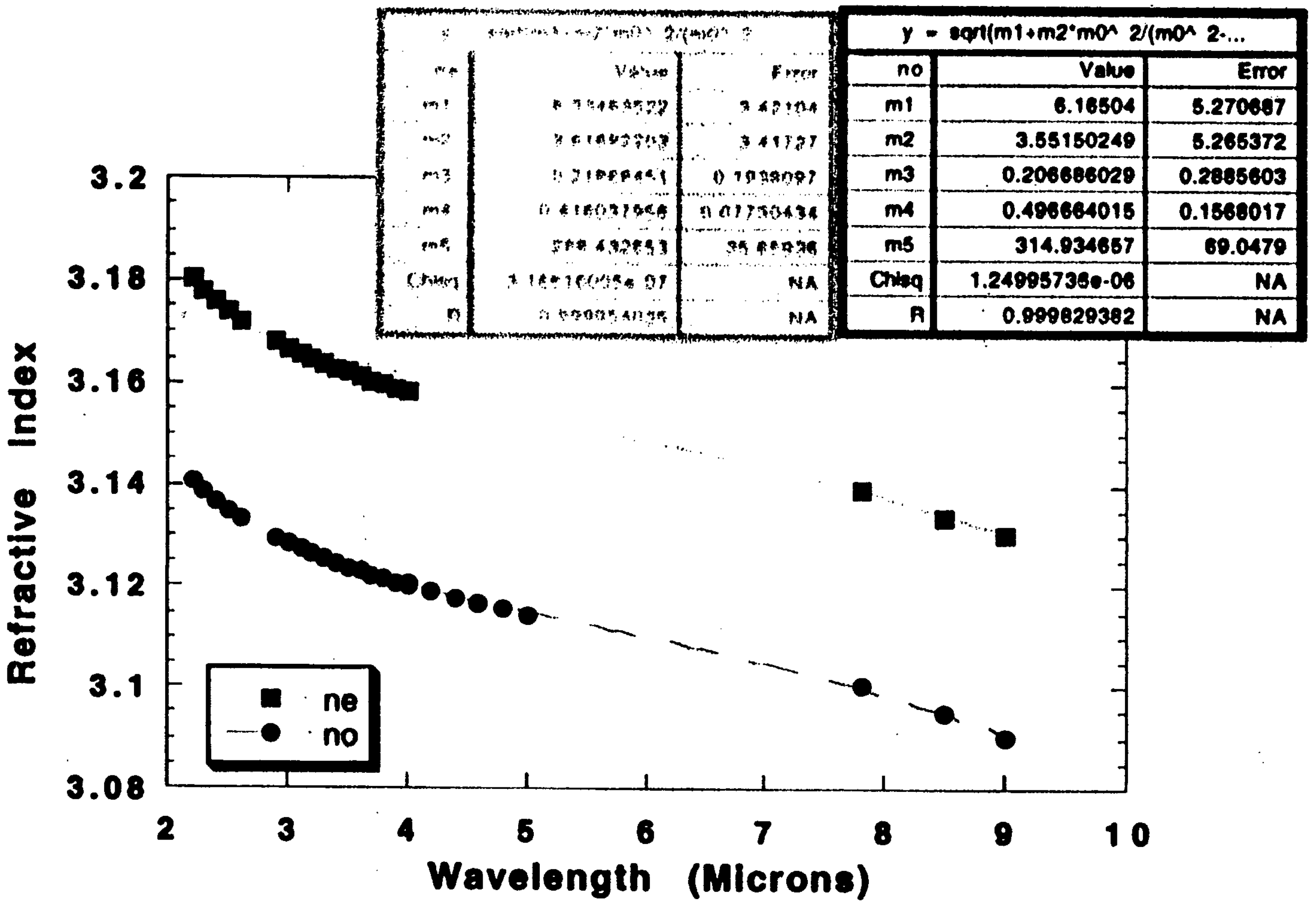
y = sqrt(m1+m2*m0^ 2/(m0^ 2-...
no | Value | Error
m1 | 6.16504 | 5.270687
m2 | 3.55150249 | 5.265372
m3 | 0.206686029 | 0.2885603
m4 | 0.496664015 | 0.1568017
m5 | 314.934657 | 69.0479
Chisq | 1.24995736e-06 | NA
R | 0.999829382 | NA
ne
no
Refractive Index
3.2
3.18
3.16
3.14
3.12
3.1
3.08
2
3
4
5
6
7
8
9
10
Wavelength (Microns)

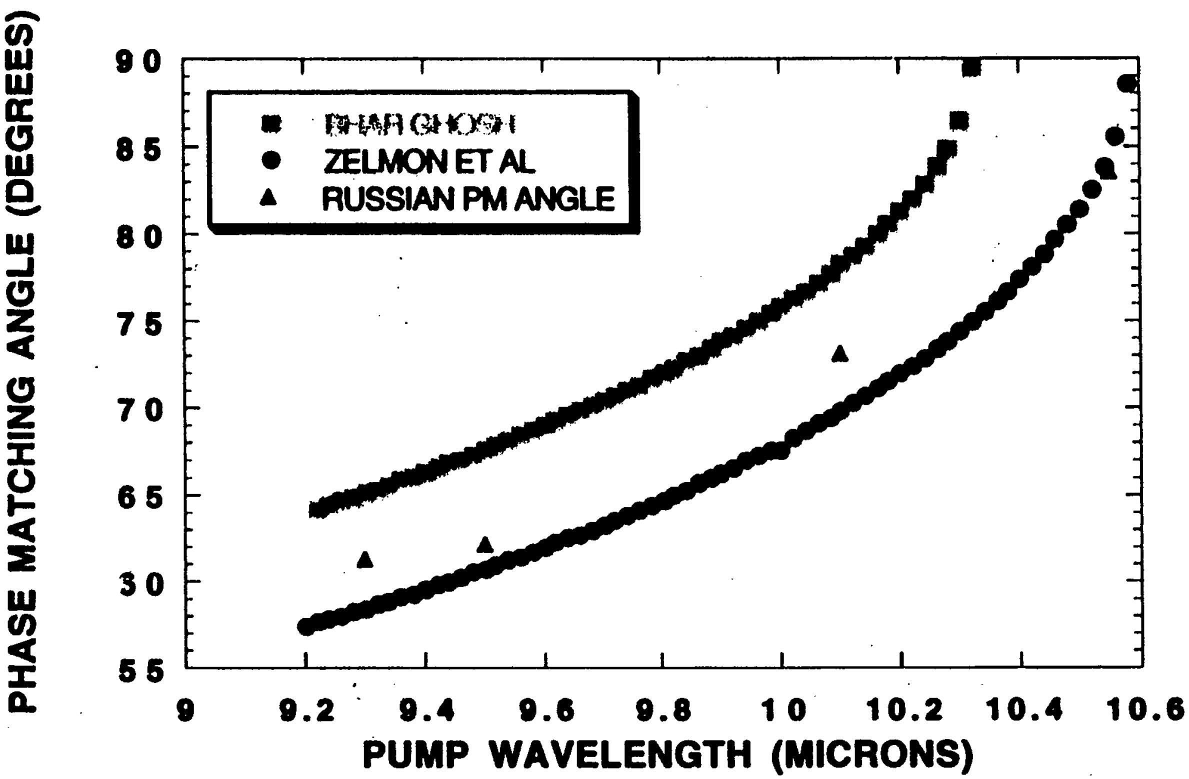
BHAR GHOSH
ZELMON ET AL
RUSSIAN PM ANGLE
PHASE MATCHING ANGLE (DEGREES)
90
85
80
75
70
65
30
55
9
9.2
9.4
9.6
9.8
10
10.2
10.4
10.6
PUMP WAVELENGTH (MICRONS)

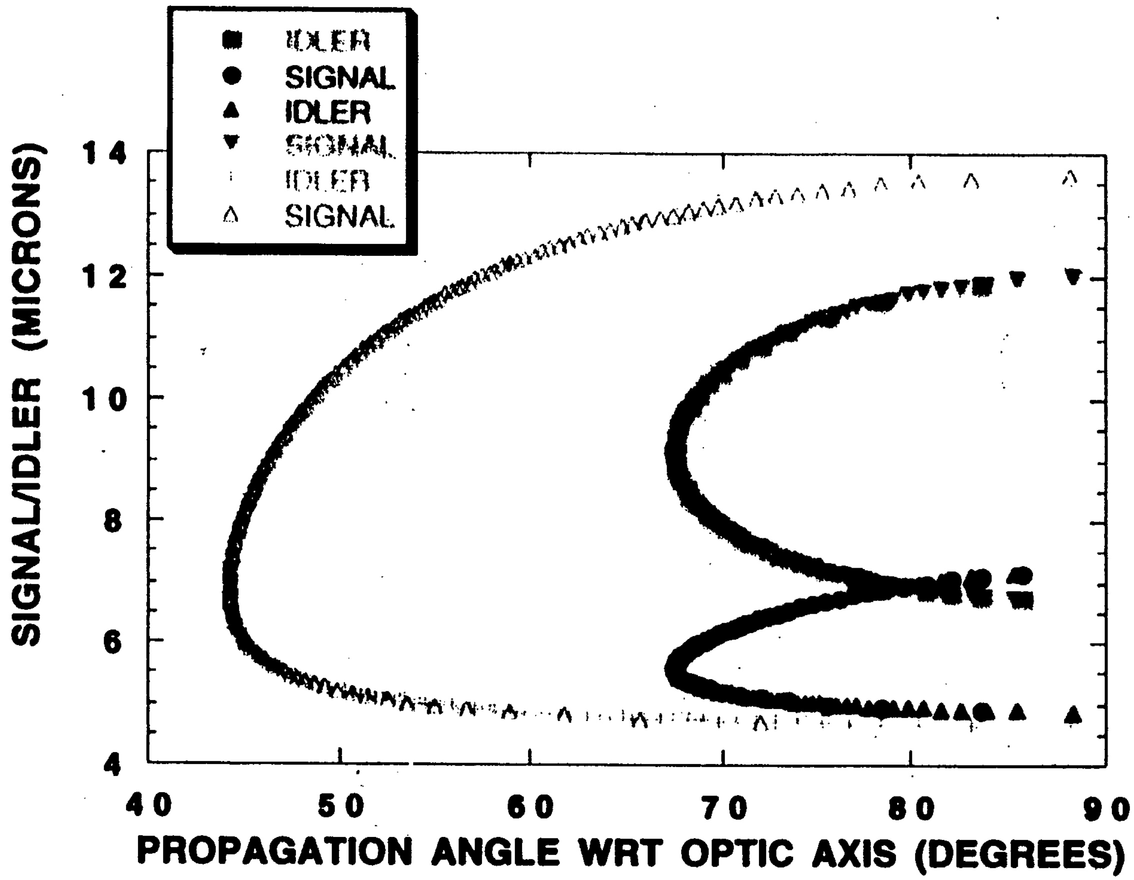
IDLER
SIGNAL
IDLER
SIGNAL
IDLER
SIGNAL
SIGNAL/IDLER (MICRONS)
4
6
8
10
12
14
40
50
60
70
80
90
PROPAGATION ANGLE WRT OPTIC AXIS (DEGREES)

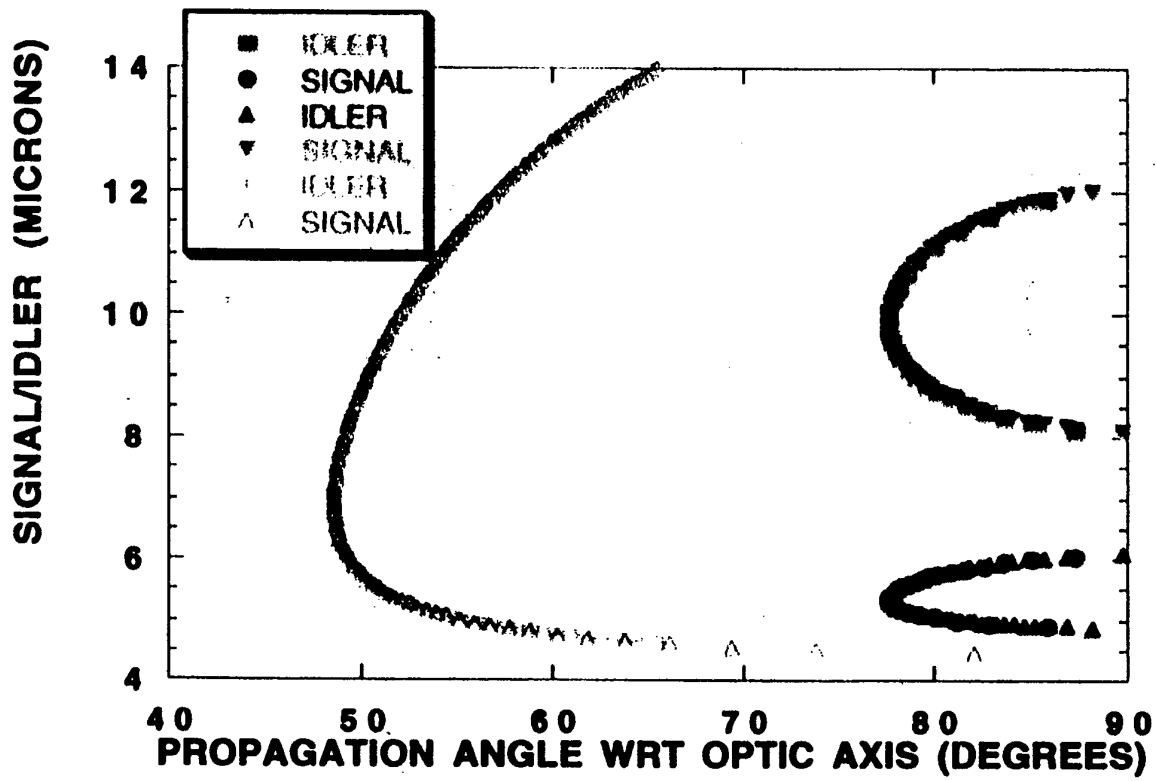
IDLER
SIGNAL
IDLER
SIGNAL
IDLER
SIGNAL
SIGNAL/IDLER (MICRONS)
14
12
10
8
6
4
40
50
60
70
80
90
PROPAGATION ANGLE WRT OPTIC AXIS (DEGREES)

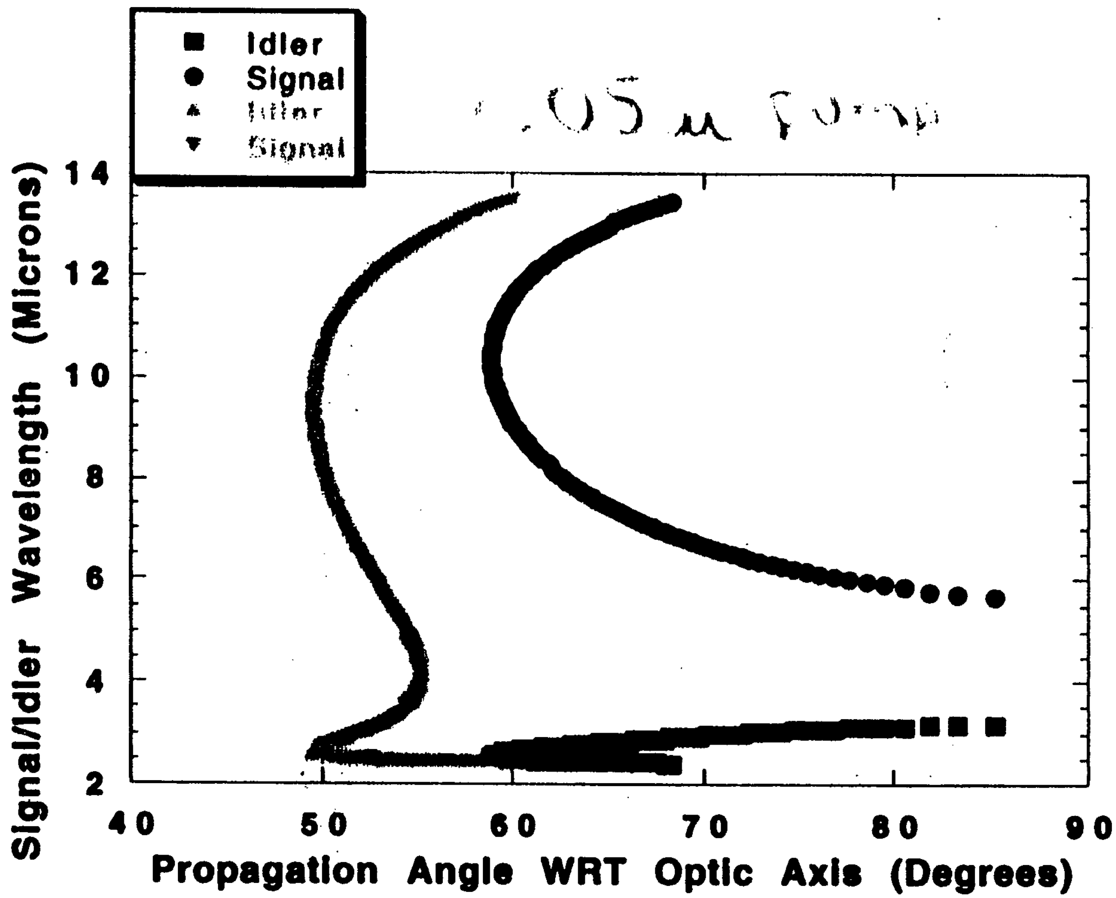
Idler
Signal
Idler
Signal
Signal/Idler Wavelength (Microns)
Propagation Angle WRT Optic Axis (Degrees)
2
4
6
8
10
12
14
40
50
60
70
80
90

Analysis of $CdGeAs_2$ using thermal admittance spectroscopy

Steven Smith

University of Dayton Research Institute

UDRI UNIVERSITY of DAYTON RESEARCH INSTITUTE

Principles of TAS

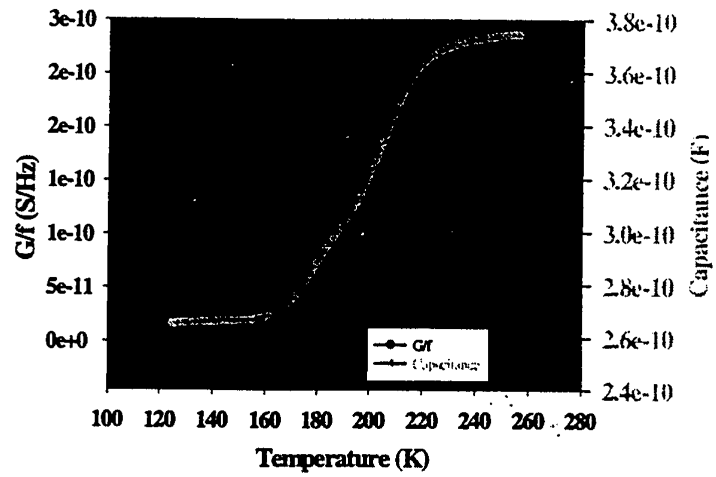

Thermal Admittance Spectroscopy (TAS) measures the response of a Schottky diode as a function of frequency and temperature. The resulting peaks in the conductance spectrum, or inflection points in the capacitance spectrum, can be used to determine the thermal activation energy(s) of the defects (impurities). Both spectra are shown in this slide.

UDRI
UNIVERSITY of DAYTON RESEARCH INSTITUTE

CGA5600a (4Q)

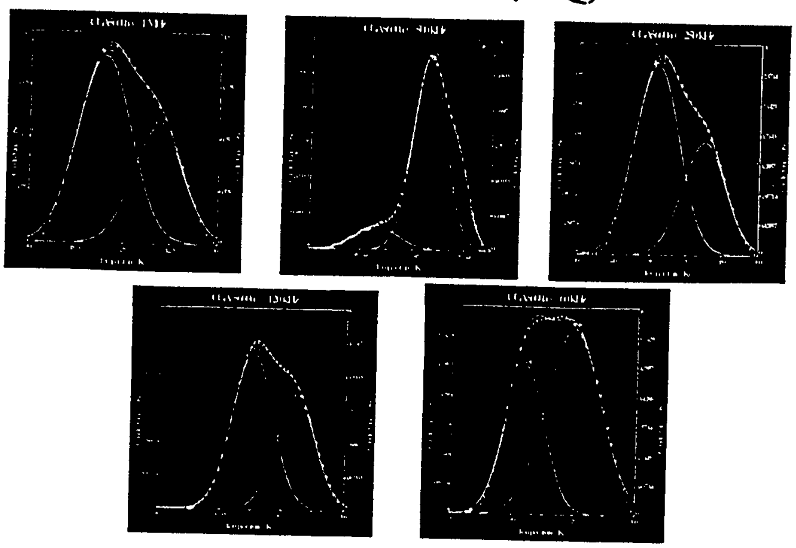

Fitting the peak in the TAS spectrum of specimen 5600 (4Q) demonstrates that more than one defect is responsible for the peak. The evolution of the shape demonstrates the relative response of the defects as a function of frequency.

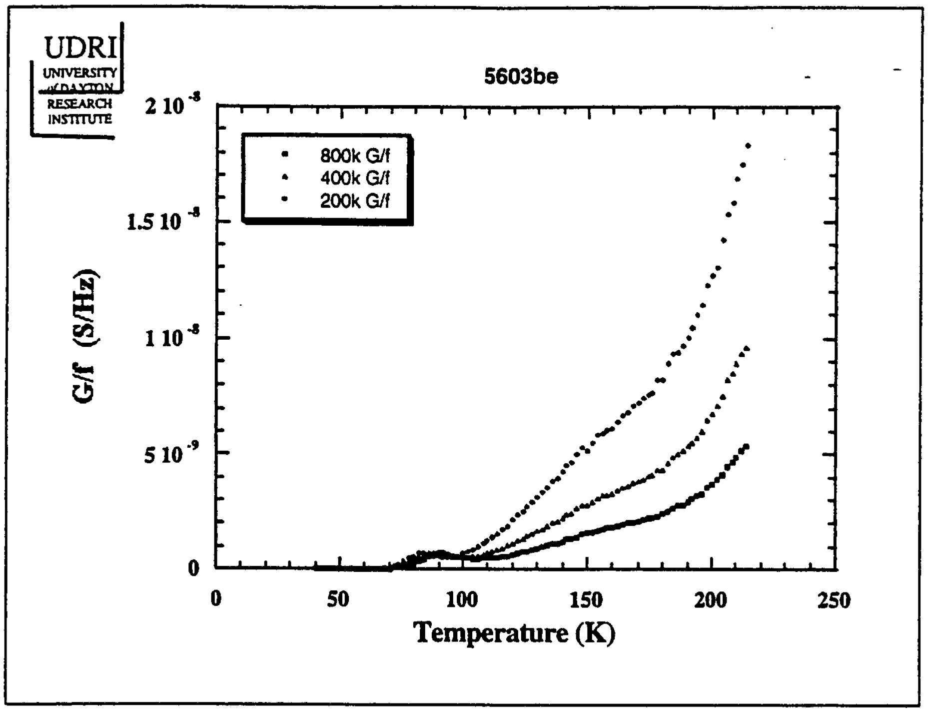

TAS spectra of specimen 5603 (4N) differs significantly from those of 5600 and 5601. A deeper level is evidenced by the broad 'bump' in the spectra around 150 K.

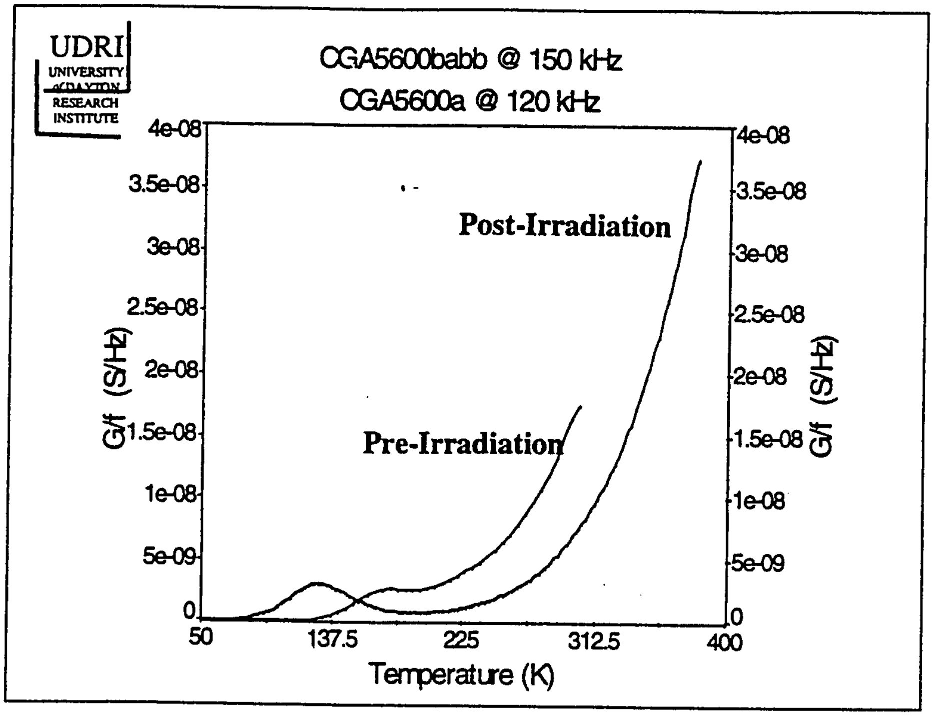

Comparison of the TAS spectra before and after electron irradiation of specimen 5600. A slight shift to lower energy is noted by the postion of the peak in the post-irradiation spectrum.

UK UNCLASSIFIED

High rep rate Tandem OPO

NLO Materials Workshop

20 - 21 September 1999
DERA Malvern

J A C Terry

© Crown copyright 1999. Published with the permission of the Defence Evaluation and Research Agency on behalf of the Controller of HMSO

DERA

Experimental - 3

- 1 μm Nd:YAG pump laser
- CEO - commercial
- ~1 kHz operation

- unreliable
- spec 18 W
- now < 8 W

- to be repaired and rebuilt

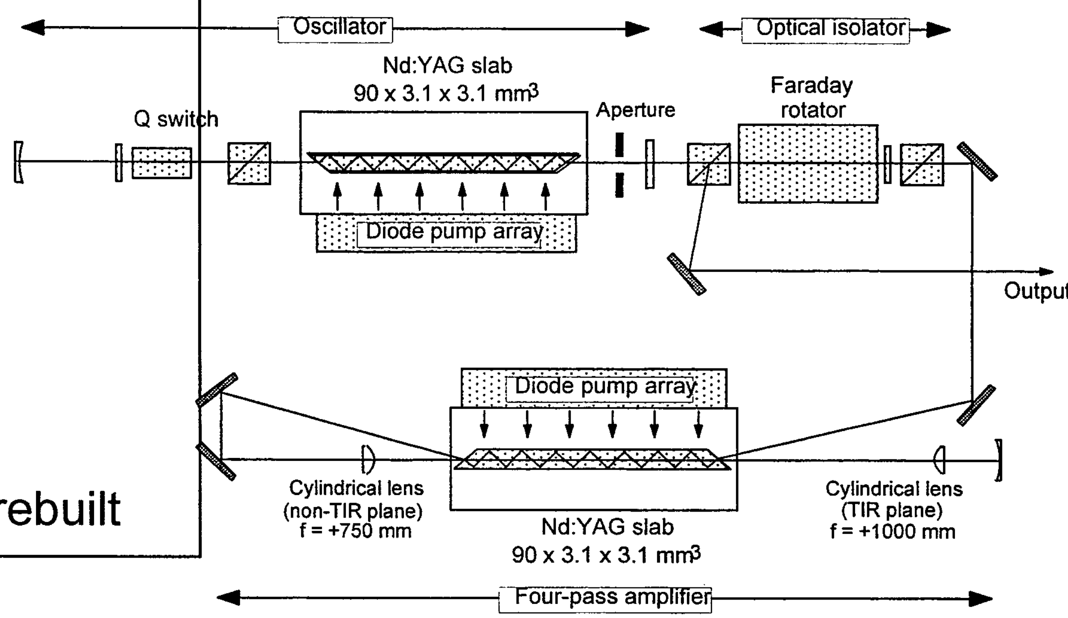

Experimental - 4

⌘ 1st OPO - wavelength doubler (3 KTP crystals)

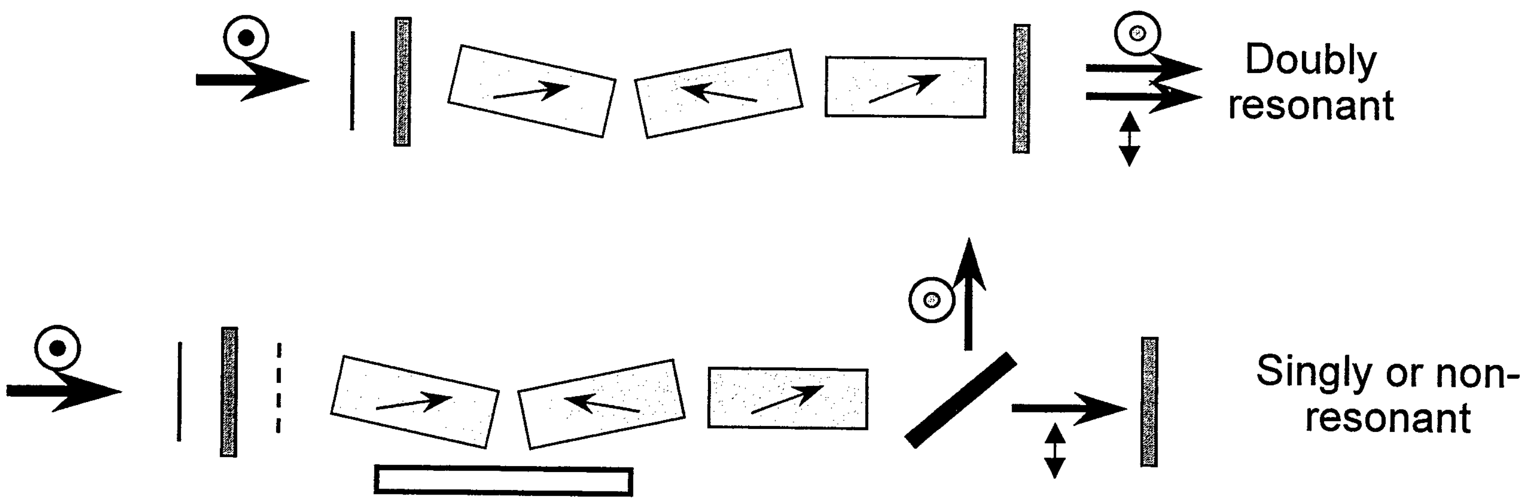

DERA

Experimental - 5

- ⌘ WD power and efficiences
  - ⌘ Doubly resonant
    - ⌘ 2.2 W (both polarisations)
    - ⌘ P_{th} - 3.9 W, s.e. - 45 %, σ - 7 %
  - ⌘ Singly resonant
    - ⌘ 2.3 W (‘single’ polarisation)
    - ⌘ P_{th} - 3.7 W, s.e. - 36 %, σ - 11 %
  - ⌘ Non-resonant
    - ⌘ 2.4 W (‘single’ polarisation)
    - ⌘ P_{th} - 4.5 W, s.e. 44 %, σ - 14 %
- ⌘ Beam quality
  - ⌘ M^2 ~ ~~1.5 x 2.3 (be~~tter in walk-off plane)

DERA

Experimental - 6

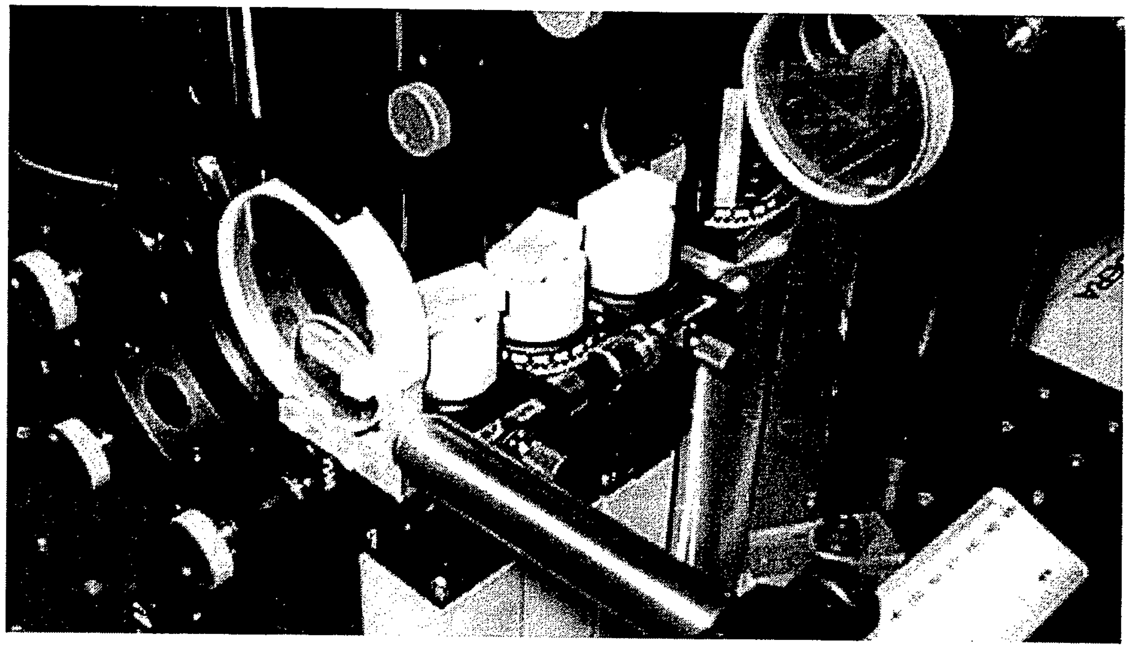

DERA

Experimental - 7

- ⌘ DERA ZGP crystal
  - ⌘ 6.5 x 6.5 x 18 mm^3
  - ⌘ nominally $\theta = 53$, $\phi = 0$
  - ⌘ actually $\theta = 90$, $\phi = 53$
  - ⌘ AR coated
    - ⌘ 2.1, 3.5-4.0 μm

Polarised transmission of coated ZGP sample VB34/2/2/2/3

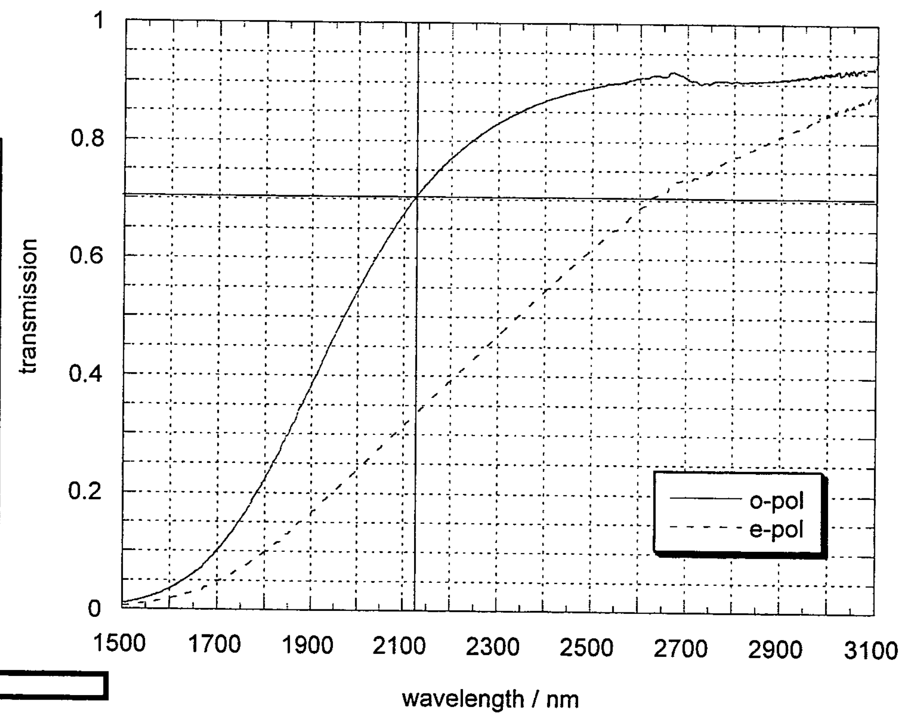

Experimental - 8

- ⌘ ZGP phasematching
  - ⌘ type I - generated waves both have same polarisation plane
  - ⌘ type II - generated waved have orthogonal polarisation planes

Type I phasematching for 2128 nm pumped ZGP ($\phi = 0$)

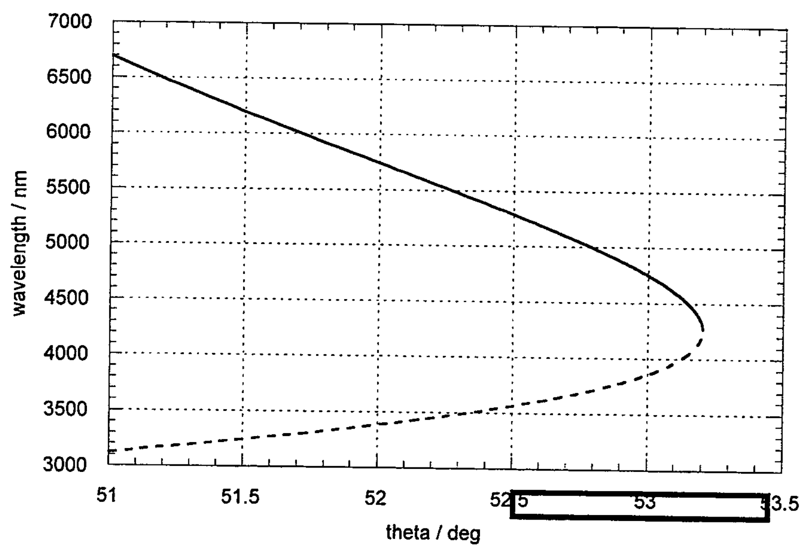

Type II phasematching for 2128 nm pumped ZGP ($\theta = 90$)

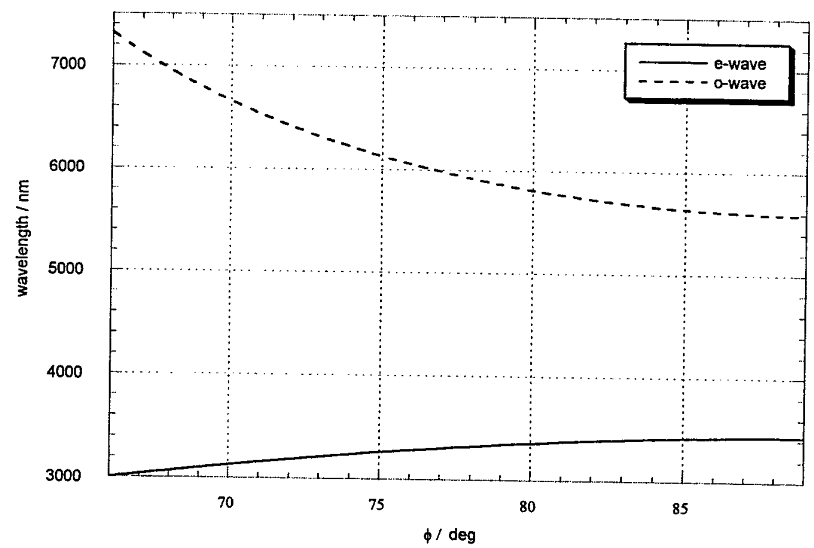

DERA

Experimental - 9

- ⌘ Ouput power, slope efficiency and threshold
  - ⌘ v incident power
    - ⌘ P_{th} ~ 350 mW
    - ⌘ s.e.
      - ⌘ total ~ 16.5 %
      - ⌘ signal ~ 10 %
      - ⌘ idler ~ 6.5 %
  - ⌘ v unabsorbed power
    - ⌘ P_{th} ~ 250 mW
    - ⌘ s.e.
      - ⌘ total ~ 23.5 %
      - ⌘ signal ~ 14.5 %
      - ⌘ idler ~ 9 %
- ⌘ Maximum out~~put ~ 100 m~~W for ~ 900 mW incident (2 μm)

Output powers v incident WD pump

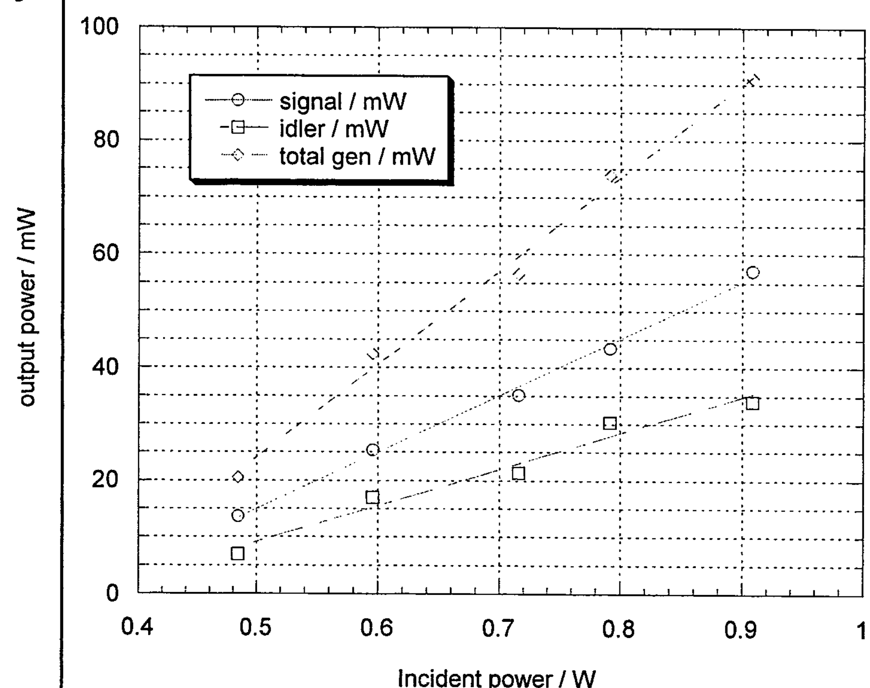

DERA

Experimental - 10

- Signal - 3.4 μm
  - $M^2 \sim 2.4$

- Idler - 5.7 μm
  - $M^2 \sim 4.8$

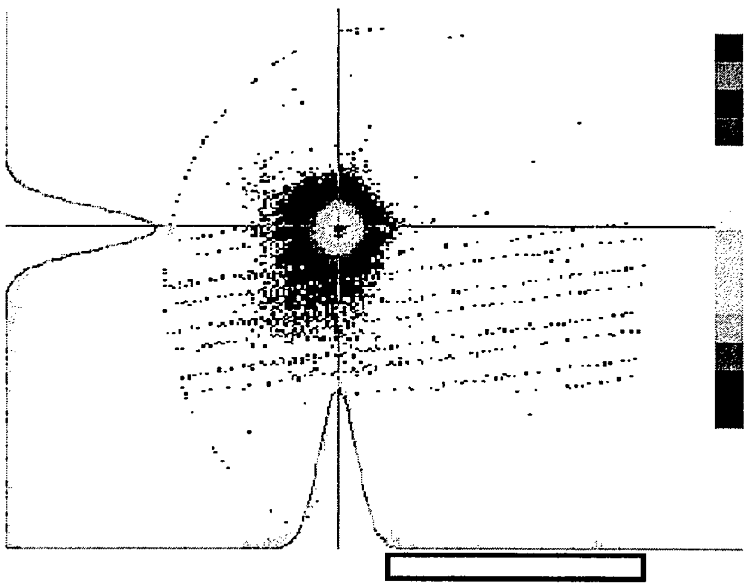

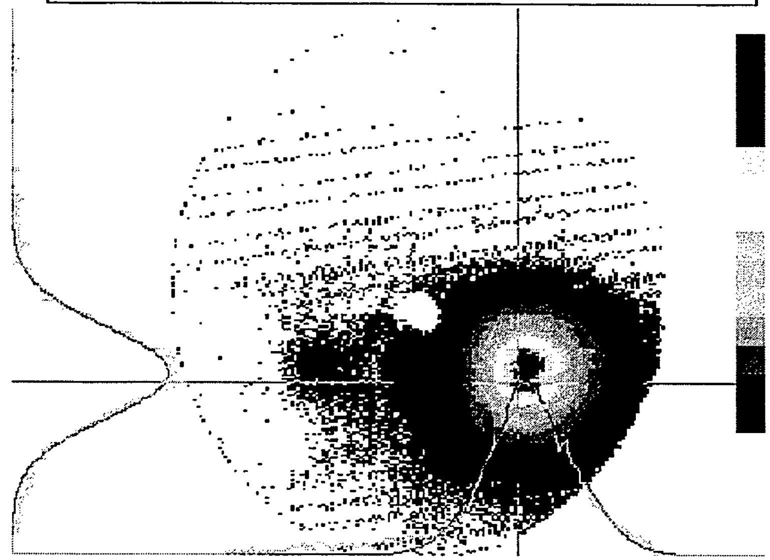

DERA

Summary

- ⌘ Operation of a tandem OPO system has been demonstrated at ~1 kHz rep rate
- ⌘ Device (wavelength doubler) with bulk NLO material demonstrated to operate with ~ 10 mJ energy per pulse
- ⌘ Demonstration of the utility of DERA ZGP
  - ⌘ In this case wrongly orientated, but reasons for this understood
- ⌘ Target of 1 W in band 4 not met
  - ⌘ Further experiments required to understand the limitations of this technology, especially thermal effects

DERA

Recent Advances in Chalcopyrites for Mid- to Far-IR Frequency Conversion

P. G. Schunemann and T. M. Pollak

SANDERS
A Lockheed Martin Company

Presented at the 1999 Nonlinear Optical Materials Workshop, (NLO 99), DERA, Malvern, UK, Sept. 20, 1999

Work supported L.N. Durvasula at DARPA (via the Air Force Research Laboratory Materials Directorate contract No. F33615 -94-C-5415) and Sanders Internal R&D Funding

Chalcopyrite Crystal Growth at Sanders

- For the past 10 years we have focused on crystal growth and processing of bulk chalcopyrites for nonlinear optical (NLO) frequency conversion:
  - Frequency doubling of CO_2 Lasers (SHG)
  - "Wavelength doubling" of 2um solid state lasers (OPO)
- The Goal:
  - Produce efficient mid-IR lasers operating in regions of high atmospheric transmission
- Applications:
  - Laser radar, remote sensing, etc.

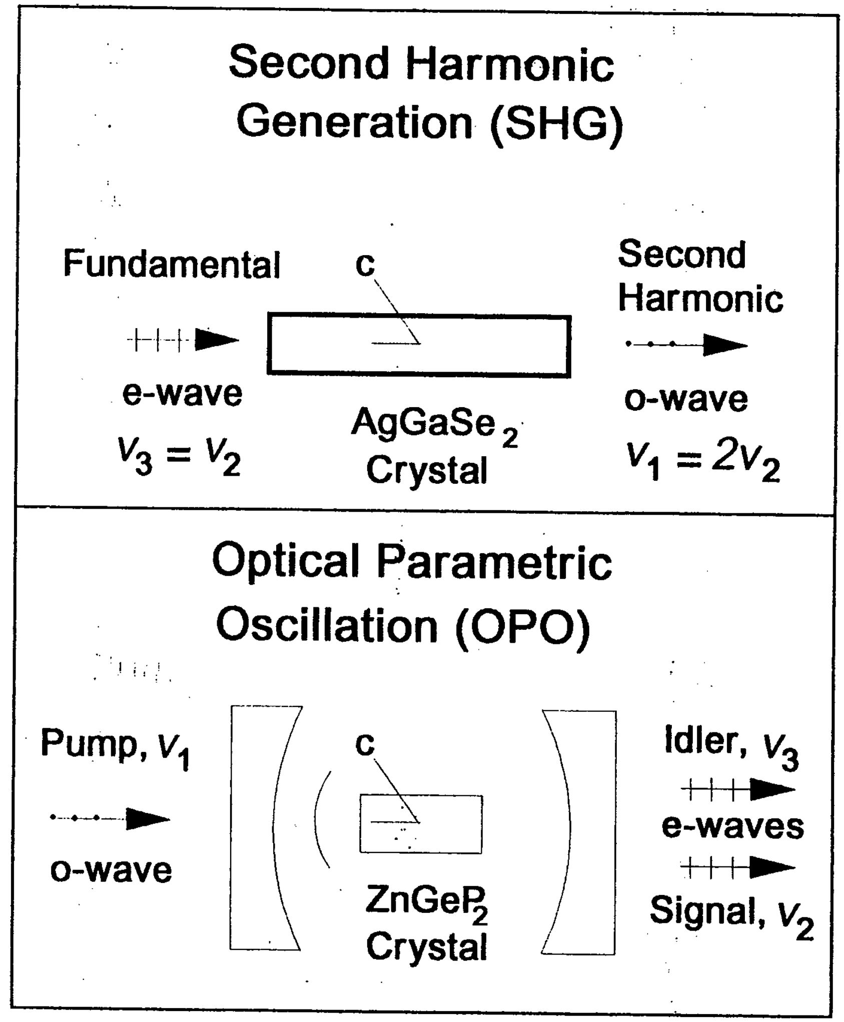

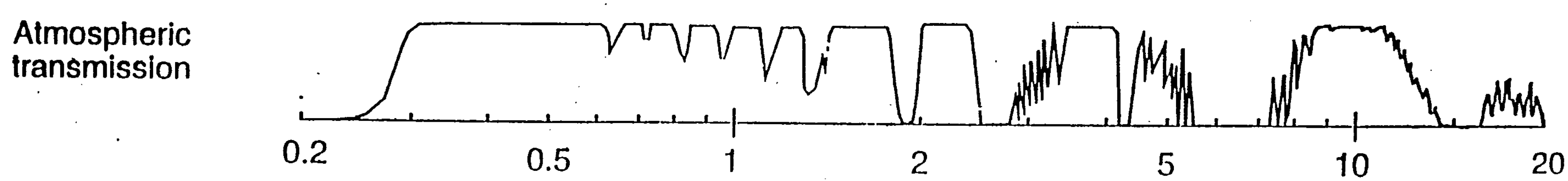

Strategies for Improved Infrared NLO Materials

2um-pumped OPO's

- Material of Choice: $ZnGeP_2$
  - Highest NLO Coefficient with sufficient band gap (d_{14}=75 pm/V)
  - High Thermal Conductivity (0.35W/cmK)
  - Reduced Losses ----> Efficient, High Power Output
- Alternatives for better performance:
  - **None:** Continue to Reduce $ZnGeP_2$ Near-IR Absorption

CO_2 Doubling

- Material of Choice: $AgGaSe_2$
  - Respectable NLO Coefficient (39 pm/V)
  - Wide transparency and phase-matching range (.78-18um)
  - Low absorption Losses
- Alternatives for better performance:
  - $CdGeAs_2$: Highest Nonlinearity (d_{14}=236 pm/V) → Reduce Absorption Loss
  - $Ag(Ga,In)Se_2$: Adjust Birefringence for Noncritical Phase-Matching (NCPM)
  - ABX_2: Continue Search for New Materials

Horizontal gradient freeze growth led to advances in NLO chalcopyrites

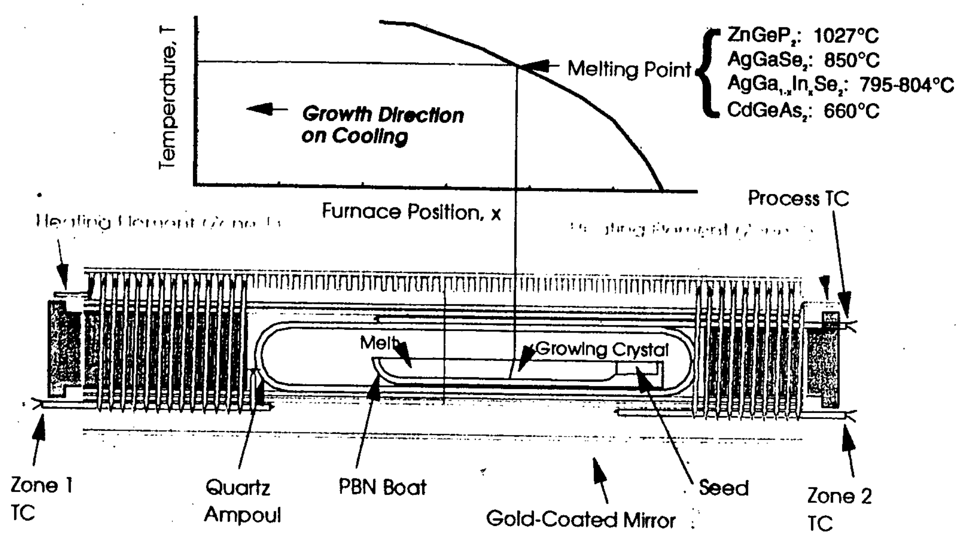

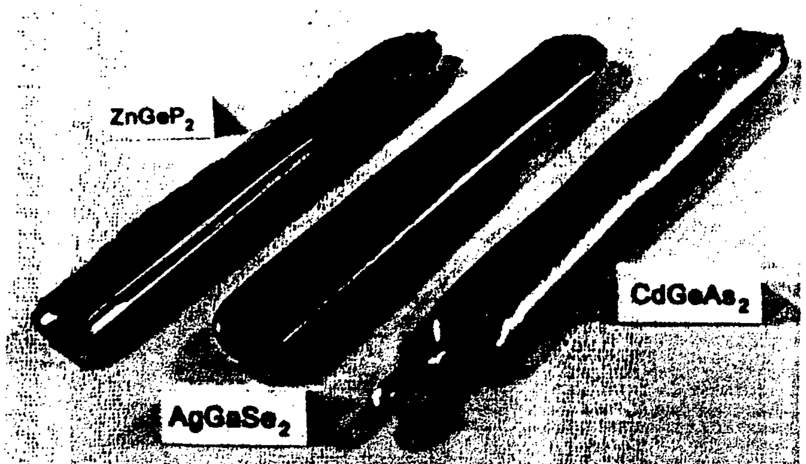

HGF Approach: Key Aspects

- **Low thermal gradients**
  - Minimize vapor transport
  - Eliminate cracking due to anisotropic thermal expansion
- **Transparent Furnace**
  - Simplifies the seeding process
  - Allows *in situ* monitoring of the S/L interface shape & position
  - Facilitates interactive growth (secondary grains can be re-melted)
- **Seeded growth**
  - Eliminates initial polycrystallinity due to supercooling
  - Optimizes orientation to accommodate negative c-axis thermal expansion
  - Enables growth along phase matching direction for max. device length & yield

SANDERS
A Lockheed Martin Company

$ZnGeP_2$: Recent Advances

Improved Single Crystal Yield

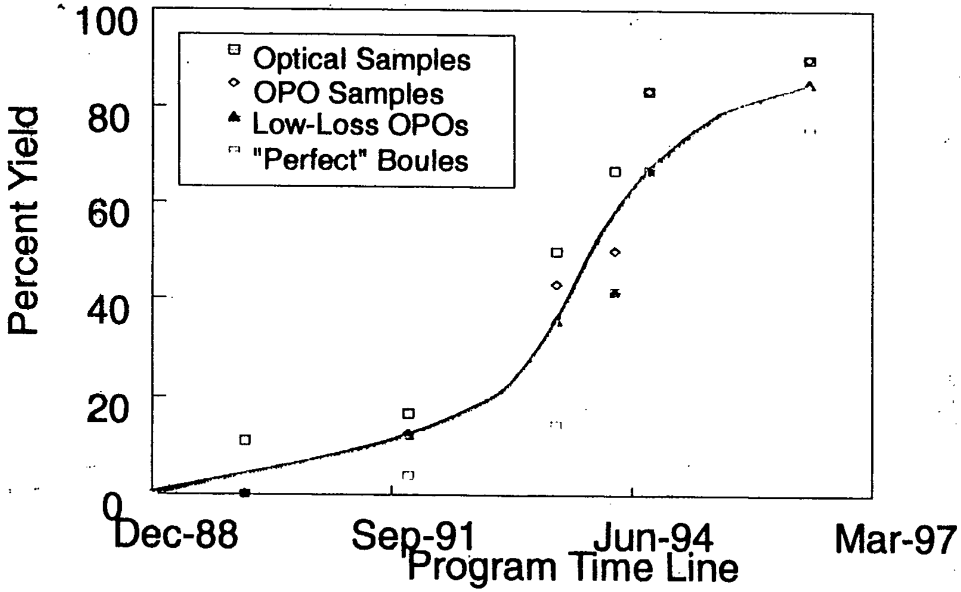

Scaled-Up Crystal Growth

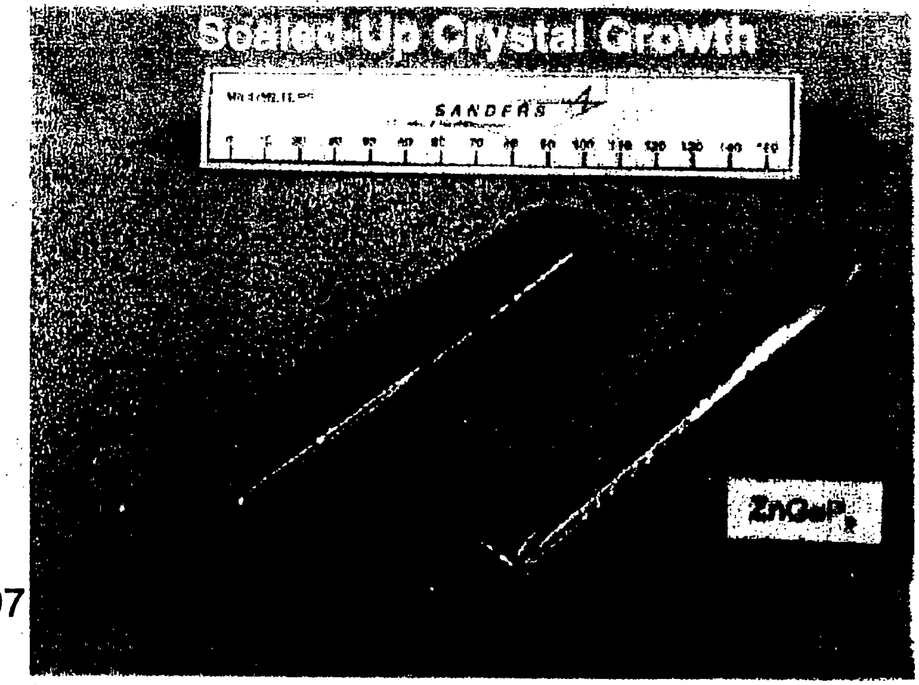

Breakthrough Reductions in Loss

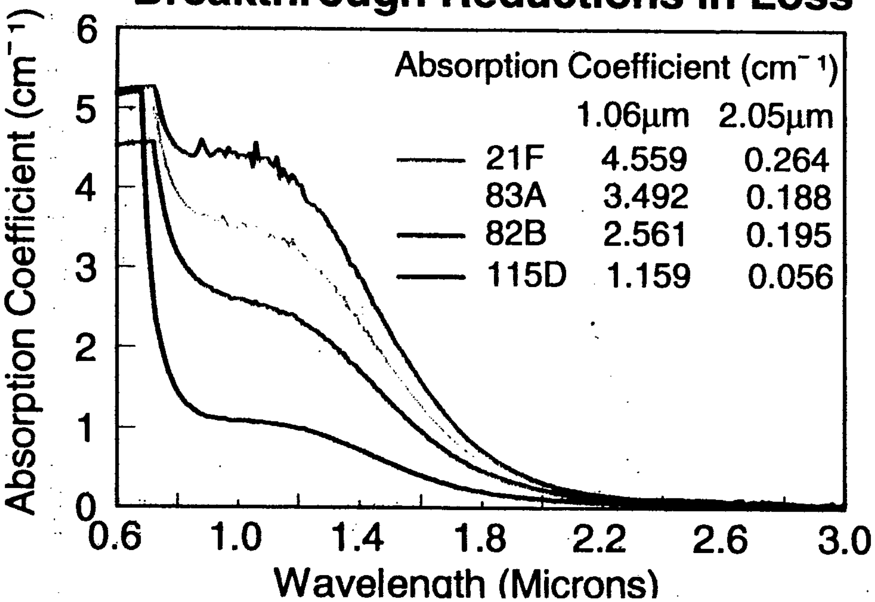

Enhanced OPO Performance

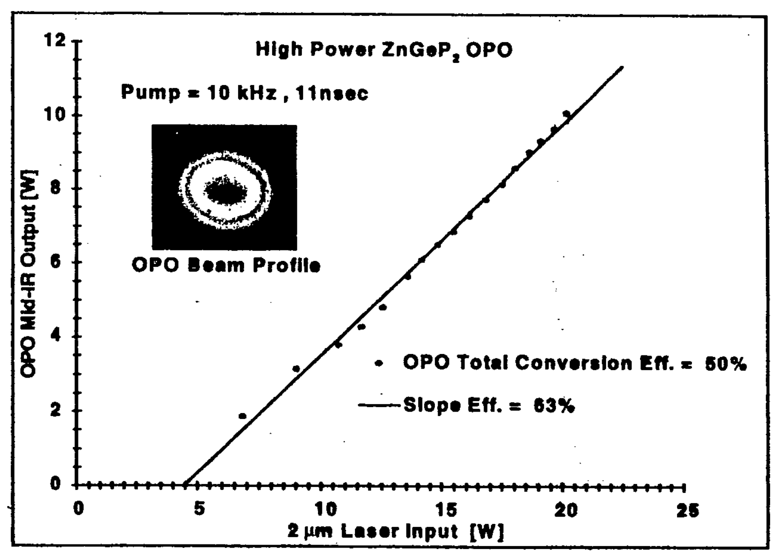

"Phase-Matched" Crystal Growth of $AgGaSe_2$

- Vertical Bridgman growth of $AgGaSe_2$ requires seeding along c-axis for unconstrained thermal expansion during cool-down
- The Horizontal Gradient Freeze (HGF) technique allows "phase-matched" growth along device orientation, yielding longer interaction lengths and minimal waste

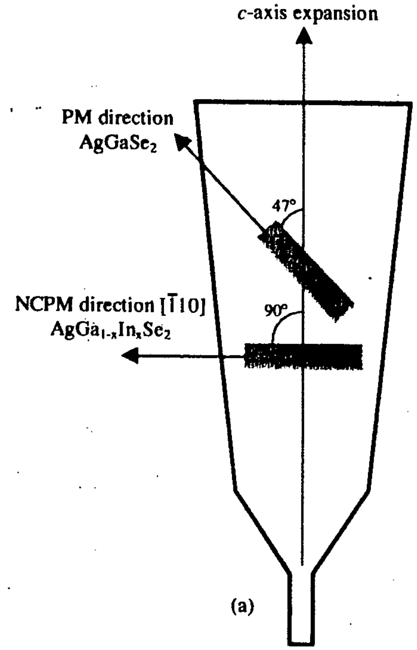

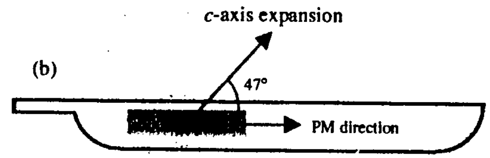

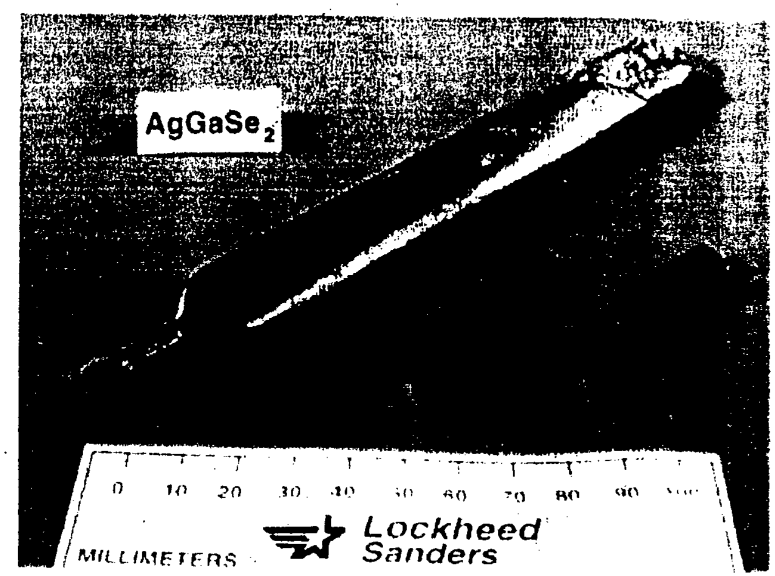

$CdGeAs_2$: Development Milestones

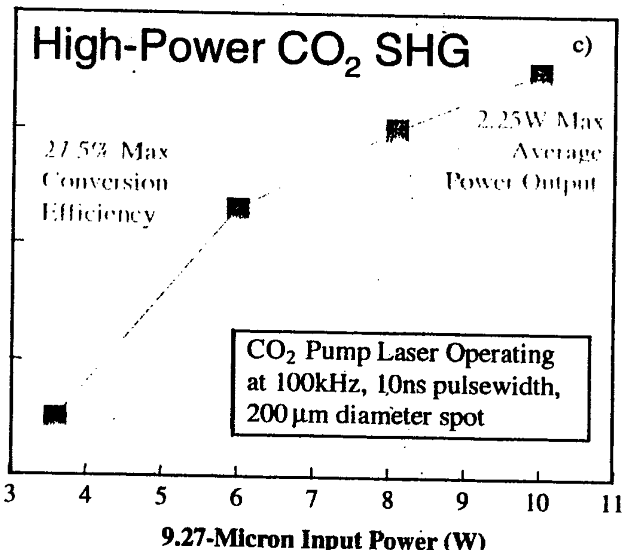

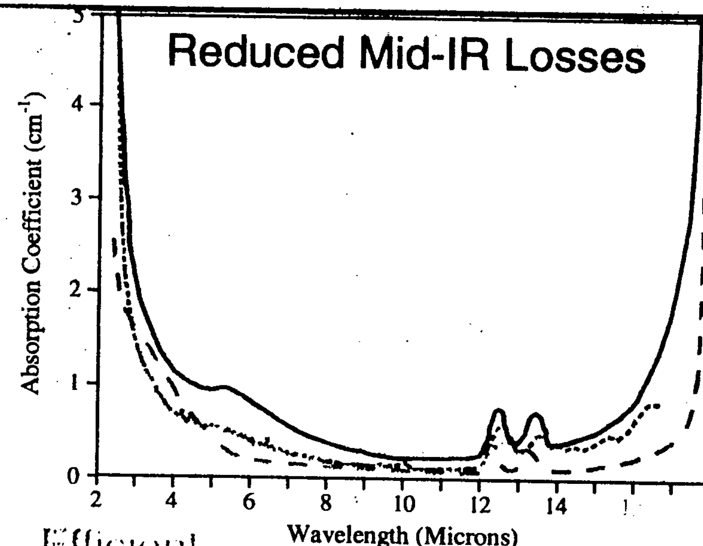

Efficient Long-wave DFG

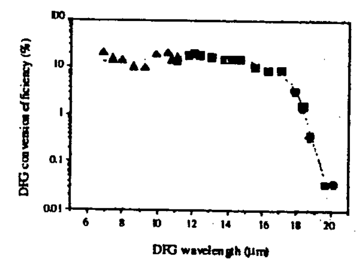

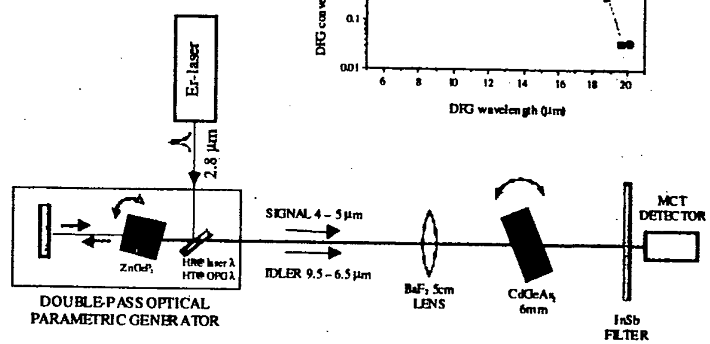

Segregation of Absorbing Defects in $CdGeAs_2$

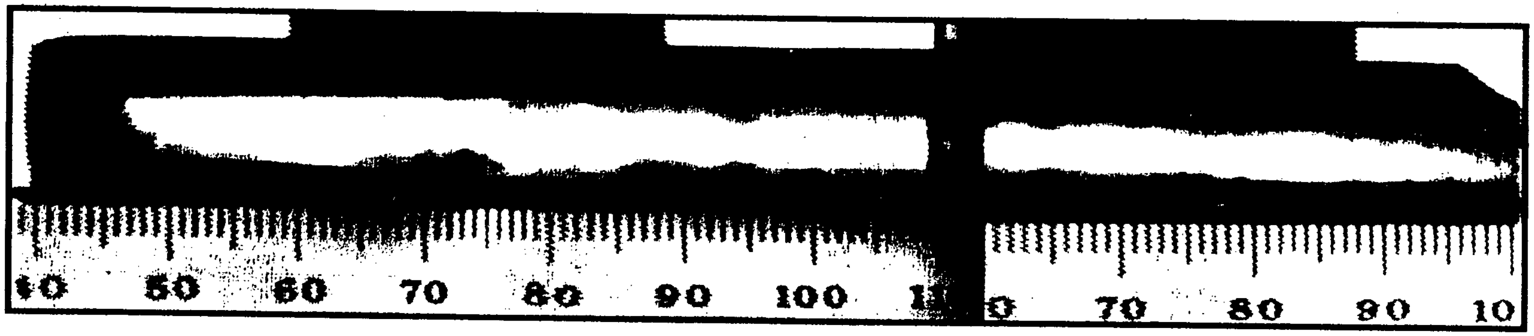

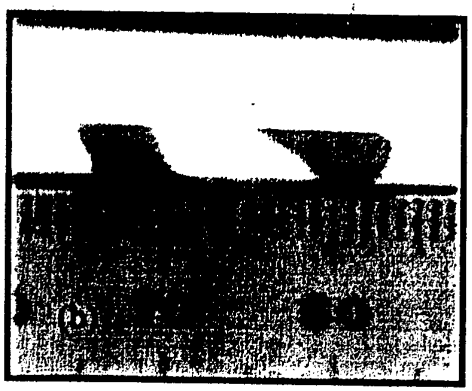

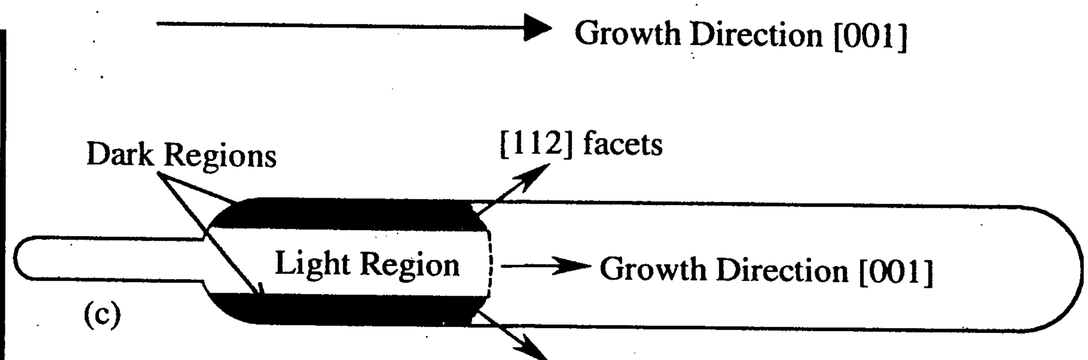

$CdGeAs_2$: Recent Advances

Reduced Mid-IR Absorption (Low-Loss Central Core)

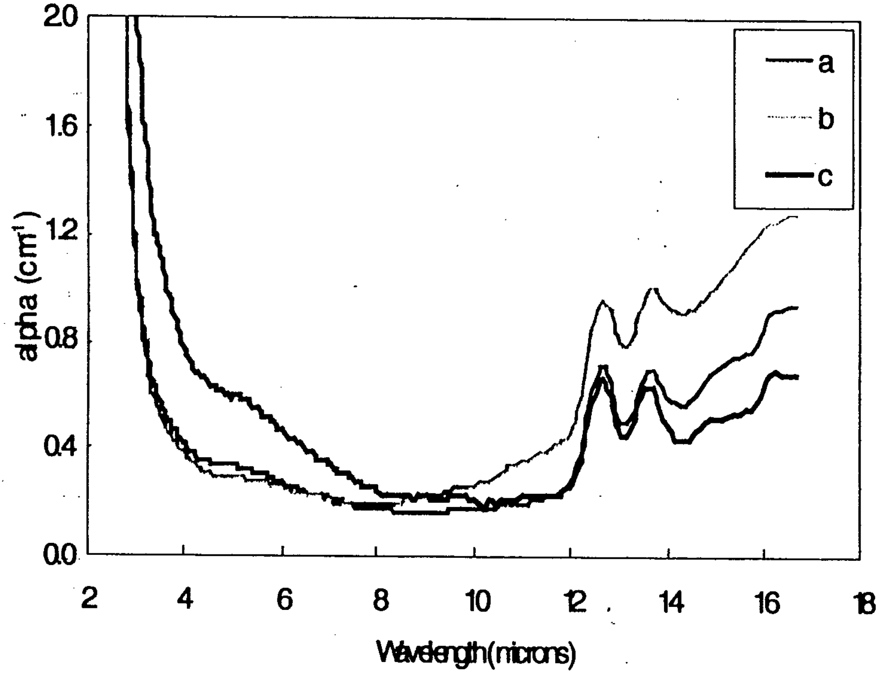

Efficient CO_2-Doubling:
η = 53% at 77K
η = 28% at 273K

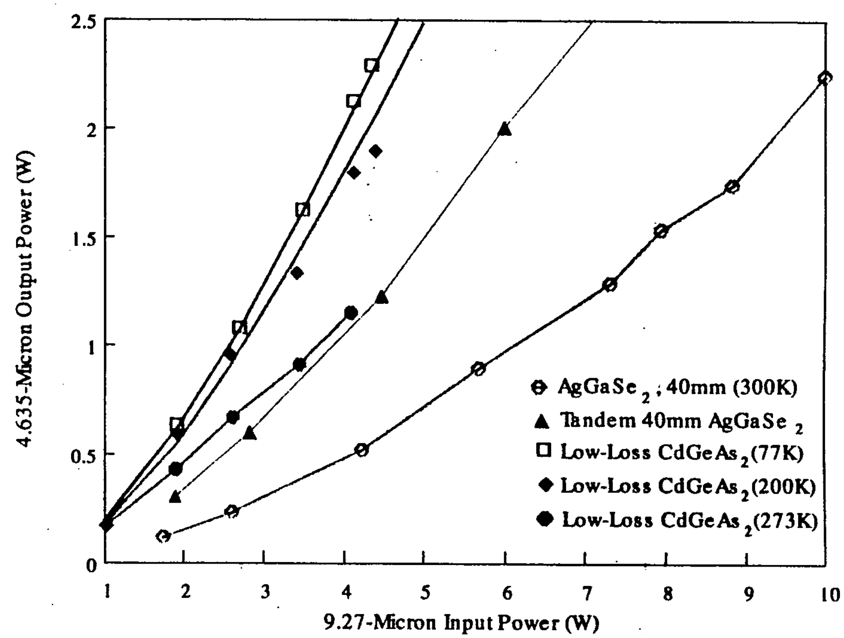

SANDERS
A Lockheed Martin Company

$AgGa_{1-x}In_xSe_2$: Engineered Birefringence for NCPM

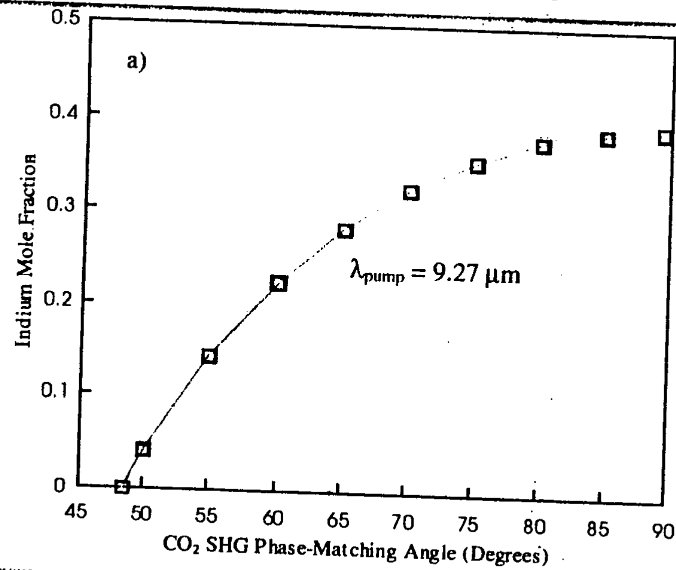

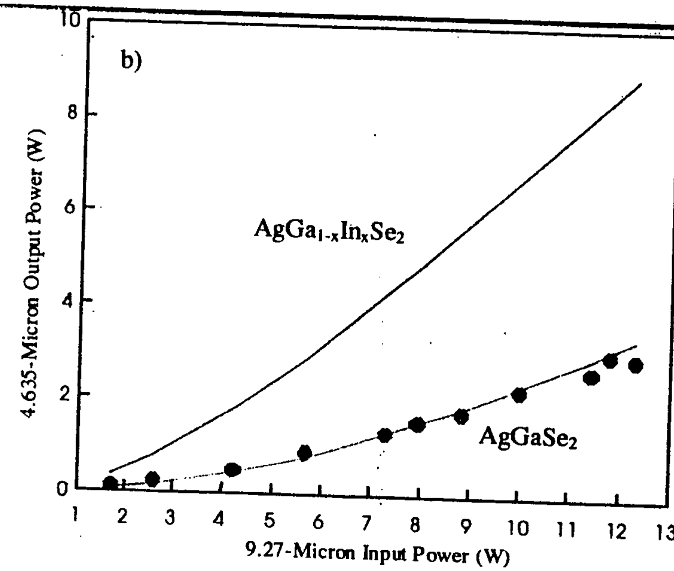

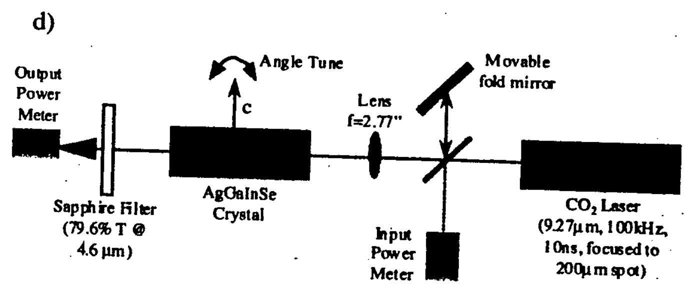

NCPM at x=0.42 (melt)

Reflection & Scattering Losses → η =1.8%

AgGaTe$_2$: a promising new nonlinear optical crystal

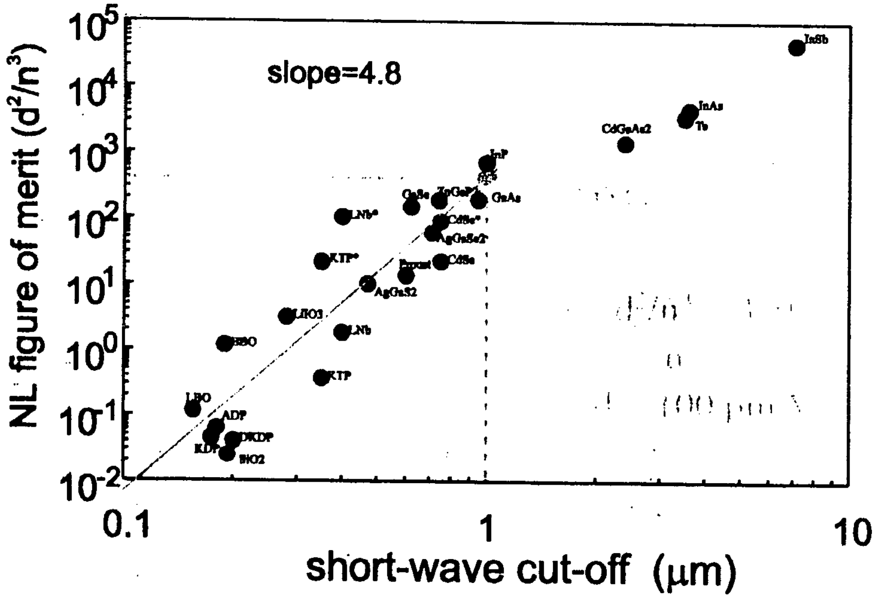

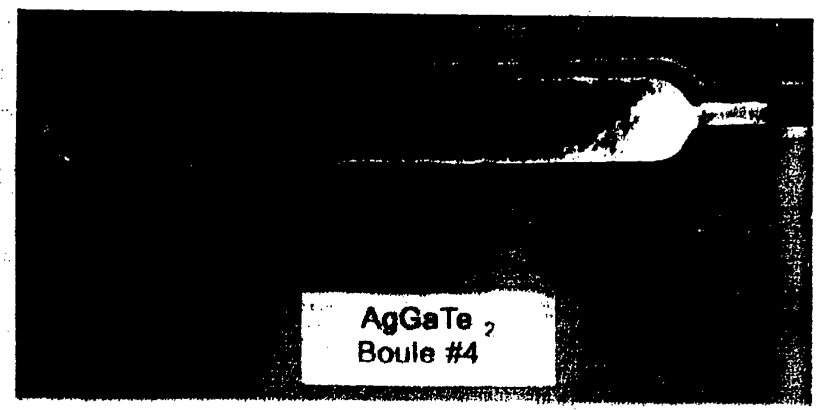

- **Motivation:**
  - Telluride analog of $AgGaS_2$ & $AgGaSe_2$
  - Substitution by Te should triple the NL coefficient and shift the transparency range further into the IR (~1-20μm)
- **Objectives of Research:**
  - Produce large, crack-free single crystals
  - Determine if birefringence is sufficient for phasematching
- **Approach:**
  - HGF Growth in Transparent Furnace
  - Fabricate prism, measure Δn

Summary

- Recent crystal growth advances have established chalcopyrites as the NLO materials of choice for mid- to far-IR laser frequency conversion:
  - Large crack-free single crystals (up to $16x28x140mm^3$) of $ZnGeP_2$, $AgGaSe_2$, and $CdGeAs_2$ can be reproducibly grown by the HGF technique
  - Substantial reductions in absorption and/or scattering losses have been achieved by feed purification, compositional control, & post-growth annealing
  - Improved crystal quality has resulted in outstanding NLO device performance
- The birefringence of mixed crystals ($AgGa_{1-x}In_xSe_2$) can be engineered to achieve non-critical phase-matching (NCPM)
- The search for new materials has led to promising NLO crystals such as $AgGaTe_2$, $CdGa_2S_4$, and $CdGa_2Se_4$
- Dy^{3+}:$CaGa_2S_4$ was demonstrated as the first sulfide mid-IR laser host

Development of Technology of $ZnGeP_2$ Single Crystal at Institute for Optical Monitoring SD RAS

By Alexander I. Gribenyukov, Galina A.Verozubova, and Valentina V.Korotkova

Laboratory of Optical Spectroscopy

Institute for Optical Monitoring

Tomsk Branch of Siberian Division

Russian Academy of Sciences

TR 3

IOM	The main directions of IOM activity & interests	• Theoretical and experimental investigations of climatic and ecological changes under effect of natural and human factors • …………
	The basic theme of the noted direction of IOM's activity	• Development of new techniques and technologies for environment remote sounding • …………
	Divisions of the basic theme	• Development of optical monitoring systems based on new generation of tunable coherent radiation sources working in the middle IR spectral range. • …………
LOS IOM	The main task	Provision of IOM works on development and multiplication of the new optical systems by optical materials needed
	The basic theme	Development of high yield and reliable technologies for production optical materials with controllable physical properties
	The main points of contents of basic theme	1. Development of high yield technology of single crystal growth 2. Investigations of possibilities of controllable manage by physical properties of material due to purposeful changes (variations) of technological parameters on all stages of crystals production – at synthesis, at crystal growth, at postgrowth annealing

TR 6

First Long-term Program

High priority problems related to $ZnGeP_2$ technology

Creation (development) of the growth equipment ensured high reproducible temperature profiles. The equipment could be working with high reliability.	Creation(development) of a new moderated (modified) synthesis technique which could assure a production of as-synthesis $ZnGeP_2$ with controllable (managed) composition.	Development of high yield single crystal technology of ZGP growth
1987 - 1988	**1988 - 1991**	**1989 - 1994**
• First prototype • Series of 6 VB furnaces	• Temperture of reaction start • Intermediate phases • Reaction velocity	• Choice of container material • Choice of seed orientation • Computer calculations of temperature profiles • K_L/K_S ratio evaluation • Calculations & measurements of real growth rate

TR9. P_4 and Zn flows in non-isothermal closed synthesis system.

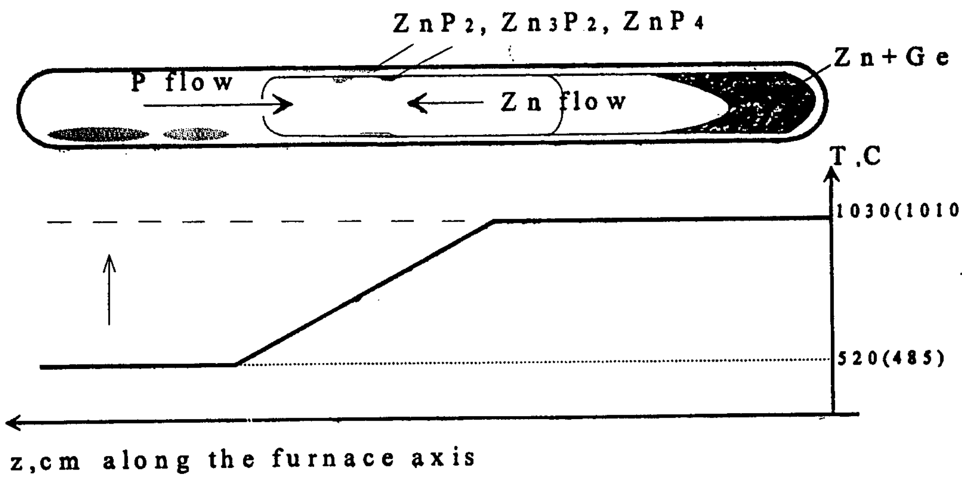

TR10 – Time dependence of expenditure velocity of P4 vapour under pressure of 10-12 atm with Zn-Ge melt at 1010 C .

Hot zone temperature - 1010 °C
Cold zone temperature - 515 °C (P_{P4} = 10 atm)

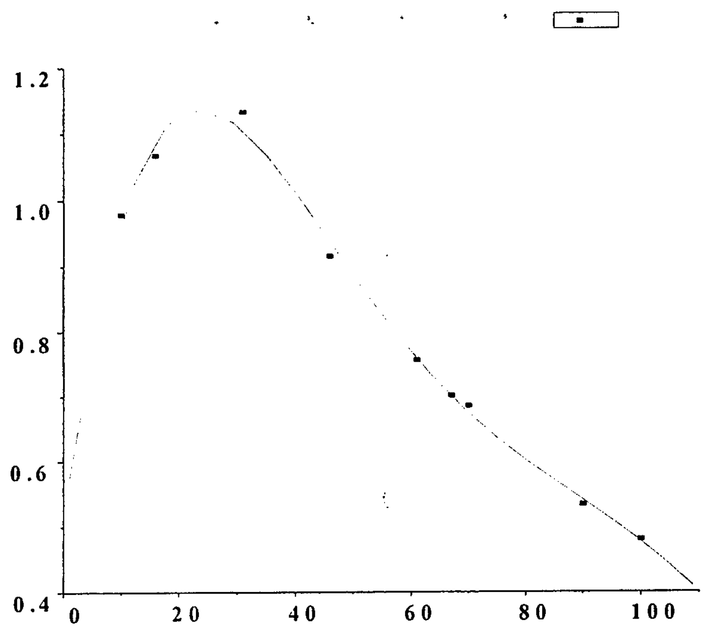

TR13

Distribution of growth failures on causes

100 %
Total quantity of cases with failured crystal growth runs

≈ 20 %	≈ 30 %	≈ 50 %
Defects of seeds	**Twinning on (112) planes**	**Unstability of liquid-solid interface near transition of cone part of growth container in cilinder** cylinder.
↓	↓	↓
Etching + selection	**Change of seed orientation**	• **Calculations and measurements of real velocity of liquid-solid interface movement** • **Evaluation of ratio liquid-to-solid thermal conductivities of ZGP**

TR12 – Probability distribution of ZGP crystalline blocks enlarged along growth axis in VB-method with spontaneous nucleation.

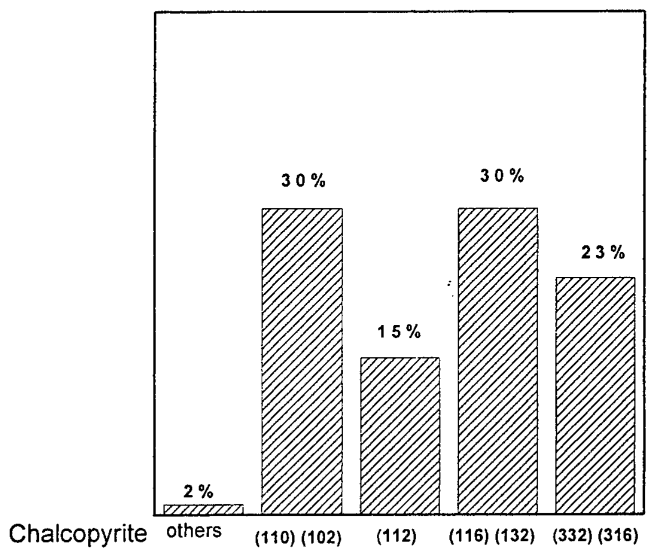

TR14 – The image of growth container surrounding structure for computer calculations.

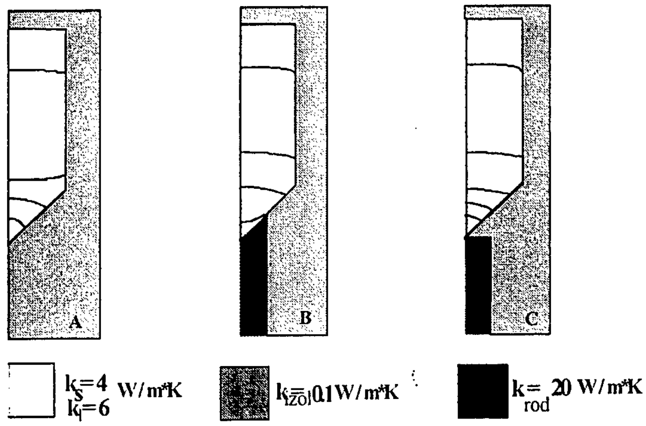

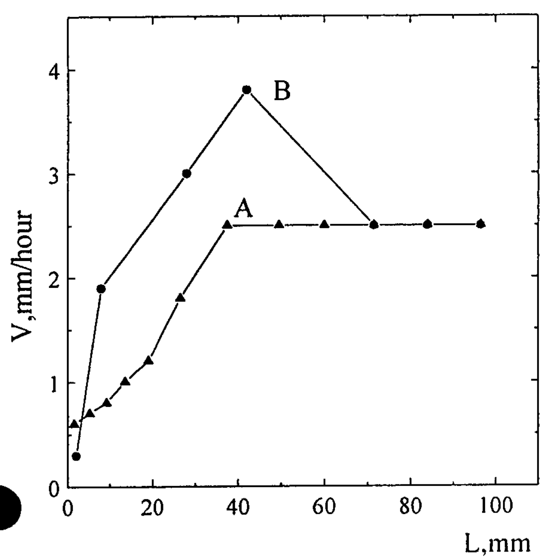

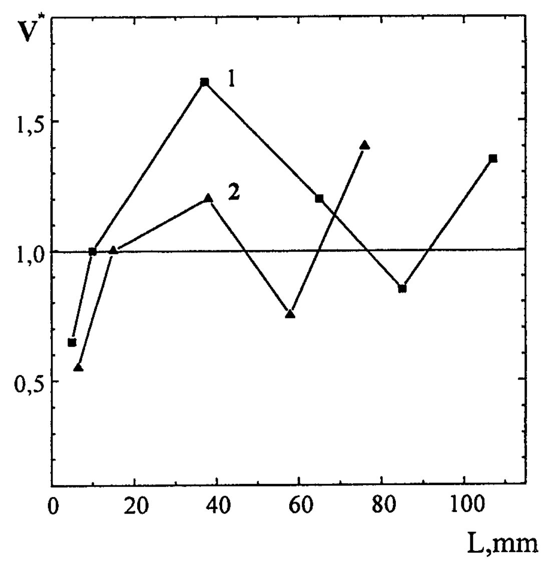

GF method:
The isotherm crystallization rate for container with A and B surrounding structure.
Cooling rate – 1 °/hour.

VB method:
Distribution of isotherm crystallization rate (in units of mechanical movement rate) along crystal axis.
A-type of surrounding structure ,$\varnothing_{furnace}$=6cm;
1 – calculation's data ,$\varnothing_{ampoule}$=3cm;
2 - experiment's data, $\varnothing_{ampoule}$=2cm;

steady

TR15. Diagram of stady state temperature distribution

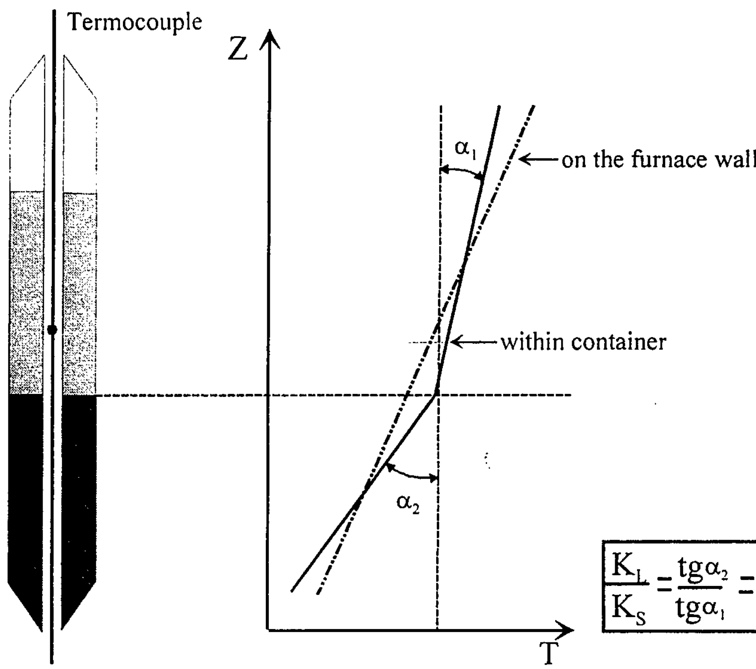

$$\boxed{\frac{K_L}{K_S} = \frac{tg\alpha_2}{tg\alpha_1} = \frac{G_2}{G_1}}$$

Material	Linear regression coefficients				Calculated values	
	Ts	Gs	TL	GL	T_{mel}	KL/Ks
Ge	942.42	4.6	940.51	2.7	937 ± 1	1.7 ± 0.1
$ZnGeP_2$	2009.9	16.24	1807.53	12.9	1027 ± 1	1.3 ± 0.1

Literature data for Ge : KL/Ks = 2.93 [3]
Corrected ratio for $ZnGeP_2$: KL/Ks = 2.3

Tr 16

The Second Long-term Program

1	2	3	4	5
Studies of properties of the ZGP crystals doped by own components from melt directly	**Studies of properties of the ZGP crystals doped by own components from vapor phase due to variation of composition and pressure above melt**	**Studies of thermal annealing conditions influence on the physical properties of the ZGP crystals**	**Determination of temperature dependencies of partial pressures of Zn and P_4 above ZGP melt.**	**Others:** • **Nature of twins** • **Nature of ultrasonic enlightenment** • **Stability of irradiation defects under laser radiation**
↓	↓	↓	↓	↓
ELM 1009	**In progress**	**ELM 1165**	**In progress**	**Current Contract (Is continued)**
↓	↓	↓	↓	↓
• **Tensions** • **Inelastic increase of unit cell volume under annealing** • **In as-grown state optical quality is the best for ZGP grown from stoichiometric composition**	**WILL BE PRESENTED BY ANOTHER REPORT**	• **Optical properties of annealed ZGP are function of melt composition used at crystals growth** • **crystals enriched by Ge indicated the most enlightenment at annealing**	• **Partial pressure of Zn above ZGP melt is not negligible**	**WILL BE PRESENTED AFTER FINISH**

TR17 Some Results of investigations of ZGP crystals doped from melt. Measurements were made in DERA. The crystals were grown in IOM

Crystal	Dopant (P_4-pres. atm)	Temperat. gradient DT/dx, °C/cm	Unit cell volume, Å^3	Unit cell volume difference ($V_{ltf} - V_{ftf}$) Å^3	Absorpt. coeff. at 2.06 μm cm^{-1}	Absorpt. coeff. difference $\alpha_{ltf} - \alpha_{ltf}$ cm^{-1}	Derivative dα/dV, cm^{-1} Å^{-3}	Unit cell volume after annealing Å^3	Absorpt. coeff. after annealing cm^{-1}
89/3 ftf	**0.2 wt%Ge**	**5.2**	319.94861	-0.03872	0.431	0.016	**<u>-0.465</u>**	320,234	0.27 –meas. **<u>0.298-calc</u>**
89/3 ltf	**(7.5)**	**15.4**	319.90989		0.449				
91/2 ftf	**Stoich**	**1.5**	319.92818	+0.120006	0.332	0.129	**<u>+1.07</u>**	320,332	0.36 –meas. **<u>0.764- calc</u>**.
91/2 ltf	**(7.1)**	**7.5**	320.04824		0.461				
93/3 ftf	**0.2 wt%Zn**	**2.5**	319.98361	-0.04372	0.615	- 0.105	**<u>+2.4</u>**	320,190	0.53-meas. **<u>1.11-calc</u>**
93/3 ltf	**(3.8)**	**>20**	319.93989		0.510				

Seeds orientation is (116) for all grown crystals.

Annealing result in an increase of unit cell volumes, but expected change of absorption coefficient with the unit cell volume indicated only for sample enriched by Ge.

ZGP GROWTH FROM MELT:
THE VAPOUR PHASE COMPOSITION AND CRYSTAL PROPERTIES

G.A. Verozubova
A.I. Gribenyukov
Yu. F. Ivanov*

Institute for Optical Monitoring SD RAS
*Tomsk Polytechnical University

in collaboration with A.Vere, DERA, Malvern

The work was fulfilled under financial support
DERA, United Kindom

327°C – $ZnGeP_2$ starts to decompose

1038°C – $ZnGeP_2$ melting point *(Seb Fiechter, 1996)*

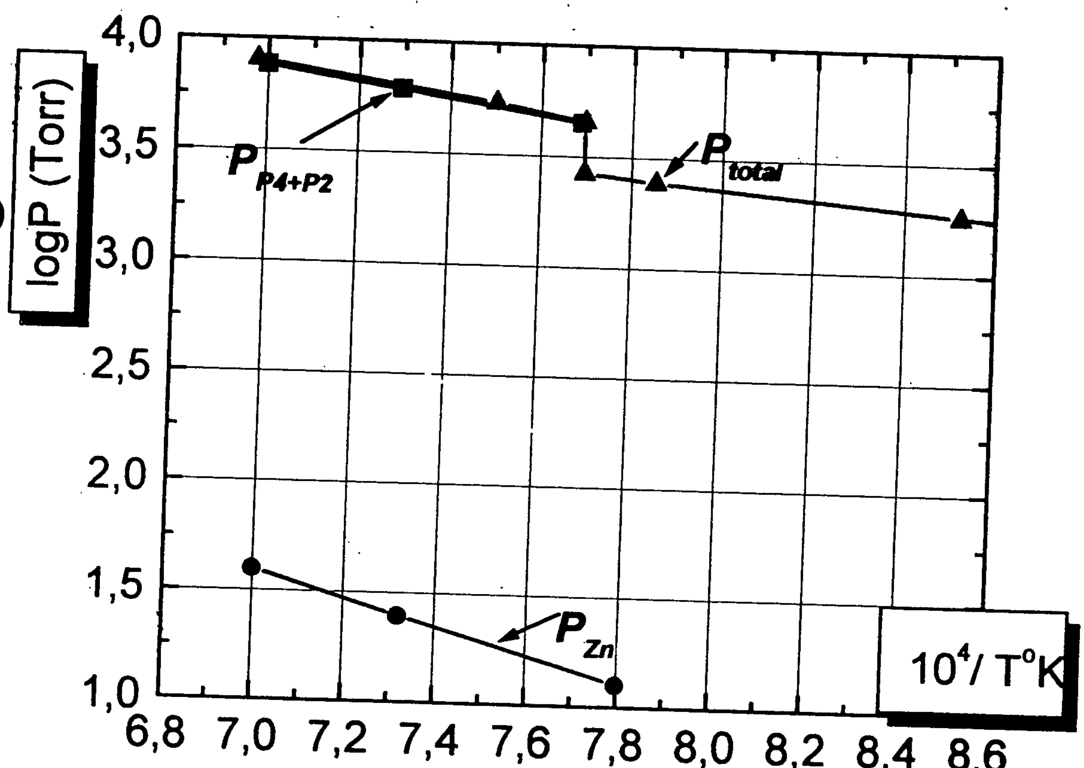

The total pressure above $ZnGeP_2$ - P_{total} *(Buehler, 1971)* and partial pressures of Zn - P_{Zn} and P - P_{P4+P2} calculated from the regular solution theory (*Roenkov, 1975*): P_{Zn} =18 Torr at 1068C

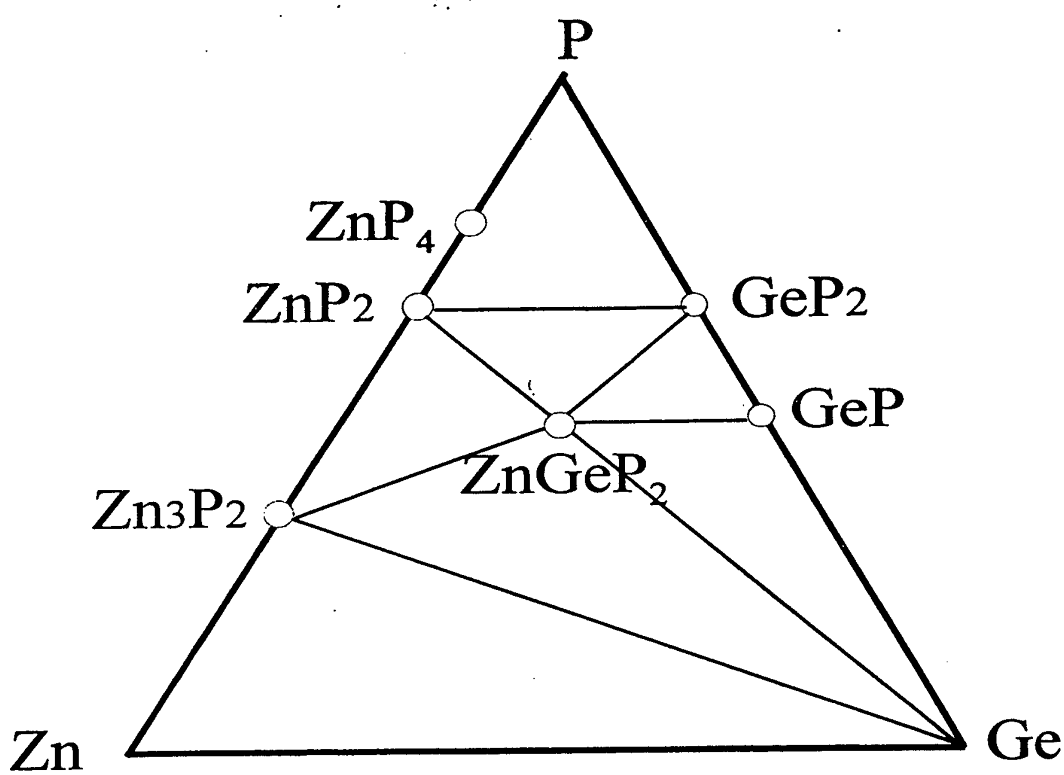

The Zn-Ge-P phase triangle

Experimental details

Synthesis: modified two-temperature technique, allowing to produce more then 500 gms of the material in one process

Growth: vertical Bridgman technique, (100) seeds

TABLE 1. Crystal growth conditions.

NUMBER OF CRYSTAL	HOT ZONE TEMRERATURE °C	COLD ZONE TEMPERATURE °C	[illegible] NEAR [illegible] POINT °C/CM	[illegible]	[illegible]	[illegible]	[illegible]
1	1060	990	6	0.5	6.9	1.1	Gas pocke
2	1060	1000	3.5	1.0	7.2	-	No pockets Single phas
3	1060	950	10	0.5	-	-	Ge eutectic on the top (the crystal

* P_{P4} (P_{Zn}) - pressures of phosphorus (zinc), created by additional charges of P (Zn), and calculated from the ideal gas law.

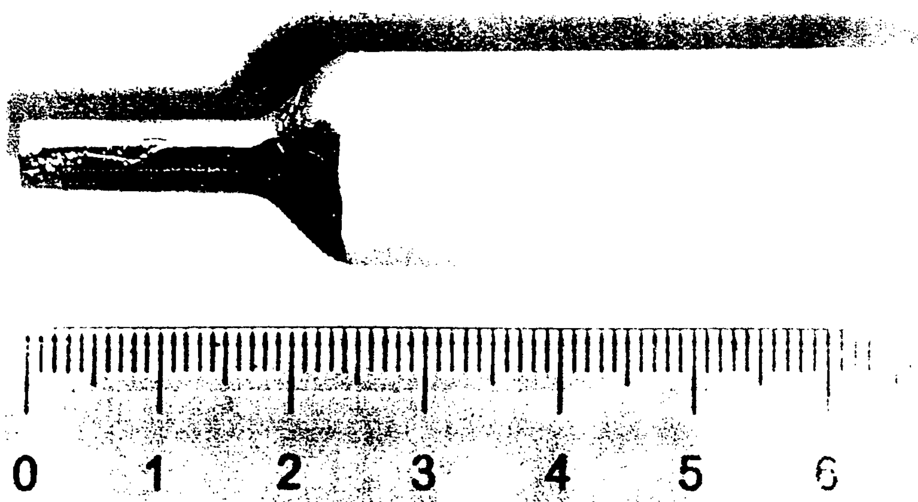
0 1 2 3 4 5 6

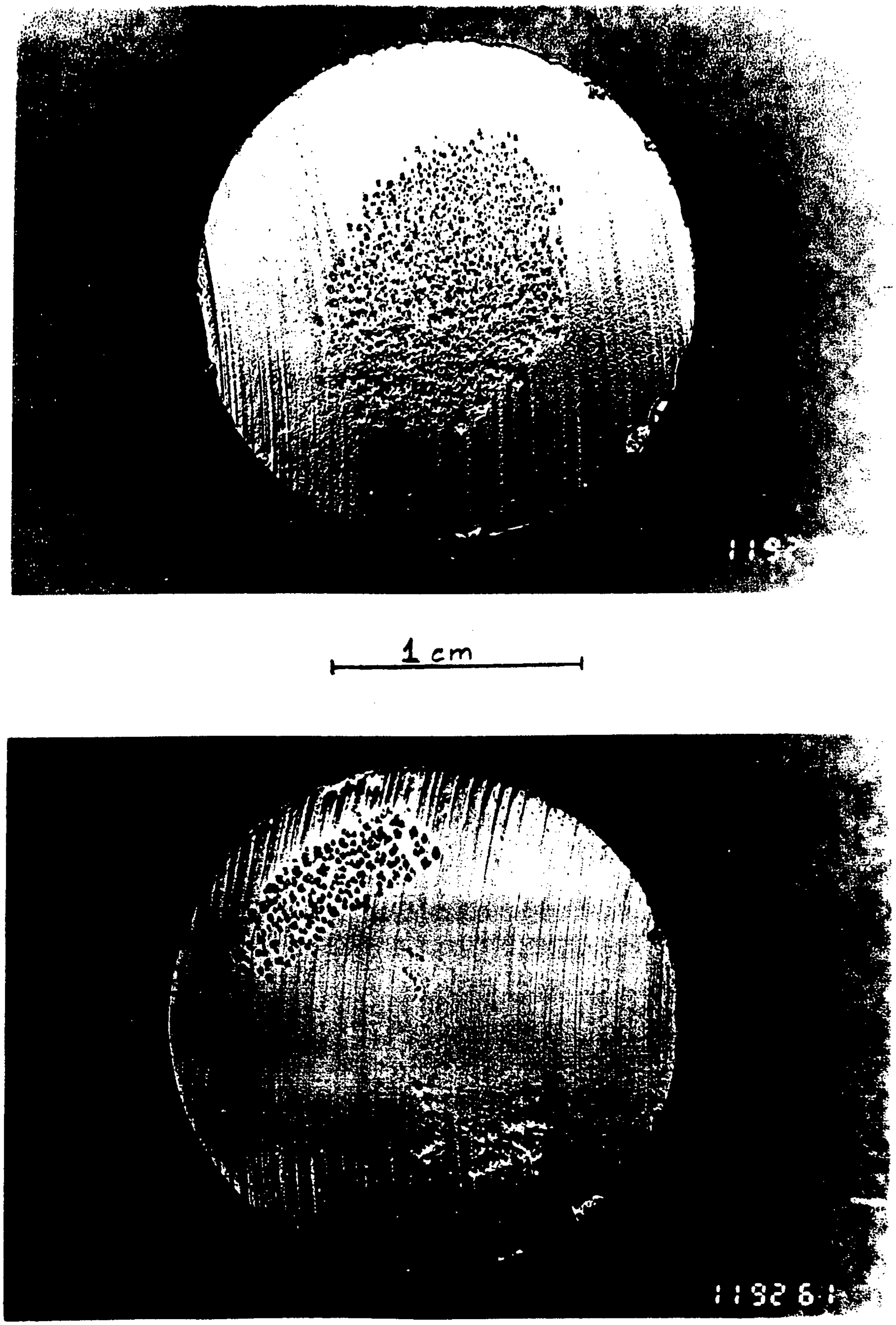

$ZnGeP_2$ slices after chemichal etching

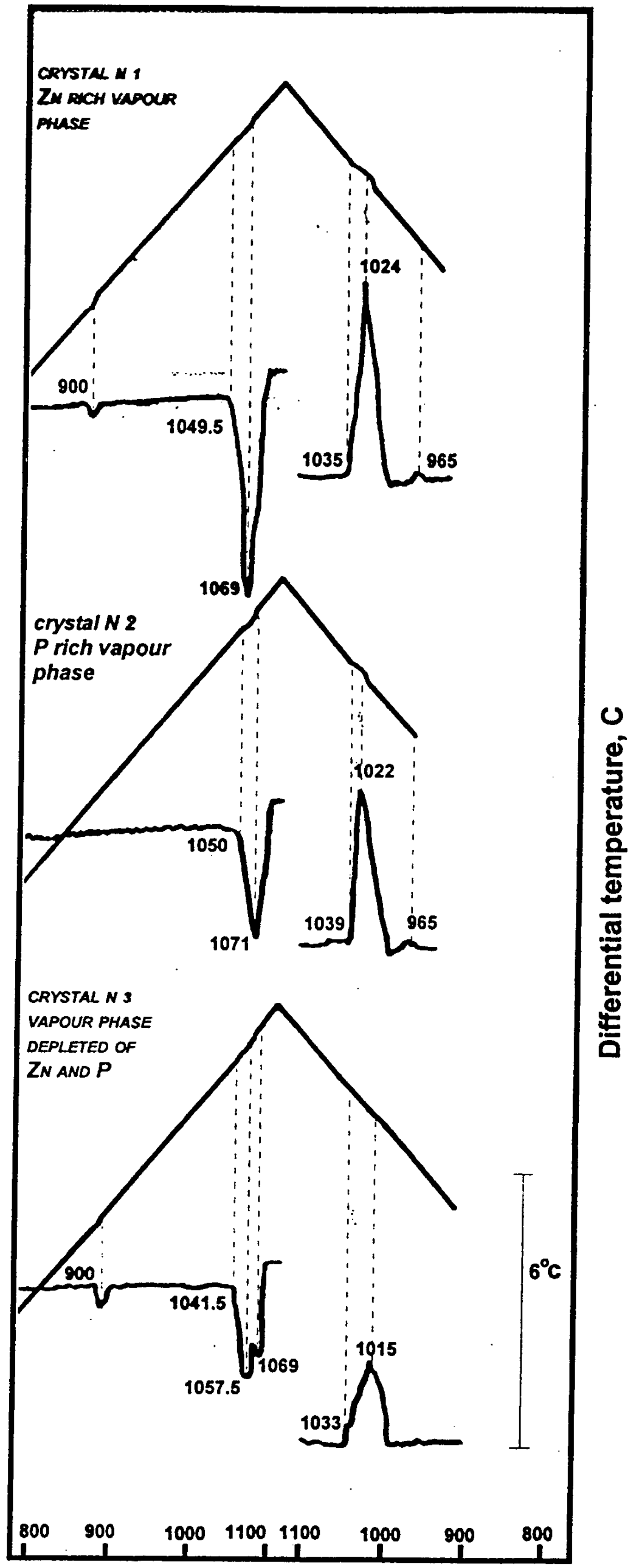

temperature, C

DTA curves of ZGP grown under various pressures of Zn and P

Experimental details: the weight of the studied samples-0.5 g , heating and cooling rates - 7.5deg/min
reference material - Al2O3, speed of the paper movement - 1mm/min

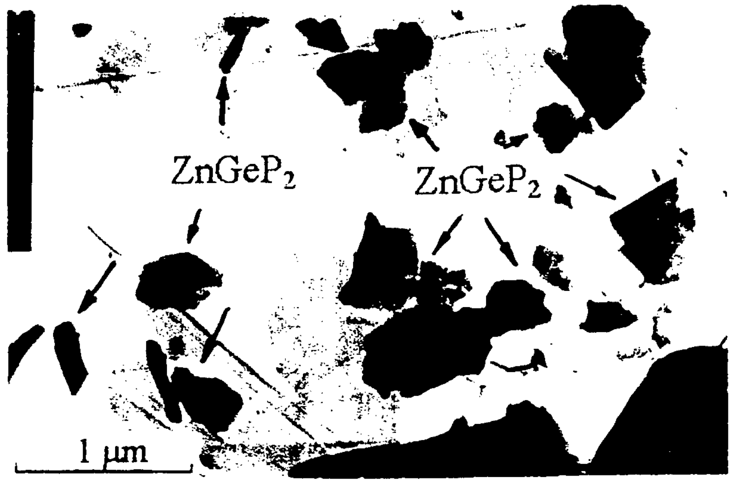

Fragments of failure (damage) of the bulk ZGP specimen
arranged on the carbon substrate

Electron microscope EM-125
Accelerating voltage 125 kV
Working Magnification 65-85 000
Resolution 7-10Å

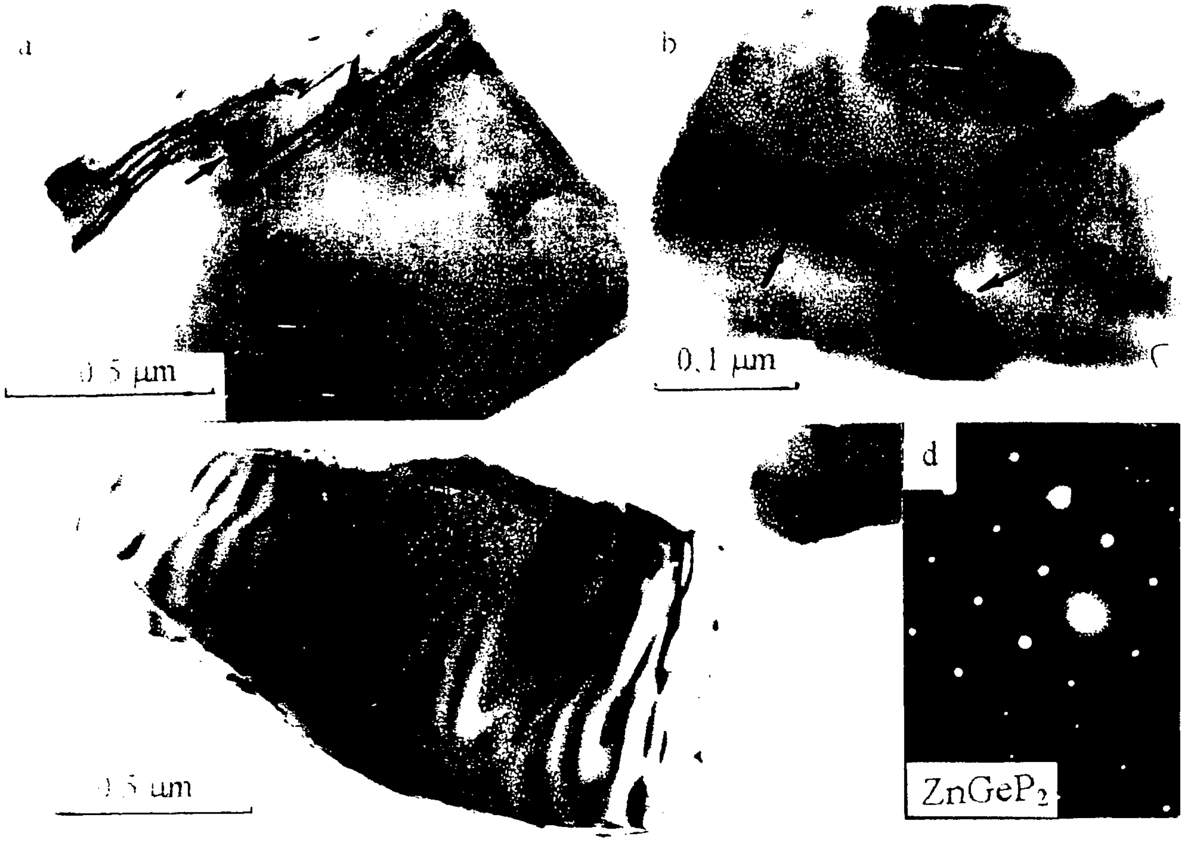

Microscopic image of $ZnGeP_2$

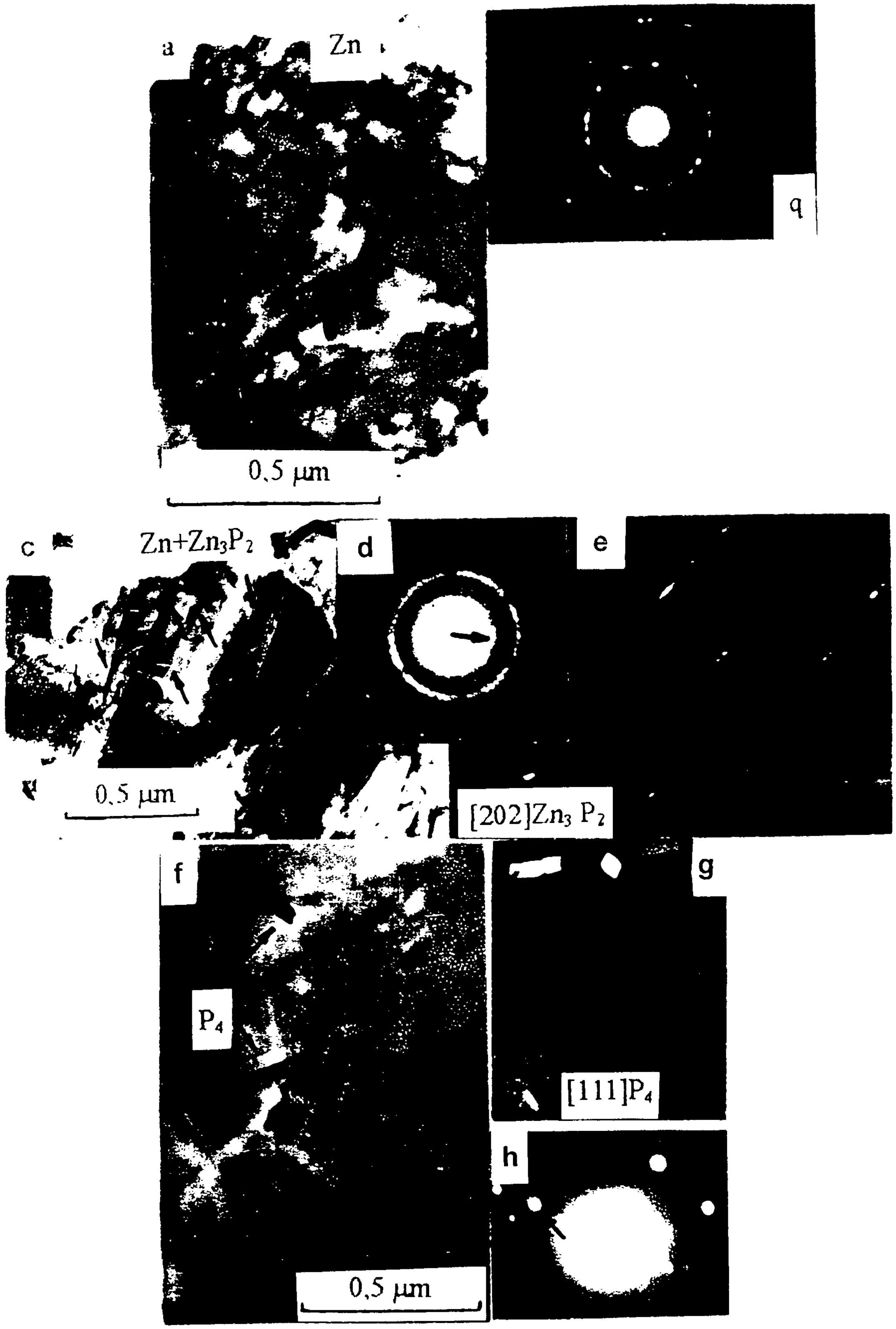

Microscopic image of $ZnGeP_2$ grown under Zn rich vapour phase (as- grown crystal N1)

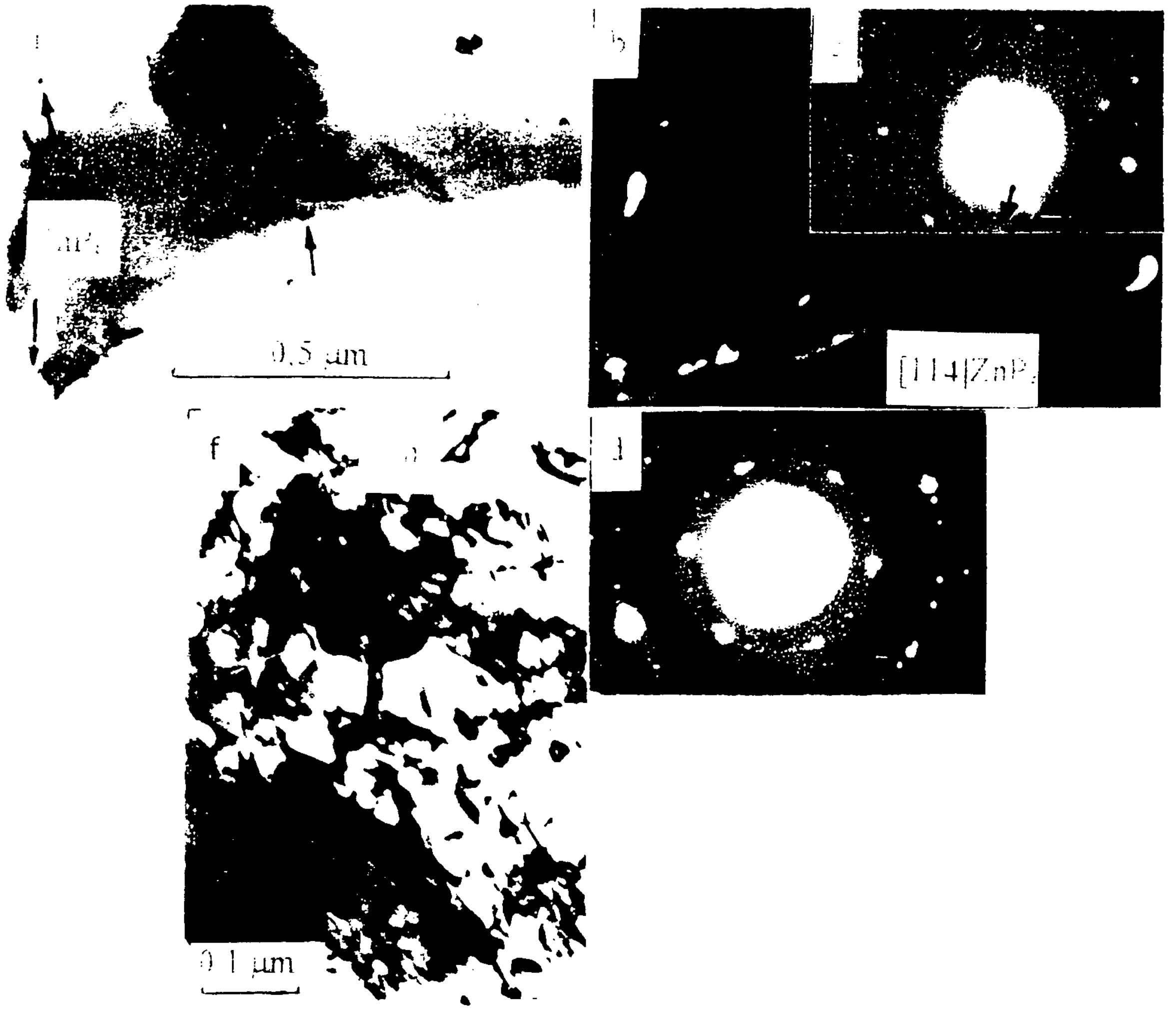

Microscopic image of $ZnGeP_2$ grown under Zn rich vapour phase (annealed crystal N1)

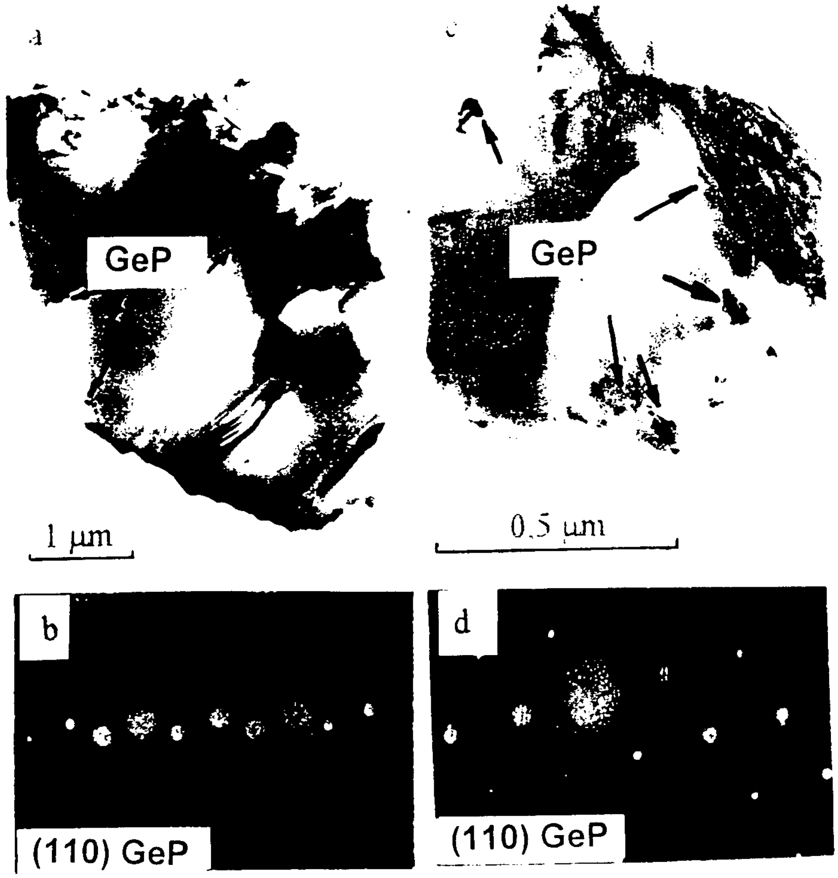

Microscopic image of $ZnGeP_2$ grown under the phosphorus pressure of 7.2 atm (crystal N2)

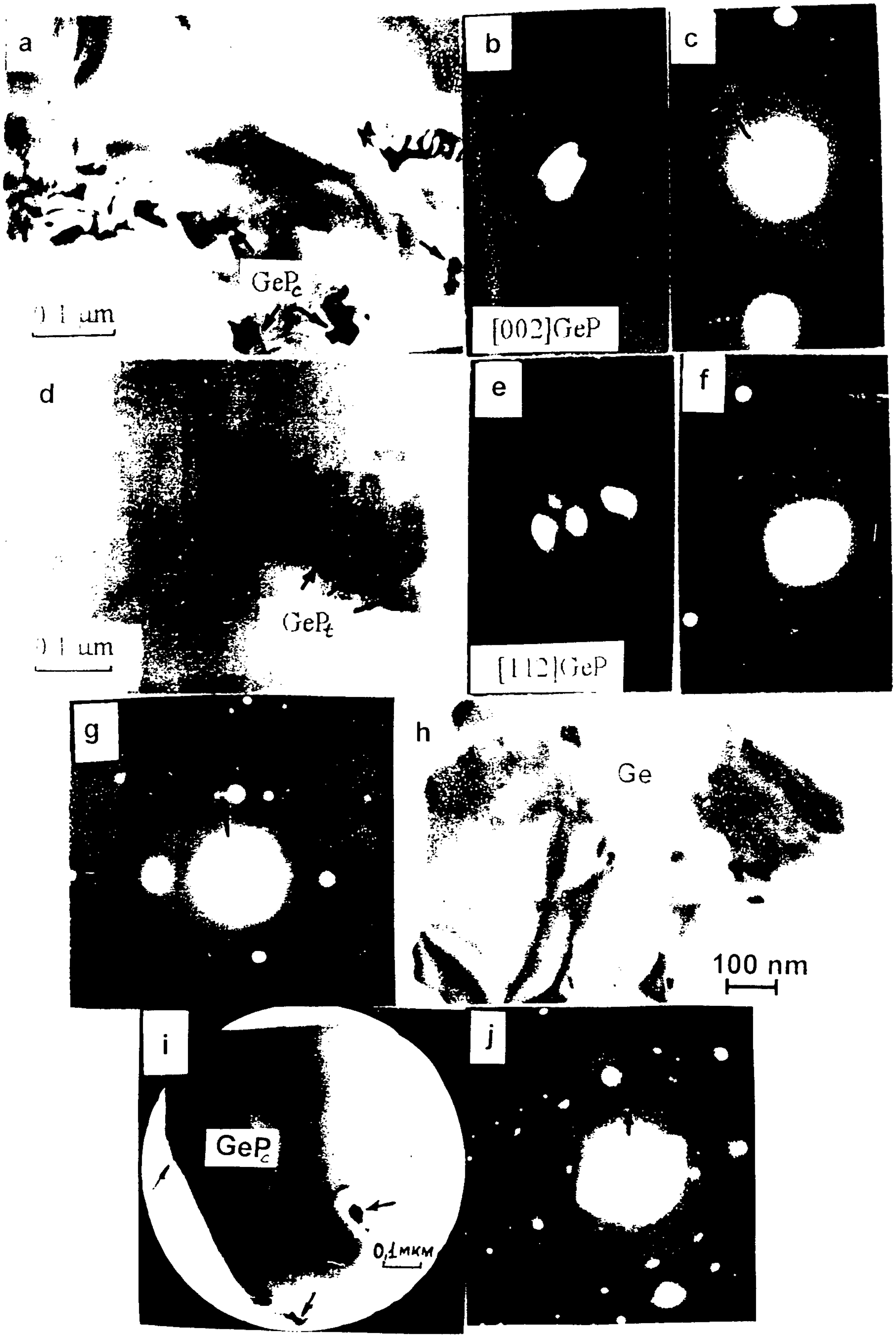

Microscopic image of $ZnGeP_2$ grown under the vapour phase depleted of volatile components (crystal N3)

TABLE 2. The vapour phase composition during growth and the phase composition of precipitates.

NUMBER OF CRYSTAL	P_{P4}* ATM	P_{Zn} ATM	EXTERNAL VIEW OF THE GROWN CRYSTAL	PHASE COMPOSITION OF PRECIPITATES	SIZES OF PRECIPITATES
1	6.9	1.1	Gas pockets	Zn	Ø 1-1.5 mkm
				Zn_3P_2 ZnP_2	10 nm×1 mkm
				P	25×300 nm
2	7.2	-	No pockets Single phase top	GeP cubic	Ø 0.2-0.3 mkm Ø 80-90 nm
3	-	-	Ge eutectic on the top of the crystal	GeP cubic	Ø 5 nm
				GeP tetrogonal	15×45 nm
				Ge	Ø 8 nm

* P_{P4} (P_{Zn}) - pressures of phosphorus (zinc), created by additional charges of P (Zn), and calculated from the ideal gas law.

Chemichal point of view:

Dissociation reaction for the melted ZGP *(Seb. Fiechter, 1996)*

$$\mathbf{ZnGeP_{2(melt)} \Leftrightarrow Zn_{(gas)} + (1-x)Ge_{(cond)} + xGeP_{(cond)} + (0.5-0.25x)\ P_{4(ga}}$$

Mass action law for the dissociation reaction of the melted ZGP:

$$K_P(T) \sim P_{Zn}\, P_{P4}^{(0.5-0.25x)}$$

TABLE 2. The vapour phase composition during growth and the phase composition of precipitates.

NUMBER OF CRYSTAL	P_{P4}* ATM	P_{ZN} ATM	EXTERNAL VIEW OF THE GROWN CRYSTAL	PHASE COMPOSITION OF PRECIPITATES	SIZES OF PRECIPITATES
1	6.9	1.1	Gas pockets	Zn	Ø 1-1.5 mkm
				Zn_3P_2 ZnP_2	10 nm×1 mkm
				P	25×300 nm
2	7.2	-	No pockets Single phase top	GeP cubic	Ø 0.2-0.3 mkm
					Ø 80-90 nm
3	-	-	Ge eutectic on the top of the crystal	GeP cubic	Ø 5 nm
				GeP tetrogonal	15×45 nm
				Ge	Ø 8 nm

* P_{P4} (P_{Zn}) - pressures of phosphorus (zinc), created by additional charges of P (Zn), and calculated from the ideal gas law.

Chemichal point of view:

Dissociation reaction for the melted ZGP *(Seb. Fiechter, 1996)*

$$ZnGeP_{2(melt)} \Leftrightarrow Zn_{(gas)} + (1-x)Ge_{(cond)} + xGeP_{(cond)} + (0.5-0.25x)\, P_{4(gas)}$$

Mass action law for the dissociation reaction of the melted ZGP:

$$K_P(T) \sim P_{Zn}\, P_{P4}^{(0.5-0.25x)}$$

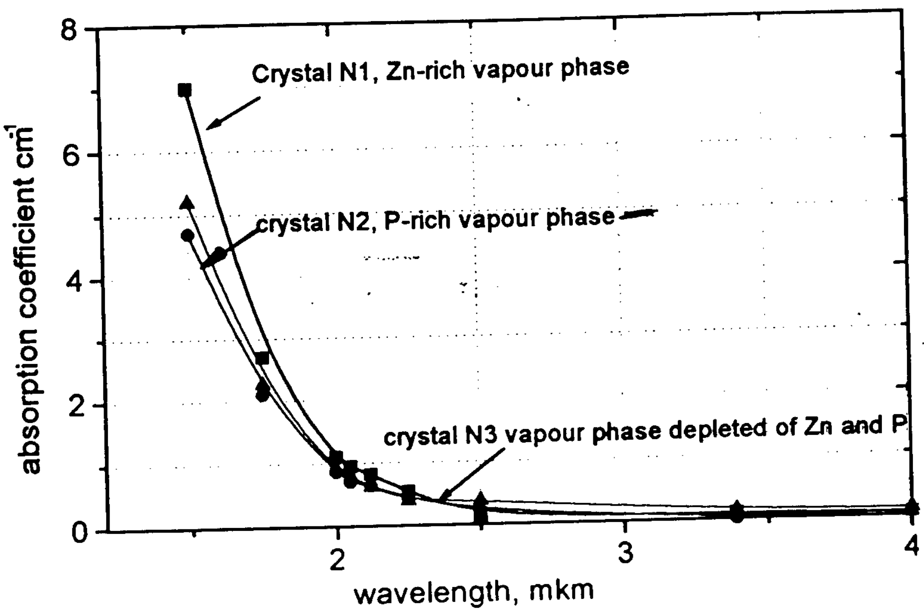

Absorption coefficient spectra for as-grown crystals
Slices were cut from the middle part of the ingot

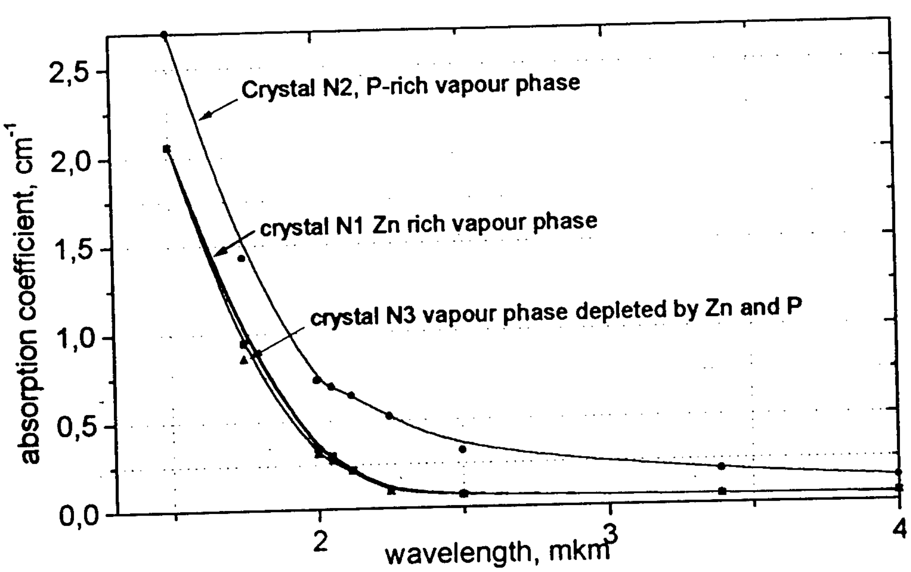

Optical absorption spectra after annealing
(vacuum, T=600°C, duration 300 hours)
Slices were cut from the middle part of the ingots

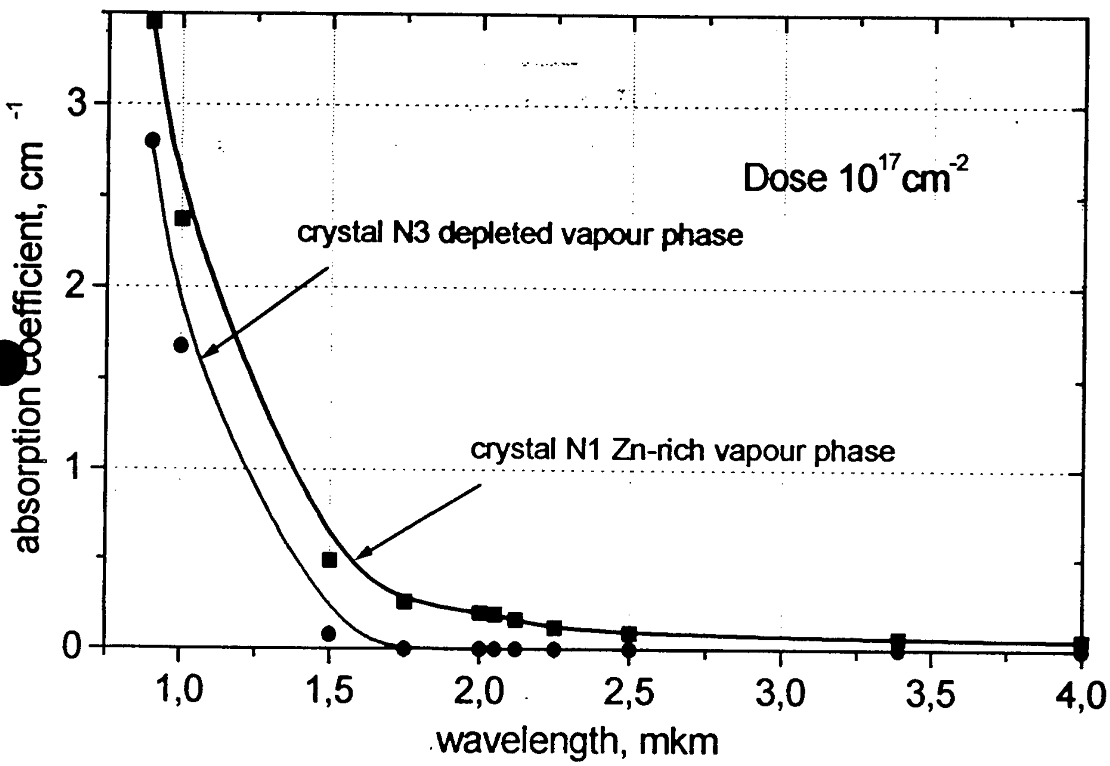

Absorption coefficient spectra of $ZnGeP_2$ after irradiation
slices were cut from the middle part of ingots, thickness is 6 mm

Conclusions

To study the influence of the vapour phase composition during growth on crystal properties three single crystals were grown from one starting material but under varied vapour phase composition.

1. DTA have shown the different composition of these crystals: their melting points are different. For the Zn and Ge rich crystals it is lowered as compared to the crystal grown with the P excess only.

2. All three crystals have the second phase particles. The second phase composition correletes with the vapour phase composition.

3. For the most part the second phase particles have a drop (splintery) form and nanometer sizes. In individual cases the second phase precipitations as the submicron – micron's areas (Zn or Zn+ Zn_xP_y) are found.

4. As a rule, the nanodimensional particles are located along boundary of areas of the crystal fracture, being responsible for the brittle cracks in ZGP.

5. $ZnGeP_2$ fragments free from the second phase particles have high elastic stress fields whereas fragments containing the latter particles are free from stresses. This could possibly indicate that the crystal areas having a high level of elastic stress fields are the places of the second phase particle formation.

6. The different improvement of the crystals grown with Zn-rich vapour phase and vapour phase depleted of volatile components on irradiation is apparently related to the different volume fraction of the second phase particles or their sizes. The lowest absorption at 2 μm attained by irradiation is $< 0.01\ cm^{-1}$.

Inelastic Light Scattering by Free Electron Gas and Coupled Electron-Phonon Excitations in Advanced Semiconductor Structures

Bahish H Bairamov

A F Ioffe Physico-Technical Institute
Academy of Sciences of the Russia

194021, St Petersburg, Russia

High resolution light scattering by LO phonons in semi-insulating GaP (n < 10 12 cm -3) in the temperature range 7 - 290K

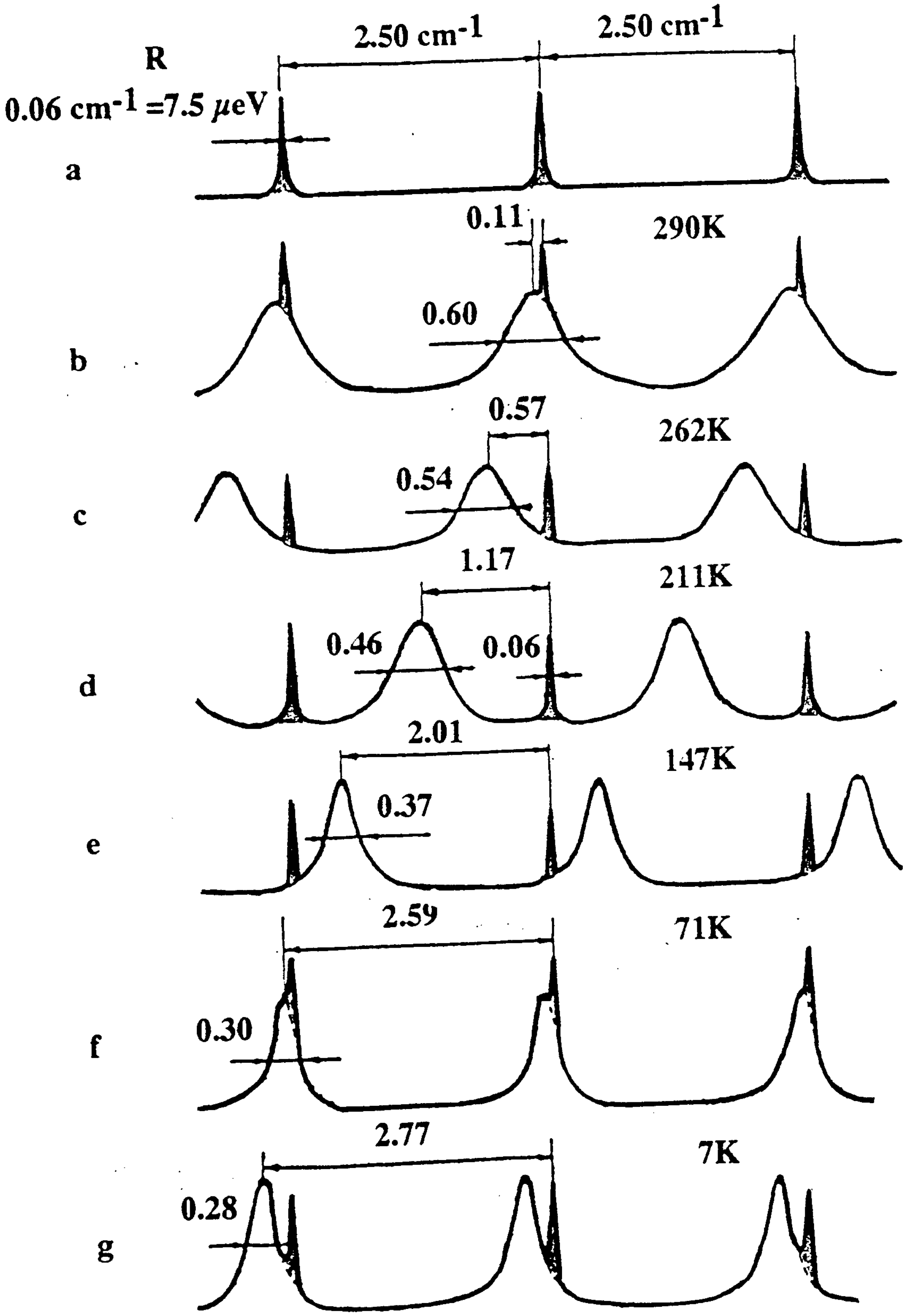

a) instrumental profile with a spectral resolution of 0.06 cm^{-1}

b-g) interference spectra of the light scattering by LO-phonons various temperatures

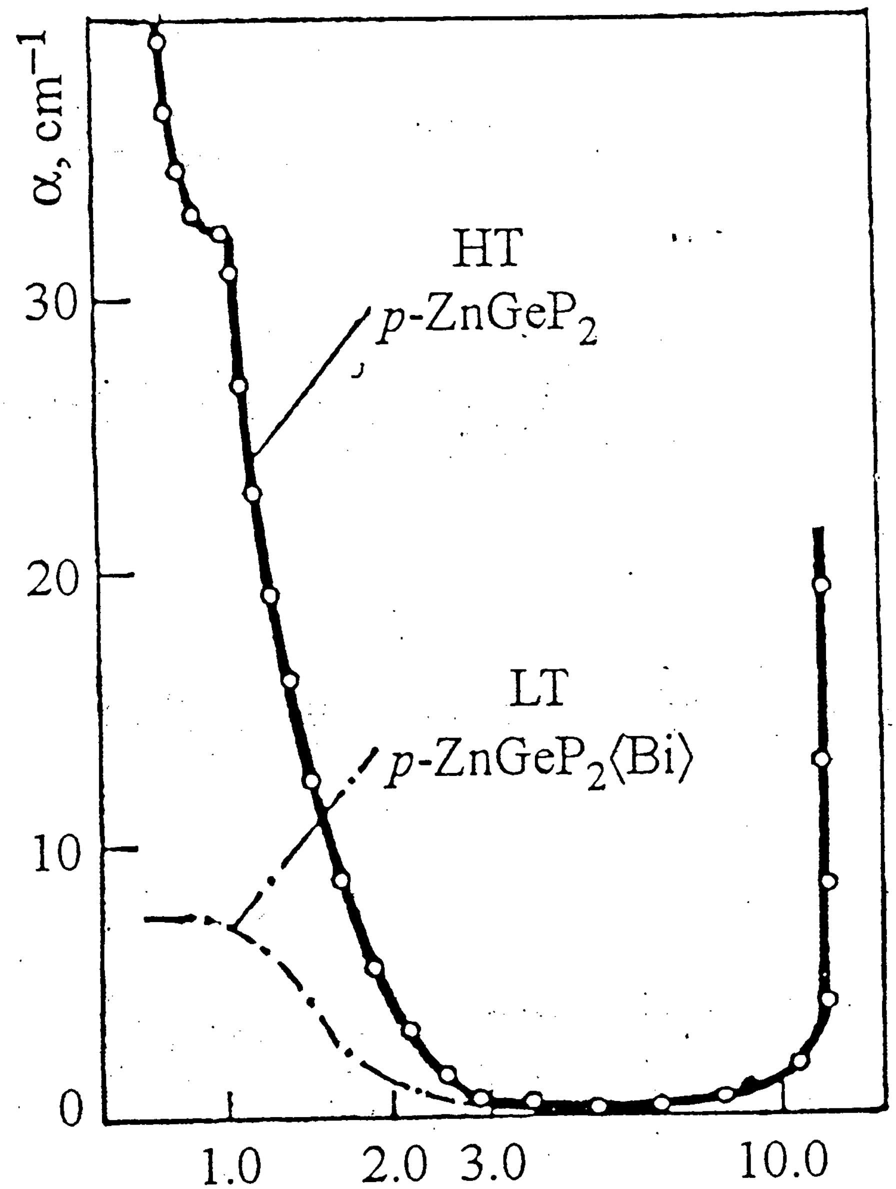

Optical absorption spectra
of the LT grown $ZnGeP_2$ <Bi>
and HT grown *p*-$ZnGeP_2$ single crystal
obtained by standard technique.

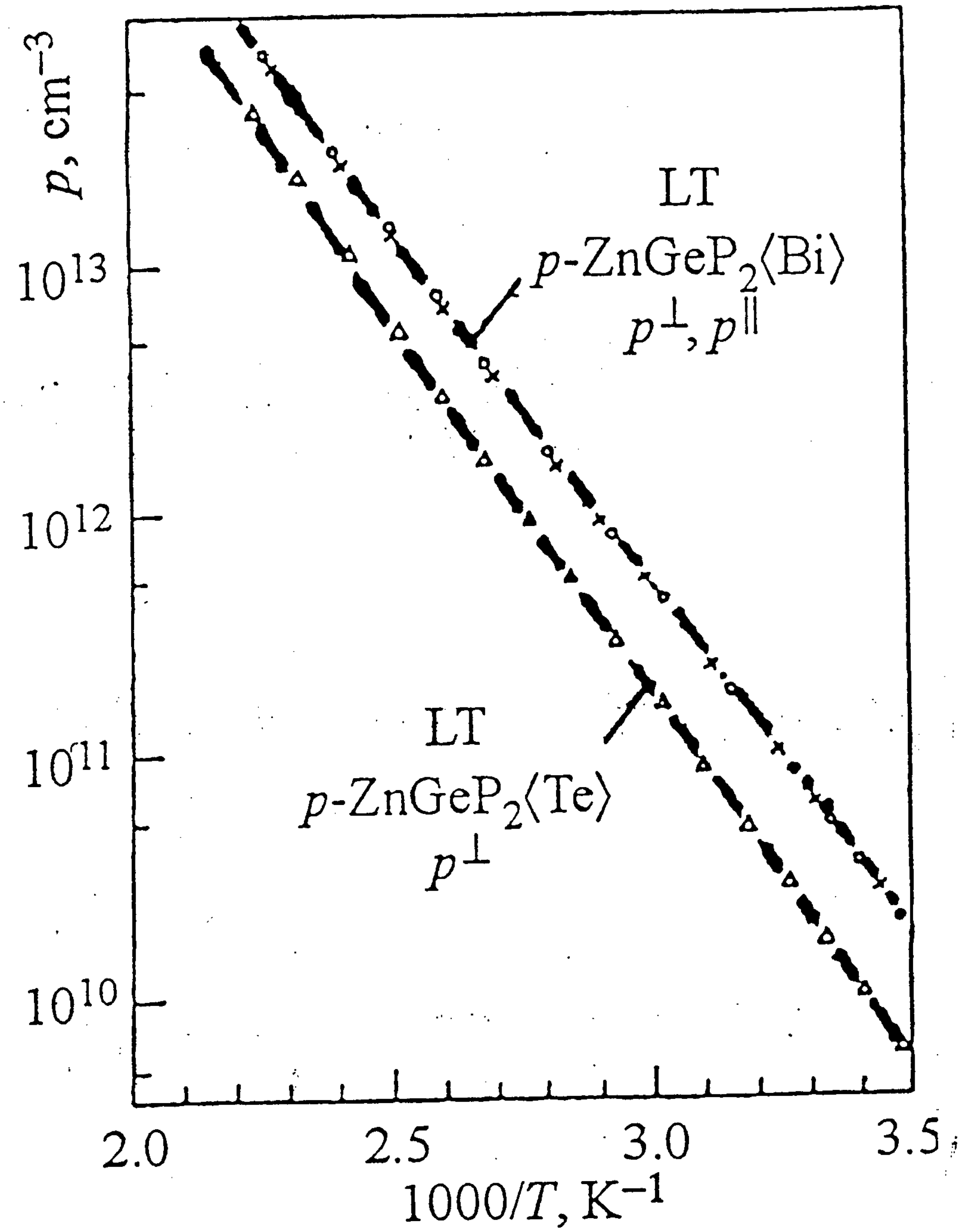

Temperature dependence
of the hole concentrations
of the two LT grown p-$ZnGeP_2$ <Bi> and <Tl>
samples.
Symbols: × and Δ for $p^{\|}$, o for $p^{\perp}$.

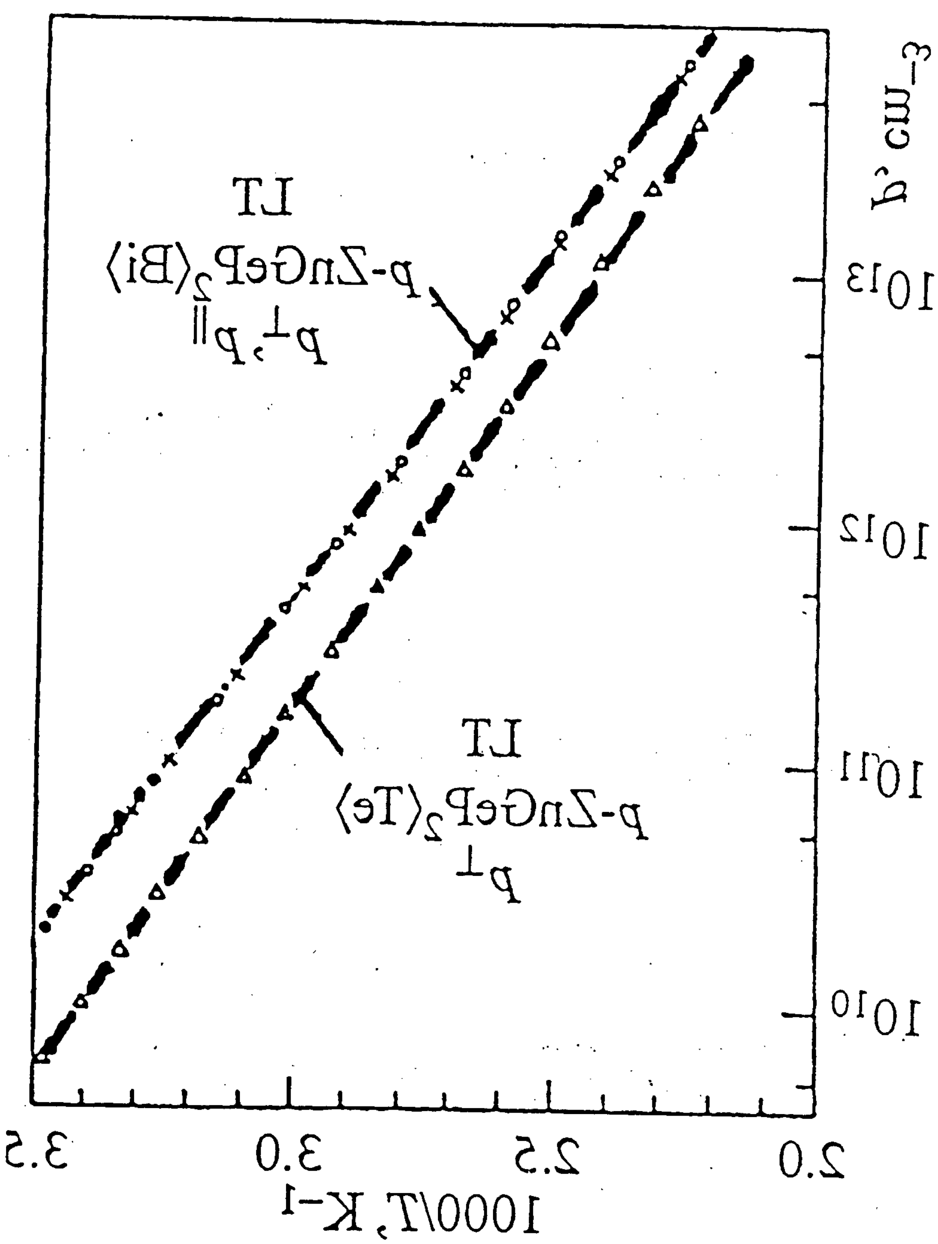

Temperature dependence
of the hole concentrations
of the two LT grown p-$ZnGeP_2$ <Bi> and <Tl>
samples.
Symbols: × and Δ for $p^{\parallel}$, o for $p^{\perp}$.

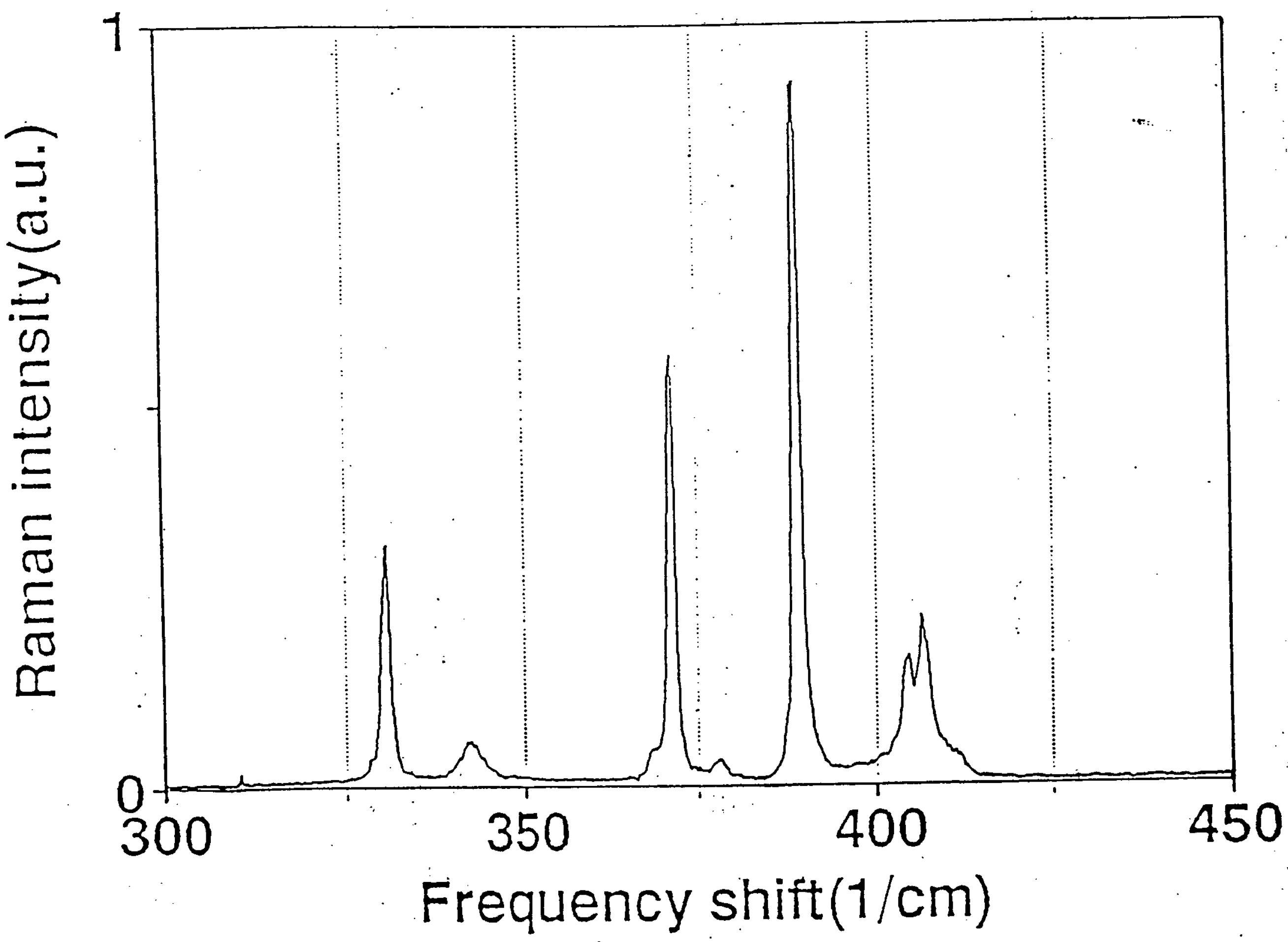

Raman spectra of p- $ZnGeP_2$ single crystals grown by low temperature method. T = 8 K. Excitation with the 514.5 nm line of an Ar+ laser, 100 mW, with slits width 0.9 1/cm .

Table IV. Symmetry assignments and frequencie[illegible] the optical pho[illegible]ns (in cm^{-1}) in Zn[illegible]$_2$ obtained from the Raman scattering (RS)and infrared reflection (IR)

Symmetry of the mode		Frequencies					
		RS[a]	RS[b]	RS[c]	IR[d]	RS[e]	
CP	ZB	T = 300 K	T = 300 K	T = 300 K		T = 300 K	T = 8 K
Γ_5	[X_5]	94 (TO+LO)	96 (TO+LO)	94 (TO+LO)		93.2	95.4
Γ_3	[W_2]	112	119	121		118.2	
Γ_5	[W_4]	142 (TO+LO)	142 (TO+LO)	143 (TO)	142(TO)	141.3	143.4
				144 (LO)	142.5(LO)		
				166*			
Γ_5	[W_3]	202 (TO)	201 (TO)	204 (TO)	205 (TO)	198	
		204 (LO)	202 (TO+LO)	205 (TO+LO)			
			203 (LO)	206 (LO)	208 (LO)	206.5	
Γ_3	[W_2]		248	249		327.4	329.8
Γ_1	[W_1]	327	328	329		334	
			328 Γ_5(TO+LO)	328 Γ_5(TO)	326.5 (TO)		
				330 Γ_5(LO)	330 Γ_5(LO)		
Γ_4	[W_2]	339 (TO)	338 (TO)	341 (TO)	342 (TO)	340	341.6
			357 (LO)	350 (LO+TO)		354.5	360
			346 (TO+LO)	361 (LO)	364.5 (LO)		
			357 (LO)				
Γ_5	[W_4]	368 (TO)	369 (TO)	369 (TO)	365.5 (TO)	368.5	371.8
		374 (LO)	374 (TO+LO)			375	377.8
			377 (LO)	377 (LO)	376 (LO)	377	377?
Γ_3	[X_3]		390				
Γ_5	[Γ_{15}]	385 (TO)	387 (TO)	387 (TO)	387.5 (TO)	384.7,385.5	389
		402 (LO)	393 $\Gamma_5 + \Gamma_4$(TO)	405 (LO)	406 (LO)	402.8	404.3
				395 [qΓ_5(TO)]***			
Γ_4	[Γ_{15}]	399 (TO)	401 (TO)	401 (TO)	397.5 (TO)	400.3?	405.2
		408 (LO)		411 (LO)	414.5 (LO)	407	
			403 Γ_5(LO)			412?	
			406 $\Gamma_5 + \Gamma_4$(TO)	396 [qΓ_4(TO)]			
			408 Γ_4(LO)	408 [qΓ_5(LO), qΓ_4(LO)]			

[a] References 53.
[b] References 52 and 56.
[c] References 50.
[d] References 49 and 5).
[e] our results.

EPR AND ENDOR CHARACTERIZATION OF DONORS AND ACCEPTORS IN $ZnGeP_2$

Larry E. Halliburton
Kevin T. Stevens
Nancy C. Giles

Physics Department
West Virginia University

Nonlinear Optical Materials Workshop
DERA
Malvern, UK
September 20 – 21, 1999

Work supported by Air Force Office of Scientific Research (in conjunction with the Materials Directorate at Wright-Patterson AFB) and by the National Science Foundation.

Work performed in cooperation with Lockheed Sanders.

Ni^+ in $AgGaSe_2$

Electron Paramagnetic Resonance

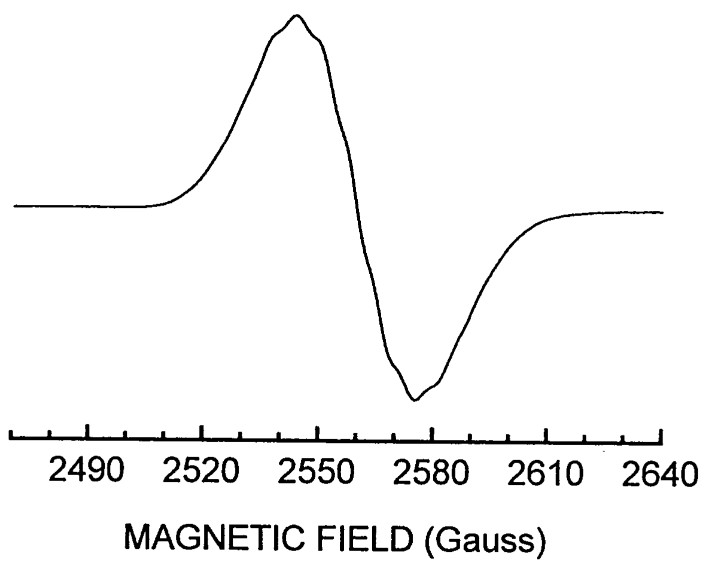

Infrared Absorption

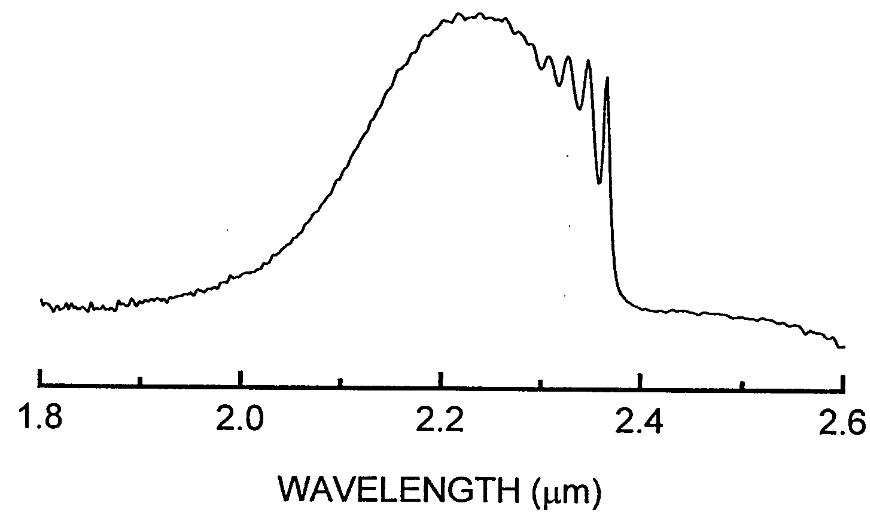

Correlation of Optical Absorption with EPR Signals from the Zinc Vacancy

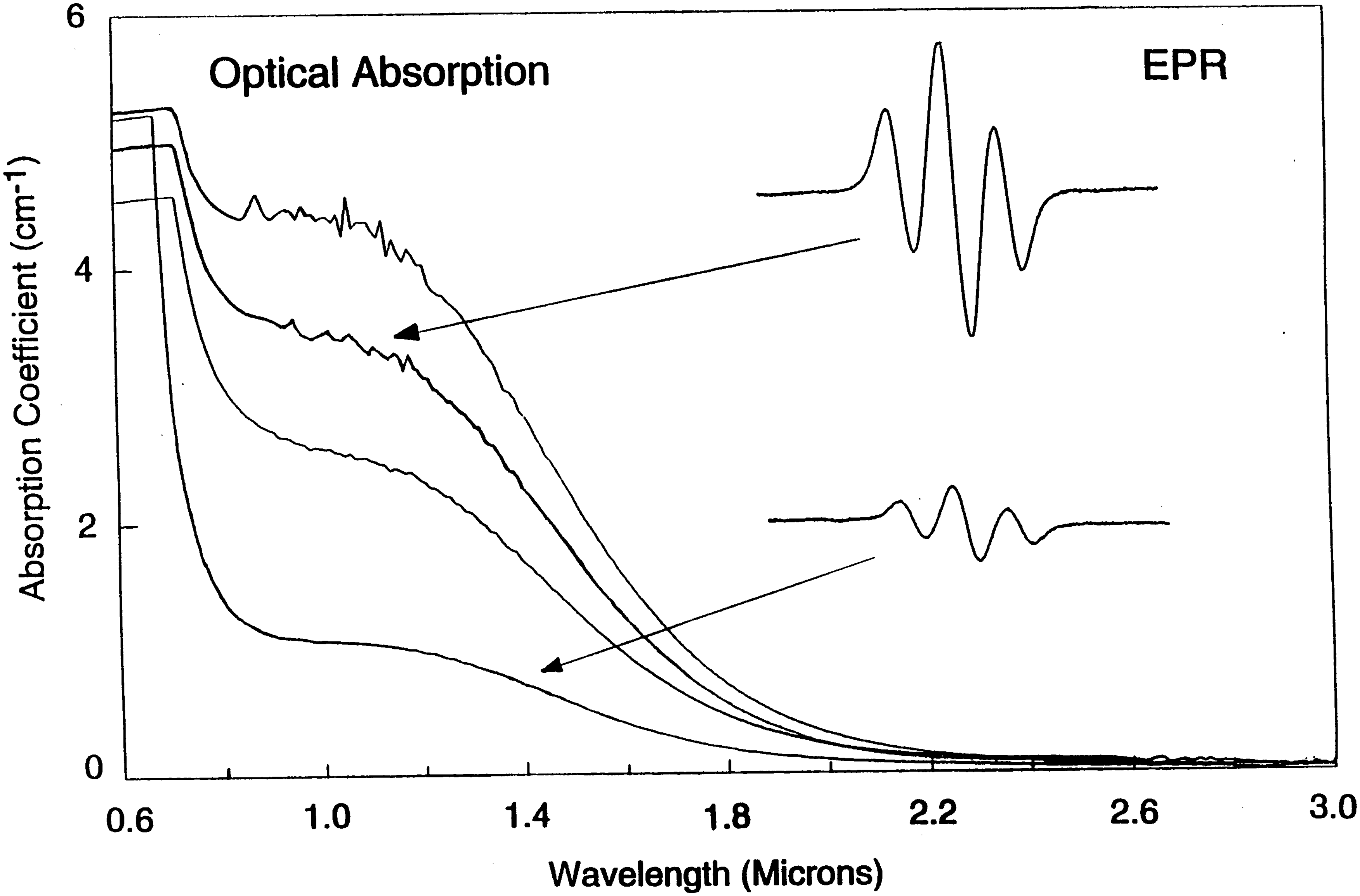

V_{Zn} EPR Intensity versus Absorption at 1 μm

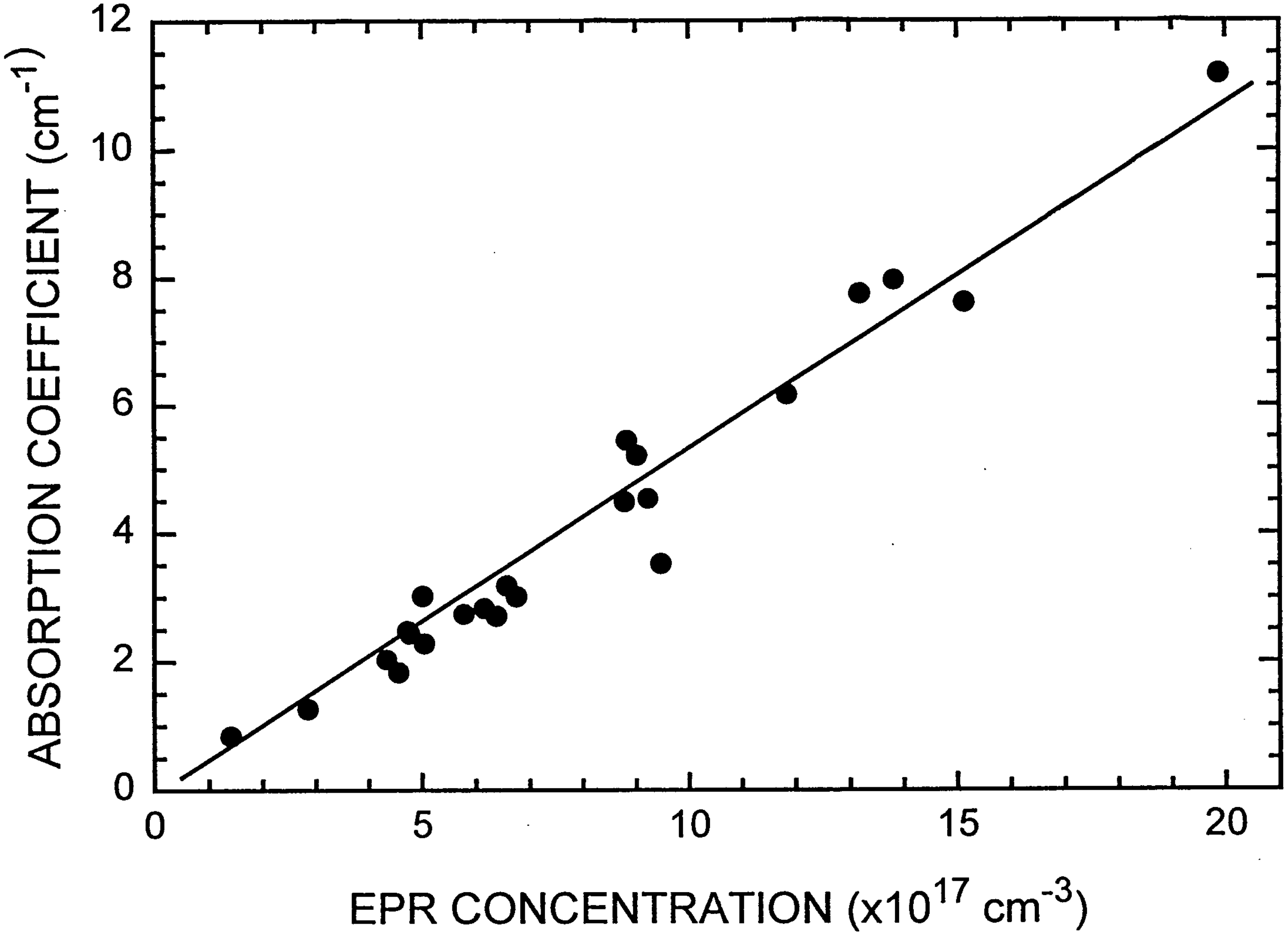

SUMMARY OF DONOR AND ACCEPTOR PROPERTIES

1. Zinc vacancies are the dominant acceptor in $ZnGeP_2$.

   - Both V_{Zn}^{-} and $V_{Zn}^{=}$ charge states are present.
   - There is no spectroscopic evidence to date for V_{Zn}^{0} in as-grown crystals.

2. Dominant donors are phosphorus vacancies and germanium antisites.

   - V_P^{+} and Ge_{Zn}^{++} in the dark.
   - V_P^{0} and Ge_{Zn}^{+} with light.

3. Effect of laser light:

   - 633 nm -- increases V_{Zn}^{-} signal
     creates V_P^{0} and Ge_{Zn}^{+} signals
   - 1064 nm -- decreases V_{Zn}^{-} signal
     creates V_P^{0}
     does not create Ge_{Zn}^{+}

Possible Optical Absorption Mechanisms

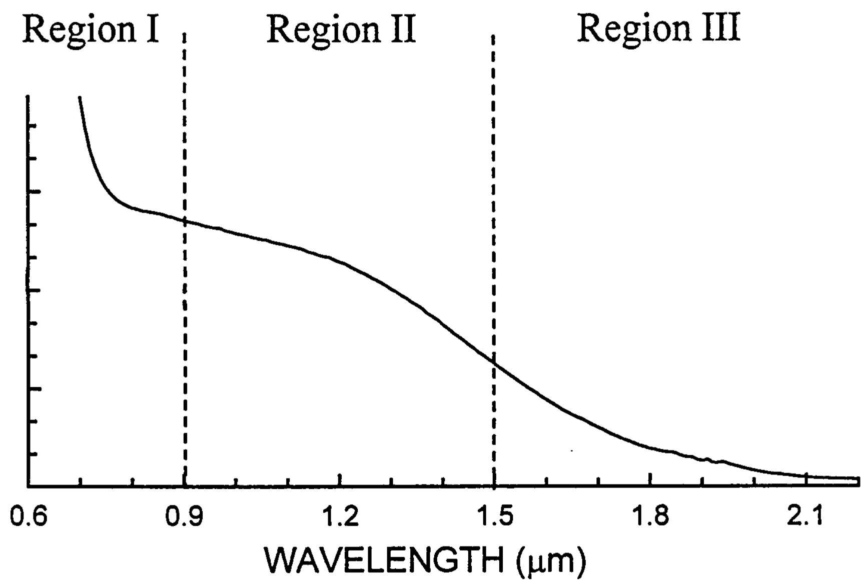

Region I

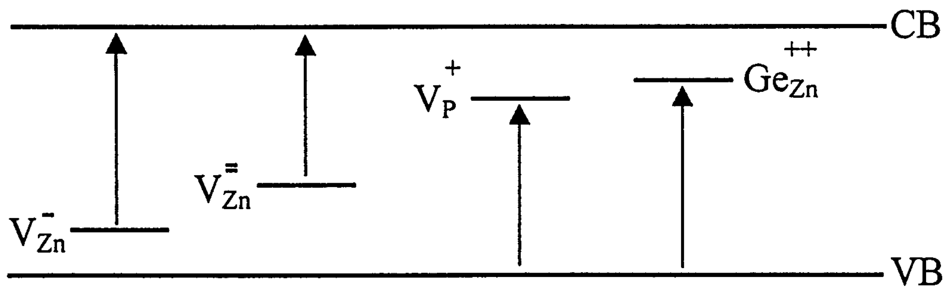

Region II

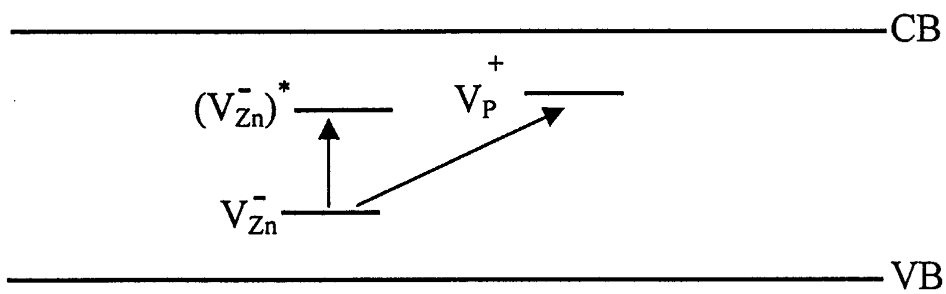

Region III

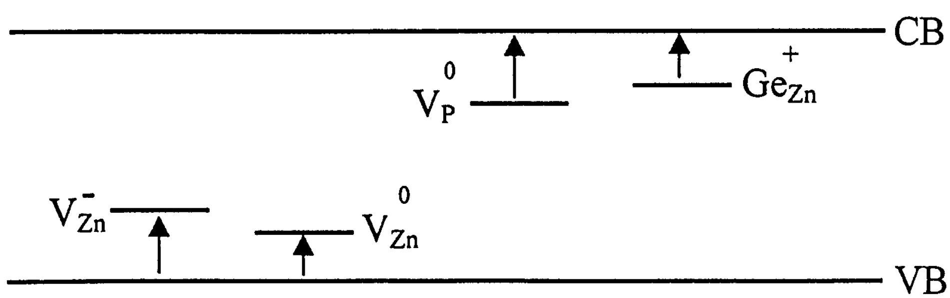

Recent Advances in Chalcopyrites for Mid- to Far-IR Frequency Conversion

P. G. Schunemann and T. M. Pollak

SANDERS
A Lockheed Martin Company

Presented at the 1999 Nonlinear Optical Materials Workshop, (NLO 99), DERA, Malvern, UK, Sept. 20, 1999

Work supported L.N. Durvasula at DARPA (via the Air Force Research Laboratory Materials Directorate contract No. F33615 -94-C-5415) and Sanders Internal R&D Funding

Chalcopyrite Crystal Growth at Sanders

- For the past 10 years we have focused on crystal growth and processing of bulk chalcopyrites for nonlinear optical (NLO) frequency conversion:
  - Frequency doubling of CO_2 Lasers (SHG)
  - "Wavelength doubling" of 2um solid state lasers (OPO)
- The Goal:
  - Produce efficient mid-IR lasers operating in regions of high atmospheric transmission
- Applications:
  - Laser radar, remote sensing, etc.

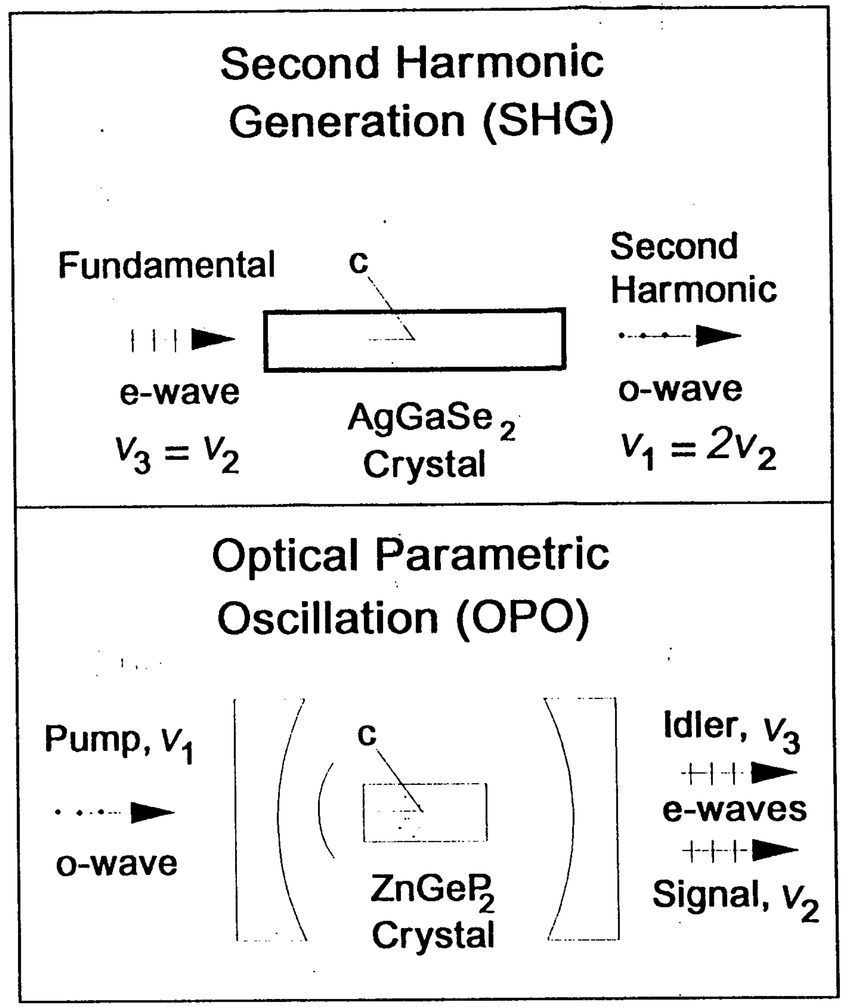

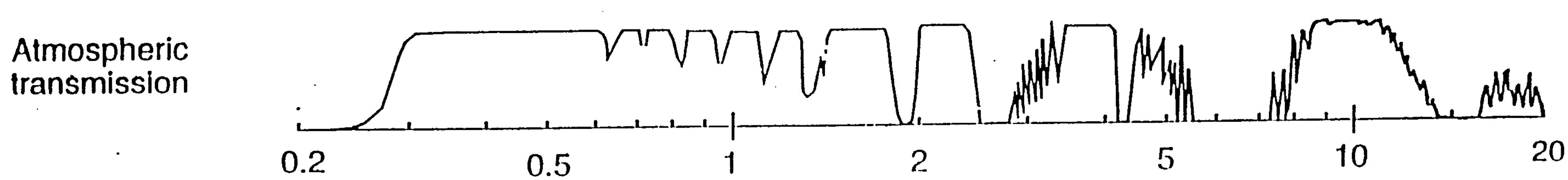

Strategies for Improved Infrared NLO Materials

2um-pumped OPO's

- Material of Choice: $ZnGeP_2$
  - Highest NLO Coefficient with sufficient band gap (d_{14}=75 pm/V)
  - High Thermal Conductivity (0.35W/cmK)
  - Reduced Losses ----> Efficient, High Power Output
- Alternatives for better performance:
  - **None:** Continue to Reduce $ZnGeP_2$ Near-IR Absorption

CO_2 Doubling

- Material of Choice: $AgGaSe_2$
  - Respectable NLO Coefficient (39 pm/V)
  - Wide transparency and phase-matching range (.78-18um)
  - Low absorption Losses
- Alternatives for better performance:
  - $CdGeAs_2$: Highest Nonlinearity (d_{14}=236 pm/V) → Reduce Absorption Loss
  - $Ag(Ga,In)Se_2$: Adjust Birefringence for Noncritical Phase-Matching (NCPM)
  - ABX_2: Continue Search for New Materials

Horizontal gradient freeze growth led to advances in NLO chalcopyrites

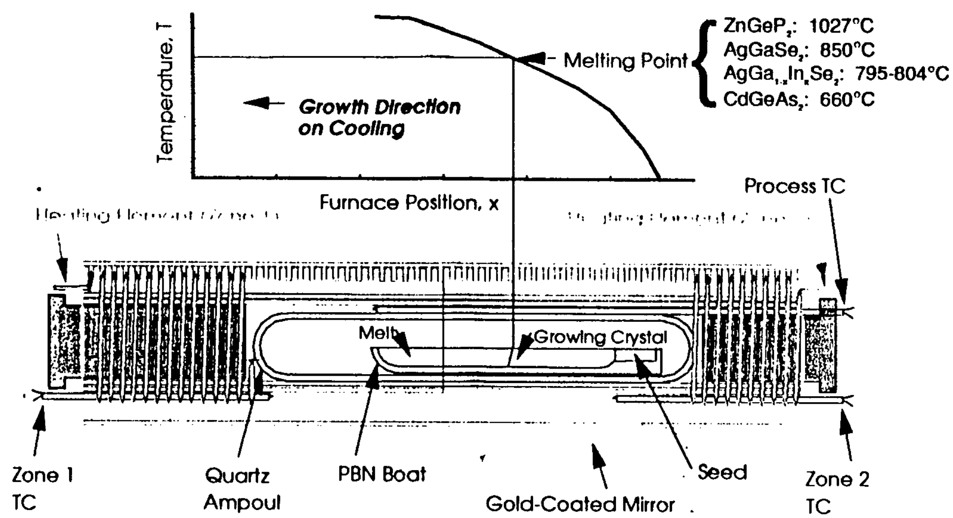

HGF Approach: Key Aspects

- **Low thermal gradients**
  - Minimize vapor transport
  - Eliminate cracking due to anisotropic thermal expansion
- **Transparent Furnace**
  - Simplifies the seeding process
  - Allows *in situ* monitoring of the S/L interface shape & position
  - Facilitates interactive growth (secondary grains can be re-melted)
- **Seeded growth**
  - Eliminates initial polycrystallinity due to supercooling
  - Optimizes orientation to accommodate negative c-axis thermal expansion
  - Enables growth along phase matching direction for max. device length & yield

$ZnGeP_2$: Recent Advances

Improved Single Crystal Yield

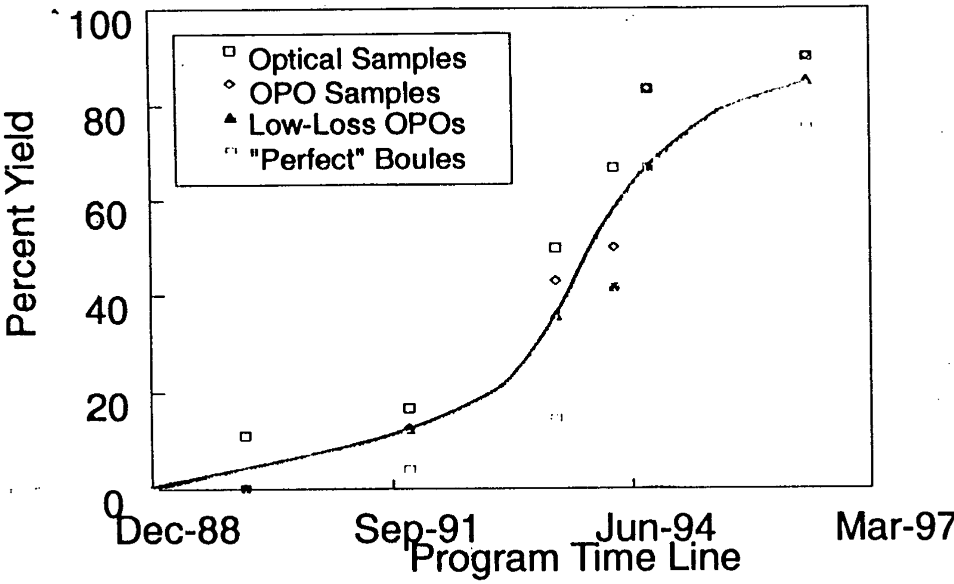

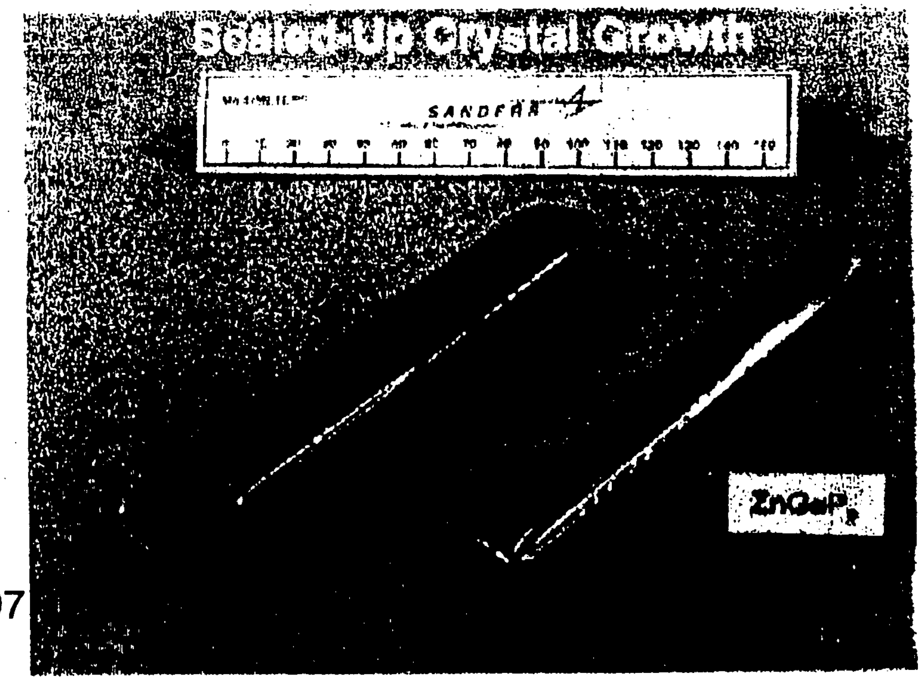

Breakthrough Reductions in Loss

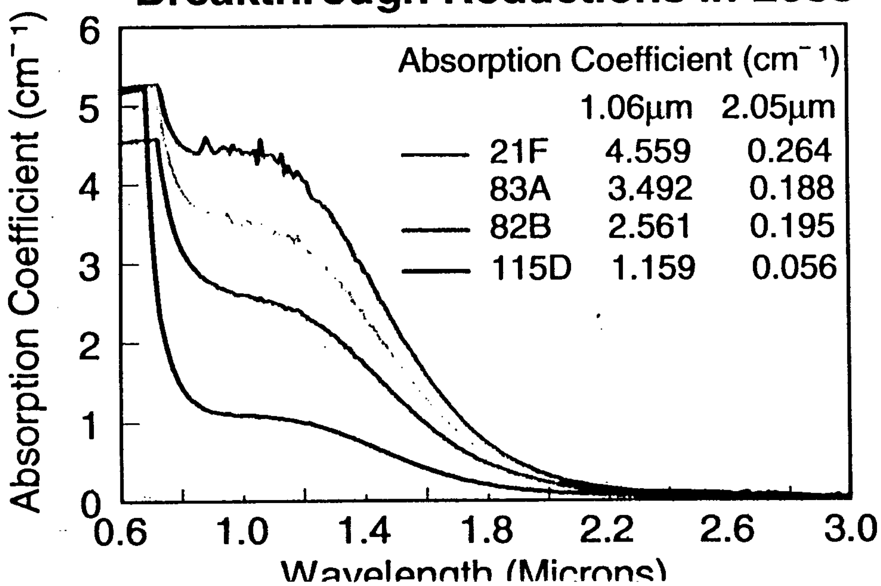

Enhanced OPO Performance

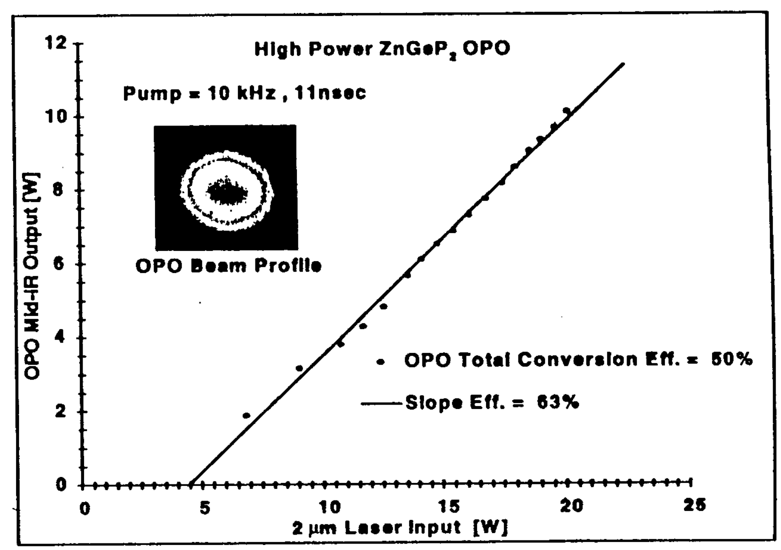

“Phase-Matched” Crystal Growth of $AgGaSe_2$

- Vertical Bridgman growth of $AgGaSe_2$ requires seeding along c-axis for unconstrained thermal expansion during cool-down
- The Horizontal Gradient Freeze (HGF) technique allows “phase-matched” growth along device orientation, yielding longer interaction lengths and minimal waste

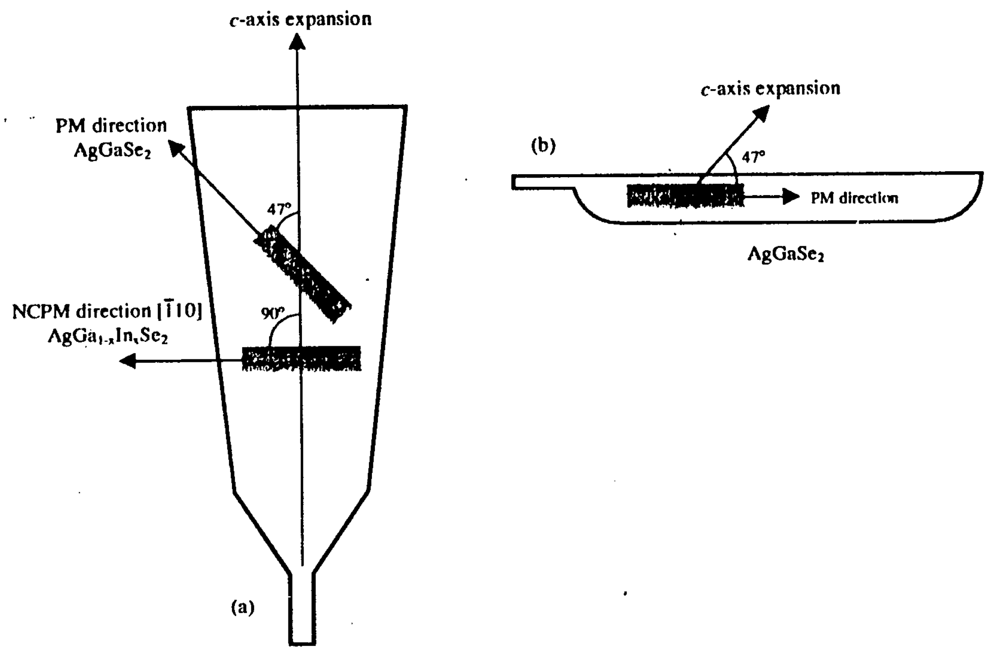

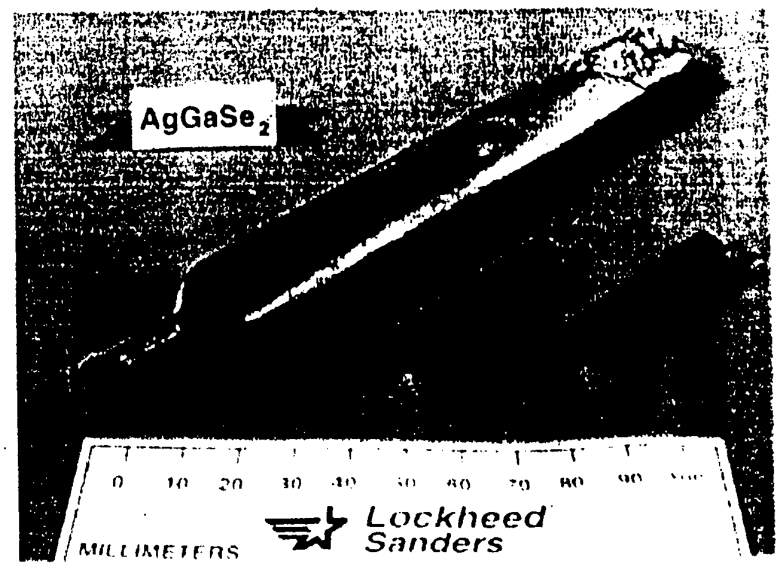

$CdGeAs_2$: Development Milestones

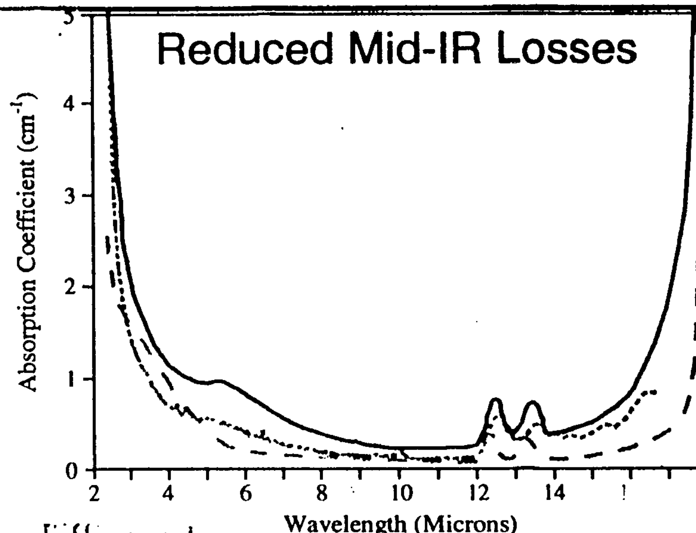

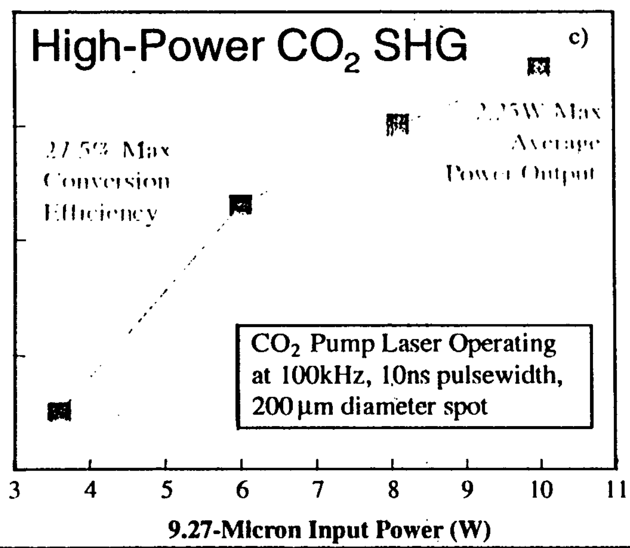

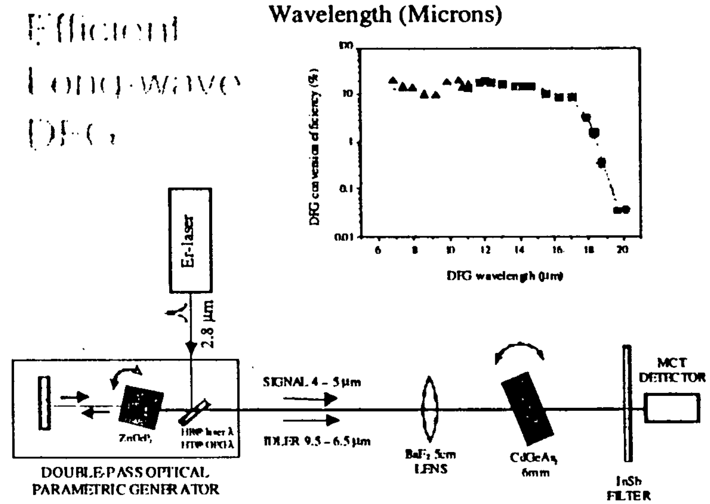

SANDERS
A Lockheed Martin Company

Segregation of Absorbing Defects in $CdGeAs_2$

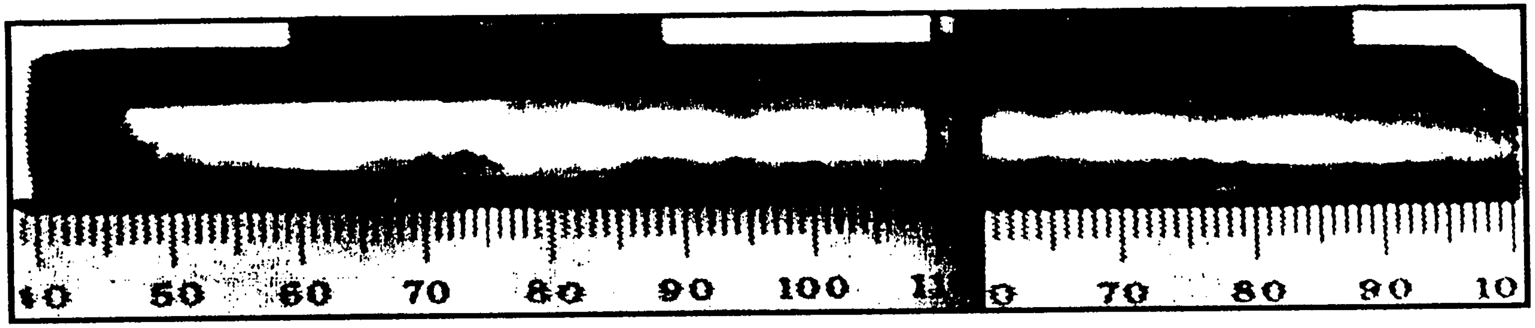

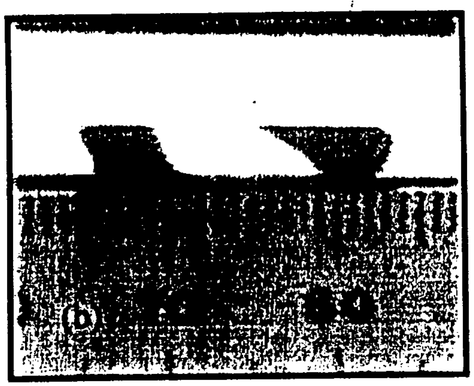

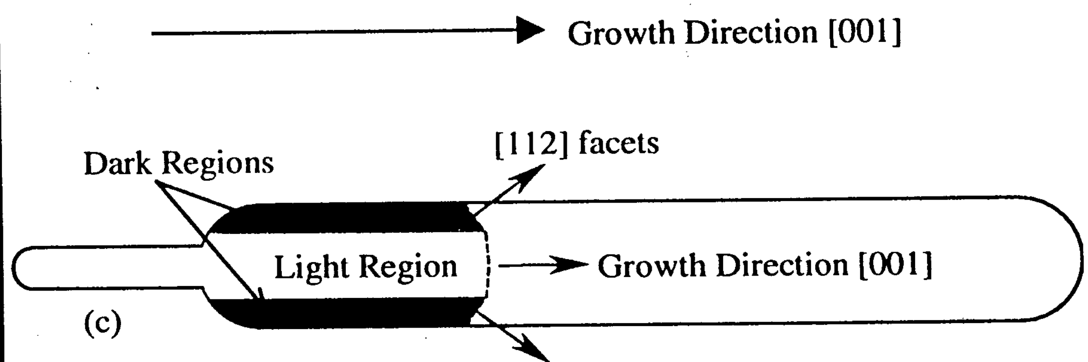

$CdGeAs_2$: Recent Advances

Reduced Mid-IR Absorption (Low-Loss Central Core)

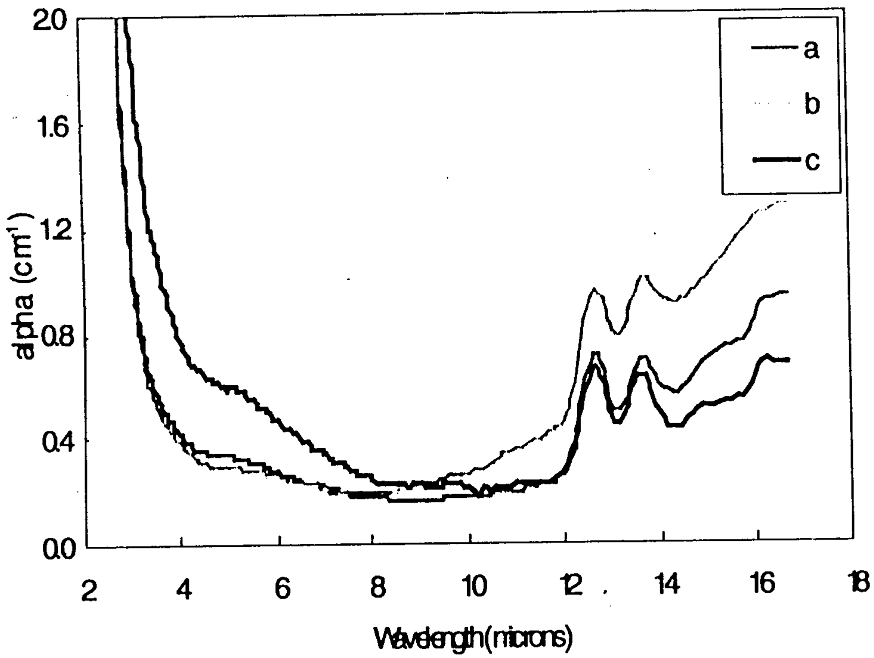

Efficient CO_2-Doubling:

η = 53% at 77K

η = 28% at 273K

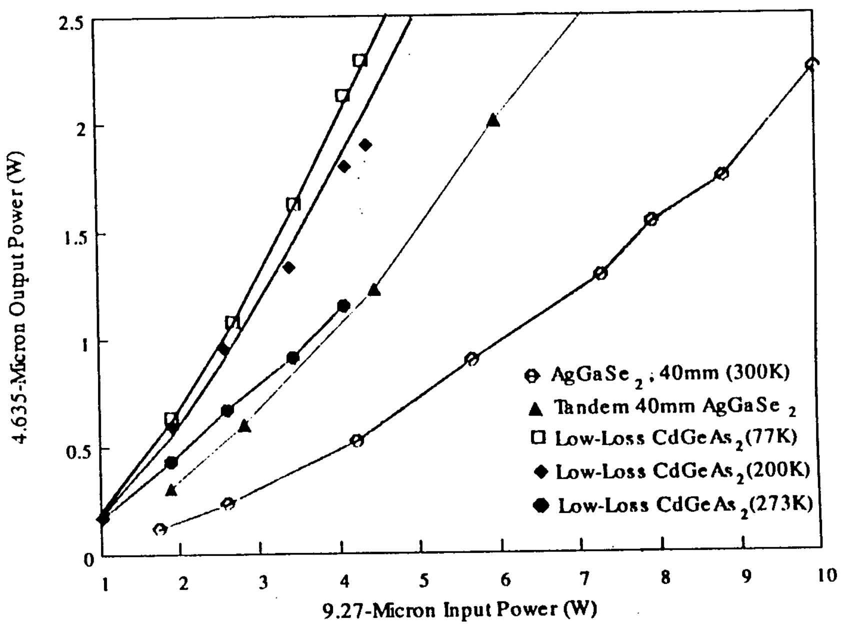

$AgGa_{1-x}In_xSe_2$: Engineered Birefringence for NCPM

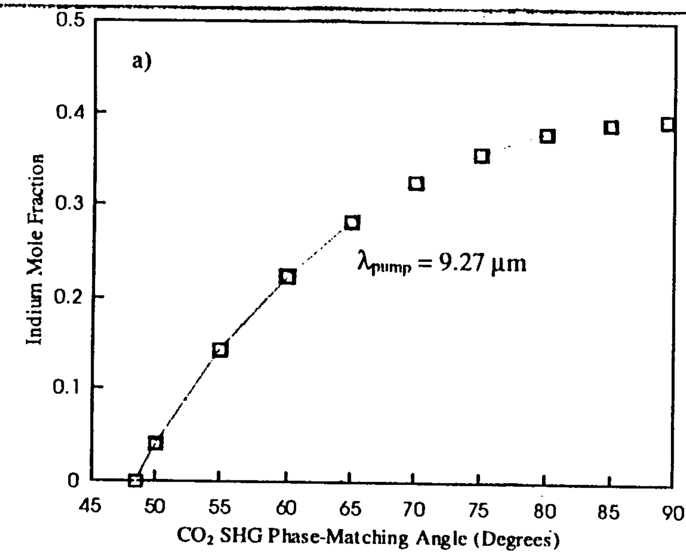

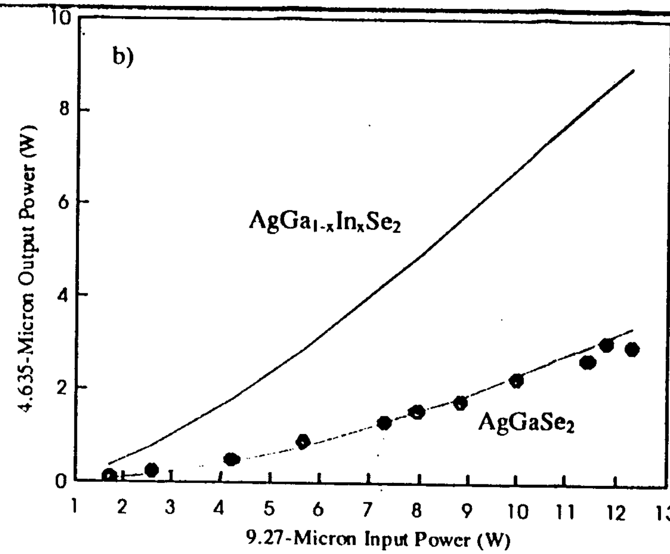

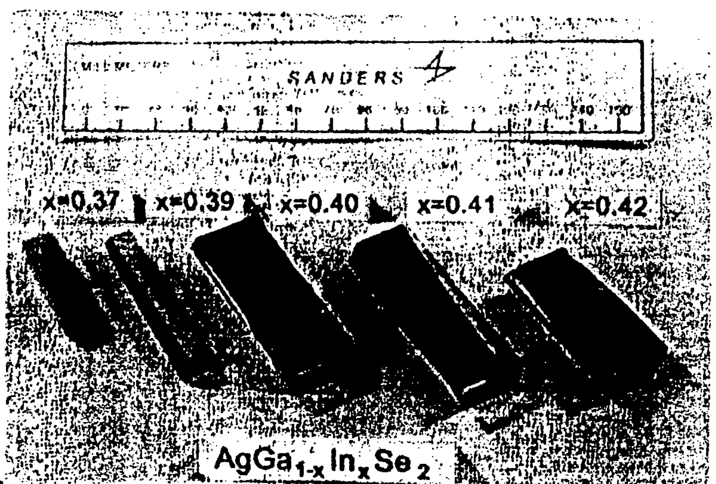

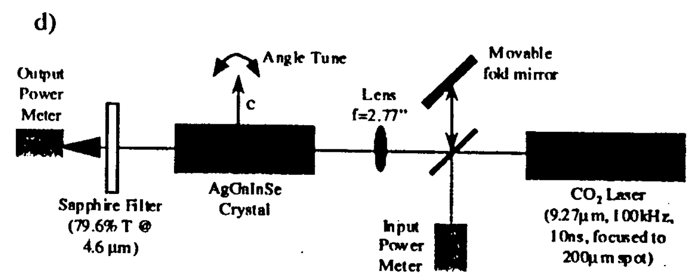

NCPM at x=0.42 (melt)

Reflection & Scattering Losses → η =1.8%

AgGaTe$_2$: a promising new nonlinear optical crystal

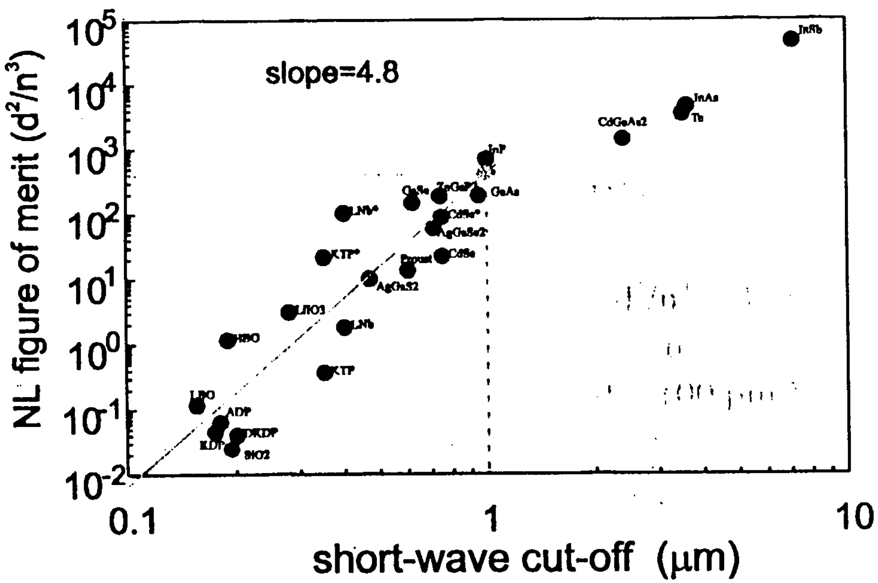

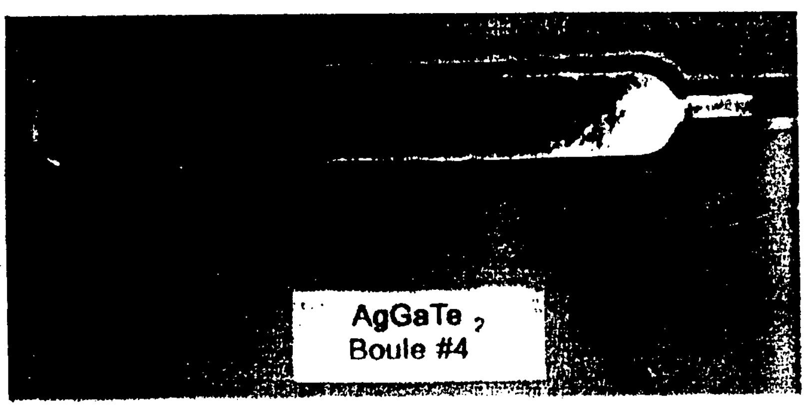

- **Motivation:**
  - Telluride analog of $AgGaS_2$ & $AgGaSe_2$
  - Substitution by Te should triple the NL coefficient and shift the transparency range further into the IR (~1-20μm)
- **Objectives of Research:**
  - Produce large, crack-free single crystals
  - Determine if birefringence is sufficient for phasematching
- **Approach:**
  - HGF Growth in Transparent Furnace
  - Fabricate prism, measure Δn

Summary

- Recent crystal growth advances have established chalcopyrites as the NLO materials of choice for mid- to far-IR laser frequency conversion:
  - Large crack-free single crystals (up to $16 \times 28 \times 140 mm^3$) of $ZnGeP_2$, $AgGaSe_2$, and $CdGeAs_2$ can be reproducibly grown by the HGF technique
  - Substantial reductions in absorption and/or scattering losses have been achieved by feed purification, compositional control, & post-growth annealing
  - Improved crystal quality has resulted in outstanding NLO device performance
- The birefringence of mixed crystals ($AgGa_{1-x}In_xSe_2$) can be engineered to achieve non-critical phase-matching (NCPM)
- The search for new materials has led to promising NLO crystals such as $AgGaTe_2$, $CdGa_2S_4$, and $CdGa_2Se_4$
- Dy^{3+}:$CaGa_2S_4$ was demonstrated as the first sulfide mid-IR laser host

Development of Technology of $ZnGeP_2$ Single Crystal at Institute for Optical Monitoring SD RAS

By Alexander I. Gribenyukov, Galina A.Verozubova, and Valentina V.Korotkova

Laboratory of Optical Spectroscopy

Institute for Optical Monitoring

Tomsk Branch of Siberian Division

Russian Academy of Sciences

TR 3

IOM	The main directions of IOM activity & interests	• Theoretical and experimental investigations of climatic and ecological changes under effect of natural and human factors • …………
	The basic theme of the noted direction of IOM's activity	• Development of new techniques and technologies for environment remote sounding • …………
	Divisions of the basic theme	• Development of optical monitoring systems based on new generation of tunable coherent radiation sources working in the middle IR spectral range. • …………
LOS IOM	The main task	Provision of IOM works on development and multiplication of the new optical systems by optical materials needed
	The basic theme	Development of high yield and reliable technologies for production optical materials with controllable physical properties
	The main points of contents of basic theme	1. Development of high yield technology of single crystal growth 2. Investigations of possibilities of controllable manage by physical properties of material due to purposeful changes (variations) of technological parameters on all stages of crystals production – at synthesis, at crystal growth, at postgrowth annealing

TR 6

First Long-term Program

High priority problems related to $ZnGeP_2$ technology

Creation (development) of the growth equipment ensured high reproducible temperature profiles. The equipment could be working with high reliability.	Creation(development) of a new moderated (modified) synthesis technique which could assure a production of as-synthesis $ZnGeP_2$ with controllable (managed) composition.	Development of high yield single crystal technology of ZGP growth
1987 - 1988	1988 - 1991	1989 - 1994
• First prototype • Series of 6 VB furnaces	• Temperture of reaction start • Intermediate phases • Reaction velocity	• Choice of container material • Choice of seed orientation • Computer calculations of temperature profiles • K_L/K_S ratio evaluation • Calculations & measurements of real growth rate

TR9. P_4 and Zn flows in non-isothermal closed synthesis system.

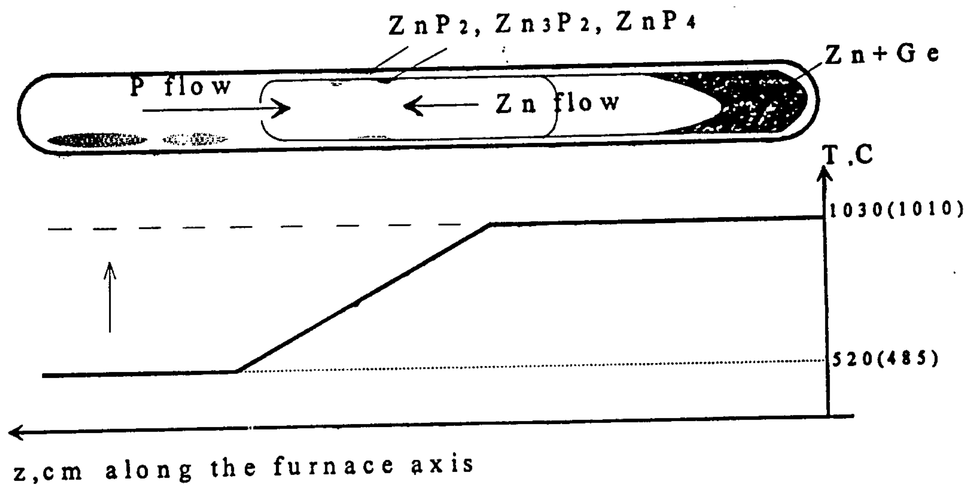

TR10 – Time dependence of expenditure velocity of P4 vapour under pressure of 10-12 atm with Zn-Ge melt at 1010 C .

Hot zone temperature - 1010 °C
Cold zone temperature - 515 °C (P_{P4} = 10 atm)

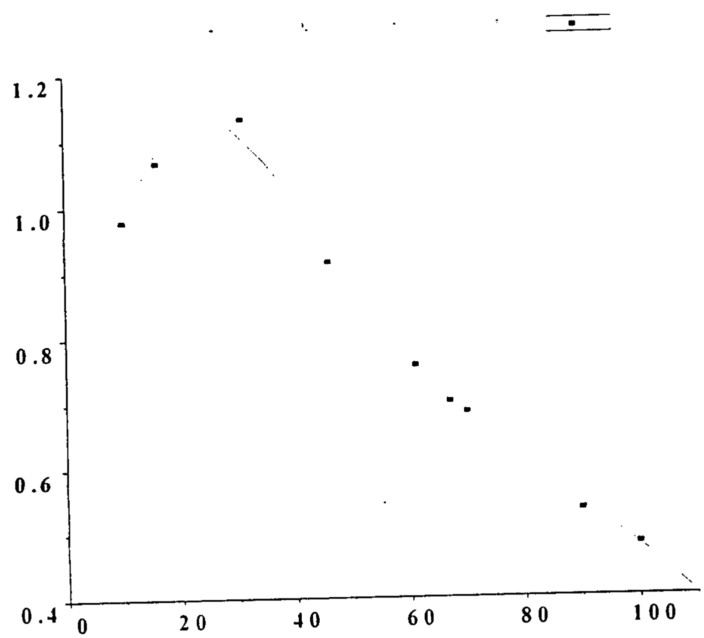

TR13

Distribution of growth failures on causes

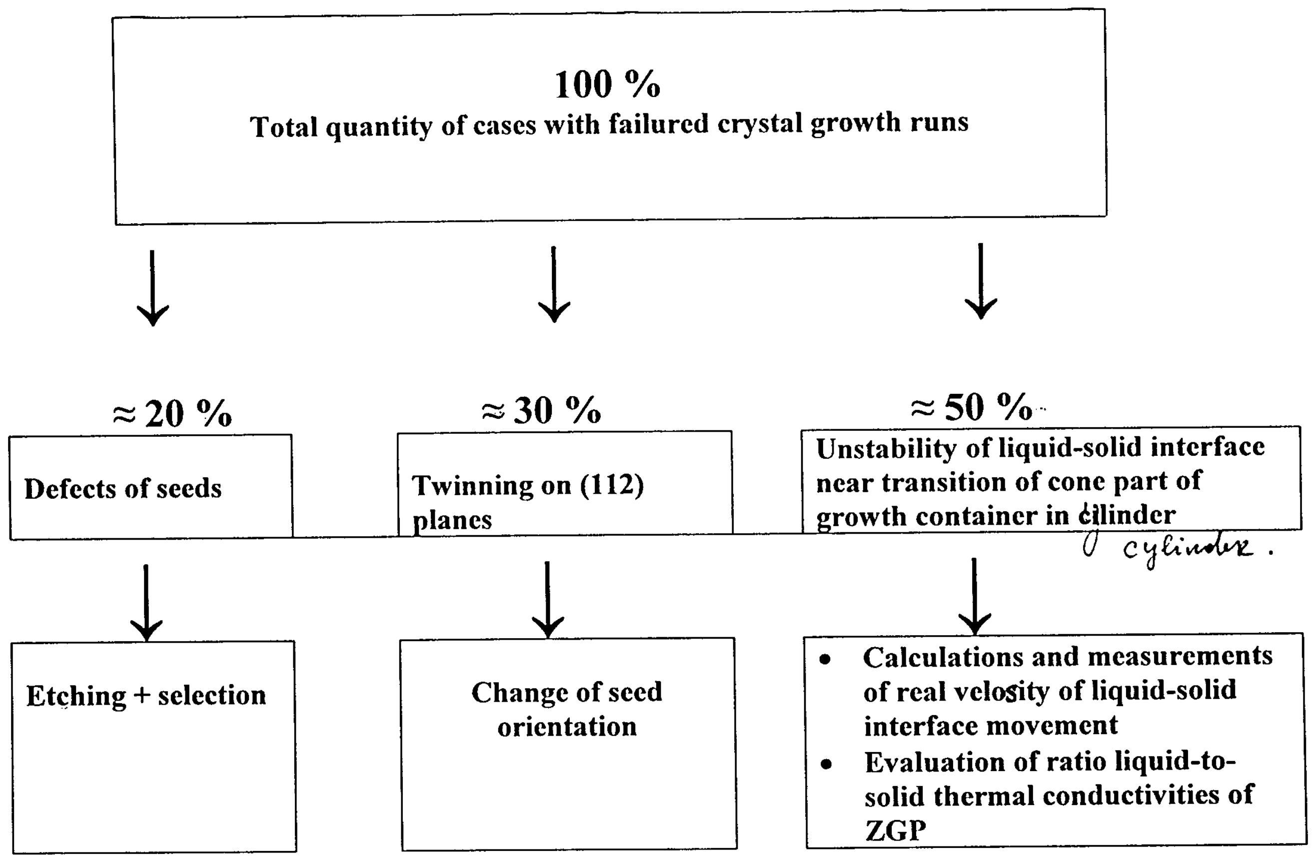

TR12 – Probability distribution of ZGP crystalline blocks enlarged along growth axis in VB-method with spontaneous nucleation.

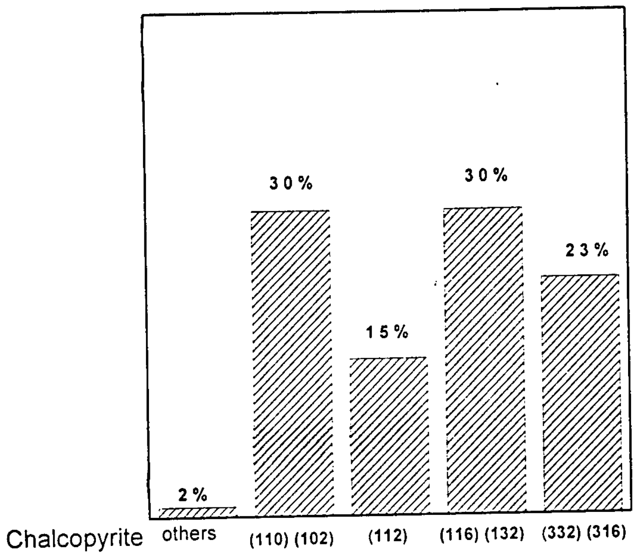

TR14 – The image of growth container surrounding structure for computer calculations.

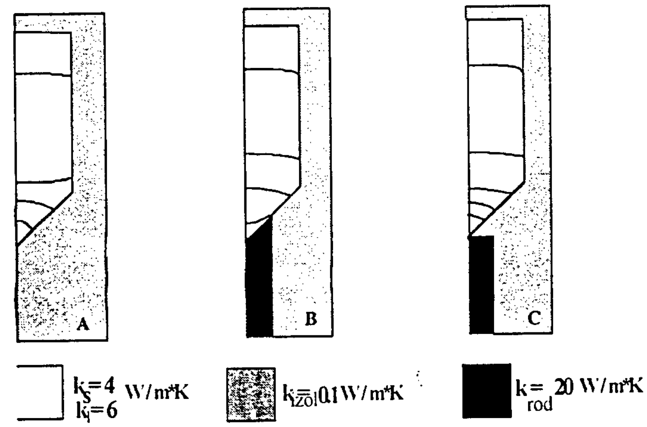

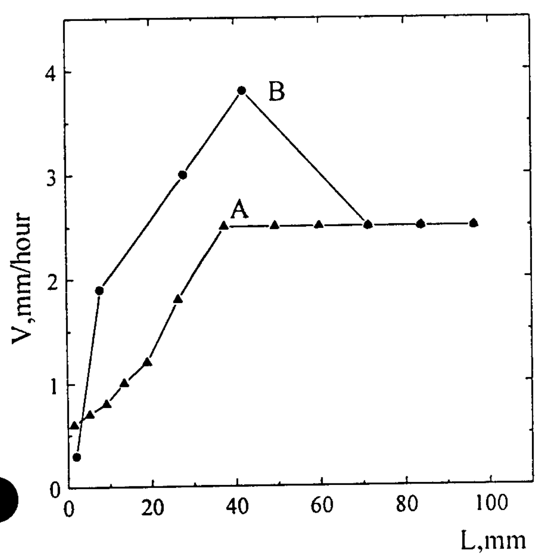

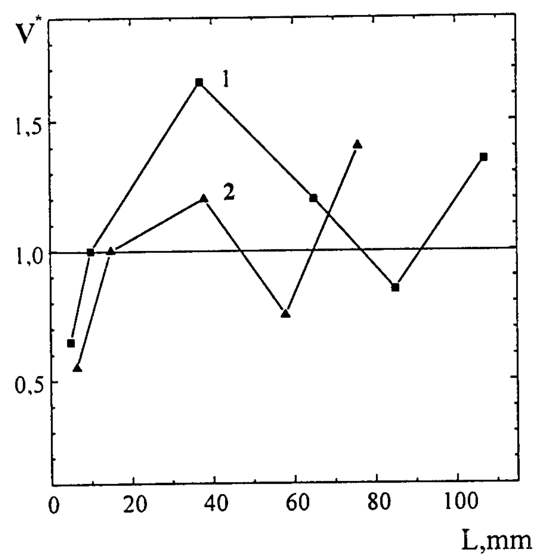

GF method:
The isotherm crystallization rate for container with A and B surrounding structure.
Cooling rate – 1 °/hour.

VB method:
Distribution of isotherm crystallization rate (in units of mechanical movement rate) along crystal axis.
A-type of surrounding structure ,$\varnothing_{furnace}$=6 cm;
1 – calculation's data ,$\varnothing_{ampoule}$=3 cm;
2 - experiment's data, $\varnothing_{ampoule}$=2 cm;

steady

R15. Diagram of stady state temperature distribution

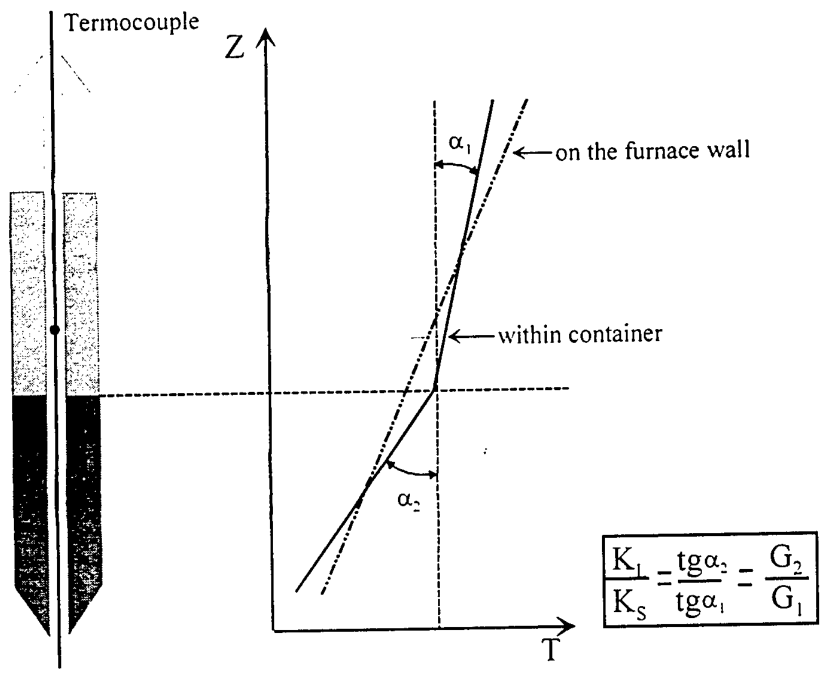

Material	Linear regression coefficients				Calculated values	
	Ts	Gs	TL	GL	T_{mel}	K_L/K_S
Ge	942.42	4.6	940.51	2.7	937 ± 1	1.7 ± 0.1
$ZnGeP_2$	2009.9	16.24	1807.53	12.9	1027 ± 1	1.3 ± 0.1

Literature data for Ge : K_L/K_S = 2.93 [3]
Corrected ratio for $ZnGeP_2$: K_L/K_S = 2.3

Tr 16

The Second Long-term Program

1	2	3	4	5
Studies of properties of the ZGP crystals doped by own components from melt directly	Studies of properties of the ZGP crystals doped by own components from vapor phase due to variation of composition and pressure above melt	Studies of thermal annealing conditions influence on the physical properties of the ZGP crystals	Determination of temperature dependencies of partial pressures of Zn and P_4 above ZGP melt.	**Others:** • Nature of twins • Nature of ultrasonic enlightenment • Stability of irradiation defects under laser radiation
↓	↓	↓	↓	↓
ELM 1009	In progress	ELM 1165	In progress	Current Contract (Is continued)
↓	↓	↓	↓	↓
• Tensions • Inelastic increase of unit cell volume under annealing • In as-grown state optical quality is the best for ZGP grown from stoichiometric composition	**WILL BE PRESENTED BY ANOTHER REPORT**	• Optical properties of annealed ZGP are function of melt composition used at crystals growth • crystals enriched by Ge indicated the most enlightenment at annealing	• Partial pressure of Zn above ZGP melt is not negligible	**WILL BE PRESENTED AFTER FINISH**

TR17 Some Results of investigations of ZGP crystals doped from melt. Measurements were made in DERA. The crystals were grown in IOM

Crystal	Dopant (P_4-pres. atm)	Temperat. gradient DT/dx, °C/cm	Unit cell volume, Å^3	Unit cell volume difference ($V_{ltf} - V_{ftf}$) Å^3	Absorpt. coeff. at 2.06 μm cm^{-1}	Absorpt. coeff. difference $\alpha_{ltf} - \alpha_{ltf}$ cm^{-1}	Derivative dα/dV, cm^{-1} Å^{-3}	Unit cell volume after annealing Å^3	Absorpt. coeff. after annealing cm^{-1}
89/3 ftf	**0.2 wt%Ge**	**5.2**	319.94861	-0.03872	0.431	0.016	**-0.465**	320,234	0.27 –meas. **0.298-calc**
89/3 ltf	(7.5)	**15.4**	319.90989		0.449				
91/2 ftf	**Stoich**	**1.5**	319.92818	+0.120006	0.332	0.129	**+1.07**	320,332	0.36 –meas. **0.764- calc.**
91/2 ltf	(7.1)	**7.5**	320.04824		0.461				
93/3 ftf	**0.2 wt%Zn**	**2.5**	319.98361	-0.04372	0.615	- 0.105	**+2.4**	320,190	0.53-meas. **1.11-calc**
93/3 ltf	(3.8)	>20	319.93989		0.510				

Seeds orientation is (116) for all grown crystals.

Annealing result in an increase of unit cell volumes, but expected change of absorption coefficient with the unit cell volume indicated only for sample enriched by Ge.

ZGP GROWTH FROM MELT:
THE VAPOUR PHASE COMPOSITION AND CRYSTAL PROPERTIES

G.A. Verozubova
A.I. Gribenyukov
Yu. F. Ivanov*

Institute for Optical Monitoring SD RAS
*Tomsk Polytechnical University

in collaboration with A.Vere, DERA, Malvern

The work was fulfilled under financial support
DERA, United Kindom

327°C – $ZnGeP_2$ starts to decompose

1038°C – $ZnGeP_2$ melting point *(Seb Fiechter, 1996)*

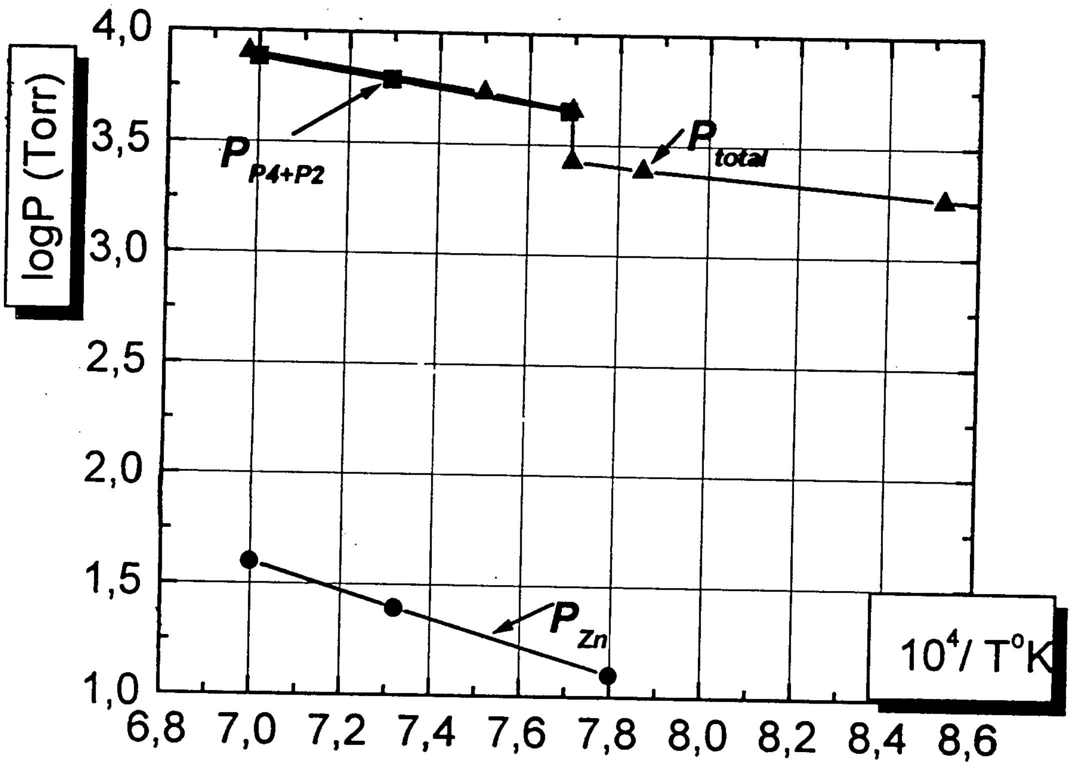

- The total pressure above $ZnGeP_2$ - P_{total} *(Buehler, 1971)* and partial pressures of Zn - P_{Zn} and P - P_{P4+P2} calculated from the regular solution theory (*Roenkov, 1975*): P_{Zn} =18 Torr at 1068C

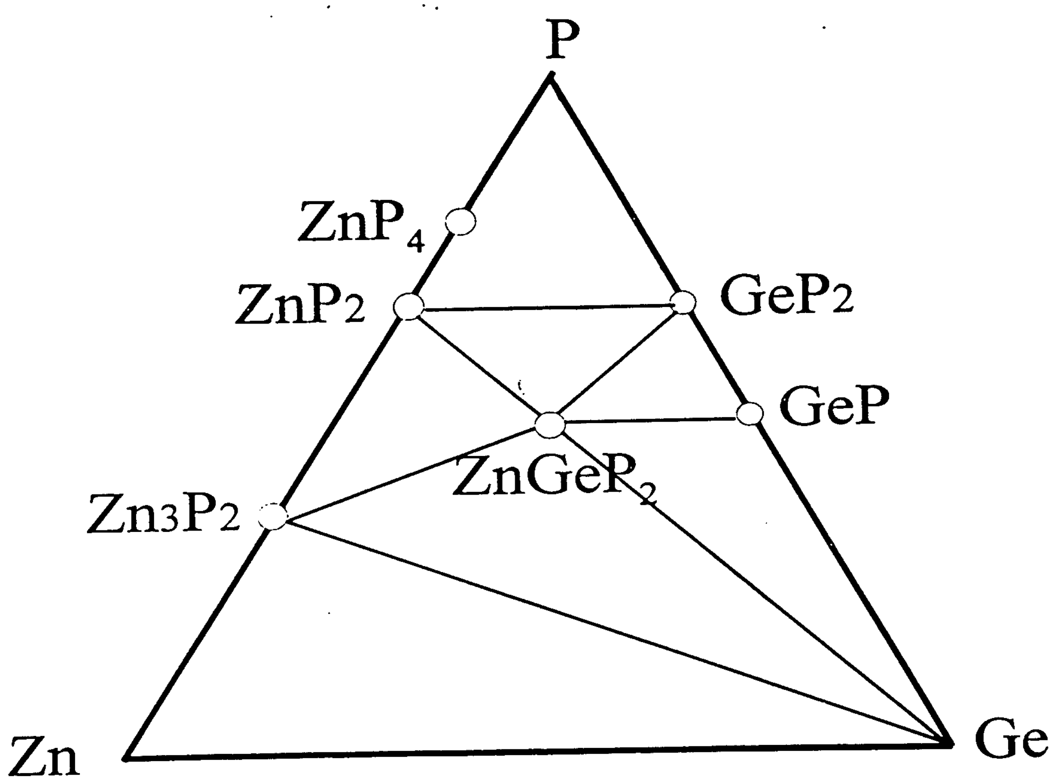

The Zn-Ge-P phase triangle

Experimental details

<u>*Synthesis:*</u> modified two-temperature technique, allowing to produce more then 500 gms of the material in one process

<u>*Growth:*</u> vertical Bridgman technique, (100) seeds

TABLE 1. Crystal growth conditions.

NUMBER OF [illegible] CRYSTAL	HOT ZONE TEMPERATURE °C	COLD ZONE TEMPERATURE °C	[illegible] NEAR MELTING POINT °C/CM	[illegible]	[illegible] ATM	[illegible] ATM	[illegible]
1	1060	990	6	0.5	6.9	1.1	Gas pocke
2	1060	1000	3.5	1.0	7.2	-	No pockets Single phas [illegible]
3	1060	950	10	0.5	-	-	Ge eutectic on the top the crystal

* P_{P4} (P_{Zn}) - pressures of phosphorus (zinc), created by additional charges of P (Zn), and calculated from the ideal gas law.

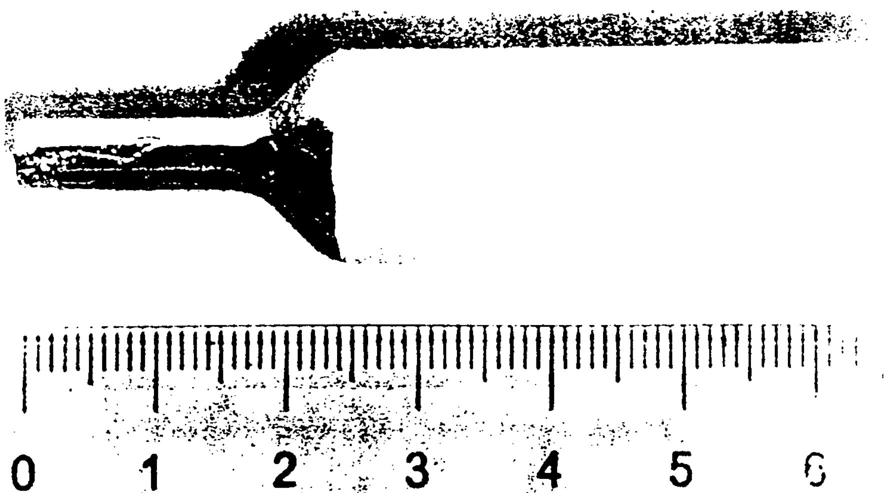
0 1 2 3 4 5 6

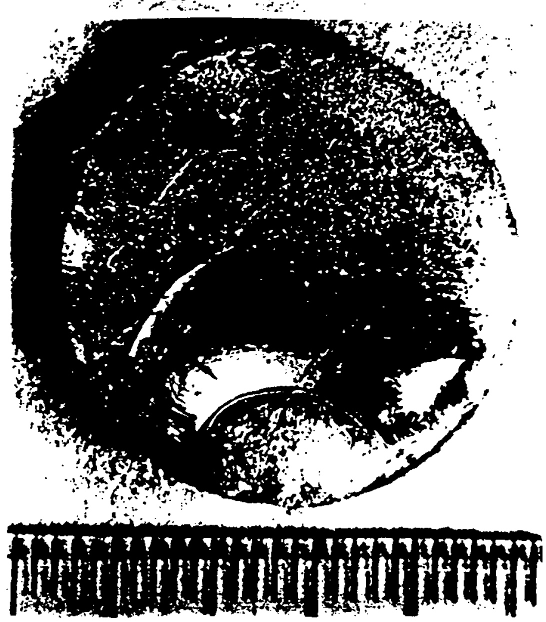

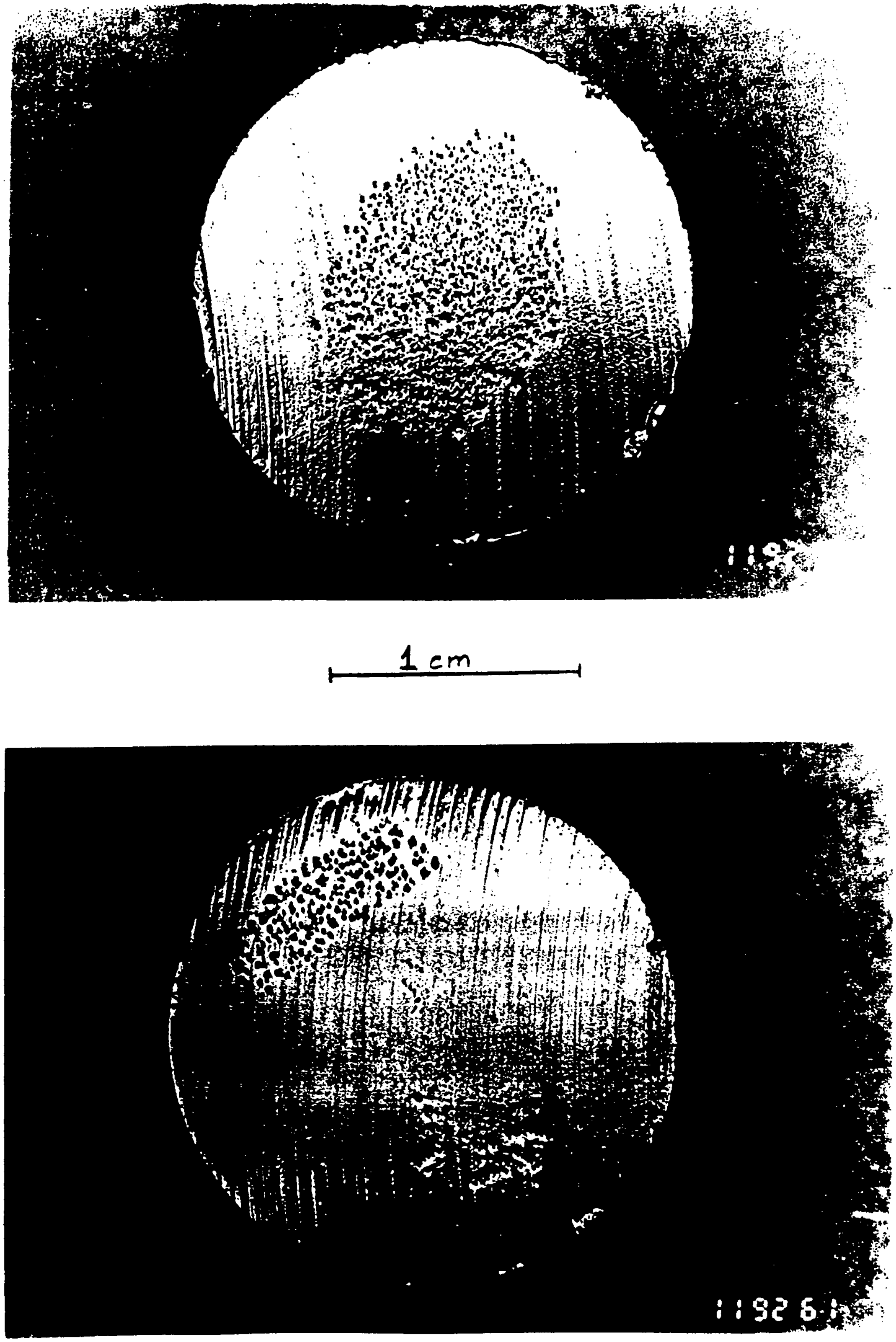

$ZnGeP_2$ slices after chemichal etching

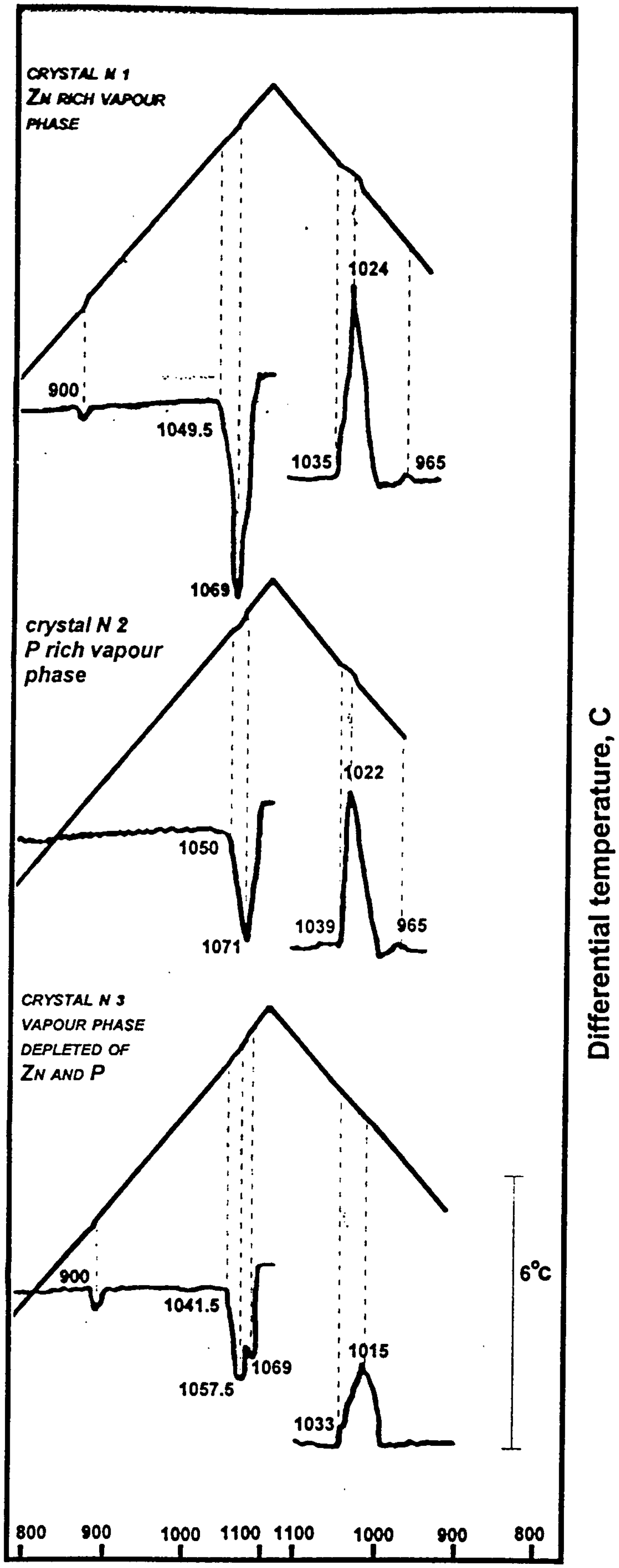

DTA curves of ZGP grown under various pressures of Zn and P

Experimental details:the weight of the studied samples-0.5 g , heating and cooling rates - 7.5deg/min reference material - Al2O3, speed of the paper movement - 1mm/min

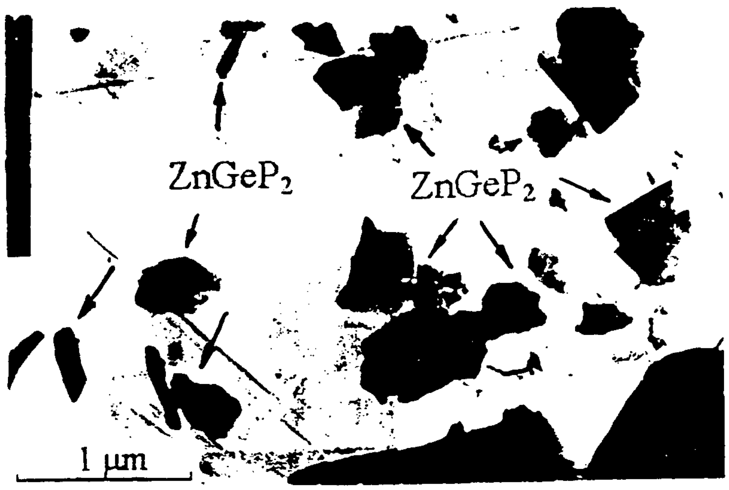

Fragments of failure (damage) of the bulk ZGP specimen arranged on the carbon substrate

Electron microscope EM-125
Accelerating voltage 125 kV
Working Magnification 65-85 000
Resolution 7-10Å

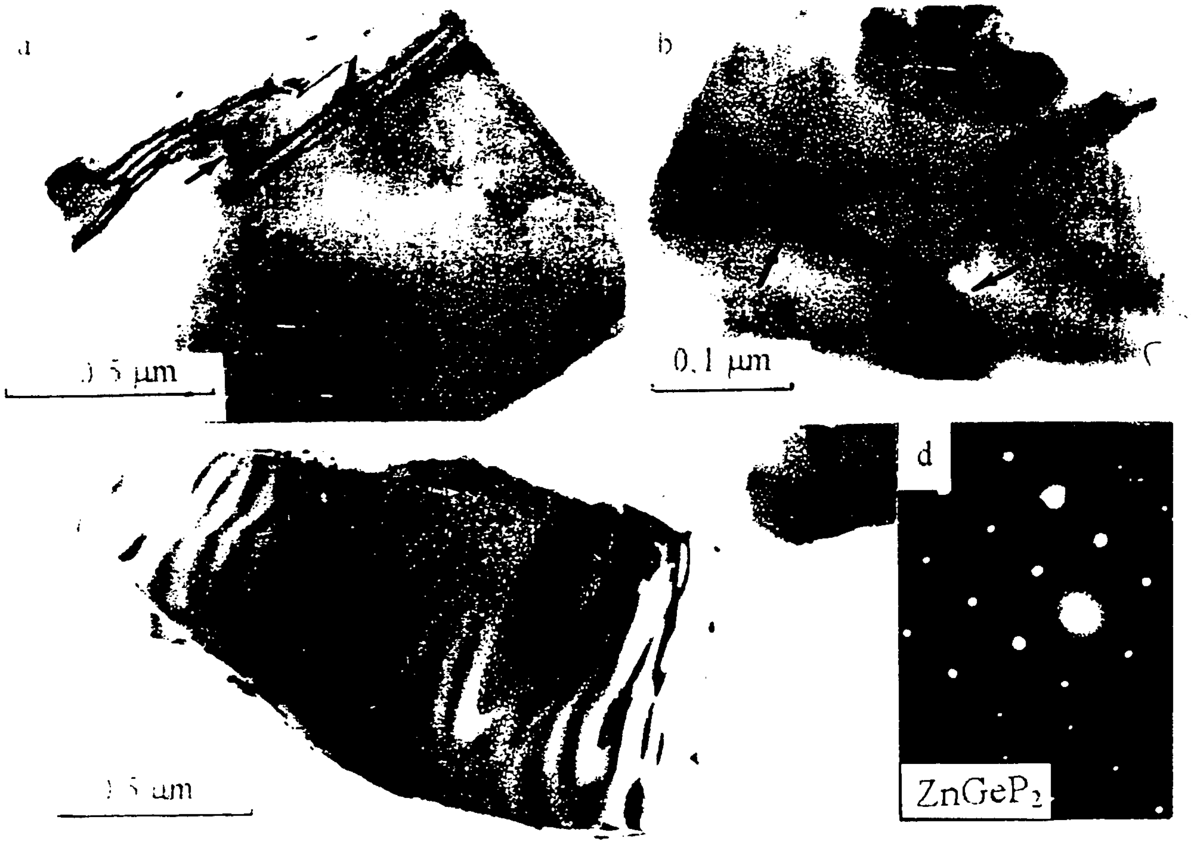

Microscopic image of $ZnGeP_2$

A Theoretical Study of Defects in $ZnGeP_2$ and $CdGeAs_2$

Ravi Pandey
Michigan Tech., Houghton, MI 49931
(pandey@mtu.edu)

(AFOSR-F49620-96-1-0319)

Approach : calculations of defect configurations and energetics in the framework of the atomistic model.

Results :

(i) Cation sublattice disorder is predicted to be the dominant native defect in both $ZnGeP_2$ and $CdGeAs_2$.

(ii) The nature of defects responsible for the near-IR absorption band in $ZnGeP_2$ and $CdGeAs_2$ appears to be different -

$ZnGeP_2$: zinc vacancy (localized hole)

$CdGeAs_2$: cadmium antisite (delocalized hole)

Defect-induced lattice distortion plays a key role in stabilizing the hole states in the lattice.

Based on the size argument, antisites in ZGP are not expected to introduce significant lattice distortion while those in CGA would be expected to cause significant distortion in the lattice.

$$R_{Zn} = 1.23\ \text{Å},\quad R_{Ge} = 1.23\ \text{Å},\quad R_{Cd} = 1.41\ \text{Å}$$

Dopant Binding Energies in $ZnGeP_2$ and $CdGeAs_2$

- selective doping of ZnGeP2 to reduce the concentration of the dominant native acceptor level via charge compensation in the lattice.
-

$ZnGeP_2$

» Au, Cu : inactive Se, Ga, In : acceptor (Gigoreva 73)

»

» Au, Cu, Ga, In, Se, Pt : acceptor (Rud 97)

»

$CdGeAs_2$

» Cu, Ga : acceptor In, Te : donor (Bairamov 98)

Summary

- Both Cu and Ag always act as acceptors.
- small hole binding energies for Cu and Ag at the Zn site.
- large hole binding energies for the group III dopants at the Ge site except B which shows a distinct behavior.
- donor levels for B, Al, Ga, In predicted to be near middle of the gap.

DEFECT IDENTIFICATION IN $ZnGeP_2$

K. J. Nash
DERA Malvern

Discussions, exchange of unpublished results, with

M. Fearn, A. W. Vere (DERA)

L. E. Halliburton, K. T. Stevens (WVU, Morgantown)

SYMMETRY THEORY

Which defect symmetry groups are possible in the ZGP structure?

- Determination of symmetry from experiments.
- Which defects have a particular symmetry?

  Which of these are consistent with
- the spin Hamiltonian?

DEFECT SYMMETRY IN ZGP

4 possibilities

- tetragonal
- monoclinic ($C_2 \parallel a$ or b)

ENDOR on the main defect in ZGP
(Halliburton et al)

$\Rightarrow$ monoclinic symmetry ($C_2 \parallel a$ or b)

suggested identity : V_{Zn}

- But the Zn site has tetragonal symmetry

tetragonal S_4
$\downarrow$
monoclinic $C_2 \parallel c$
$\downarrow$
triclinic

reduction of symmetry

- So V_{Zn} does not have the right symmetry

Other Models

$X_D - X_E$ where D is a defect site that is close to one P atom and D, E are related by the C_2 symmetry axis

- $P_{Ge} - X_P - P_{Ge}$

  $P_{Zn} - X_P - P_{Zn}$

  $P_{CI} - X_P - P_{CI}$ (CI = interstitial site on cation sublattice)

-

↳ unpaired spin localised on X; two P atoms related by symmetry

SPECULATION

$$P_{Ge} \underset{}{\overset{\text{P, Ge exchange}}{\rightleftharpoons}} P_{Ge} - Ge_P - P_{Ge}$$

EPR3 EPR1?

-
- no evidence for this! but...
- P_{Ge} has already been found in ZGP
- $P_{Ge} - Ge_P - P_{Ge}$ would explain the
- EPR1 signal, if the unpaired spin is localised on Ge_P.

Optical Properties of Tellurium Rich $Te_xSe_{(1-x)}$ Nonlinear Optical Semiconductors

G.J. Brown*, Cindi L. Dennis*,
M. C. Ohmer*, and Arnold Burger**

*Air Force Research Laboratory, Materials & Manufacturing Directorate, AFRL/MLPO, Wright-Patterson AFB, OH 45433-7707

** Fisk University, 1000 17th Ave., N, Nashville, TN 37208-3051

ASC-99-1822

Outline

- Infrared photoresponse and the energy gaps of tellurium rich oriented crystals of the form $Te_xSe_{(1-x)}$ for x= 1, 0.9, and 0.8 are reported.
- Band gaps are comparisoned
  - Te 0.33 eV 3.76 microns
  - $Te_{0.9}Se_{0.1}$ 0.38 3.26
  - $Te_{0.8}Se_{0.2}$ 0.498 2.48
  - Se 1.7 0.73
- The composition $Te_{0.286}Se_{0.714}$ is estimated to have an energy gap of 1 eV or 1.24 microns from literature data

WHAT IS A LARGE SECOND ORDER NONLINEAR SUSCEPTIBILITY (a.k.a. CHI2)?

- The largst reported value for a birefringent element is 650 pm/V for Te. The value for Se is 97 pm/V.
- The largest reported value for a birefringent compound is 470 pm/V for $CdGeAs_2$
- The value of 11 pm/V for lithium niobate ($LiNbO_3$) is usefully large for optical signal processing applications
- Two state of the art IR materials, $AgGaS_2$ and $AgGaSe_2$ have Chi2 values of respectively 36 pm/V and 66 pm/V
- $ZnGeP_2$ has a very respectable value of 150 pm/V, but not birefringnent
- The above numbers are normalized to GaAs at 180 pm/V
- Upper limit for bound electrons is 4000-5000 pm/V

Oriented Tellurium Crystal
Perkin Elmer FTIR (Raw Source Beam)

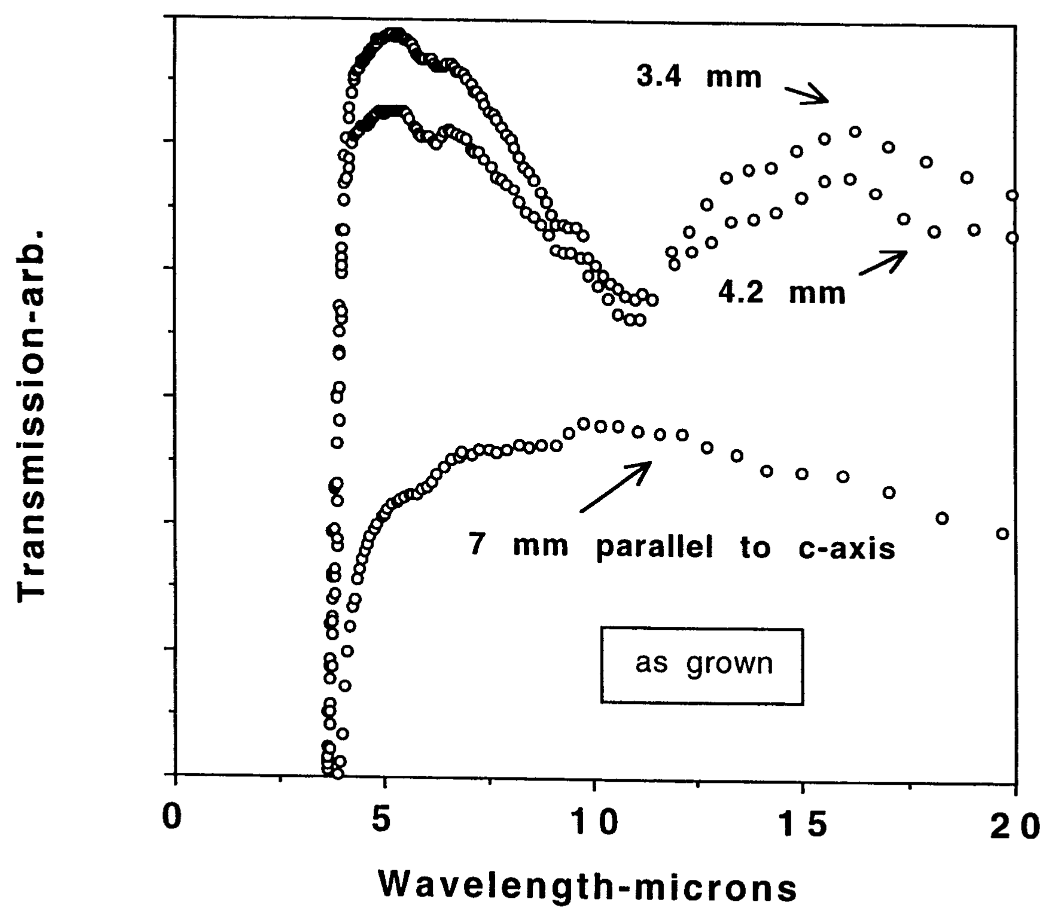

Photoresponse of Te and $Te_{0.8}Se_{0.2}$

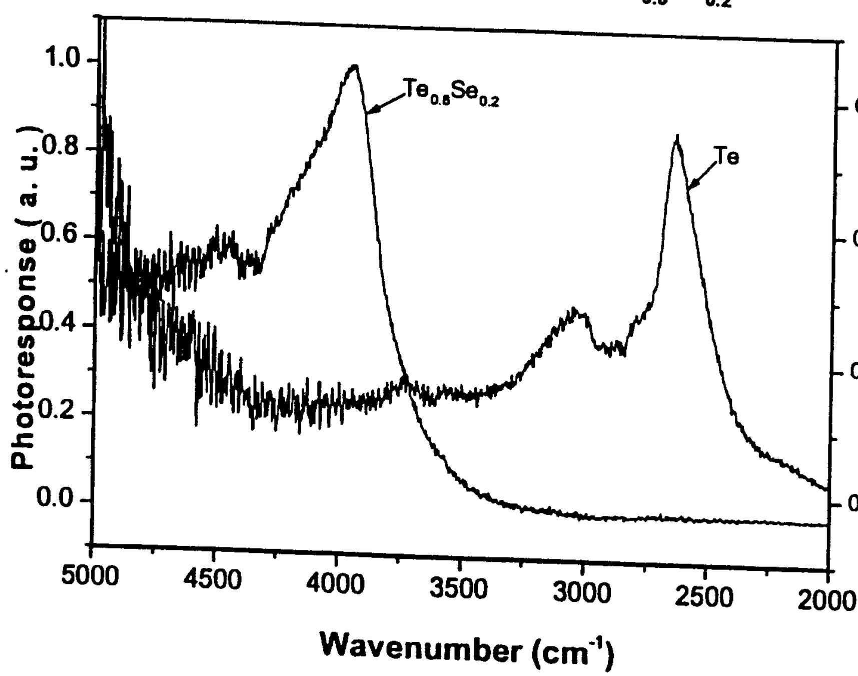

Comparison of Tellurium and Its Alloys

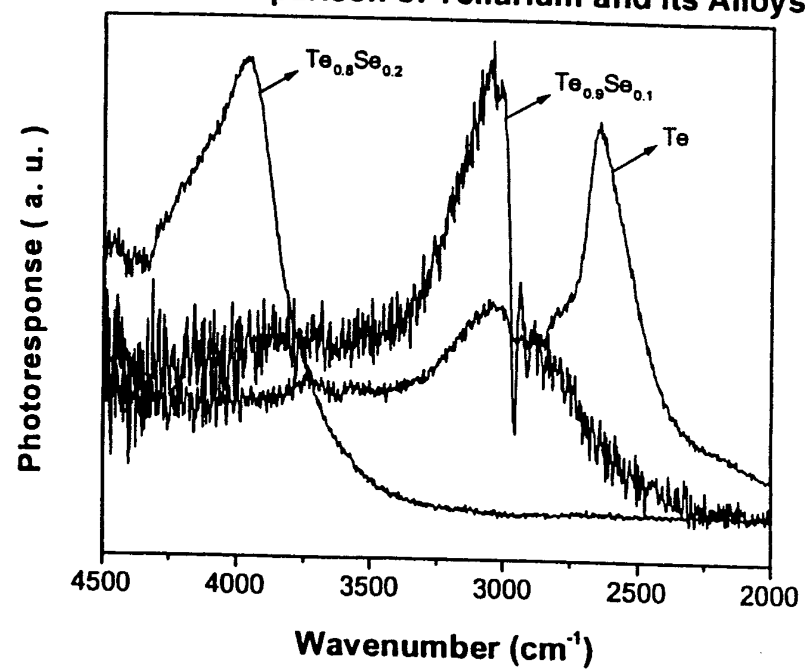

AFRL Materials Directorate Efforts in Nonlinear Optical Crystal Development for Laser Wavelength Shifting

NILS C. FERNELIUS*, F.K. HOPKINS,
& M.C. OHMER
Materials Directorate,
Air Force Research Laboratory,
Wright Patterson Air Force Base,
Dayton, Ohio *45433*

DESIRED PROPERTIES FOR NLO UNOBTAINIUM

BROAD WAVELENGTH OPTICAL TRANSMISSION
LOW LOSS: ABSORPTION & SCATTER
LARGE NONLINEAR SUSCEPTIBILITY or d
rather d_{eff}^2/n^3
NEED LARGE BIREFRINGENCE FOR PHASE MATCHING
(or USE QUASI-PHASE-MATCHING STRUCTURES)
TOO LARGE LEADS TO BEAM WALK-OFF PROBLEMS
NEED UNIFORM REFRACTIVE INDEX THROUGHOUT CRYSTAL
LASER DAMAGE RESISTANCE
WANT SMALL dn/dT TO AVOID SELF-FOCUSSING
WANT HIGH THERMAL CONDUCTIVITY
WANT STRONG MECHANICAL PROPERTIES
STABLE CHEMICAL PROPERTIES
CRYSTALS EASY TO GROW
INEXPENSIVE

THRUSTS OF BULK CRYSTAL PROGRAM

BIREFRINGENT CRYSTALS:

KTP {$KTiOPO_4$} ISOMORPHS- KTA {$KTiOAsO_4$},
RTA {$RbTiOAsO_4$}, CTA {$CsTiOAsO_4$},
KRTA {$K_{1-x}Rb_xTiOAsO_4$}

KTP GREY TRACK

CHALCOPYRITES- $ZnGeP_2$, $CdGeAs_2$, $AgGaS_2$,
$AgGaSe_2$, $AgGa_{1-x}In_xSe_2$, $AgGaTe_2$

GaSe

$HgGa_2S_4$

CGC {$CsGeCl_3$}

CGB {$CsGeBr_3$}

UV MATERIALS(borates) - LBO {LiB_3O_5},
BBO { β-BaB_2O_4}, CLBO { $CsLiB_6O_{10}$ },

KBBF {$KBe_2BO_3F_2$}, $CsLaB_7O_{13}$,
low birefrigence: SBO {SrB_4O_7} & PBO {PbB_4O_7}
$MM'(B_3O_5)_3$ where M = Sr, Ba, Pb; M' = Li, Na

Figure of Merit for Many Common NLO Materials

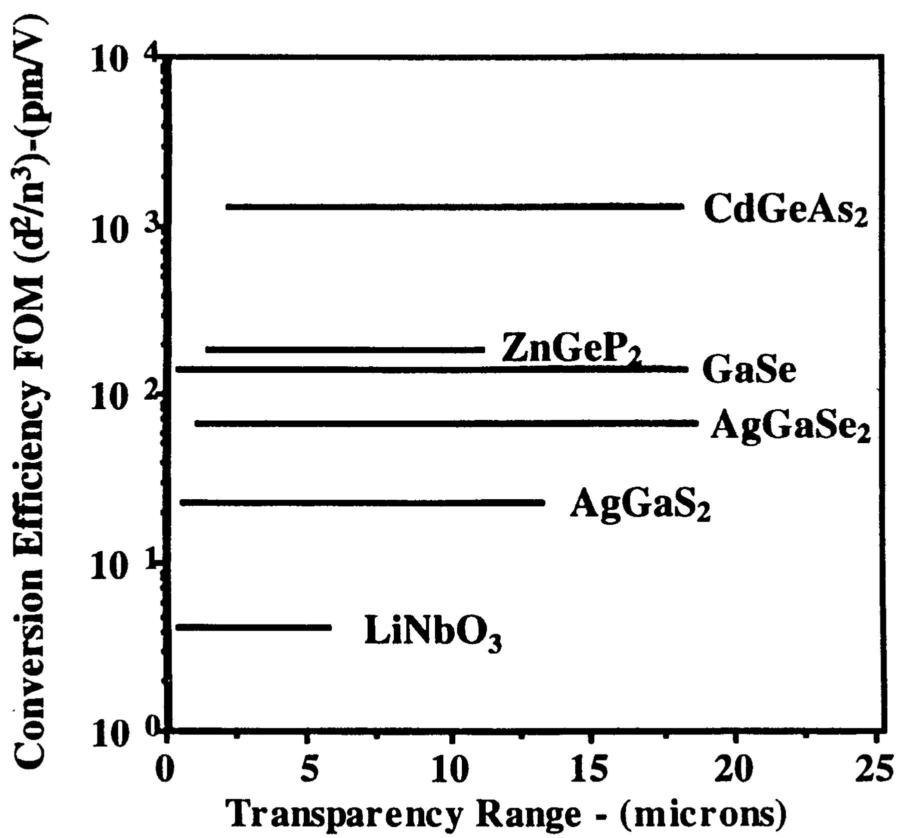

TRANSMISSION
KTA vs. KTP

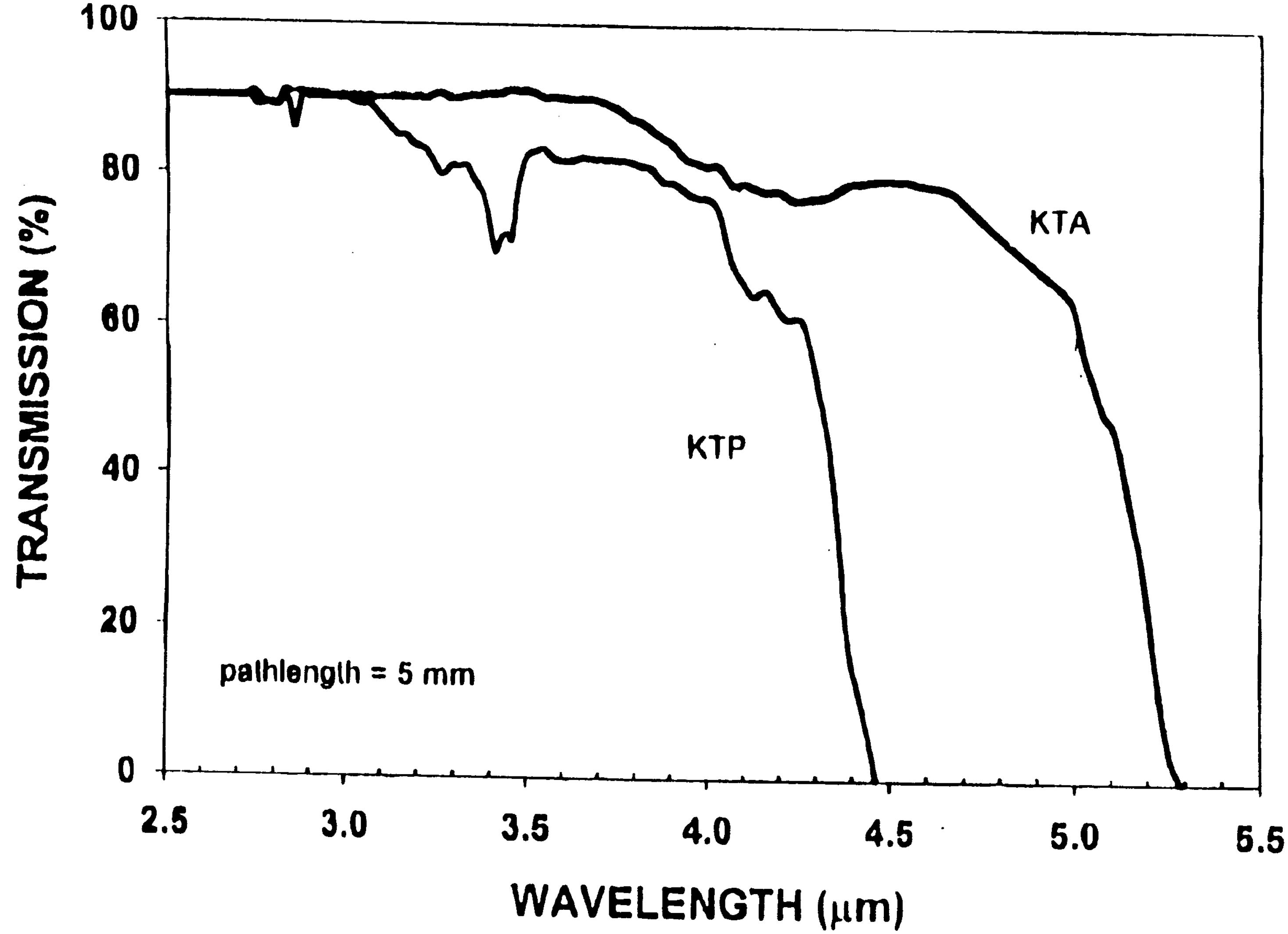

CRYSTAL ASSOCIATES, INC.

GRAY TRACKS IN KTP

Nd:YAG laser produces 355 nm photons (third harmonic generation or sum of fundamental & second harmonic)

KTP room temperature band edge at 350 nm.

The above-band-gap photons generate electron-hole pairs.

Many recombine but a portion are trapped at stabilizing defects such as vacancies or impurities to form "stable" gray tracks. When these complexes contain an unpaired electron, they can be studied by ESR and ENDOR.

Flux grown KTP:

$$Fe^{3+} + h^{+} \underset{\text{decay}}{\overset{\text{formation}}{\rightleftarrows}} Fe^{4+}$$

$$Ti^{4+}\text{-}V_O + e^{-} \underset{\text{decay}}{\overset{\text{formation}}{\rightleftarrows}} Ti^{3+}\text{-}V_O$$

Hydrothermal grown KTP:

$$Fe^{3+}\text{-}OH^{-} + h^{+} \underset{\text{decay}}{\overset{\text{formation}}{\rightleftarrows}} Fe^{4+}\text{-}OH^{-}$$

$$Ti^{4+}\text{-}OH^{-} + e^{-} \underset{\text{decay}}{\overset{\text{formation}}{\rightleftarrows}} Ti^{3+}\text{-}OH^{-}$$

Halliburton & Scripsick, SPIE Proc. 2379 235 (1995)

CHALCOPYRITES

$A^{II}B^{IV}C^{V}_{2}$ or $A^{I}B^{III}C^{VI}_{2}$

Some examples for IR NLO:

$ZnGeP_2$, $AgGaS_2$, $AgGaSe_2$, $CdGeAs_2$, $AgGaTe_2$

See July, 1998 issue MRS Bulletin 23(7)

● K. L. Vodopyanov ●

1724 J. Opt. Soc. Am. B/Vol. 10, No. 9/September 1993

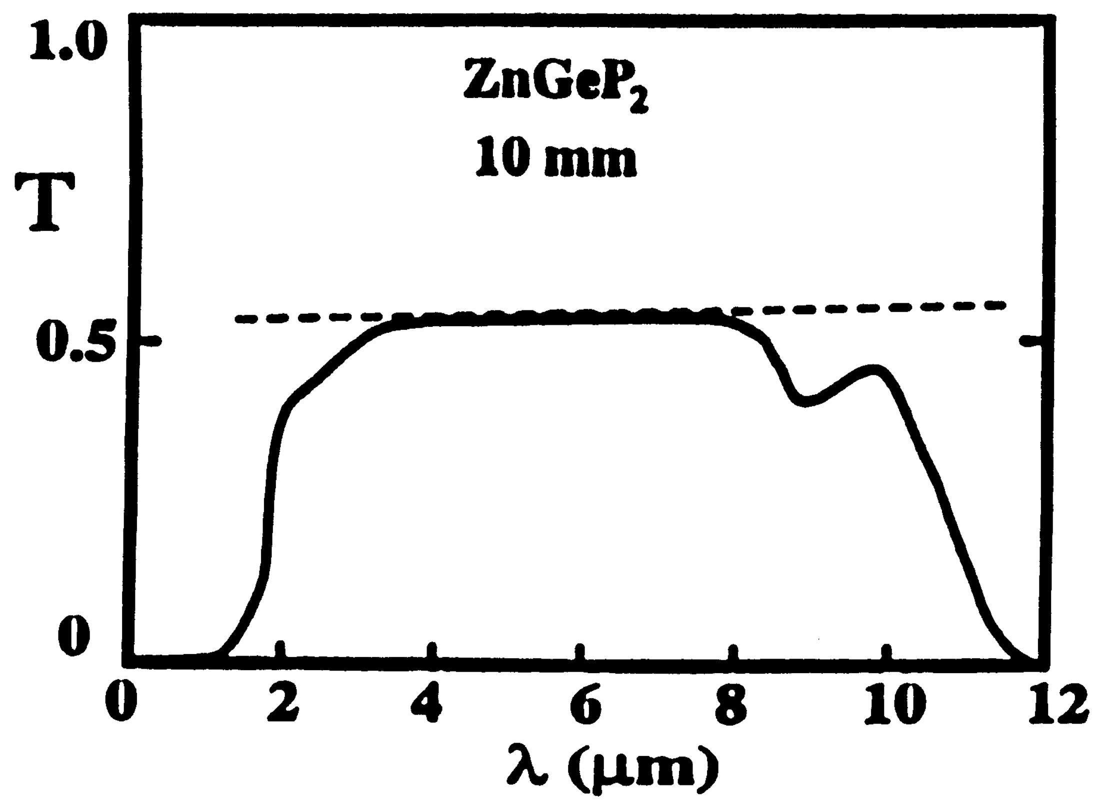

Transmission spectra taken at room temperature. $ZnGeP_2$ (L = 10 mm). Dashed curves, Fresnel losses.

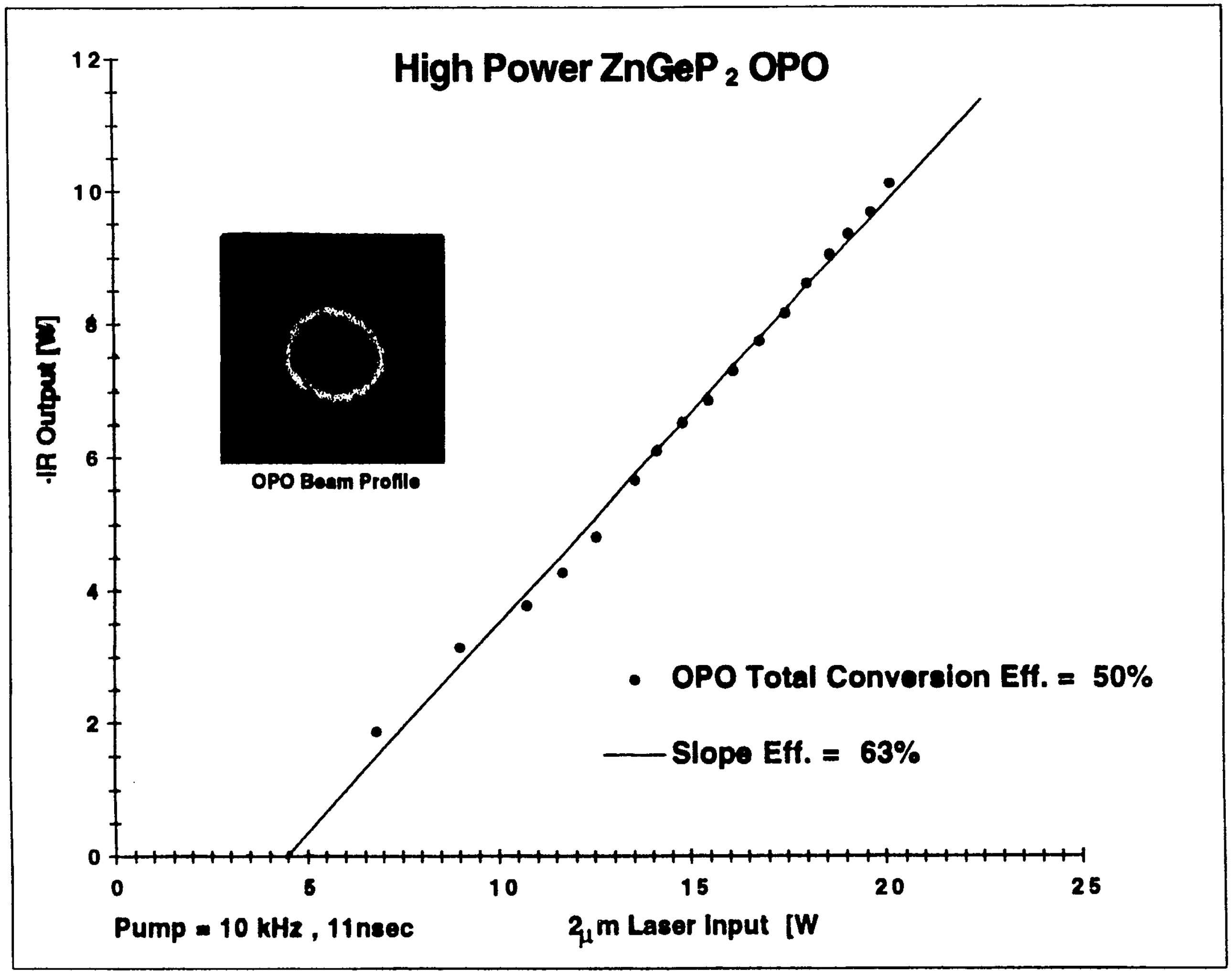

High Power ZnGeP 2 OPO
-IR Output [W]
12
10
8
6
4
2
0
0
5
10
15
20
25
OPO Beam Profile
• OPO Total Conversion Eff. = 50%
Slope Eff. = 63%
Pump = 10 kHz , 11nsec
2μm Laser Input [W

Vodopyanov & Schunemann, Optics Lett. 23 1096 (1998)

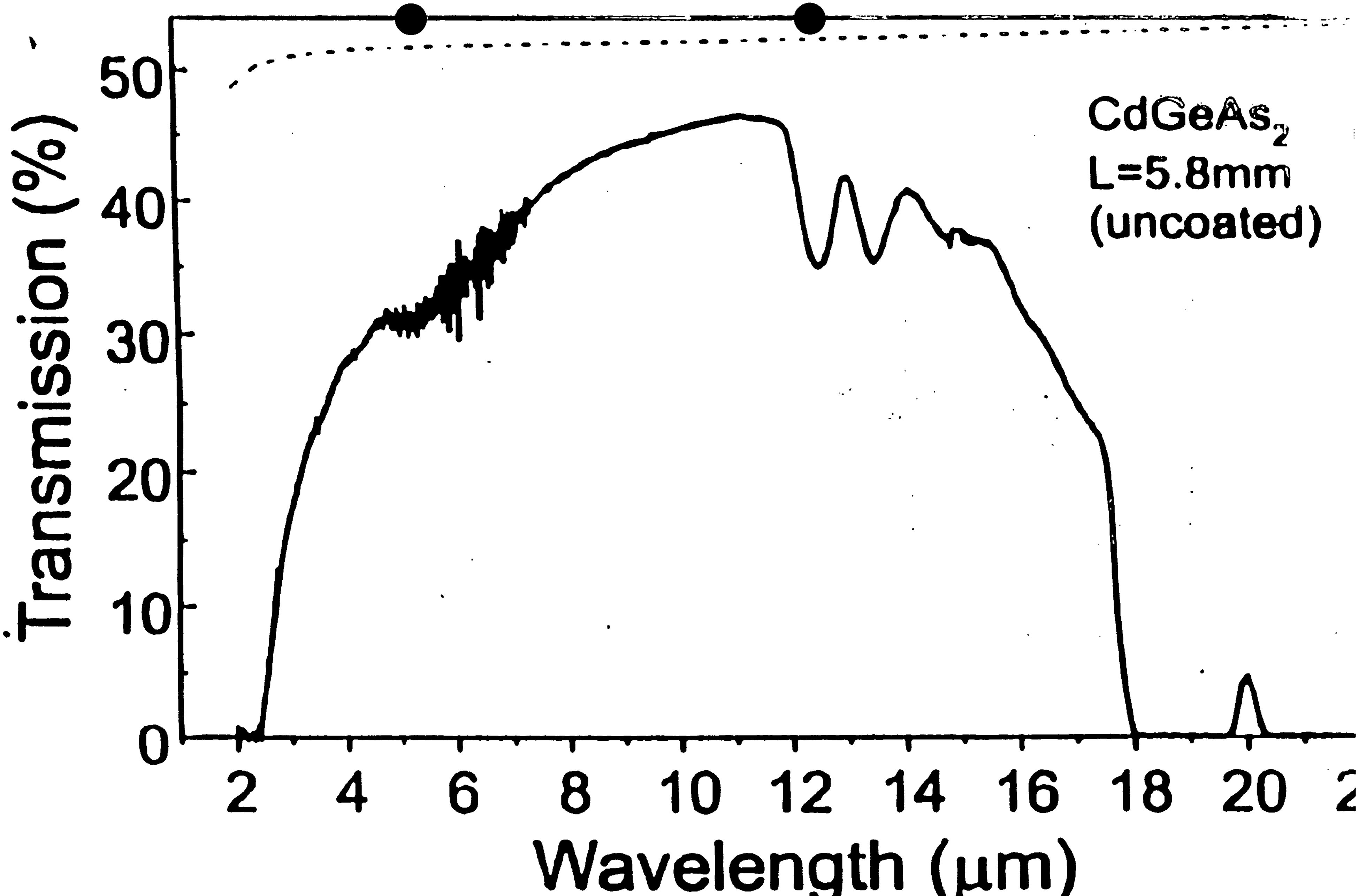

Measured transmission spectrum of an uncoated,

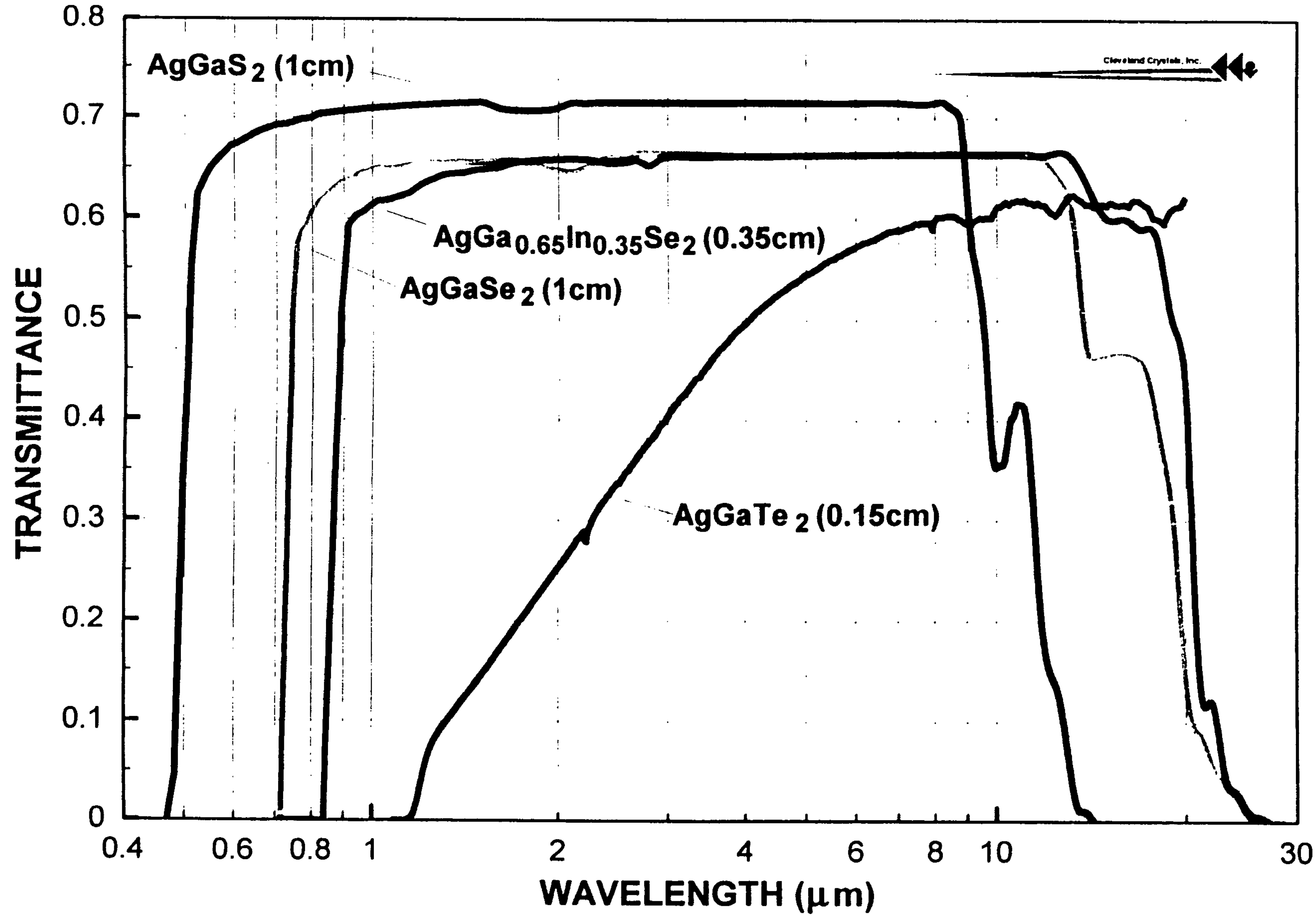

AgGaS2 (1cm)
AgGa0.65In0.35Se2 (0.35cm)
AgGaSe2 (1cm)
AgGaTe2 (0.15cm)
TRANSMITTANCE
0.8
0.7
0.6
0.5
0.4
0.3
0.2
0.1
0
0.4
0.6
0.8
1
2
4
6
8
10
30
WAVELENGTH (µm)

[redacted]

- GaSe has extremely high NLO coefficient (76 pm/V) and merit (d^2/n^3 331) compared to ZGP, TAS and $AgGaSe_2$ crystals.
- GaSe transmits between 0.65 to 20 micrometer wavelength region without any absorption band.
- GaSe has very high damage threshold and did not damage up to 180 MW/cm^2 power

NORTHROP GRUMMAN

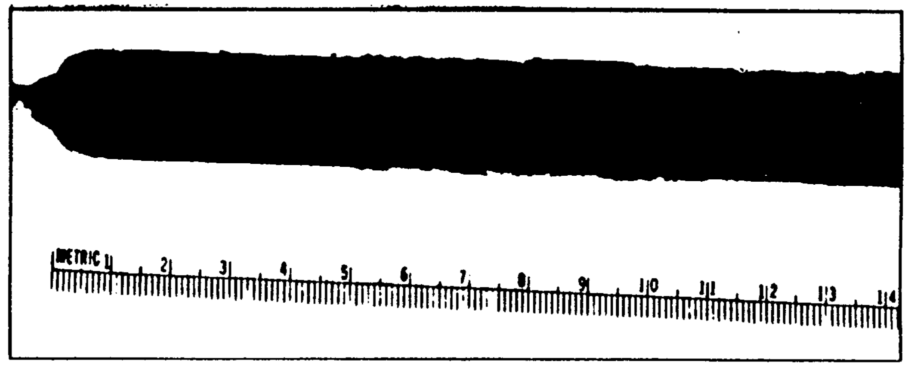

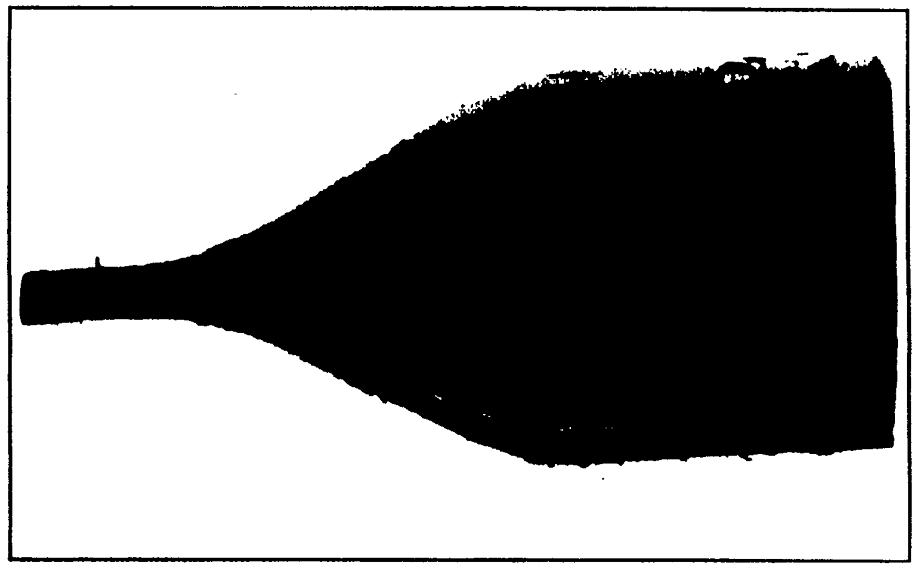

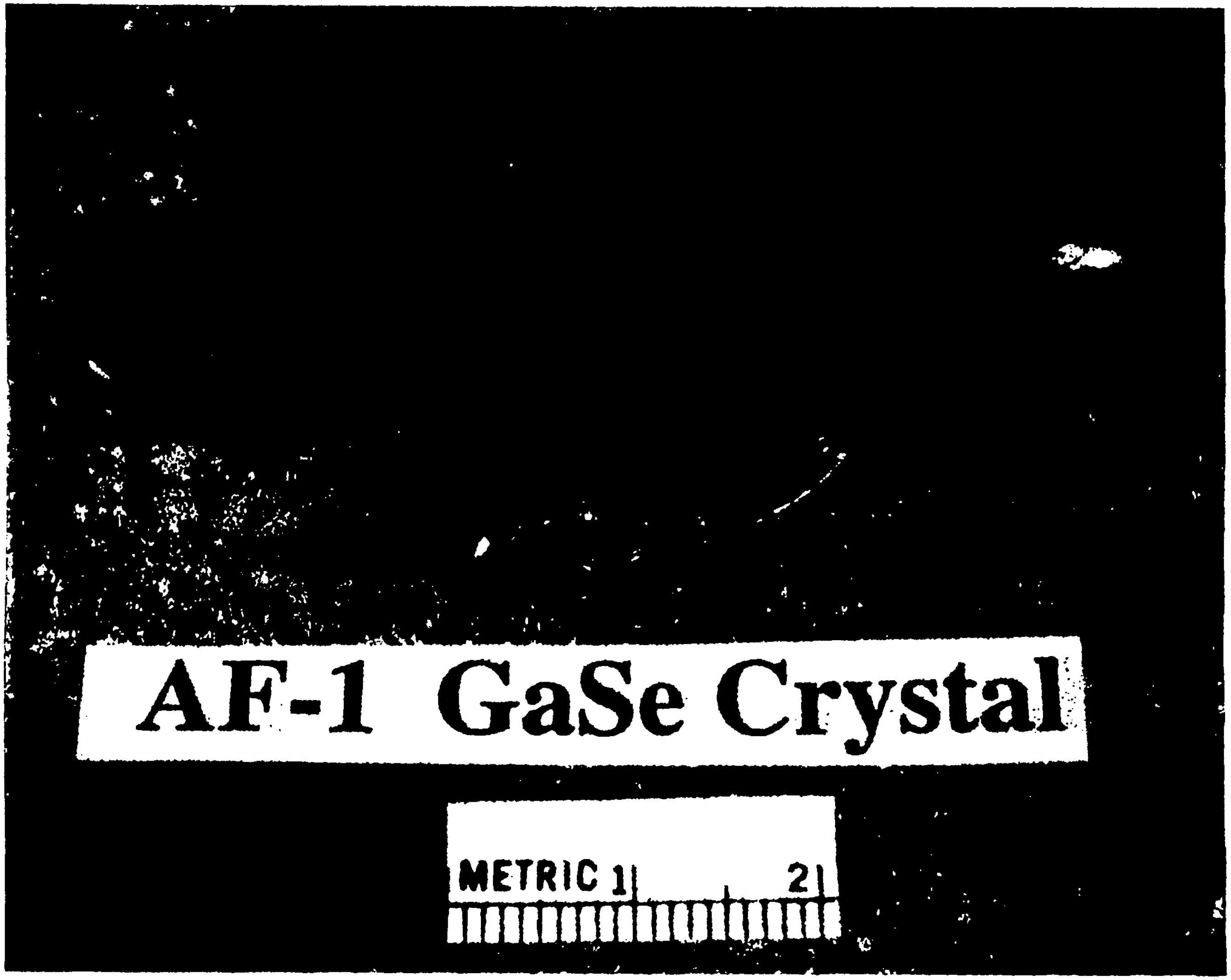
AF-1 GaSe Crystal
METRIC 1 2

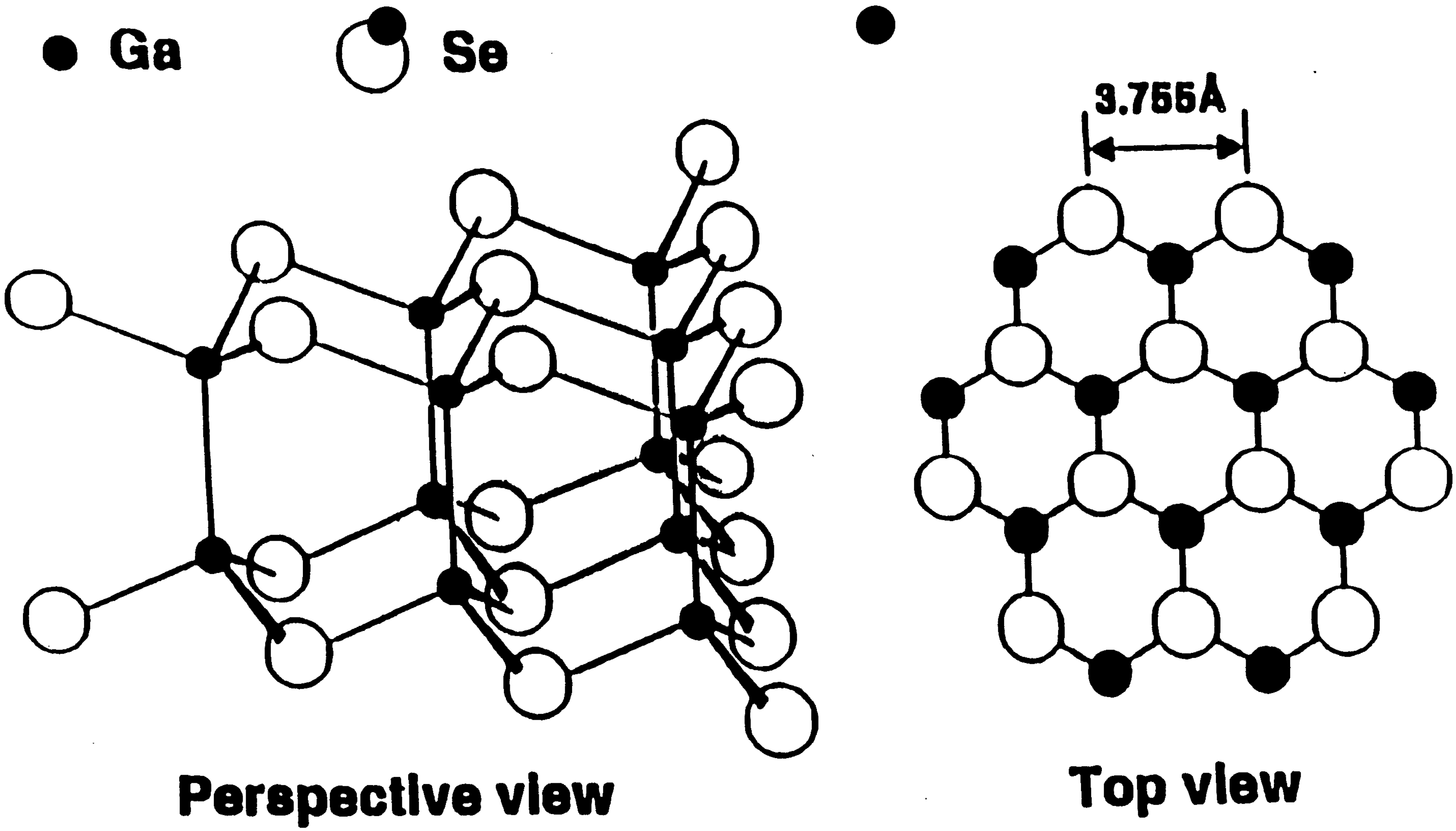

Perspective and top views of a unit layer of GaSe.

Uneo,Abe, Suiki & Koma, Jap.J.Appl.Phys.Lett., 30 L1352 (1991)

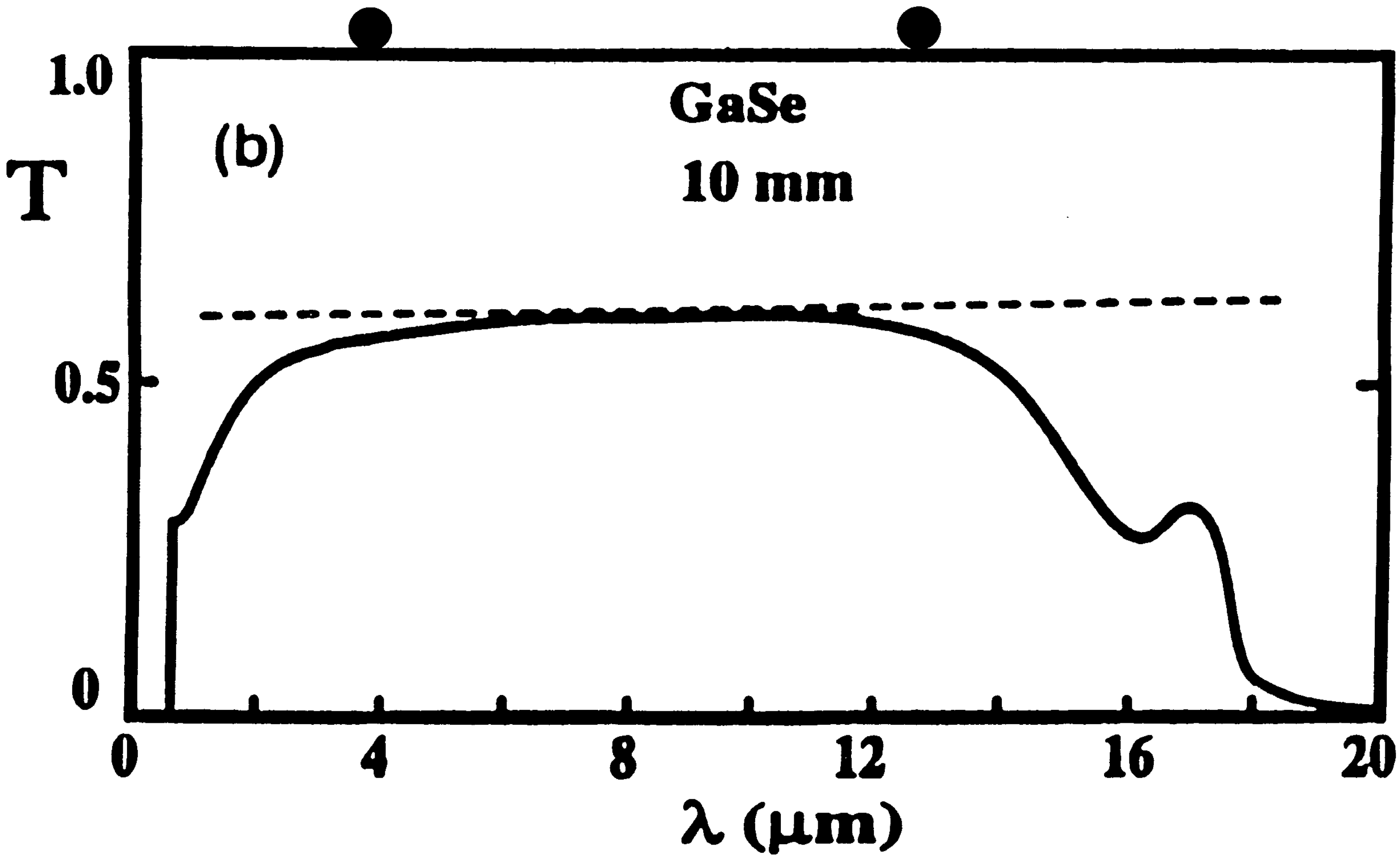

Transmission spectra taken at room temperature. GaSe (L = 10 mm). Dashed curves, Fresnel losses.

K. L. Vodopyanov

RECENT GaSe USES

W.C. Eckhoff, R.S. Putnam, S. Wang, R.F. Curl, F.K. Tittel
A continuously tunable long-wavelength cw IR source for high-resolution spectroscopy and trace-gas detection
Appl. Phys. B 63, 437-441 (1996)
Difference frequency generation (DFG) of two synchronously pumped Ti:sapphire lasers yields continuosly tunable light over 8.8-15.0 μm region.

- K.L. Vodopyanov & V. Chazapis
Extra-wide tuning range optical parametric generator
Optics Communications 135, 98-102 (1997)
Optical parametric generator (OPG) yields continuously tunable light over 3.3-19 μm range.

-

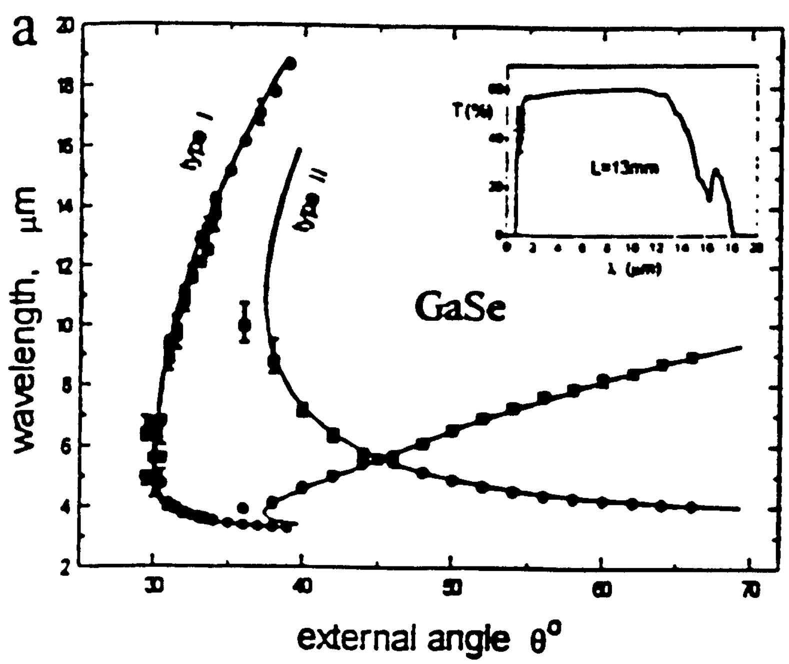

Fig. 2. GaSe and $ZnGeP_2$ angular tuning curves at $\lambda = 2.8$ μm pump for the two types of phase-matching. Vertical bars correspond to experimental half-maximum linewidths. Solid lines - calculated tuning curves. Insets show linear transmission spectra for the two crystals;

Quasi-Phase Matching

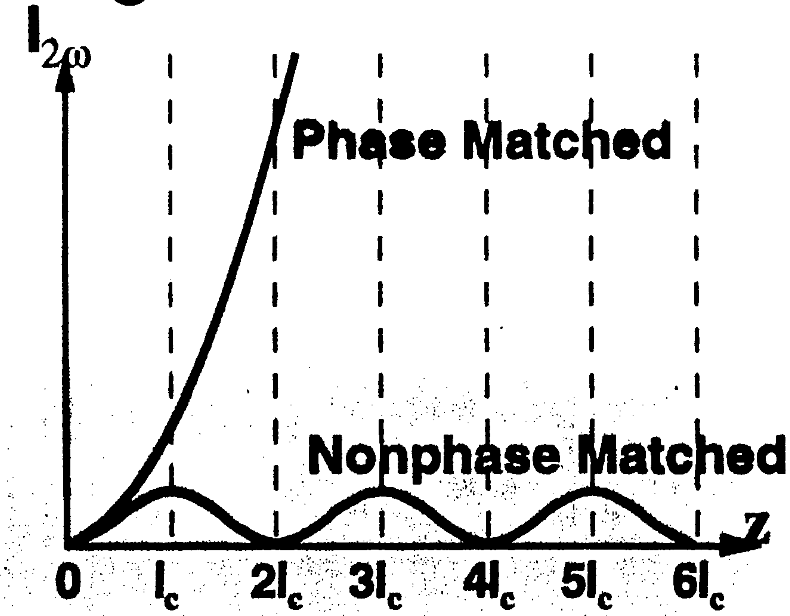

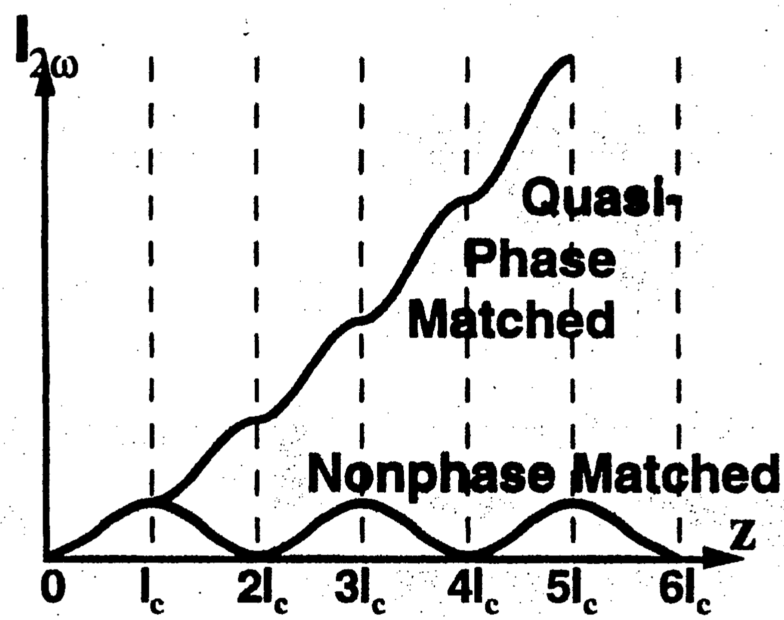

QUASI-PHASE-MATCHING TECHNIQUES

Inverted Segments

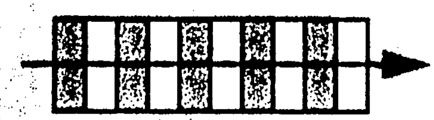

- Diffusion bonded - GaAs
- Periodically poled - $LiNbO_3$, $LiTaO_3$, KTP, RTA, KTA, SBN
- Periodic doping
  - diffusion exchange
  - ion implantation

Total Internal Reflection Devices

- GaAs, ZnSe

THRUSTS OF BULK CRYSTAL PROGRAM

QUASI-PHASE-MATCHING TECHNIQUES:

INVERTED SEGMENTS

- DIFFUSION BONDED - GaAs
- PERIODICALLY POLED- 3-5μm: $LiNbO_3$ {PPLN}, $LiTaO_3$ {PPLT}, KTP, RTA, KTA, $Pb_xBa_{1-x}Nb_2O_6$ (PBN)
  - 8-12μm: $CsGeCl_3$, $CsGeBr_3$, Tl_3PbBr_5, Tl_4PbI_6, Tl_4HgI_6

PERIODIC DOPING - diffusion exchange
ion implantation

PERIODIC PRESSURE TO INVERT DOMAINS

TOTAL INTERNAL REFLECTION DEVICES - GaAs, ZnSe

Mid IR Multigrating PPLN

- Tuning from ~1.4 - 4.8 μm
- Multi -Watt Output Power
- Suffers from Photorefractive Effects
- Low Cost Material
- Uses 1.06 μm Laser Pump

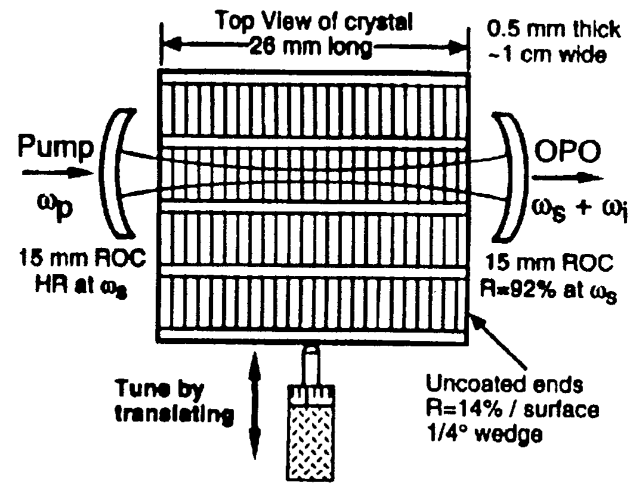

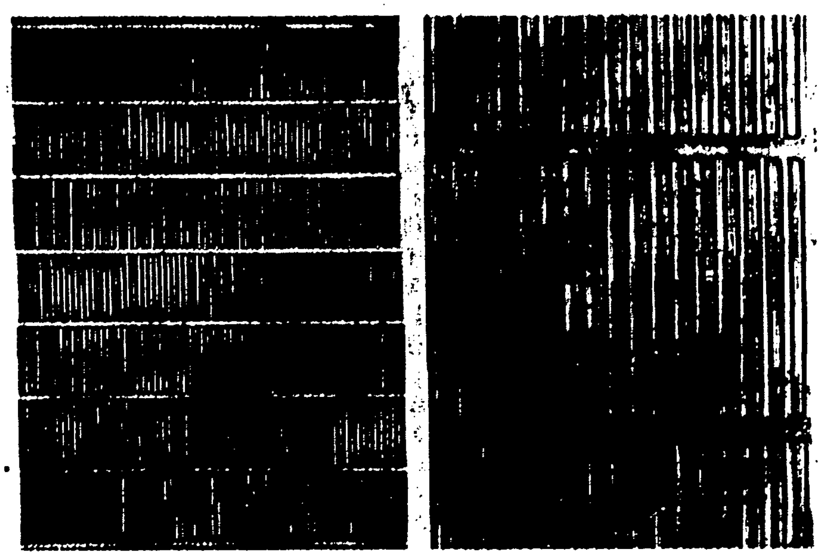

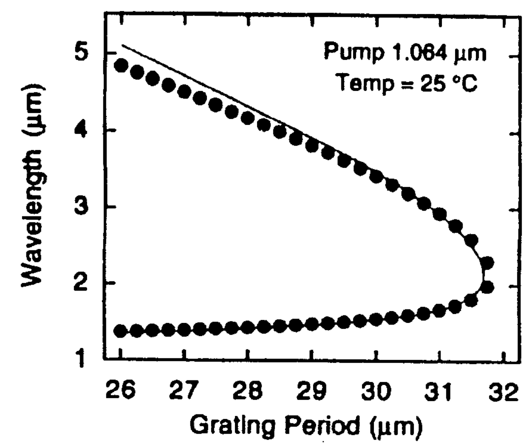

MATERIALS WHICH HAVE BEEN PERIODICALLY POLED

$LiNbO_3$	(PPLN)
$LiTaO_3$	(PPLT)
$KTiOPO_4$	(KTP)
$RbTiOAsO_4$	(RTA)
$KTiOAsO_4$	(KTA)
$Sr_{0.6}Ba_{0.4}Nb_2O_6$	(SBN)
$BaTiO_3$	(PPBT)

PERIODICALLY POLED LITHIUM NIOBATE-$LiNbO_3$ (PPLN)

GOOD POINTS:

- USE d_{33}= 42 pm/V INSTEAD OF d_{31}= 5 pm/V AS IN
  - BIREFRINGENT PHASE MATCHING
    - IMPROVES FIGURE OF MERIT BY ~ 25
- NO WALK OFF PROBLEMS
- CAN USE Nd:YAG 1.06 μm AS PUMP

BAD POINTS:

- SMALL INPUT APERTURE WHICH LIMITS POWER OUTPUT
  - SO FAR SAMPLES 0.5-1 mm THICK
  - UNLESS DIFFUSION BOND A STACK
- M^2 PROBLEMS OF OUTPUT BEAMS EVEN WITH STACK
- PHOTOREFRACTIVE DAMAGE
  - HEAT SAMPLE IN OPERATION TO ANNEAL OUT DAMAGE

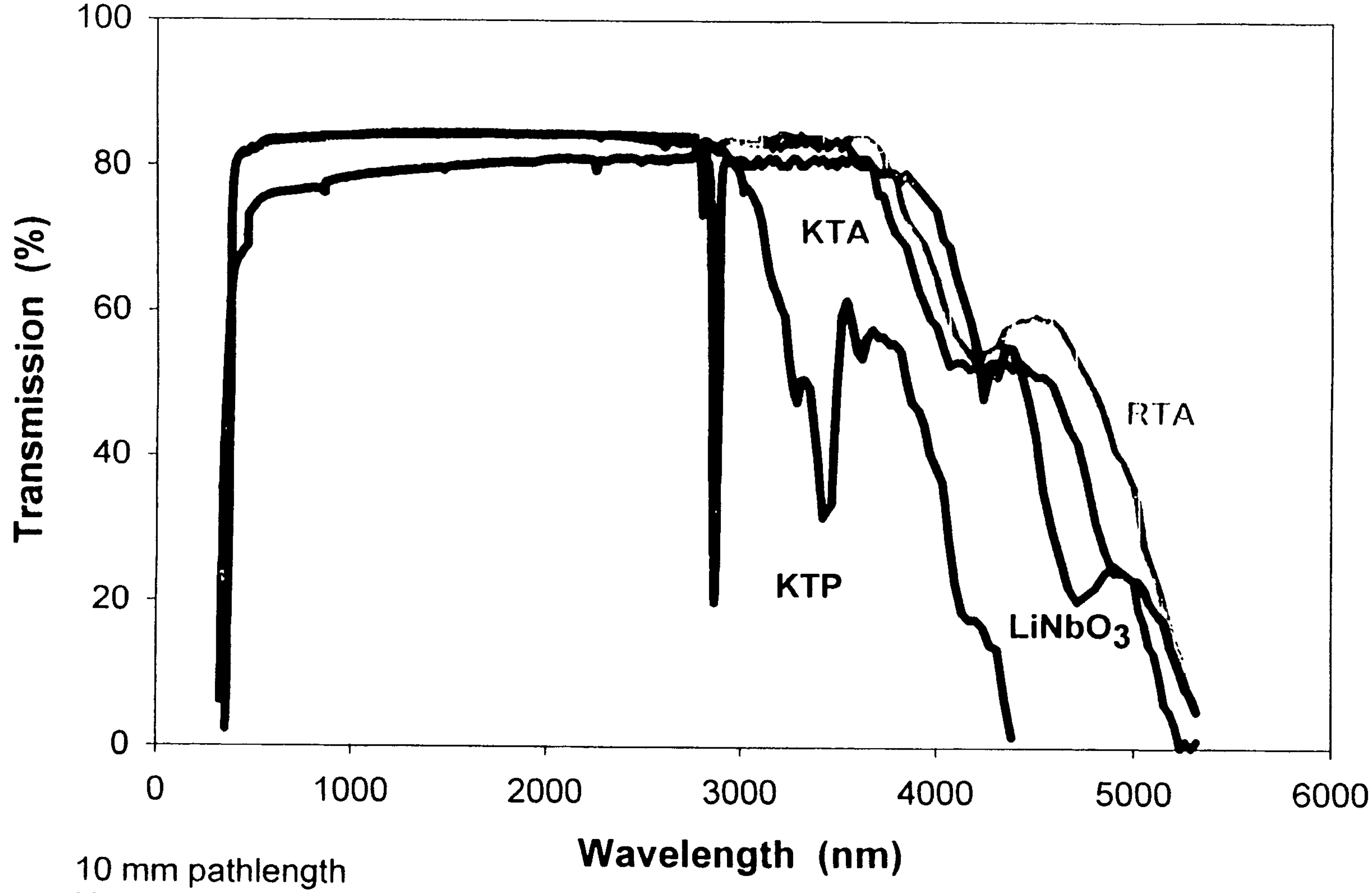

10 mm pathlength
Uncorrected for Fresnel reflections

MWIR (3-5 μm) THRUSTS

PMNT : $Pb\{Mg_xNb_yTi_{1-x-y}\}O_3$ (PMNT) — Rockwell Science Center to cover 4.5-6 μm band

Difficult to grow optically clear. Switch to $Pb_xBa_{1-x}Nb_2O_6$ (PBN) to cover 4.5-5.5 μm band

KRTA : $K_xRb_{1-x}TiOAsO_4$ — Crystal Associates
Best for $x = 0$

LWIR (8-12 μm) THRUSTS

$CsGeCl_3$
$CsGeBr_3$ — Rockwell Science Center

Tl_3PbBr_5
Tl_4PbI_6
Tl_4HgI_6 — Northrop Grumman (Pittsburgh) → (Baltimore)

Comparison of Spectral Transparencies in Ferroelectric Oxides

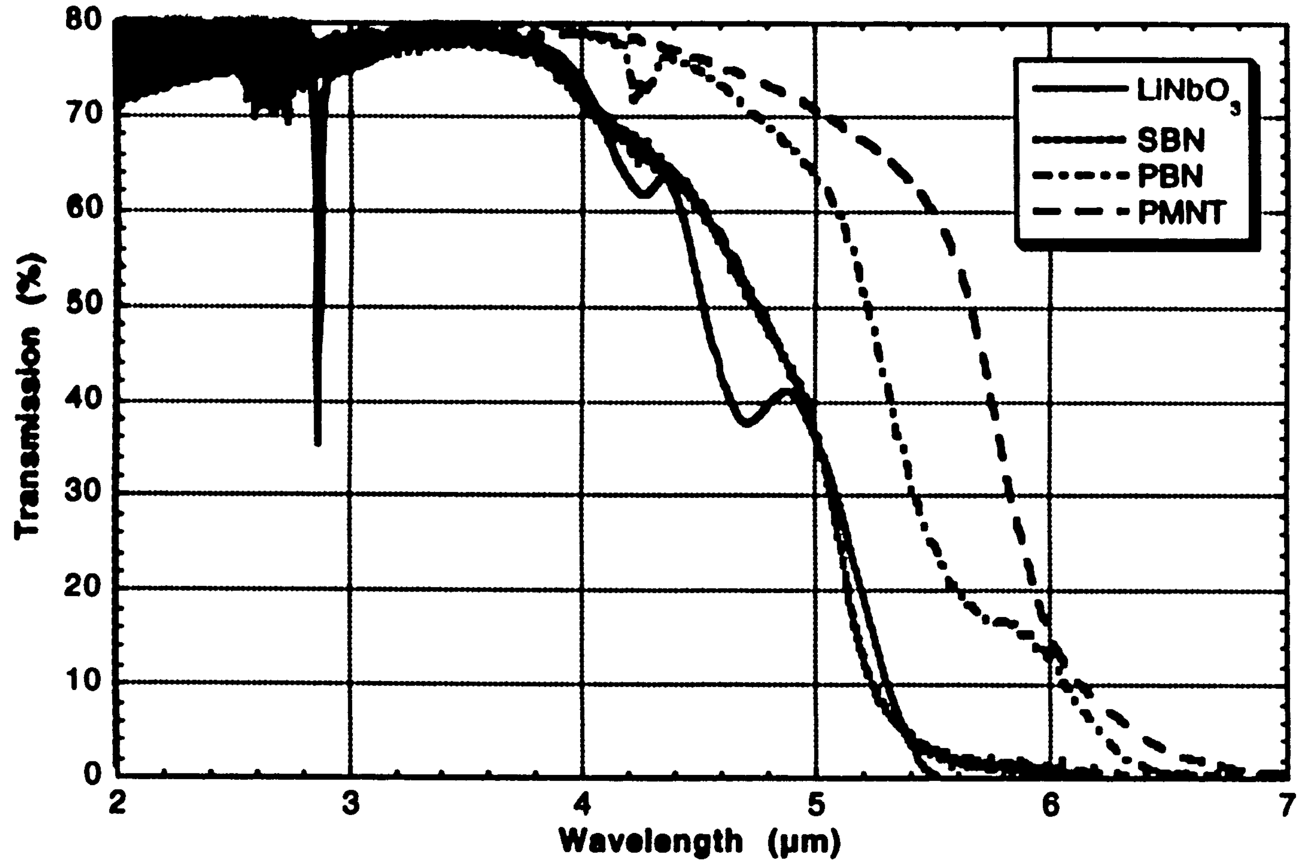

Rockwell

New Family of NLO Materials: CGX

DPM Loci & d_{eff} in $CsGeCl_3$

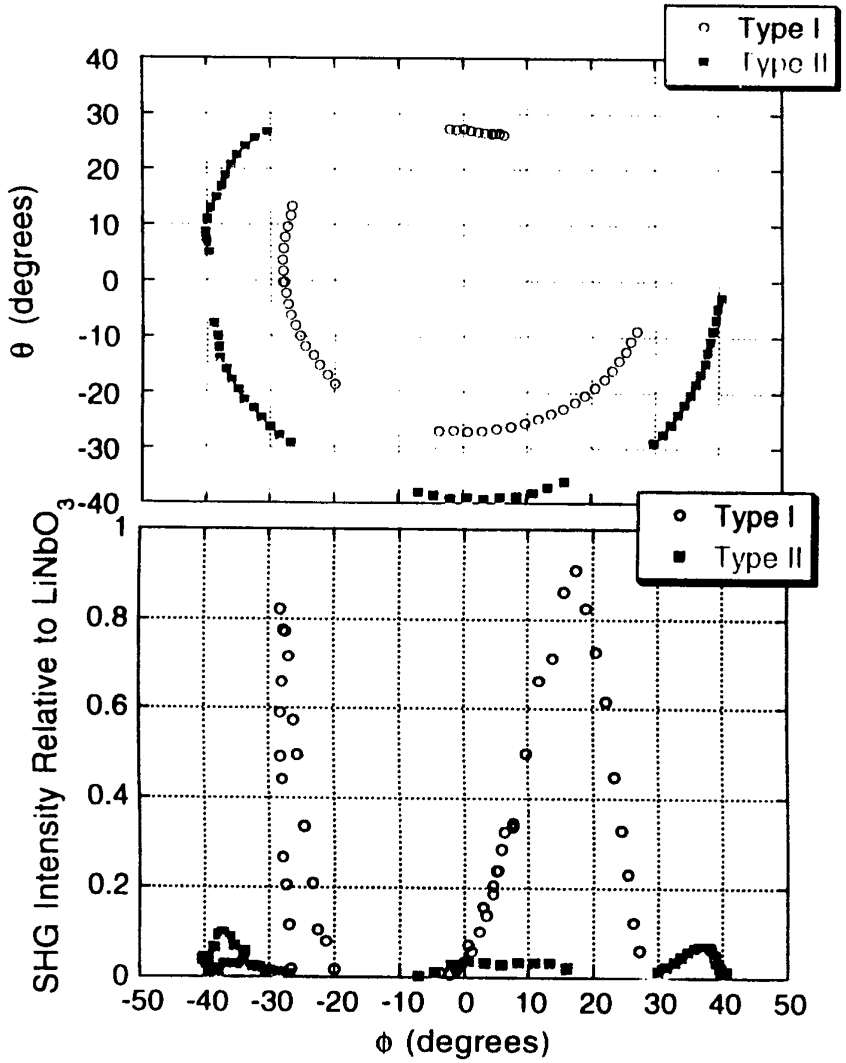

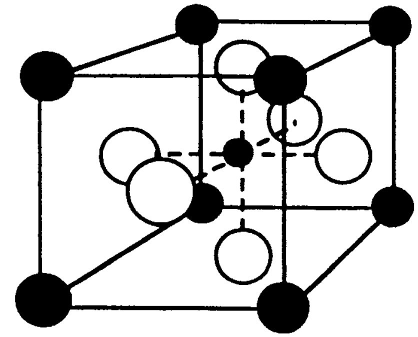

- Ge, Sn, Pb (2+)
- Cs, Rb (1+)
- Cl, Br, I (1-)

Ferroelectric Halides

- Perovskite structure
- Wide IR transparency
- Solution-grown semiconductor
- Mechanically robust
- Nonlinearity ~$LiNbO_3$
- Periodically poleable?

Rockwell Science Center

Progress in Crystal Growth of $CsGeCl_3$

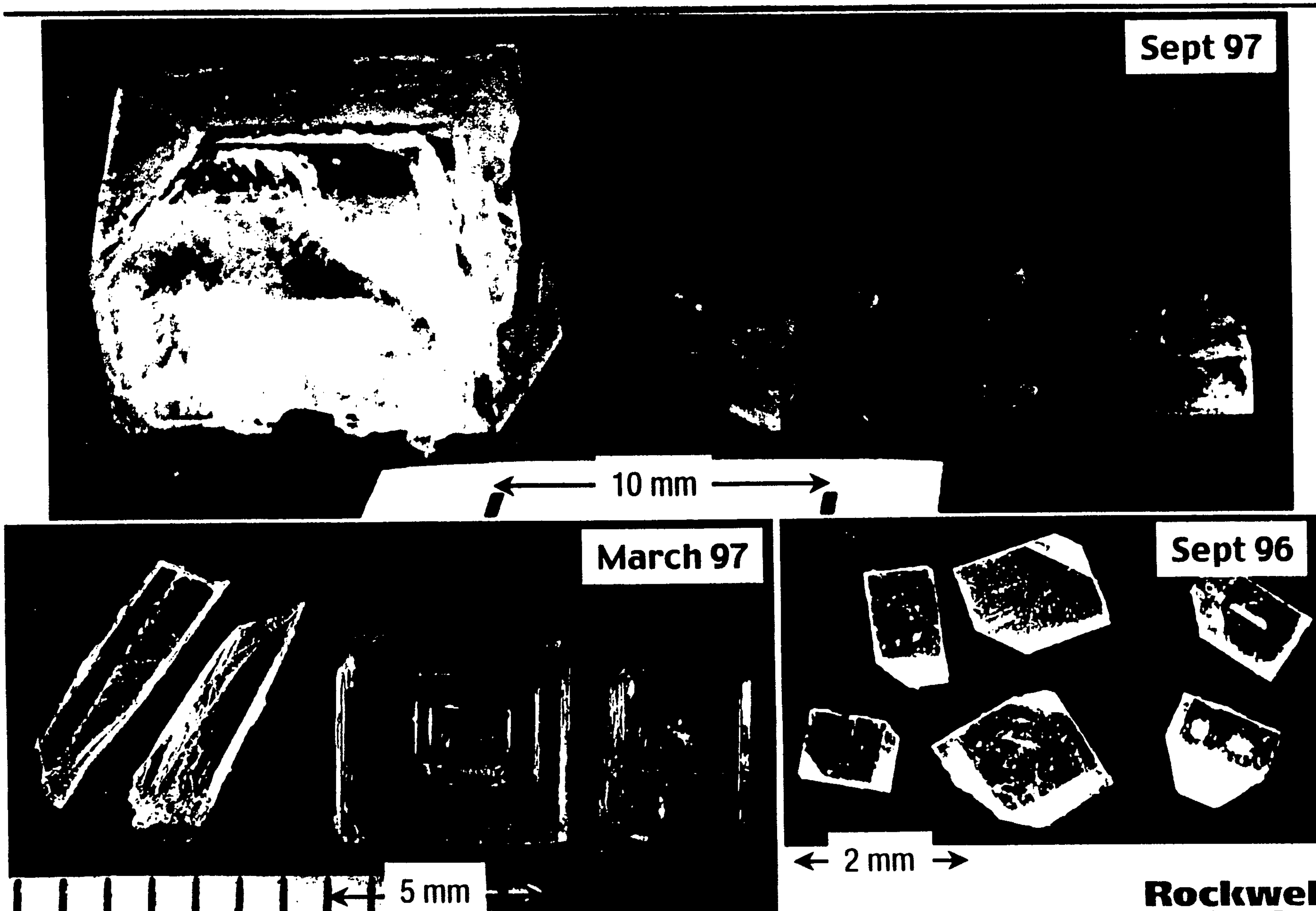

Rockwell
Science Center

$CsGeBr_3$ Transmission Spectra

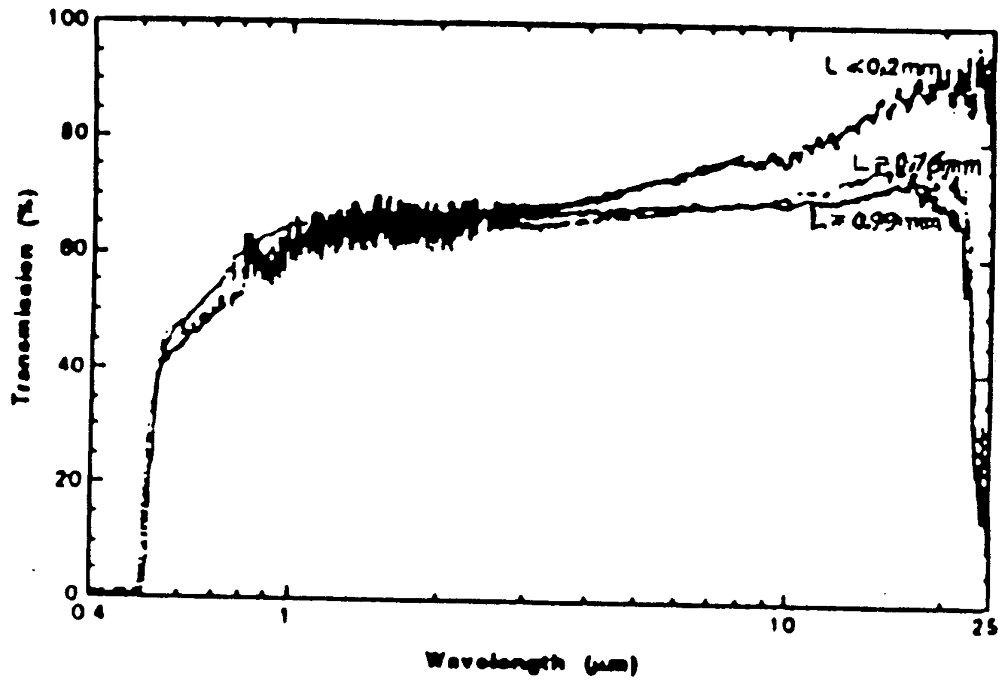

Rockwell
Science Center

$CsGeCl_3$ Transmission Spectra

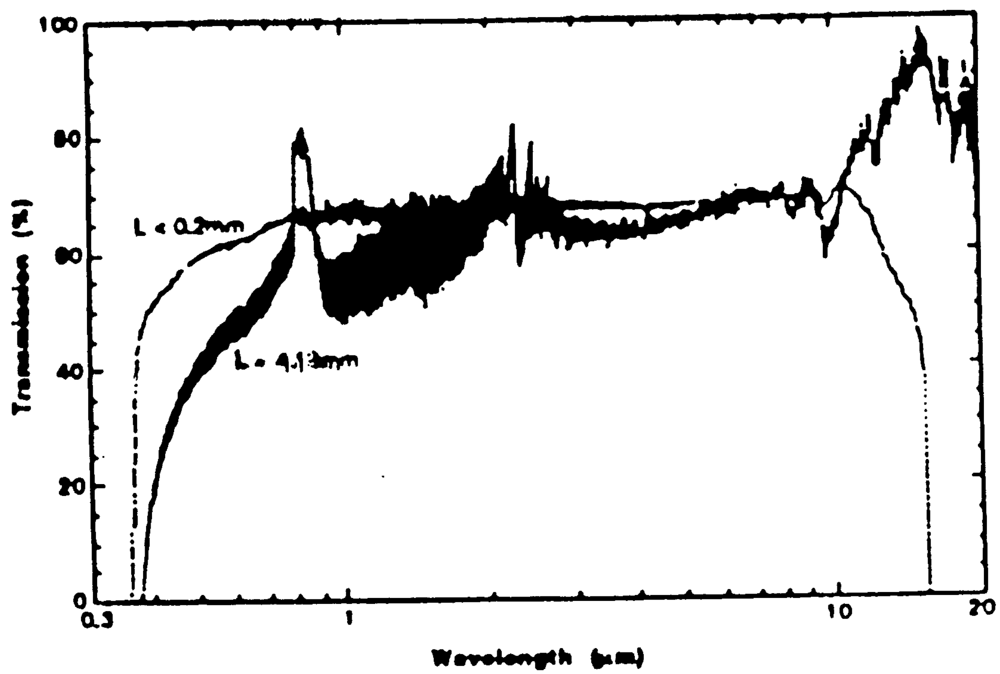

Rockwell
Science Center

We disclose a novel class of binary halides for the tunability of dielectric constant. This will enable very efficient tunable devices suitable for radar applications. These materials are combinations of $A^{+} B^{++} X$ (where A is mono valent, B is divalent and X=F, Cl, Br and I). We have experimentally demonstrated the growth feasibility of $Tl_3 PbBr_5$, $Tl_3 PbI_5$ and $Tl_4 HgI_6$ stoichiometry. Many other compounds such as $Rb_2 ZnCl_4$, K_2ZnF_4, $K_2 ZnBr_4$ and $K_2 ZnCl_4$ also belong to this category. These compounds were grown by Bridgman method in large sizes and were fabricated in desired shape and sizes. The devices of these crystals will provide high performance rf tunable filters for radar receivers and communications for receivers such as SC-21 and JSF.

TOTAL INTERNAL REFLECTION QUASI PHASE MATCHED WAVELENGTH CONVERTER

- GaAs TIR QPM Converter
- Couple Pump Into Plate With GaAs Prism
- Output Via Prism Also Allows Use Of High CHI Two Materials With Little Or No Birefringence

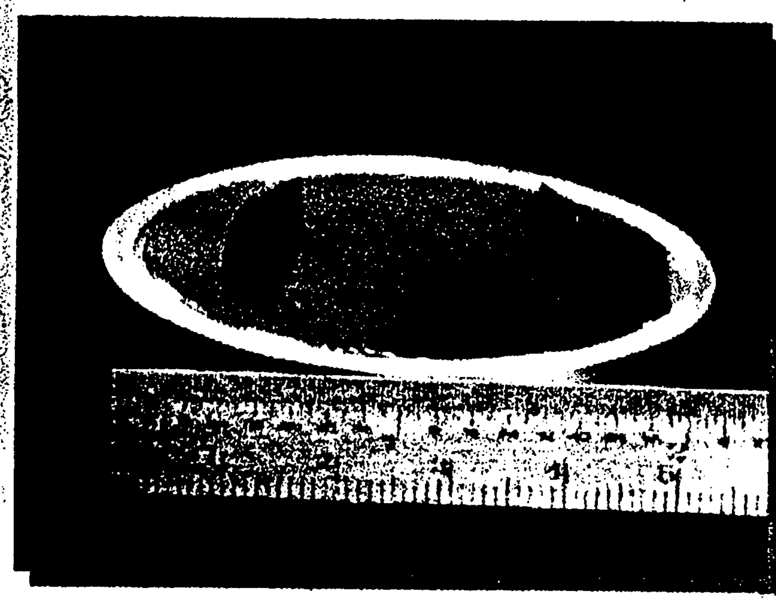

Non-linear for IR region in DTIM

L. I. Isaenko

Design & Technological Institute of Monocrystals SB RAS, 630090, Novosibirsk, Russia, E-mail: lisa@lea.nsk.su

Outlines

I. **Design & Technological Institute of Monocrystals SB RAS:**
- field of activity, main crystals;
- contacts and collaborators;

II. Crystal real structure.

1. Investigation techniques;
2. Pyroelectric properties effect on processes of crystallization and defect formation (on example of KTA, $LiInS_2$);
3. Defects, appearing at deviation from stoichiometry (KTA, $AgGaS_2$ $LiInS_2$);

III Structural investigation

1. Structural features responsible for spontaneous polarization P_s, in KTA, $LiInS_2$
2. Structural simulation of doping process:
- KTA, doped by Nd and Yb;
- $LiInS_2$, doped by Nd;
- $AgGaS_2$, doped by Yb

IV. Spectroscopic parameters of polyfunctional crystals

V. Double chlorides as active media for IR region

VI. Conclusions

Design & Technological Institute of Monocrystals,
Russian Academy of Sciences, Siberian Branch,
founded in 1978

The main trends of the scientific research:

1. The complex physic-chemical study of the growth processes of the optic quality single crystals for the laser technique and optoelectronics.
2. Experimental modeling of the diamond crystallization processes and the refinement of the methods of diamond instruments manufacturing.
3. Experimental modeling of the natural mineral formation processes and the improvement of the methods of gem crystals growth..

Main growth techniques:

TSSG, Czochralski, Bridgeman-Stockbarger, Kyropulos,
low temperature growth from aqueous and organic solutions

The main groups of crystals under consideration:

- 0xides; halogenides, chalcogenides (Tables);

Foreign collaborators:

1. The Lawrence Livermore National Laboratory, U.S.A.;
2. Tohoku University, Japan;
3. Observatory of Pariş, Bureau of Metrology, Paris, France;
4. University of Bourgogne, Dijon, France,

Financial support:

1. Grant of the Civil research and Development Foundation (CRDF);
2. INCO-Copernicus grant;
3. Contracts with the LLNL beginning from 1992;
4. Contracts with other universities/ companies all over the world.

Table 2. SOME CHARACTERISTICS OF OBTAINED NONLINEAR SINGLE CRYSTALS

Crystal	Transparency µm	Max size of element (mm)	SHG cut off (nm)	Walk off angle (degree)	Optical damage threshold (MW/cm^2)	Conversion efficiency (%)
LBO	0.16 - 2.6	10 x 10 x 20	554	0.43(I) 0.22(II)	>10 000 (1.064 µm, 20 ns, 50 Hz)	70(1.064µm, 20ns,50Hz,2W) 30(0.8µm, 20ns, 50Hz, 2W) 55(1.064µm, quasi CW, 2W) 50(1.064µm, 20ns, 3W)
BBO	0.19 - 2.6	4 x 4 x 20	411	4.80	>2000 (1.064 µm, 10 ns)	30(1.064µm, 20ns, 3W)
CLBO	0.18 - 2.8	5 x 5 x 15	471	1.83	>10 000	1.064µm, 2W-5W
a-$LiIO_3$	0.28 - 5.6	30 x 30 x 30	630	4.0	500 + 100 (1.064µm, 20ns)	50(1.064µm, 20ns, 50Hz,2W) 35(0.780µm, 20ns,10Hz,2W) 20(1.064µm, 20ns,50Hz,3W)
KTP	0.35 - 4.5	5 x 5 x 15	990	0.06	500 (1.064µm, 20ns)	60(1.064µm, 10ns,50Hz,2W)
KTA	0.35 - 5.5	5 x 5 x 20	1083	0.06	>10 000 (1.064 µm, 70 ps)	OPO pumping by 20-30 (1.064µm, 20ns) to 3-5µm
POM	0.44 - 2.1	8 x 8 x 8	1000		2000(1.064µm,15ns) 75(0.53µm,15ns)	20(1.32µm, 10ns, $10MW/cm^2$ L=4mm
DLAP	0.23 - 1.95	10 x 10 x 10	532	2.0	>10 000 (1.064µm, 20ns)	
$LiInS_2$	0.4 - 12	5 x 5 x 10			>100 (1.064µm, 10 ns)	OPO up to 10 µm
$LiInSe_2$	0.6 - 15	5x5x5			>50(1.064, 10 ns)	
$AgGaS_2$	0.46 - 12	10 x 10 x 20	1736		8000(1.06µm, 15ps, 10Hz) 75(1.06µm, 10ns, 20Hz	OPO up to 10 µm (1.064µm, 20ps, 10mJ)
$AgGaSe_2$	0.65 - 18	5x5x5			>50	OPO up to 10 µm DFG up to 18 µm
GaSe	0.7 - 18	5x5x5			3.7 J/sm^2 (9.25 µm) 0.5 (cw 10.6 µm)	1 (OPO 2.94 µm, 100 ps) DFG up to 18 µm

Specific effects at crystallization/cooling
of pyroelectric (ferroelectric) crystals

1. **A strong anisotropy in growth rates** along and across polar axis;
2. **Self-organization of extended defects** structure directed to lower or compensate completely the large pyroelectric fields inside crystal appearing at crystallization or cooling:
   - Formation of **twin or domain structures** from several blocks with different (opposite) direction of spontaneous polarization vector P_s.
   - Formation of **channel type defects** extended along polar axis and filled by different phases with lower melting temperature which operates as a conductor removing the fields appearing in the «ideal» pyroelectric lattice.
3. **Cracking of the crystals** is particularly dangerous in temperatures where pyroelectric coefficient γ has maximum.
4. Pyroelectric fields stimulate **migration of alkali cations** and **formation of defects** in the cation sublattice.
5. The electric discharge as a result of huge pyroelectric fields inside crystals is one of the mechanisms of their **mechanical damage** at cooling or during operation in laser schemes.

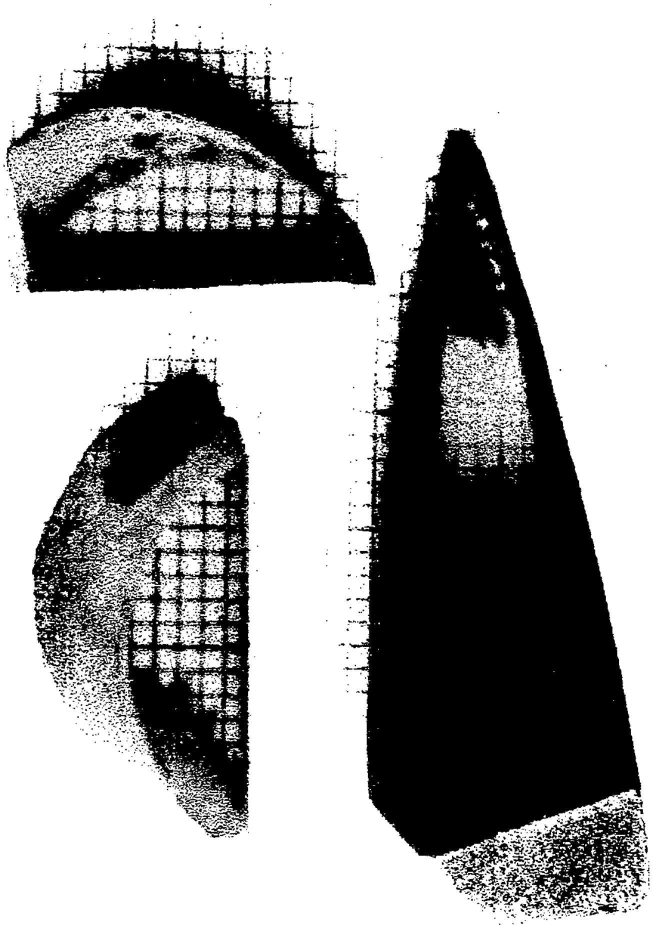

Single crystals

$KTiOAsO_4$	$LiInS_2$	$AgGaS_2$
pyroelectrics ferroelectrics	pyroelectrics	nonpyroelectrics

Symmetry

(point group)

mm2	mm2	$\bar{4}2m$

Lattice parameters

a= 13.103 A	a= 6.887 A	a= 5.757 A
b= 6.558 A	b= 8.05 A	
c= 10.746 A	c= 6.474 A	c=10.305 A
	density (G/cm^3)	
d=3.45	d= 3.5	d=4.56

Growth techniques

($T_{cryst.}$=850-1000 C)

TSSG with pulling from selfflux in K_2O-As_2O_5--TiO_2 system	Bridgeman-Stockbarger from melt	Bridgeman - Stockbarger from melt

Boule size (mm^3)

50x55x45	20x20x50	25x25x100

The technique of differential dissolving combined with the ICP analysis (inductively coupled plasms)

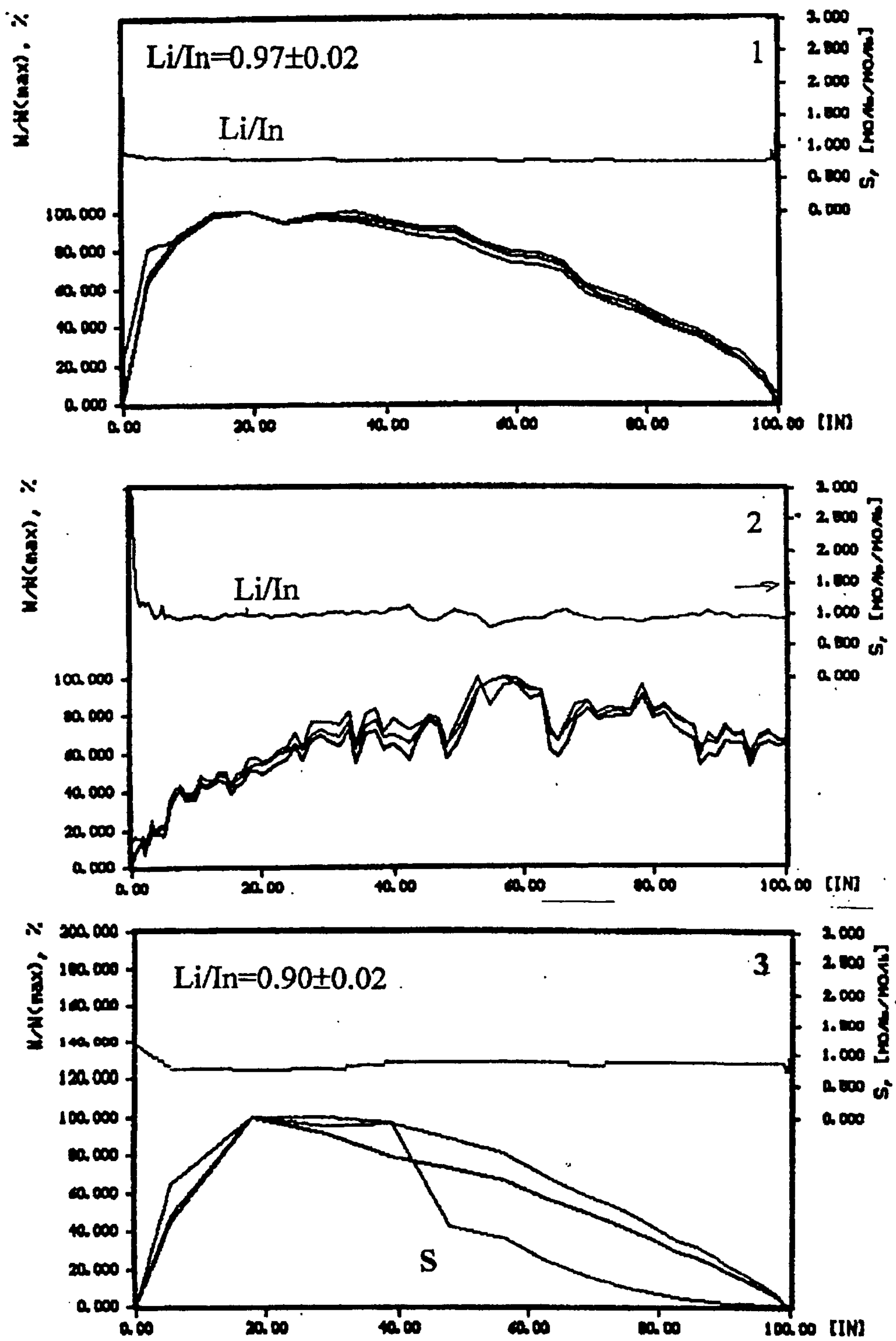

Kinetic curves of dissolving, Li/In stoichiogramms for:
1, 2 – grown samples, 3 – annealed in S_2 sample

	KTA		$LiInS_2$	$AgGaS_2$	
Dopant	Yb	Nd	Nd	Yb	Nd
Segregation coefficient C_{cryst}/C_{melt}	0.2	10^{-3}-0.1*	0.02	0.02-0.3**	$<10^{-3}$
Possible position of dopant ion in the lattice	Distorted TiO_6 prism, two sites: Ti(1),Ti(2)	K-O(8,9) polyhedral Formation of NdO_7	Octahedral cavity	Octahedral cavities Distorted octahedral	
Absorption cross-section, cm^2 (300K)	1.2×10^{-20}		2×10^{-20}		

Notes: * for KTA:Me^{2+}
** for milky as grown $AgGaS_2$ sample

Necessary conditions for dopant stability in the crystal structure:

- Coordination number ≥6;
- Similarity of sizes for dopant ion and host site;
- Charge compensation

Design & Technological Institute of Monocrystals SB RAS
43 Russkaya str.,
Novosibirsk 630058 Russia
E-mail: alex@elis.nsk.ru

Spectroscopic properties of pure and Rare Earth-doped nonlinear crystals for the mid-IR

A.Elisseev

Outline:

A. Spectroscopic features of pure nonlinear crystals

1. Absorption /luminescence of pure nonlinear single crystals for the mid -IR: excitation mechanisms

- $KTiOAsO_4$ (KTA);
- $AgGaS_2$;
- $LiInS_2$.

B. Spectroscopic properties of RE-doped crystals

1. Option of RE dopants for nonlinear crystals as

- Polyfunctional laser elements;
- Chalcogenides as an active media for the mid IR;

2. Spectroscopy of Nd and Yb: spectra, decay times,
3. Radiation and radiationless multiphonon relaxation, stimulated emission in the mid-IR

Photoluminescence in $AgGaS_2$, T=80K

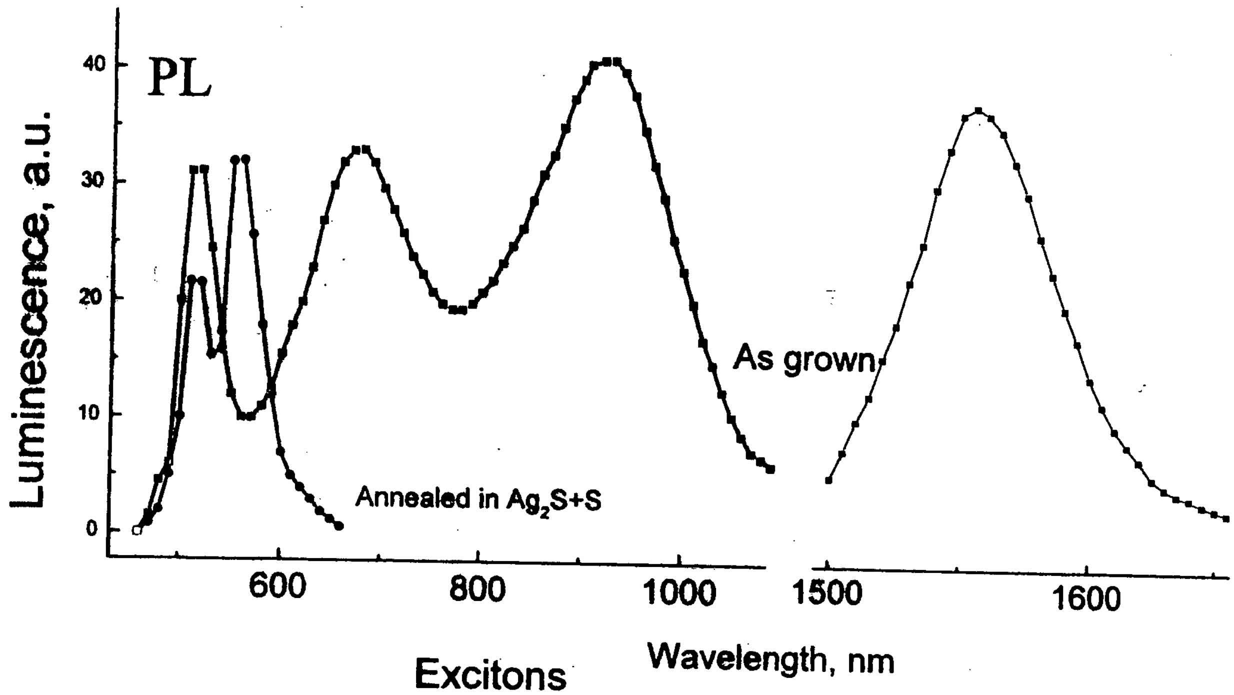

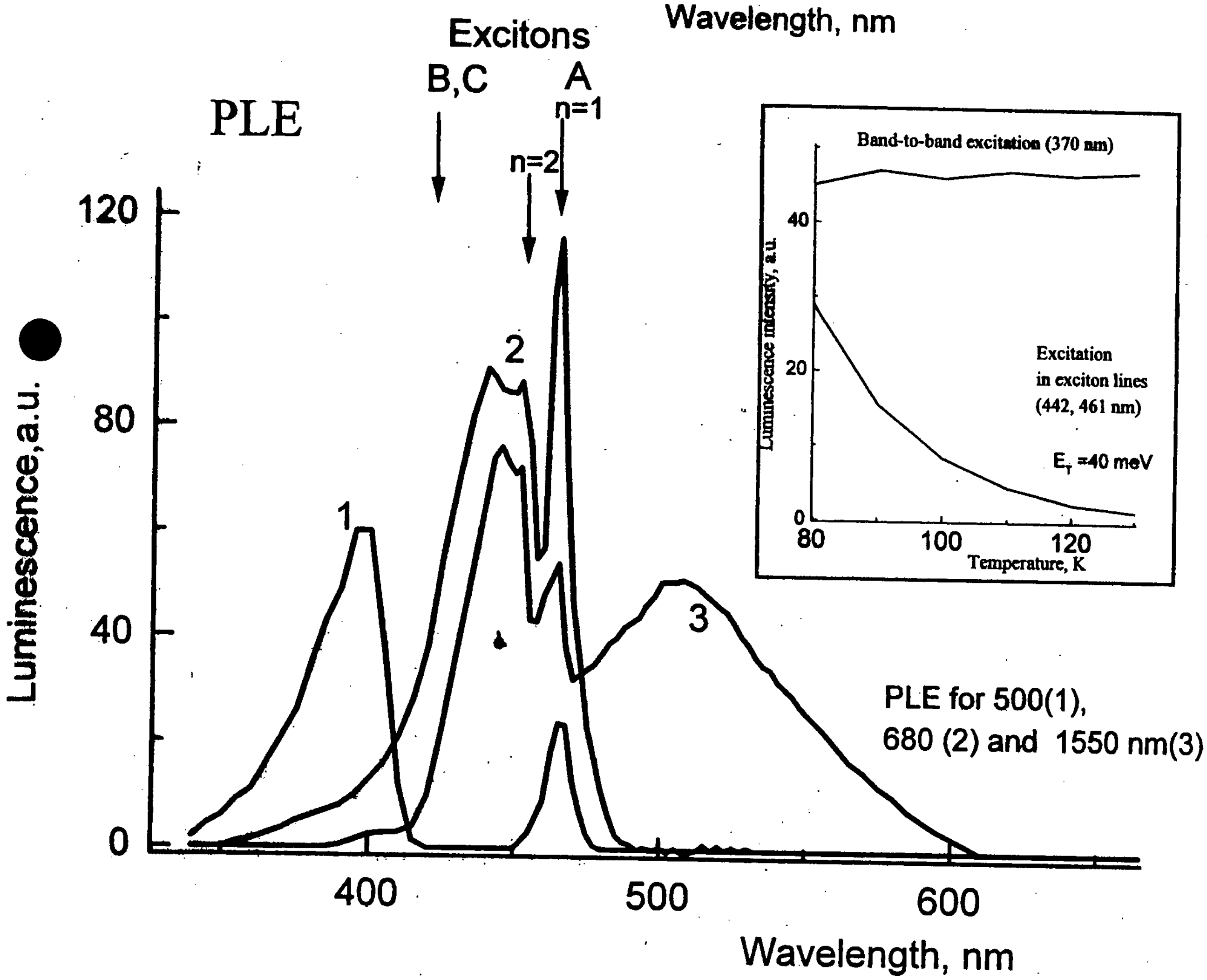

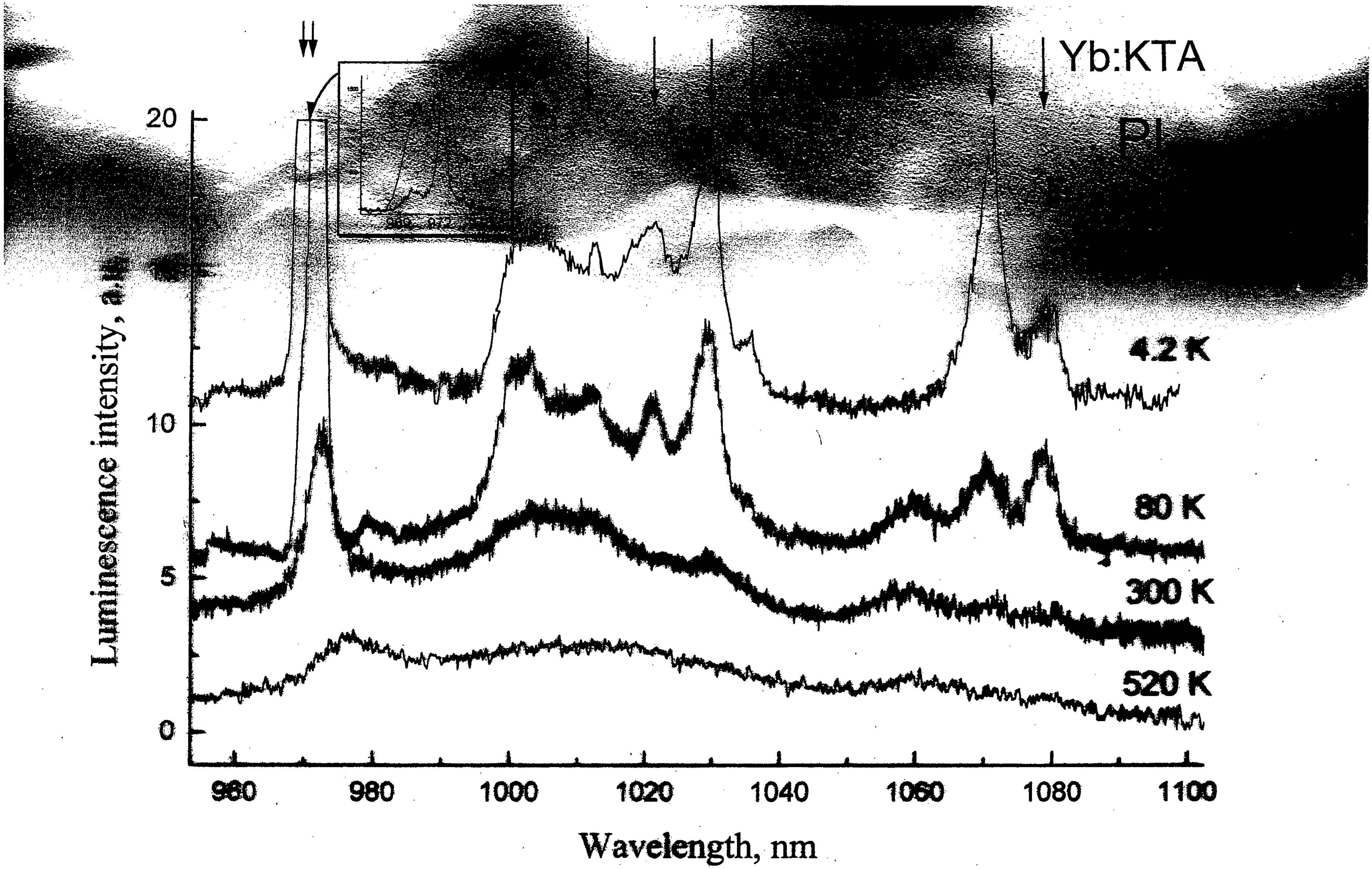

Yb:KTA
PL
4.2 K
80 K
300 K
520 K
Luminescence intensity, a.u.
Wavelength, nm
0
5
10
20
960
980
1000
1020
1040
1060
1080
1100

Luminescence spectra of $LiInS_2$:Nd
versus temperatureat 825 nm excitation

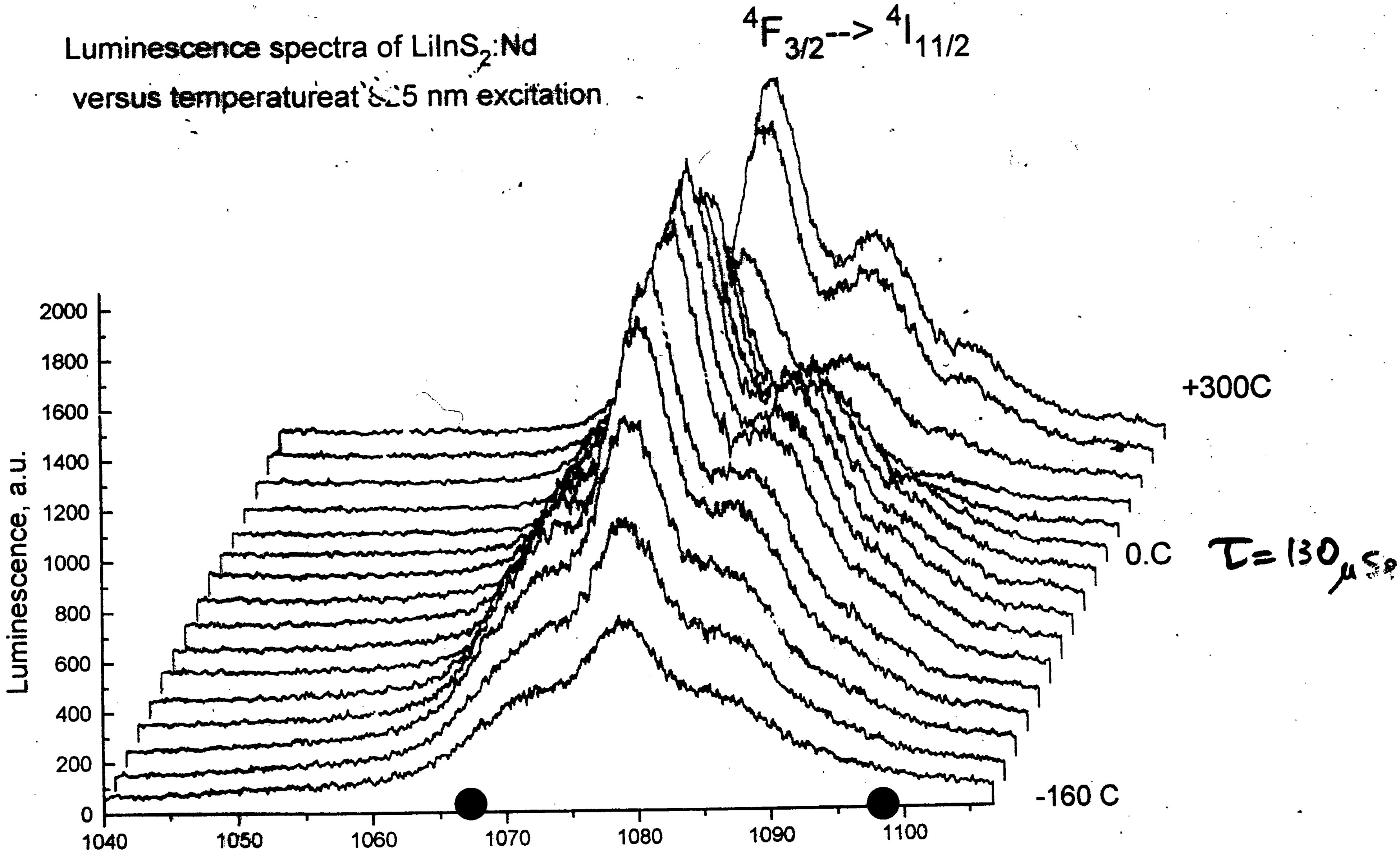

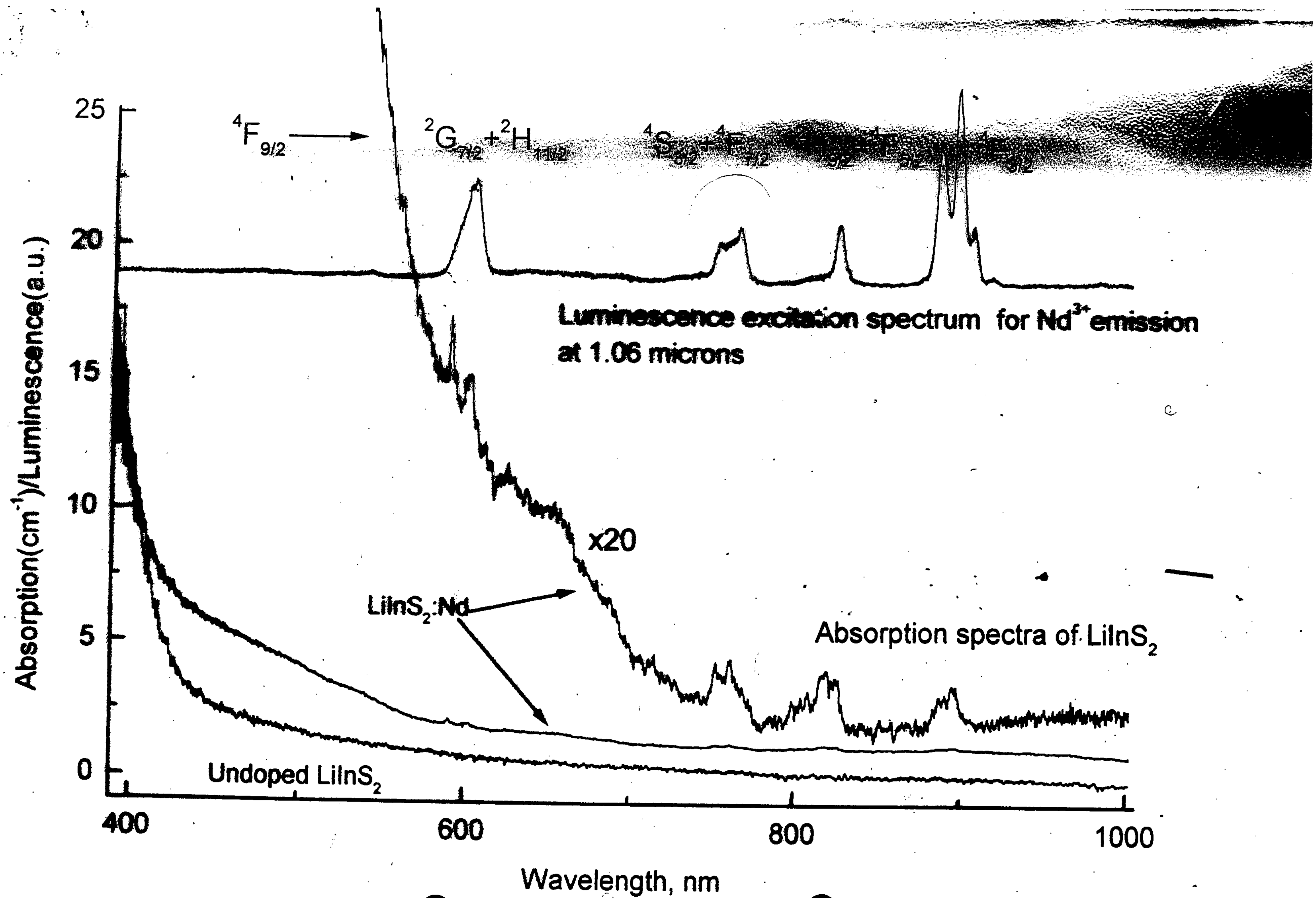

Absorption(cm-1)/Luminescence(a.u.)
25
20
15
10
5
0
4F9/2
2G7/2+2H11/2
4S3/2+4F7/2
Luminescence excitation spectrum for Nd3+ emission
at 1.06 microns
x20
LiInS2:Nd
Absorption spectra of LiInS2
Undoped LiInS2
400
600
800
1000
Wavelength, nm

Growth and Optical Properties of $LiNbO_3$-WO_3 and $LiNbO_3$-MoO_3 solid solutions

A. Hill, A. Pirie, T. P. J. Han and H. G. Gallagher

Optical Materials Research Centre
Department of Physics and Applied Physics
University of Strathclyde
Glasgow G1 1XN, Scotland, UK

Tel: +44-141-548 4015 ; Fax: +44-141-553 4162
E-mail: h.g.gallagher@strath.ac.uk

Crystal Growth

- Method: Czochralski
- Composition: $X < 10$ mol%

  Solid solution range of $Li_{1-x}Nb_{1-x}W_xO_3$:-

  At T = 860 °C, X = 0 - 50 mol% Blasse et al, 1970

  At T = 750 °C, X = 0 - 20 mol% Foulon et al, 1998

  Solid solution range of $Li_{1-x}Nb_{1-x}Mo_xO_3$:-

  At T = 860 °C, X = 0 - 30 mol% Blasse et al, 1970

- Melting temperature: 1180 - 1250 °C
- Poling: 1 -2 mA/cm^2 at 1200 °C

Variation in Powder SHG for $LiNbO_3$ Doped with Various Concs. of WO_3

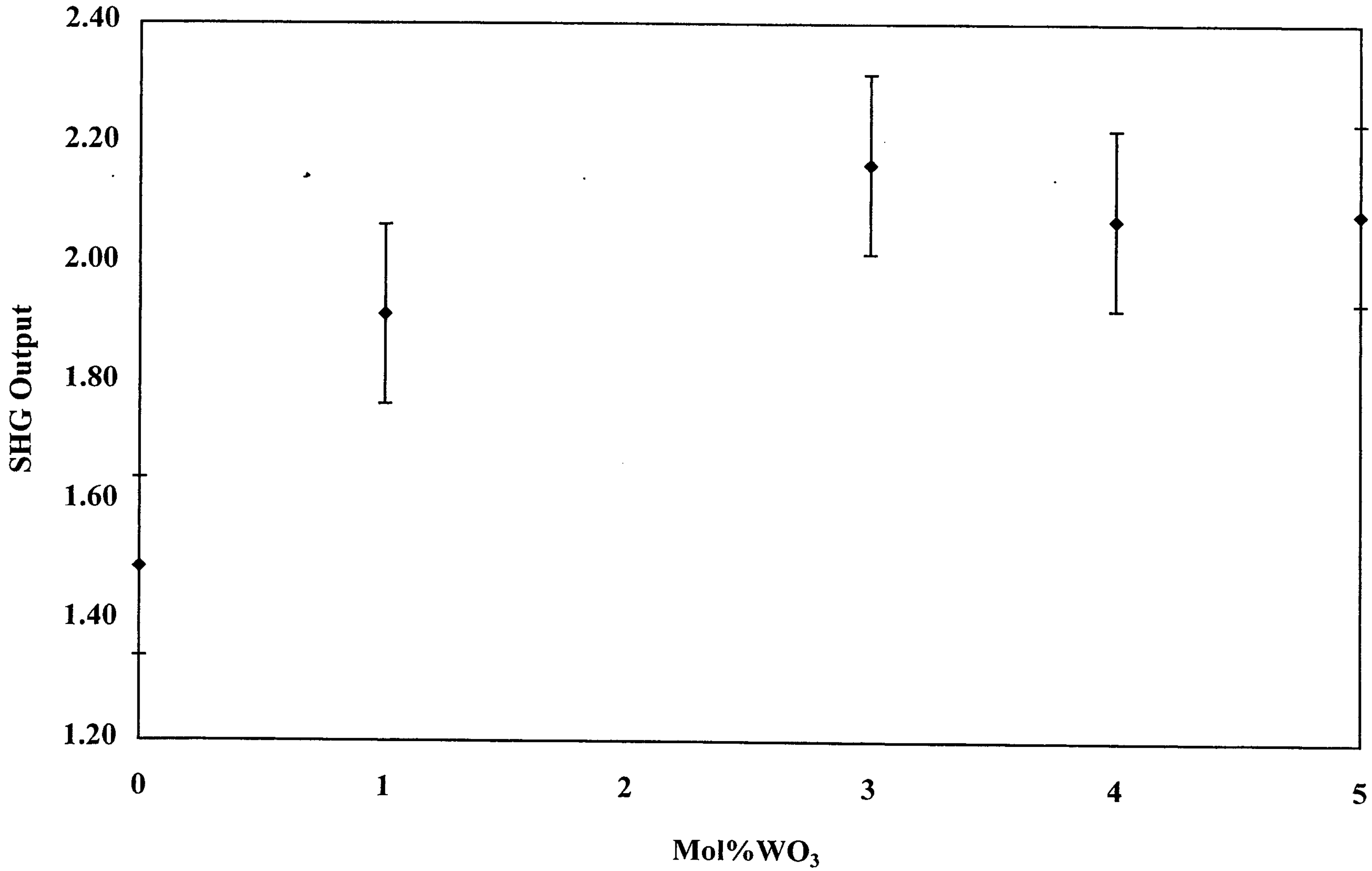

Variation in Powder SHG for $LiNbO_3$ Doped with Various Concs. of MO_3

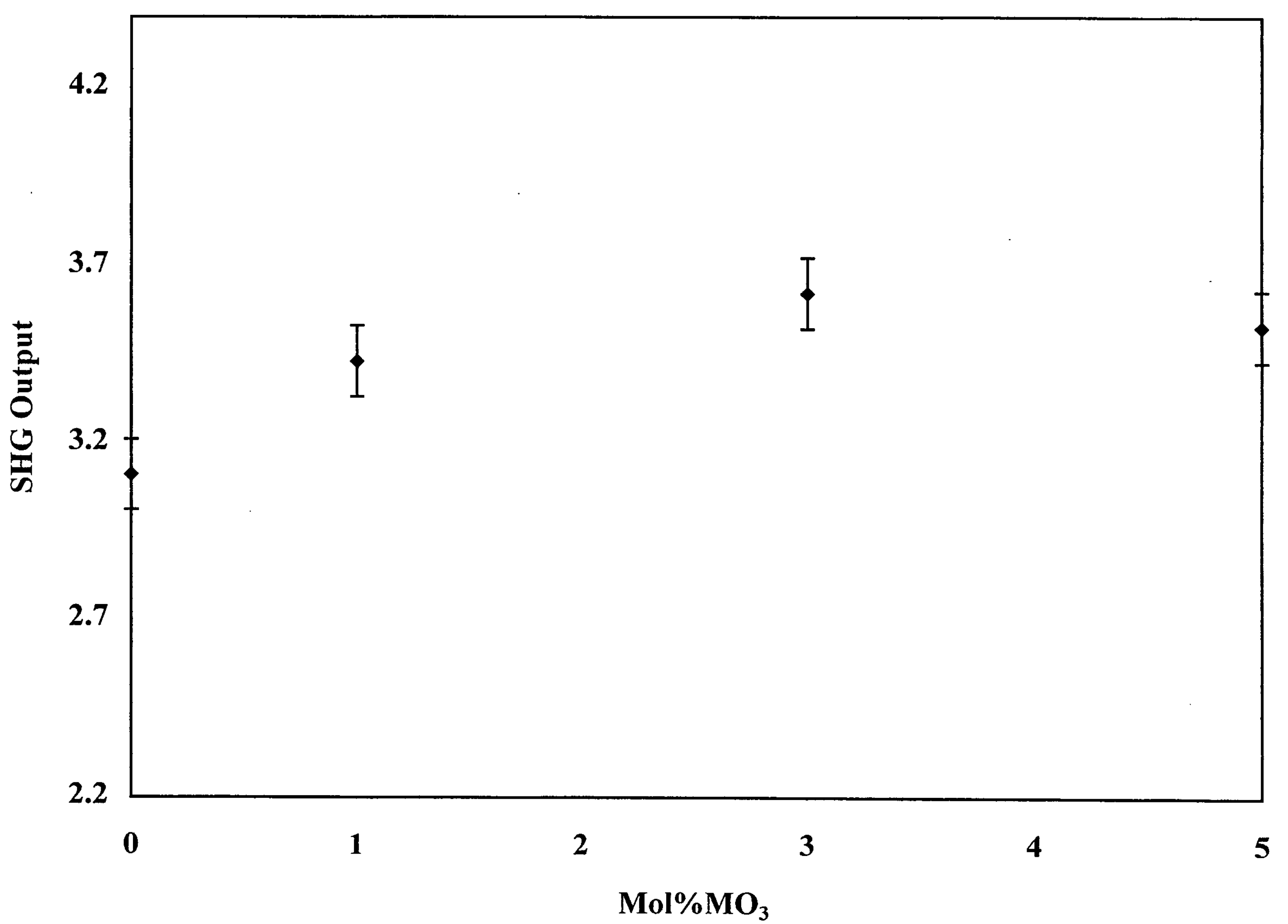

Variation of d_{33} Coefficient for $LiNbO_3$ Doped with Various Concentrations of WO_3

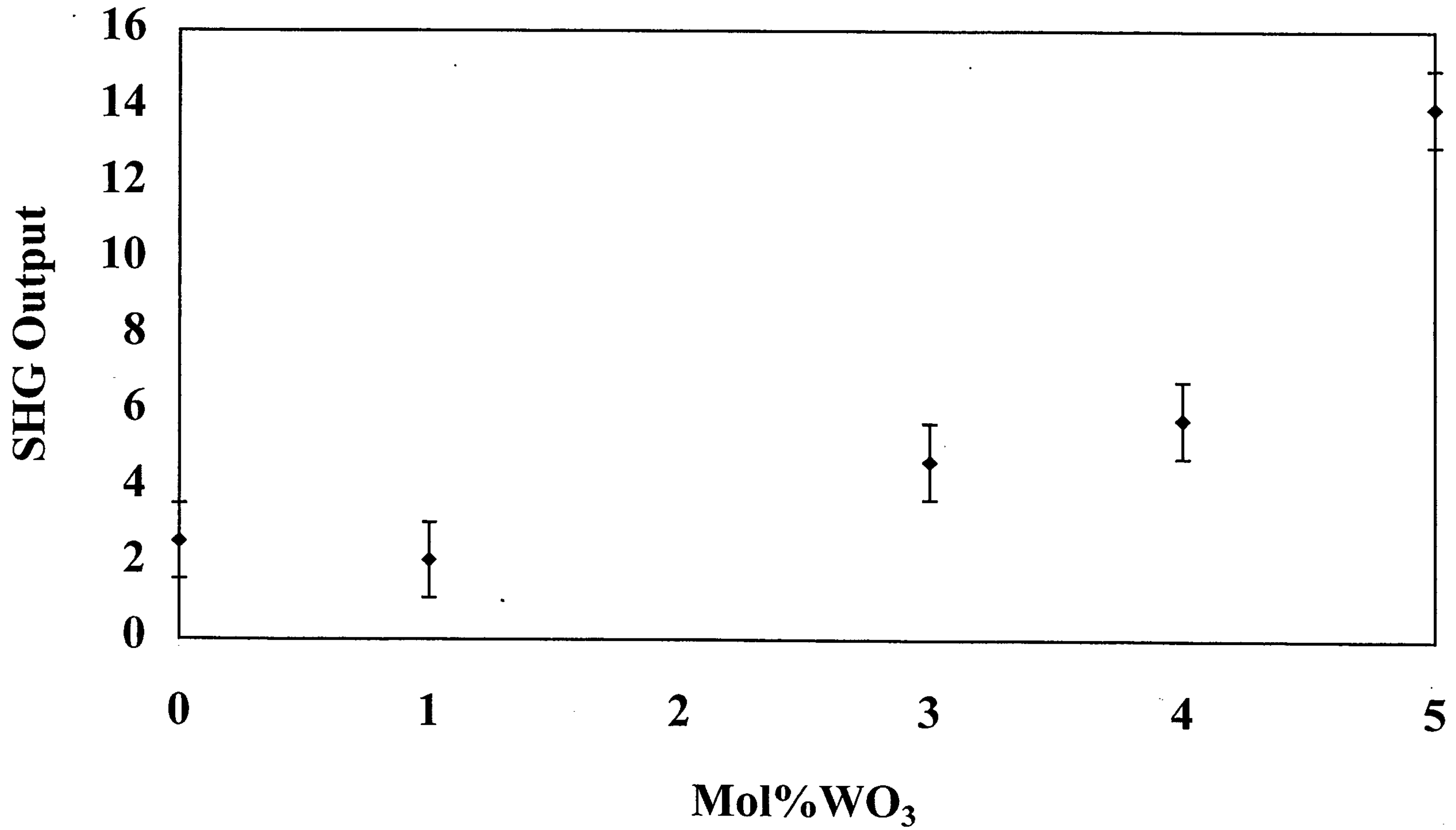

Variation of d_{33} Coefficient for $LiNbO_3$ Doped with Various Concs. of MO_3

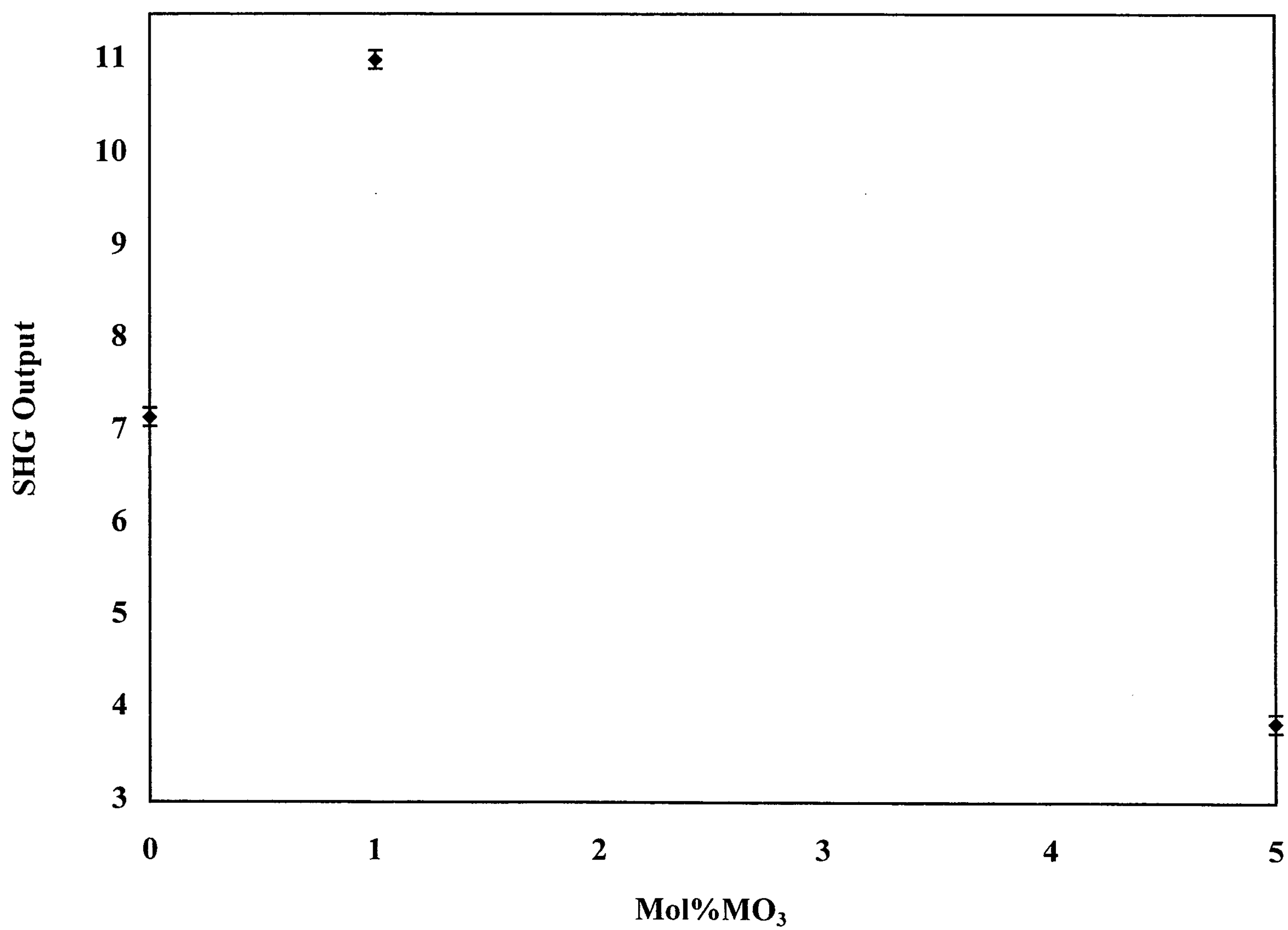

Conclusions

- The solid solution range for growth of $Li_{1-x}Nb_{1-x}W_xO_3$ and $Li_{1-x}Nb_{1-x}Mo_xO_3$ crystals is limited to $x = 0.5$ due to cracking and constitutional cooling, respectively
- Optical properties vary (linearly?) with concentration of WO_3 and MoO_3
- Further work is required to refine growth conditions and eliminate optical defects
- More detailed optical characterisation is necessary

Growth and Characterisation of Photorefractive Materials

Craig.J. Finnan, H.G. Gallagher, T.P.J. Han.
Optical Materials Research Centre (OMRC),
University of Strathclyde
G. Cook, D. Jones
DERA Malvern

THE UNIVERSITY OF STRATHCLYDE IN GLASGOW

DERA

Czochralski Growth Technique

- Both single and co-doped $Fe{:}LiNbO_3$ samples have been grown.
- Congruent Lithium Niobate is best grown from a melt by the Czochralski technique.
- Congruent composition is 48.6mol% Li_2O, 51.4mol% Nb_2O_5.
- To reduce thermo-Mechanical Strain, a Platinum Afterheater must be used.
- Surface cracking can occur due to Li_2O evaporation.

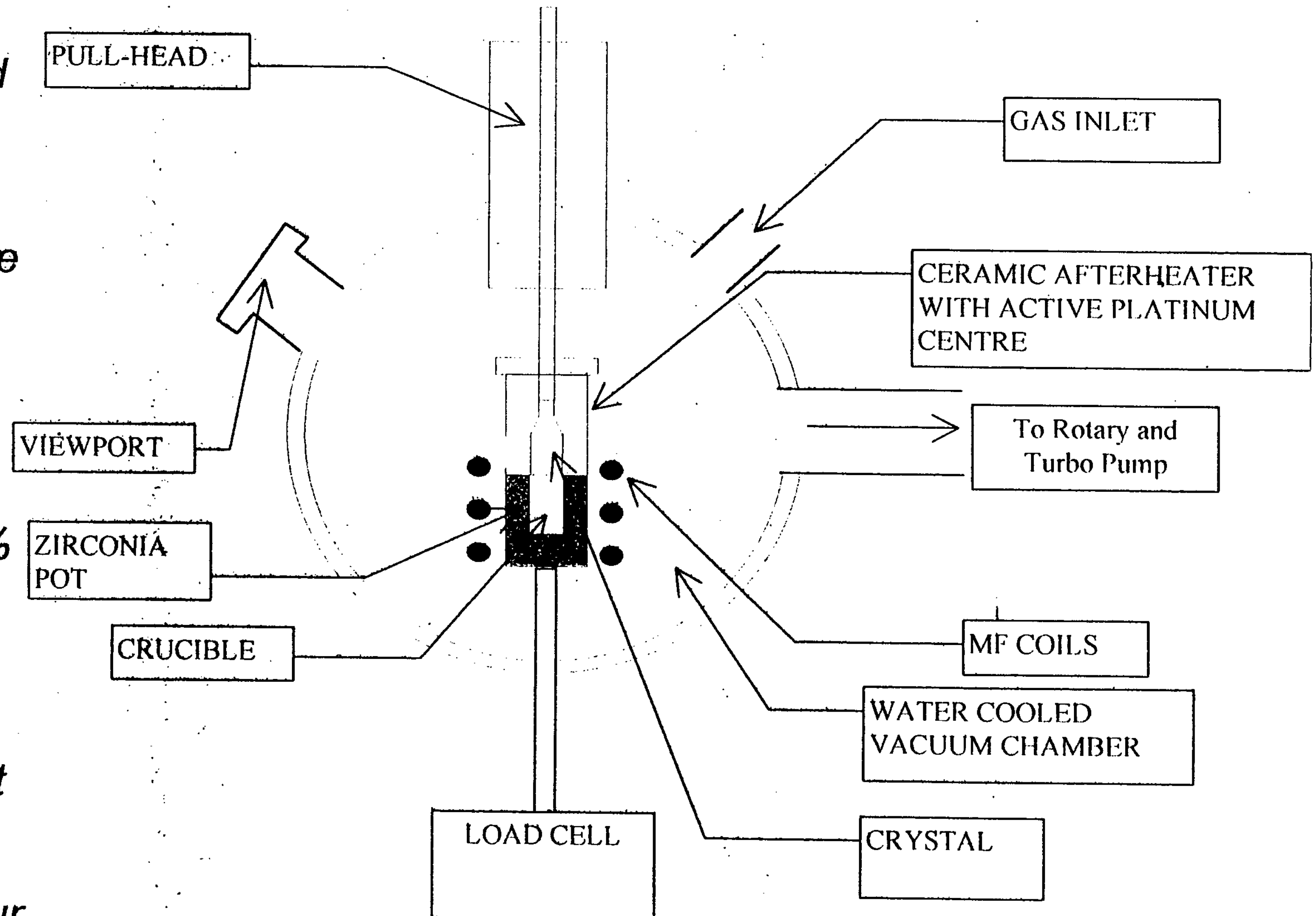

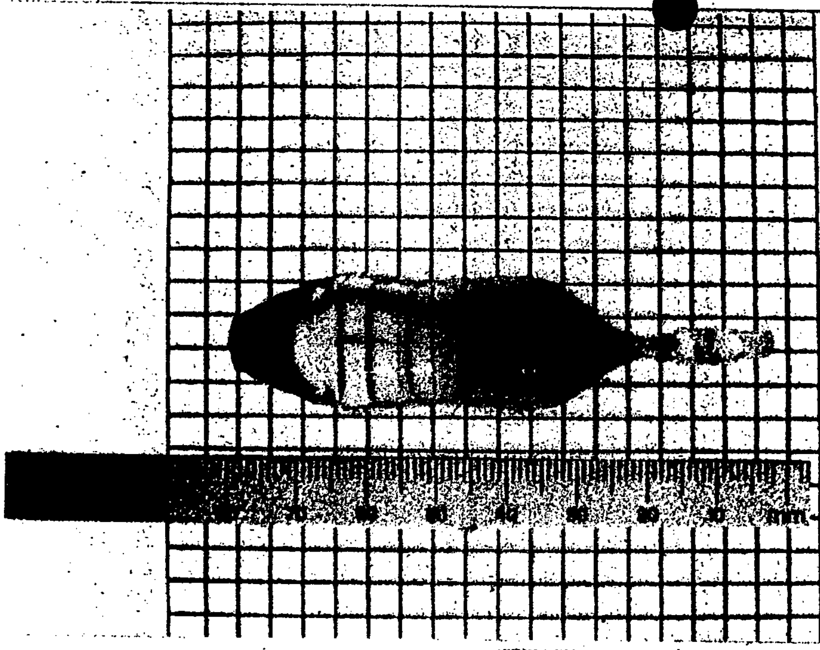

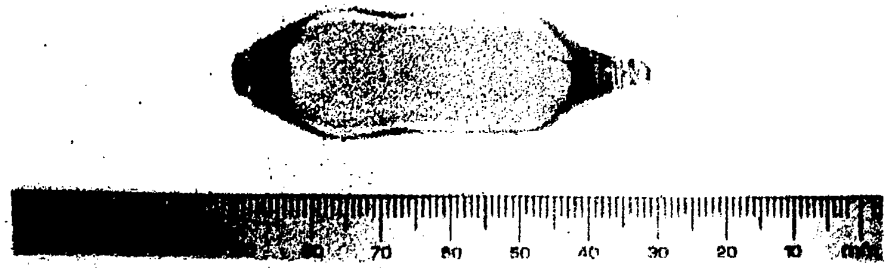

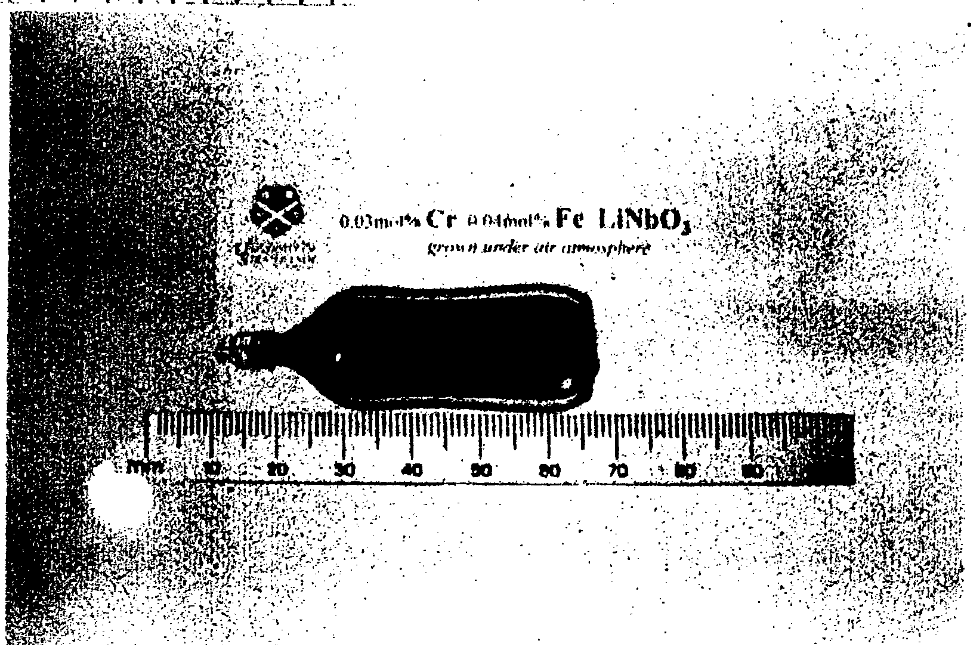
0.03mol% Cr 0.04mol% Fe LiNbO3
grown under air atmosphere

EXPERIMENTAL SETUP

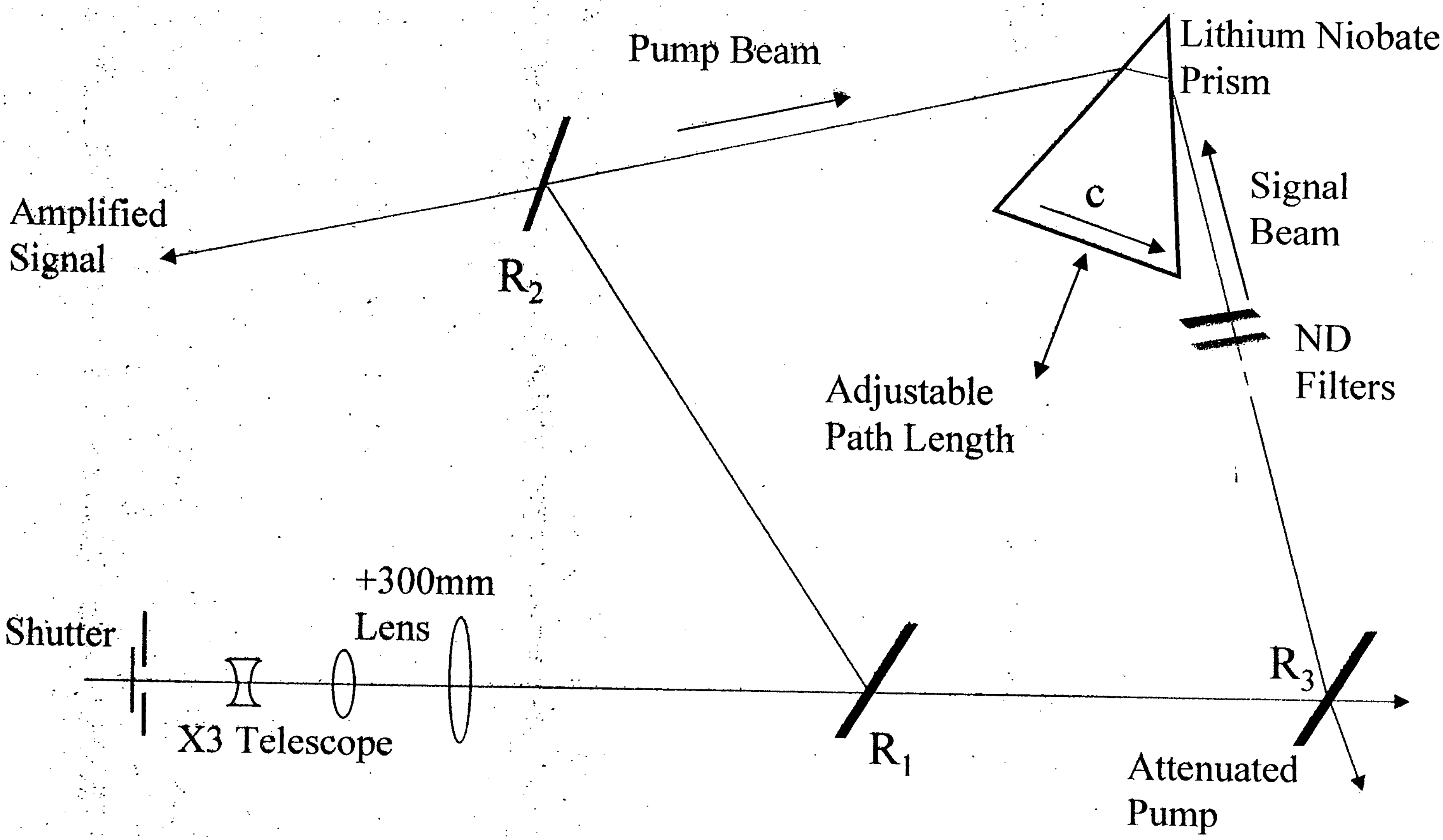

LiNbO$_3$ optical gain as a function of Signal Intensity.

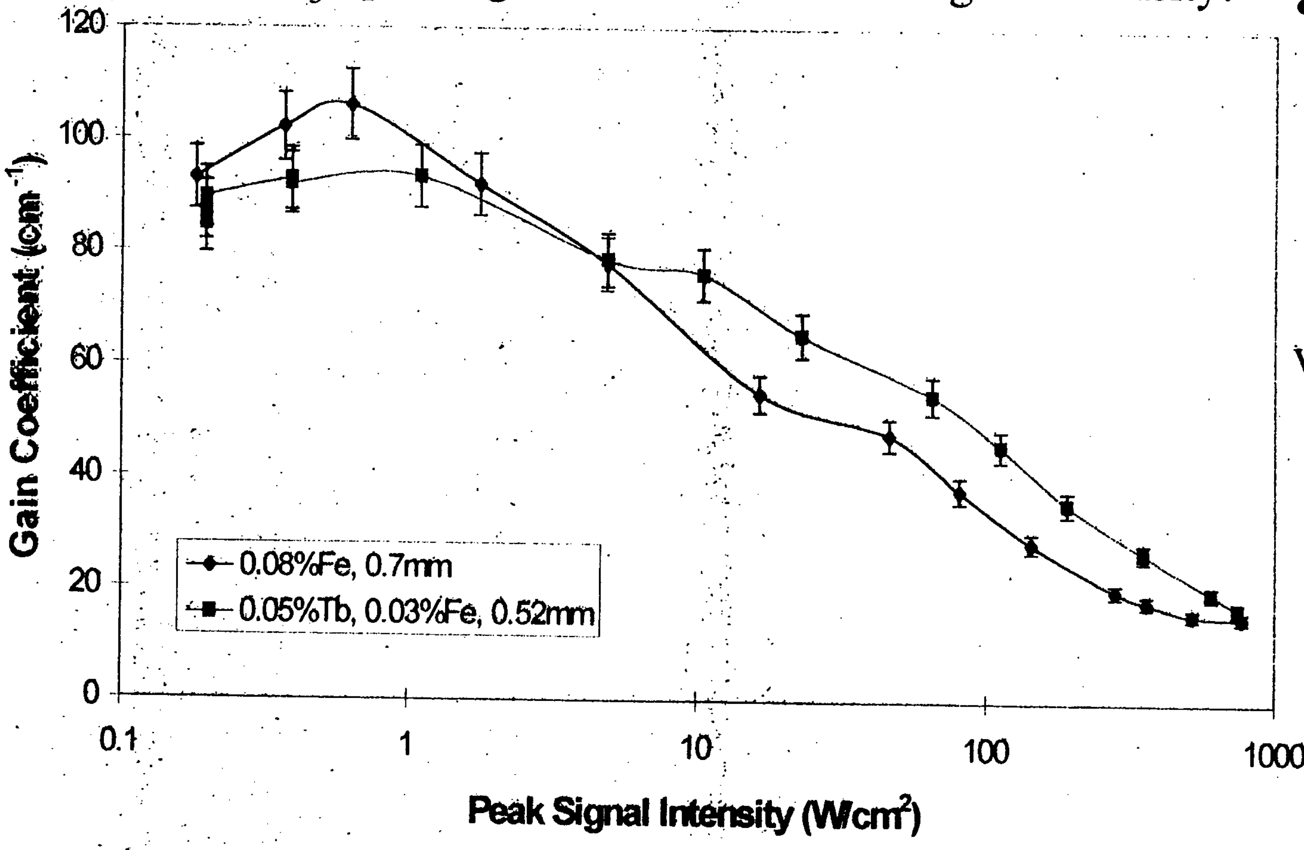

- Pump intensity is constant at 1kW/cm^2.
- Gain Coefficient is calculated from,

$$G = \frac{\ln\left[\frac{(I_A - I_B)}{I_S}\right]}{l}$$

where I_B is the background intensity with no pump beam, I_S and I_A are the intensities of the transmitted signal beam in the presence and absence of the pump, and l is the sample thickness

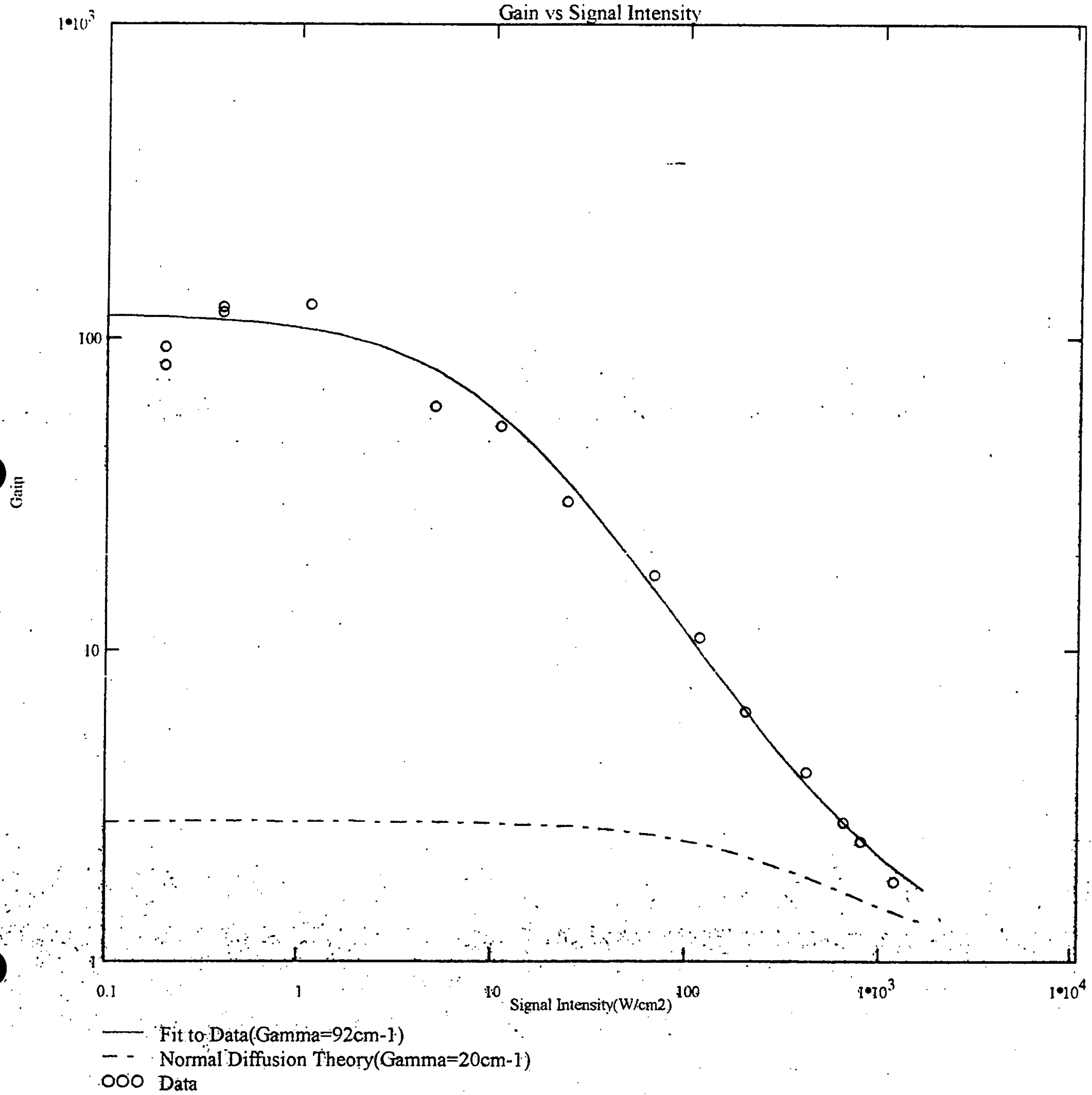

Gain vs Signal Intensity
1•10³
100
10
1
Gain
0.1
1
10
100
1•10³
1•10⁴
Signal Intensity(W/cm2)
Fit to Data(Gamma=92cm-1)
Normal Diffusion Theory(Gamma=20cm-1)
OOO Data

Developments in PPLN Fabrication at the ORC

Dr. Peter G.R. Smith

Prof. D.C. Hanna, Prof. D.J. Richardson
Dr R.W. Eason, Dr. Graeme Ross, Dr. Neil Broderick
Dr. H.L. Offerhaus
Paul Britton, Cowin Gawith, Joyce Abernethy, Ian Barry

Outline

- PPLN Fabrication 1mm material
- PPLN OPOs and fibre lasers
- Etched PPLN microstructuring
- HeXLN

PPLN Fabrication 1mm material

- DERA Supported Project
- Constructed a current controlled poling rig for 1mm samples
- Successfully fabricated 1mm thick PPLN at coarse periods >25μm.
- Issues are breakdown through the material, electrode design, yield.
- Future - how to improve quality, how to improve yield? Can push to 2mm?

Experimental Setup

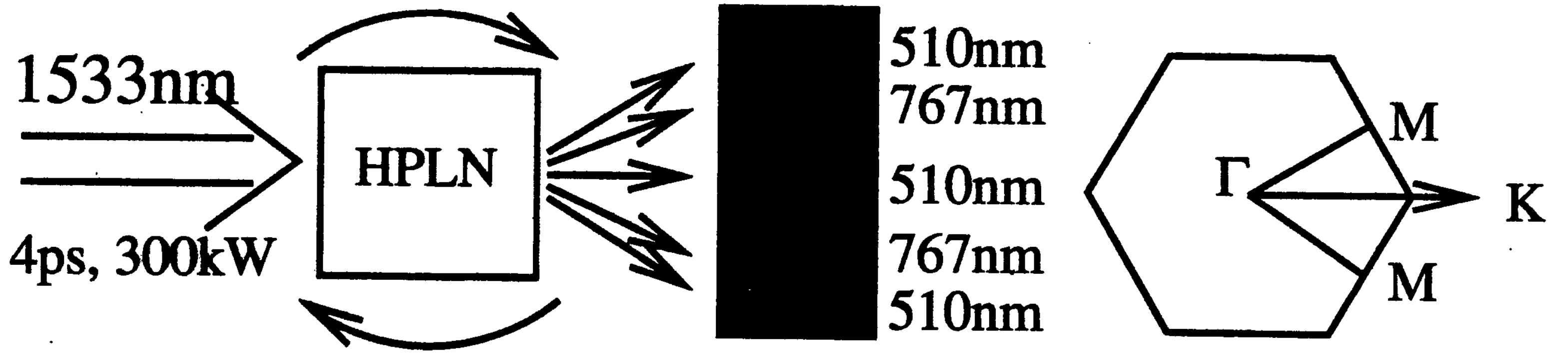

- A schematic of the experimental setup is shown above. The pulse source is a high power all-fibre CPA source.

- The input pulses were ~ 3ps long with a bandwidth of 2nm and a maximum peak power of 300kW.

2D patterned PPLN

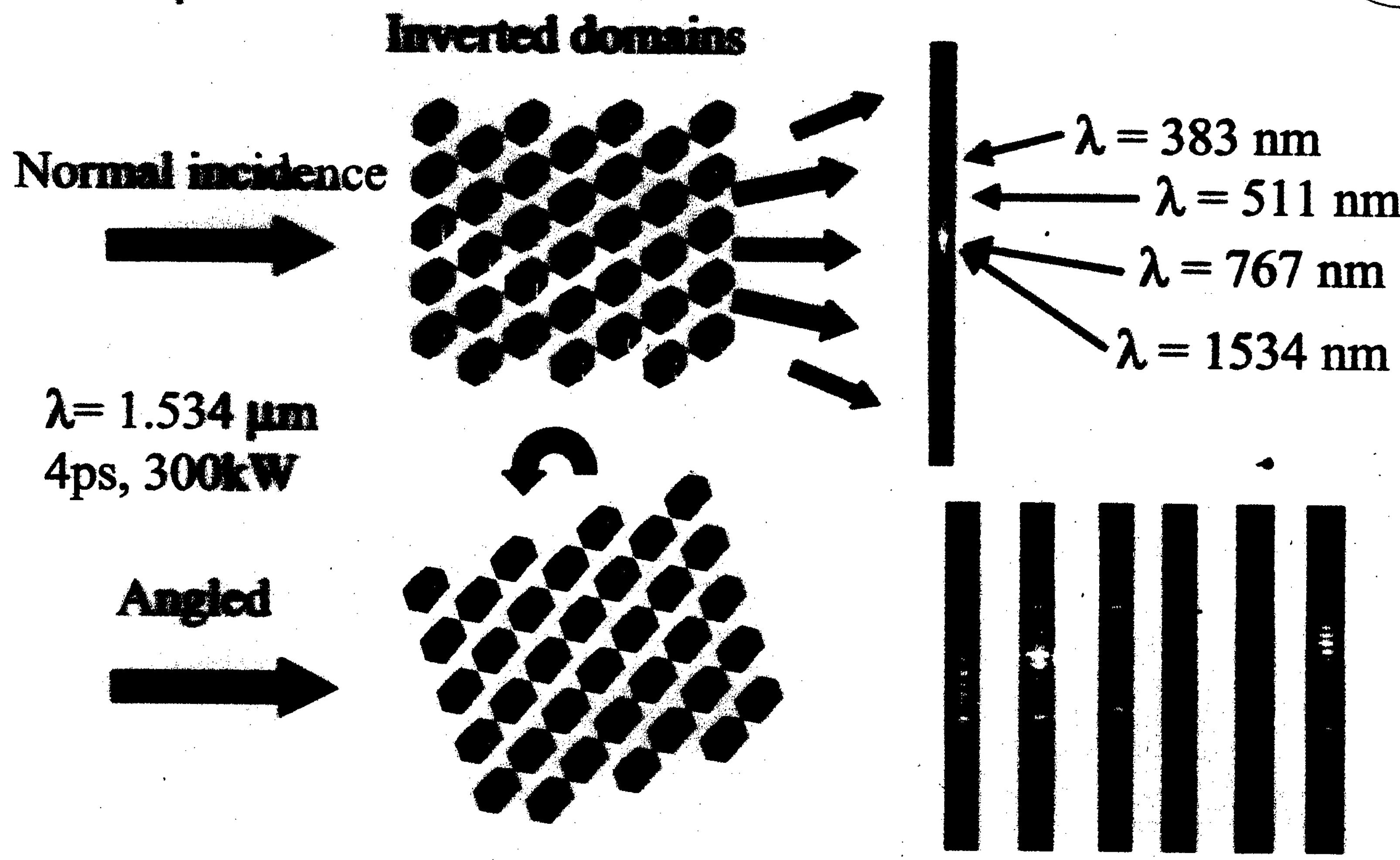

Introduction

- Recently V. Berger [Phys. Rev. Lett. **81**, 4136 (1998)] developed the idea of a nonlinear photonic crystal in which the linear refractive index is constant but the nonlinear suspectibility varies periodically.

- We have fabricated such a crystal in Lithium Niobate. Due to the crystal symmetry of $LiNO_3$ our crystal has hexagonal symmetry – hence HeXLN.

- Such a crystal is able to phase-match nonlinear interactions in any direction where there is a suitable reciprocal lattice vector (RLV).

- For certain angles of incident this should result in multiple output beams for a single input beam. Or it could phase-match multiple wavelengths at different angles simultaneously.

Lithium Niobate: differential etching

- +z untouched
- -z etches 700nm/hr (room temp.)

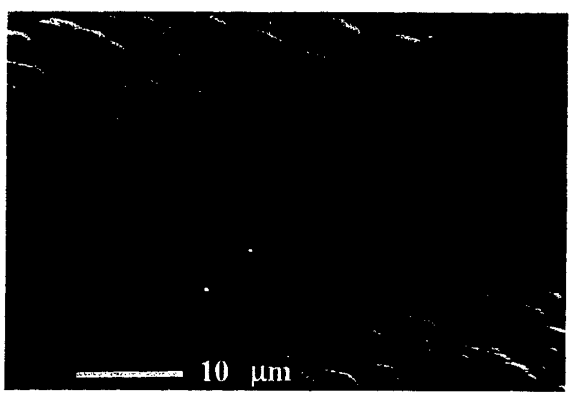

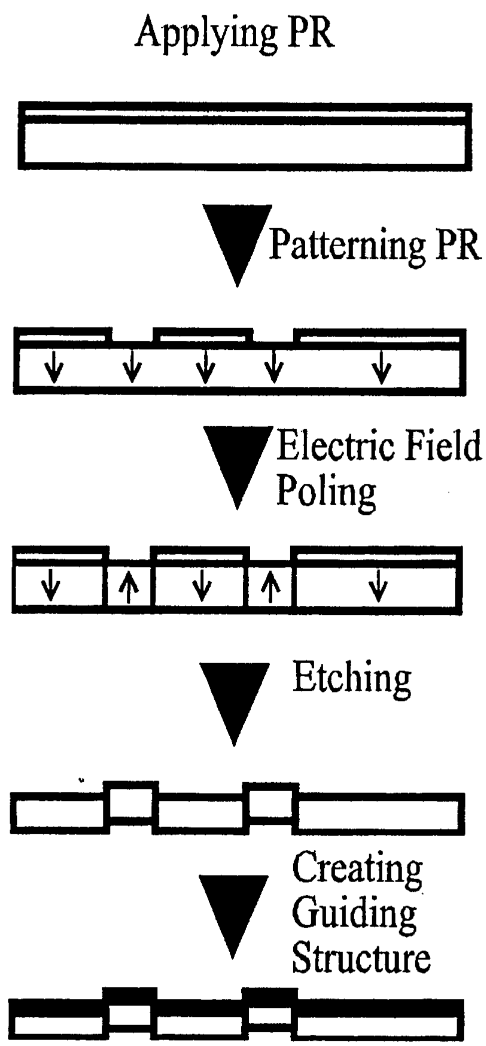

Optoelectronics Research Centre
University of Southampton
UK

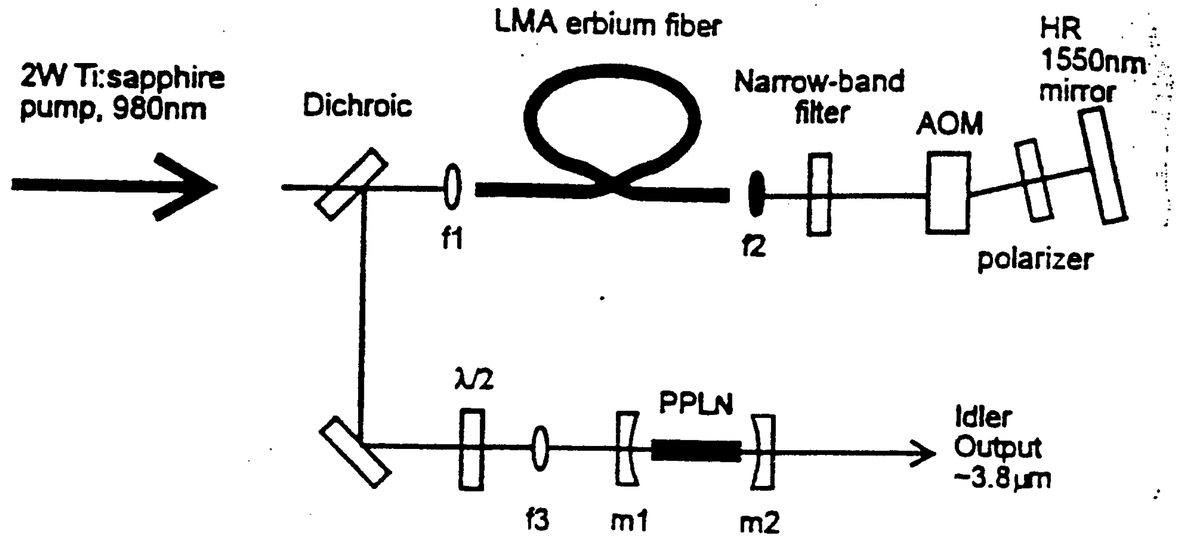

Fig. 1. Schematic of the setup: LMA, large-mode-area. AOM, acousto-optic modulator; HR, highly reflecting.

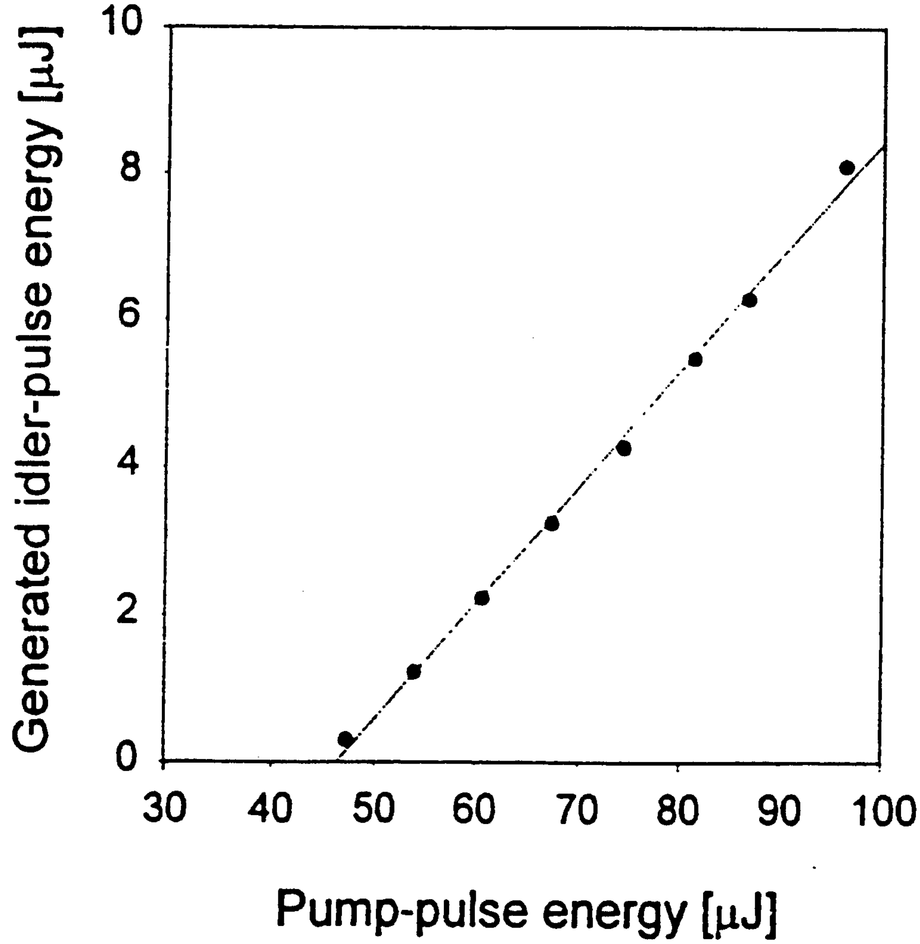

Fig. 2. Energy characteristics of the generated idler output at 2.61 μm.

Oxford Crystal Growth Group

Growth of phosphates and arsenates for periodic poling

K.B.Hutton and R.C.C.Ward

Clarendon Laboratory, Parks Road, Oxford OX1 3PU

- Properties of phosphates and arsenates
- Material requirements for periodic poling
- Growth programme using self fluxes
- Assessment of results

Collaborators

P.A.Thomas, Warwick Univ.

D.C.Hanna, P.Smith, Southampton ORC

M.H.Dunn, St.Andrews Univ.

Acknowledgements

EPSRC, DERA Fort Halstead

NLO 99

Optical and electrical properties of KTP isomorphs

	KTP	RTP	KTA	RTA
Curie point (°C)	946	785	873	750
Trans. range (μm)	0.35 - 4.3	0.35 - 4.3	0.35 - 5.3	0.35 - 5.3
SHG NCPM y cut-off (nm)	994	1038	1075	1138
1.06 μm PM $\phi°$	25	60	-	-
d_{33}	16.9	17.1	16.2	15.8
d_{eff} type II, 1.06μm	3.3	2.4	-	-
ionic conduc^y 0.1kHz (S/cm)	5×10^{-7} *	2×10^{-8}	2×10^{-7}	10^{-11}

* Can be reduced to 2×10^{-9} by doping with trivalent ions

Sources : Cheng et al, J.Crystal Growth <u>137</u> 107 (1994)
Cheng & Bierlein, Ferroelectrics <u>142</u> 209 (1993)

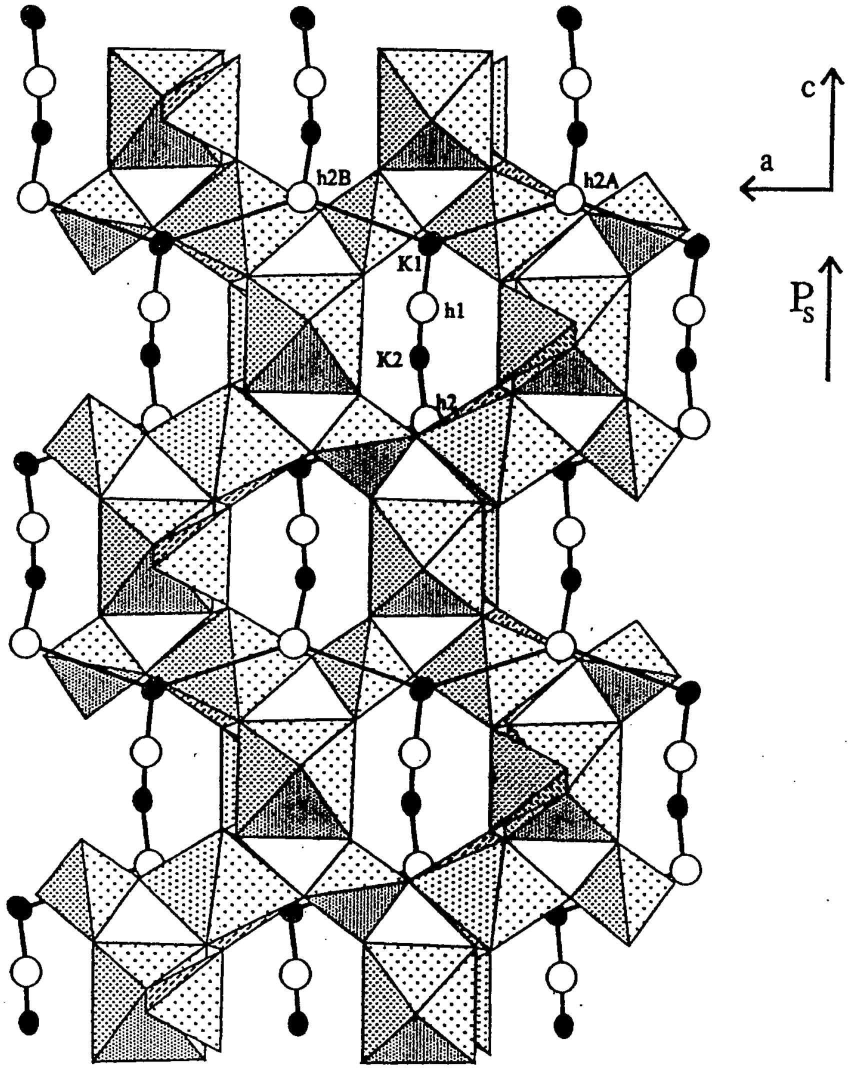

Crystal structure of $K^+Ti^{4+}OP^{5+}O_4$

(from P.A.Thomas & A.M.Glazer, *J.Appl.Cryst.* **24** 968 (1991))

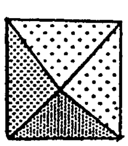

TiO_6 octahedra

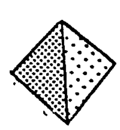

PO_4 tetrahedra

Morph[illegible]
and orientat[illegible]
[illegible] shown [illegible]

Electric field poling of KTP and analogues

- Electric field poling of hydrothermal KTP

  Q.Chen & W.P.Risk, Electron.Lett. ***30*** *1516 (1994)*

- Periodic poling of RTA

  H.Karlsson, F.Laurell et al, Electron.Lett. ***32*** *556 (1996)*

- Periodic poling of flux-grown KTP with Rb-exchanged layer

  H.Karlsson & F.Laurell, Appl.Phys.Lett. ***71*** *3474 (1997)*

- Low-temperature poling of flux-grown KTP

  G.Rosenman et al, Appl.Phys.Lett. ***73*** *3650 (1998)*

Advantages of KTP analogues for periodic poling

- Lower poling voltage than $LiNbO_3$
- Highly anisotropic crystal structure inhibiting domain broadening
- Stable device operation due to small *dn/dT*

Growth of KTP analogues for periodic poling

- ### Objectives

1. Production of high-quality, flux-grown KTP for poling trials

2. Investigate methods of lowering conductivity of KTP
   Doping - Ga^{3+} *(ref: Morris et al, J.Cryst.Growth* ***109*** *367 (1991))*
   Ce^{4+} *(correlation with increased transmission?)*
   Rb^{+} *(ref. RTP properties)*

3. Establish UK source of KTA and RTA
   Extended IR transmission and inherently low conductivity (RTA)

4. Investigate in-situ poling techniques

- ### Growth methods

TSSG method using self fluxes

$NH_3H_2P(As)O_4 + K(Rb)_2CO_3 + TiO_2$

Synthesis of high-purity arsenate starting material

Production of arsenate seed crystals by spontaneous nucleation

Optimisation of growth conditions

flux composition, growth temperature, doping

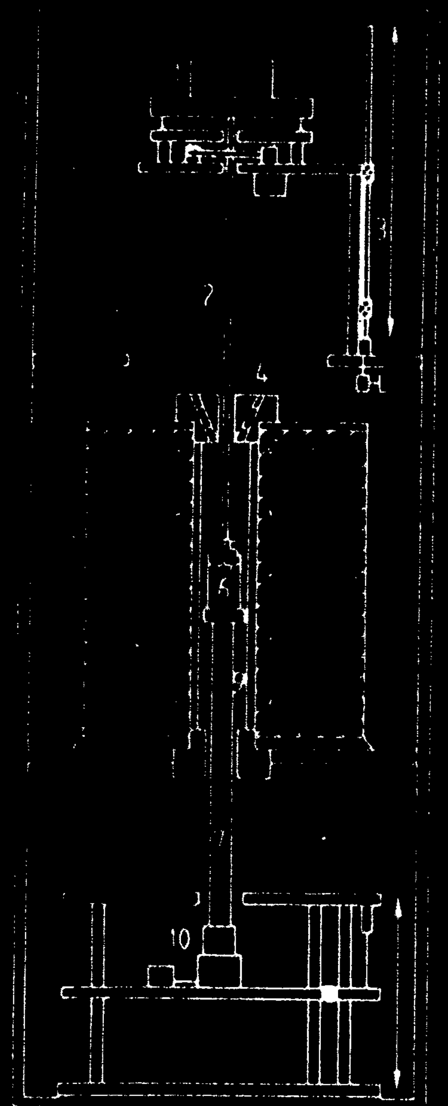

Fig. 1 Top Weighing TSSG Furnace

1. Electronic Balance
2. Seed Rod
3. Vertical Adjustment Stages
4. Optical Windows
5. Seed Crystal
6. Platinum Crucible
7. Alumina Crucible Support Rod
8. Three Zone Furnace
9. Silica Liner
10. ACRT Motors

Self fluxes for KTP and analogues

Polyphosphate $K_2O - P_2O_5$ solvents :

K_2O / P_2O_5	Flux	
2	$K_4P_2O_7$	Corresponding
1.67	$K_5P_3O_{10}$	Rb and As analogues.
1.5	$K_6P_4O_{13}$	
1.33	$K_8P_6O_{19}$	

Solubility curves for KTP/K_6 and RTP/R_n

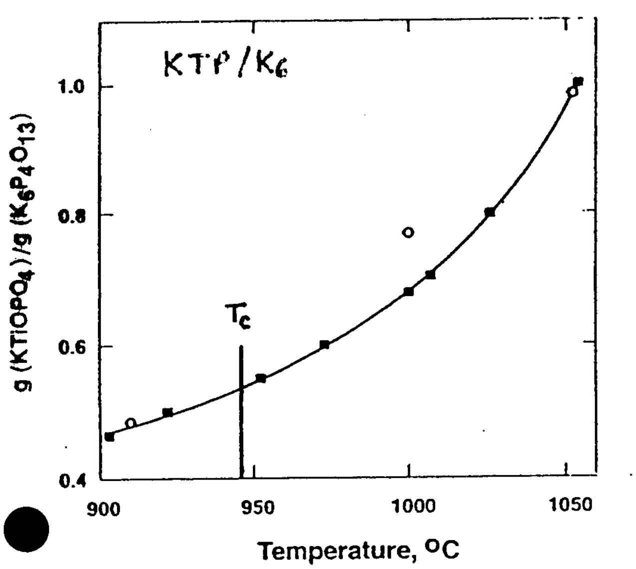

Ref: Angert et al, J.Cryst.Growth **137** 116 (1994)

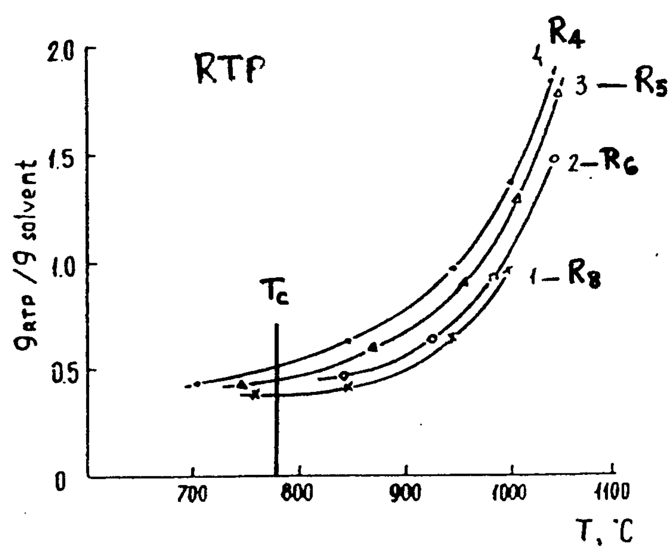

Ref: Oseldchik et al, J.Cryst.Growth **125** 639 (1992)

Viscosity

- KTP/K_6 – viscosity increases from 75cP at 950°C to 300cP at 800°C

High viscosity and flat solubility curve set limits for very low temperature growth

Results to date of growth programme

- Undoped KTP, Ga:KTP, Ce:KTP

  Routine production of large crystals (≈100g) established

- Rb-doped KTP

  5, 10, 20 mol% concentrations, growth temp. ≈ 860°C
  Growth rate low along a-axis
  Quality appears higher than undoped KTP

- RTP crystals

  Growth along a-axis enhanced (a:b:c≈1:1:1)
  Melt very viscous at 830°C - higher temp. under test

- Arsenates

  Synthesis of starting materials established

  KTA run in progress (886°C using K_6 flux)
  Volatility of solution higher than KTP

  RTA - small crystal grown at 893°C(R_5) to provide seeds
  Evidence that *a*-axis growth enhanced in arsenates

Shekhar Guha and Chris Reyerson*
AFRL/MLPJ
Wright Patterson Air Force Base, OH 45433-7702
* Anteon Corporation

shekhar.guha@afrl.af.mil

NLO99 Workshop, DERA, Malvern, UK, 20 - 21 September, 1999

AR coating wafers:

1. Coating 2 inch diameter single wafer, dicing in oriented pieces and stacking three coherence length thickness 320 micrometers

2. Growing 100 wafers 1 inch diameter, three coherence length thick Then IR AR coating at 5.3 and 10.6 micrometer

Results:

1. Up to 5 μJ of MWIR energy generated

2. Saturation of generated power observed

Possible causes of saturation being investigated

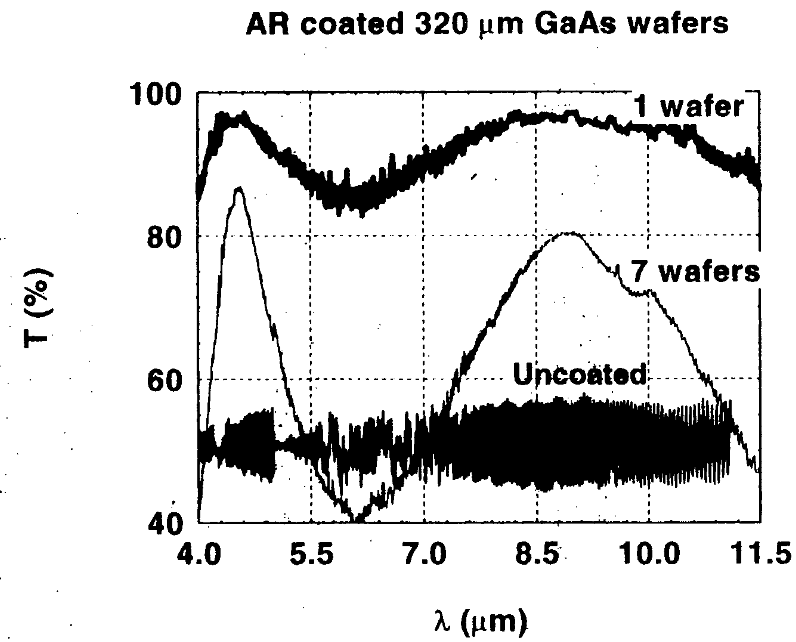

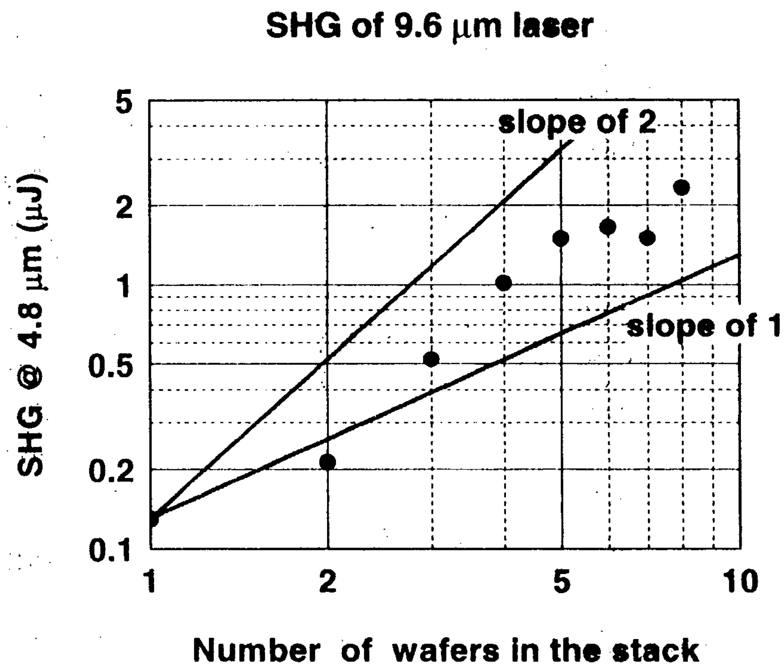

- SHG is not increasing quadratically
- Saturation of generated signal

SHG in AR coated GaAs Wafers at 10.6 μm

1 Coherence length each

1 inch diameter, 107 μm GaAs Wafers

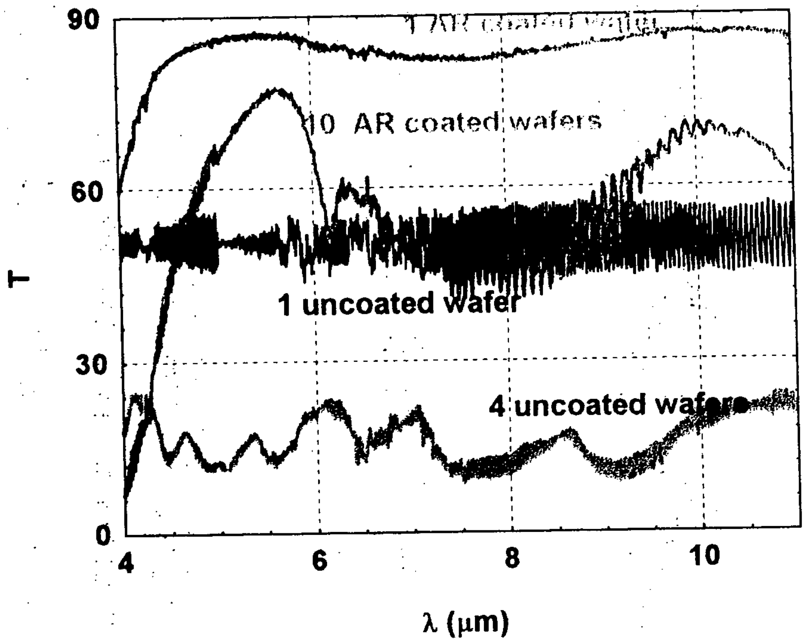

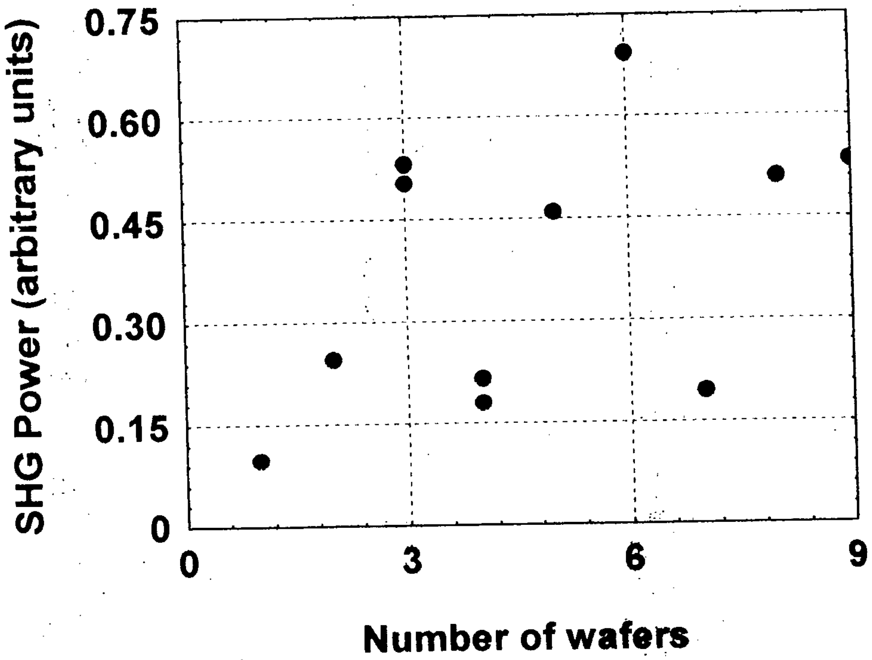

Worse SHG performance

	d_{eff}	n	K	α	dn/dT	FOM_1	FOM_2
GaAs	61	3.3	55	0.01	1.5	2.5	633
ZnSe	37	2.4	18	5×10^{-4}	0.64	2.4	9333
CdTe	28	2.7	6.3	0.001	0.5	1	867

ZGP	70	3.1	35	0.1 (1996)	1.7	4	55
CGA	154	3.5	4.2	0.2 (1996)	5	13.5	5
$AgGaSe_2$	27	2.6	1	0.01	0.7	1	1

d: pm/V
K: W/m/K
α: cm^{-1}
dn/dT: $10^{-4}\,K^{-1}$

$$FOM_1 = \frac{d^2}{n^3}$$

$$FOM_1 = \frac{d^2}{n^3} \times \frac{K}{\alpha\ (dn/dT)}$$

Reflectivity of a single AR coated GaAs wafer

1 coherence length (106 ± 10 μm)

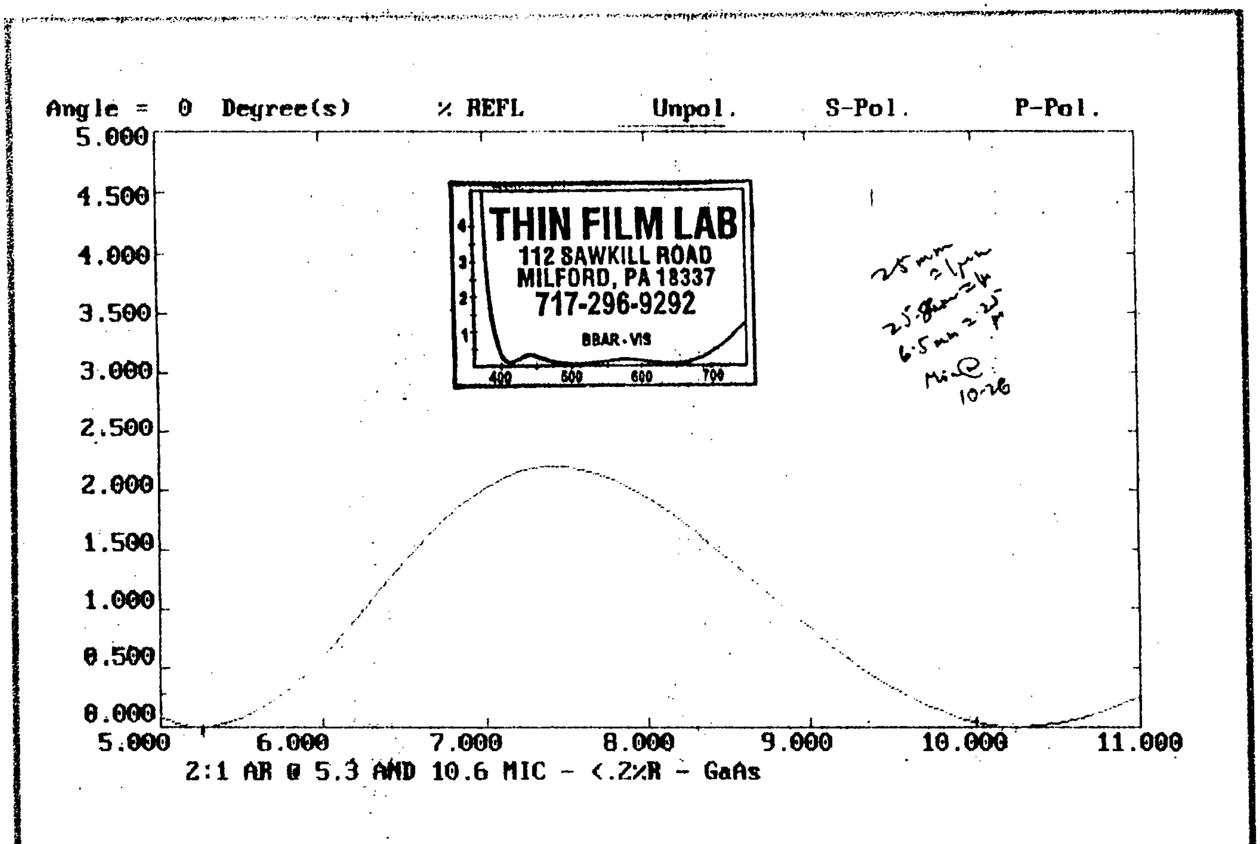

Very low reflectivities shown at 5.5 and 10.26 μm

AR coating GaAs for efficient QPM SHG of CO_2 laser was attempted

Coating performance still not adequate

A New Nonlinear Optical Material: Periodically-Poled Barium Titanate (PPBT)

P. G. Schunemann, S. D. Setzler, T. M. Pollak

SANDERS
A Lockheed Martin Company

Presented at the 1999 Nonlinear Optical Materials Workshop, (NLO 99), DERA, Malvern, UK, Sept. 21, 1999

Work supported L.N. Durvasula at DARPA (via the Air Force Research Laboratory Materials Directorate contract No. F33615 -94-C-5415) and Sanders Internal R&D Funding

Periodically-Poled Barium Titanate

SANDERS
A Lockheed Martin Company

Advanced Engineering and
Technology Division

$BaTiO_3$ Offers Very Attractive Properties for Periodically-Poled OPOs

- Longer IR cut-off than PPLN (allowing full 3-5 micron coverage)
- Low Coercive Field (100V/mm, 200x lower than PPLN)

↓

- Larger Apertures
- Large Nonlinear Coefficient
  d_{15}=17pm/V

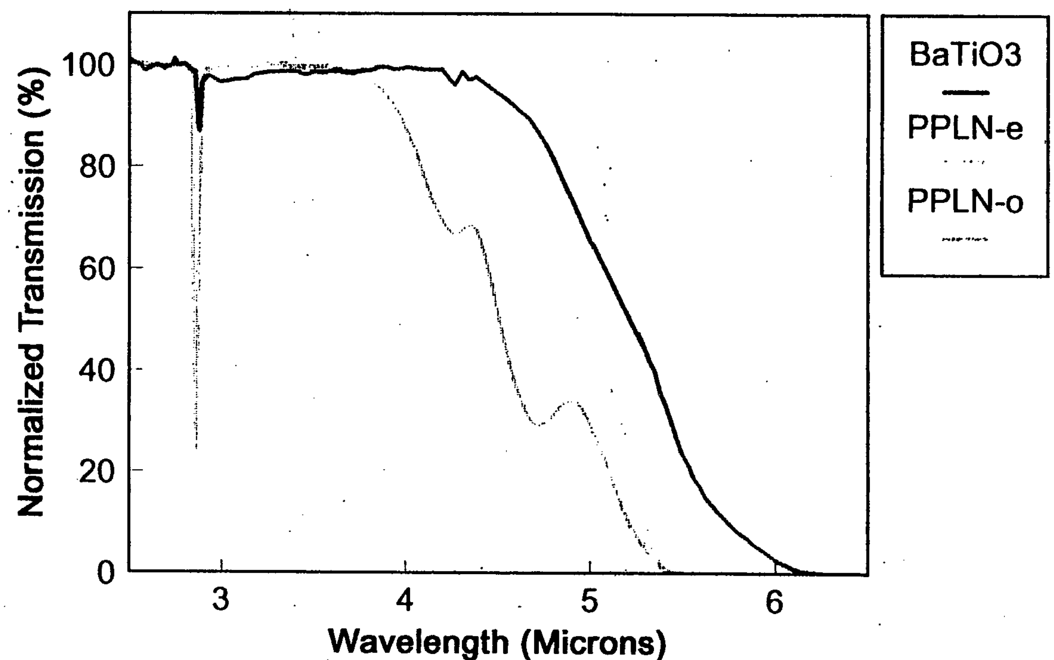

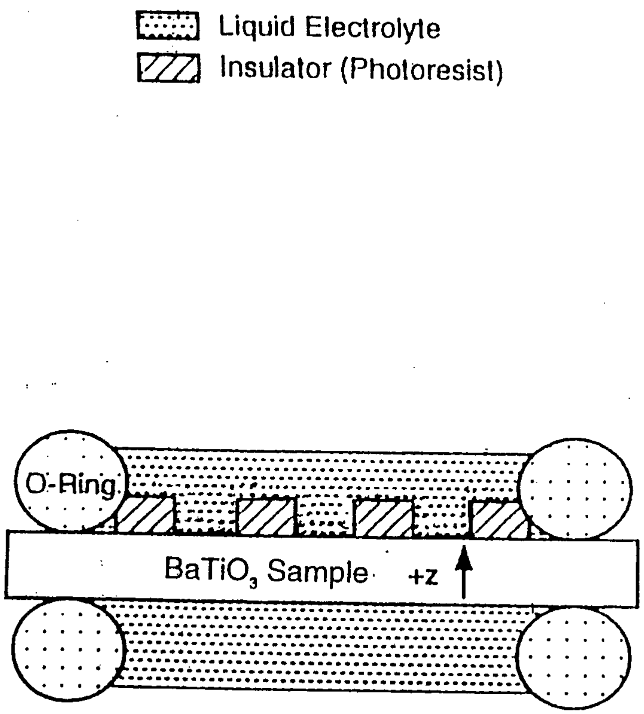
Liquid Electrolyte
Insulator (Photoresist)
O-Ring
$BaTiO_3$ Sample
+z

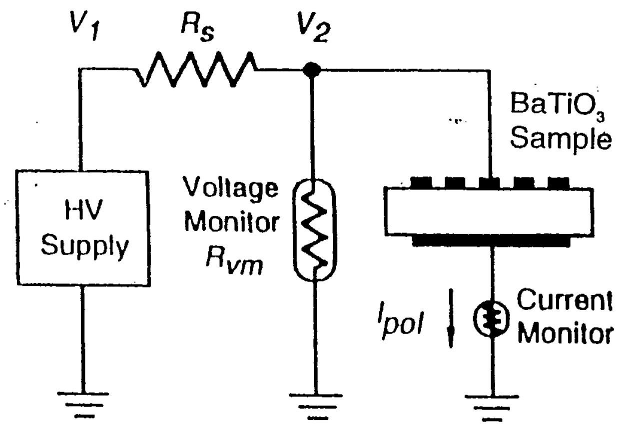
V_1
R_s
V_2
HV Supply
Voltage Monitor R_{vm}
$BaTiO_3$ Sample
I_{pol}
Current Monitor

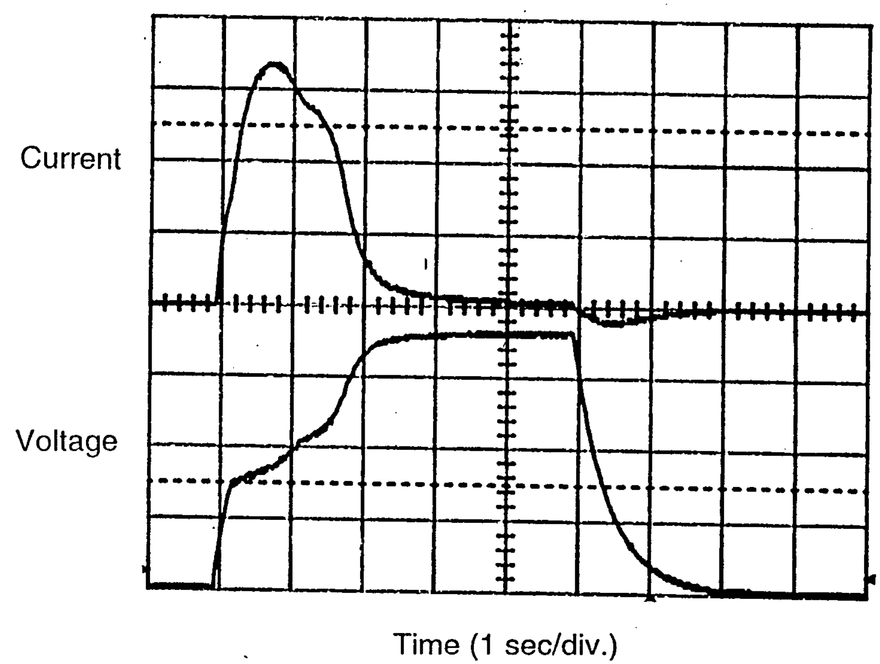
Current
Voltage
Time (1 sec/div.)

Images of sample #296G (Total poling depth ~0.5 mm)

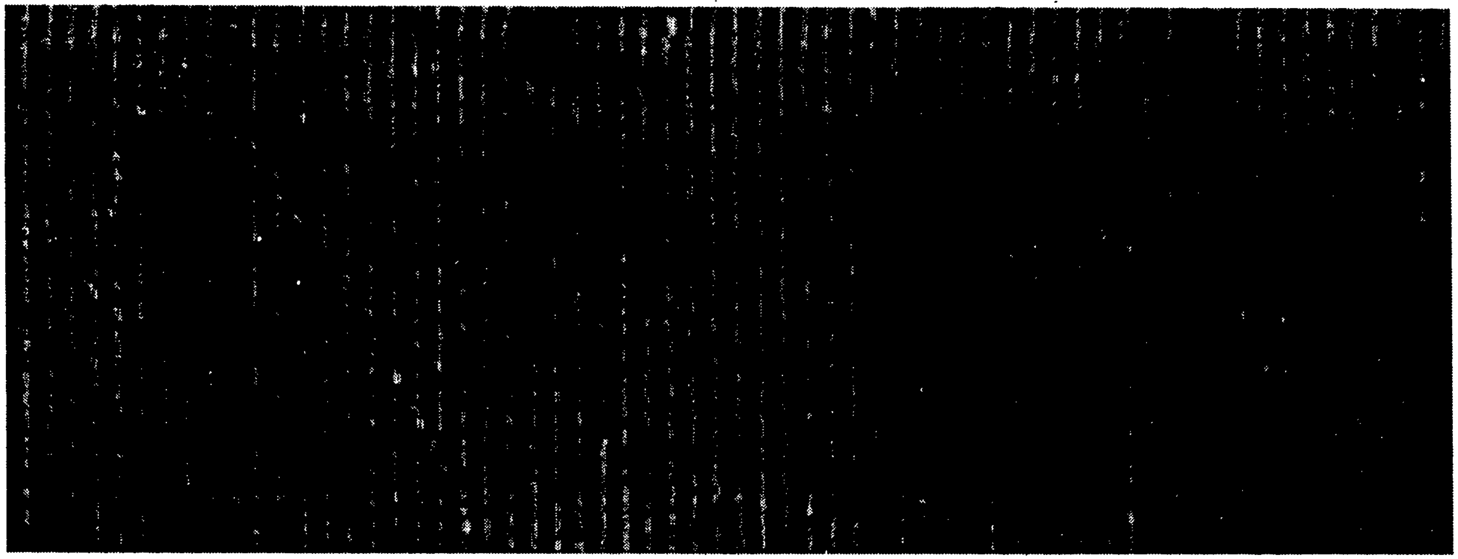

150X magnification

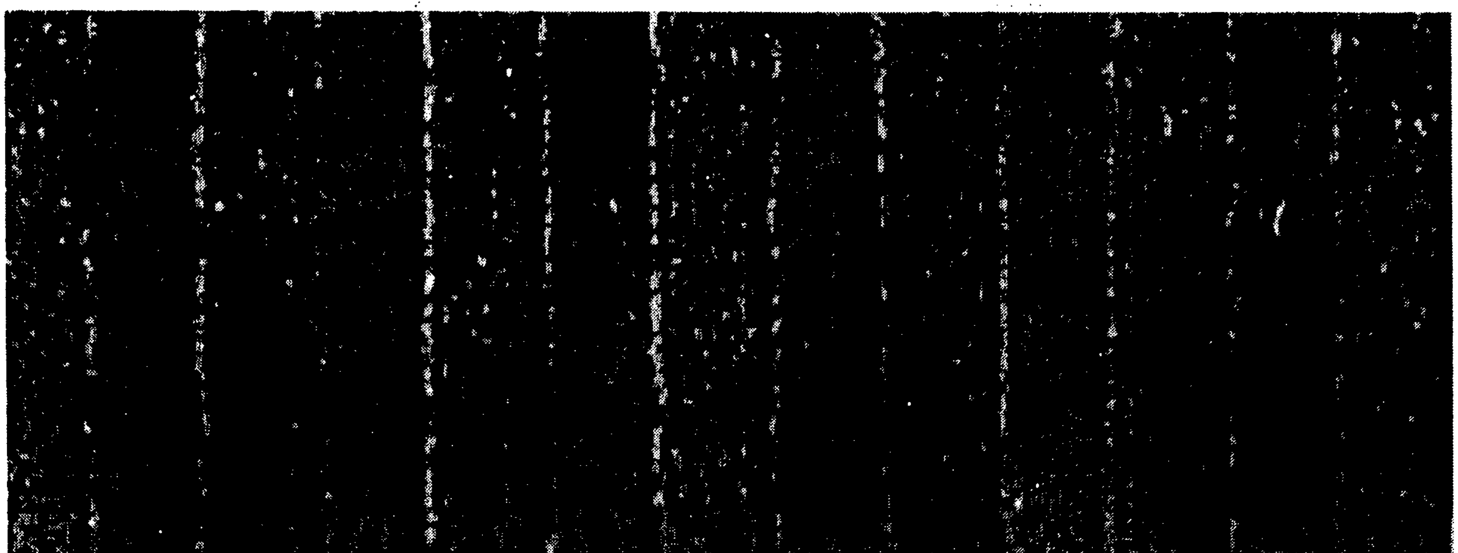

1500X magnification

17 μm

Periodically-Poled Barium Titanate

SANDERS
A Lockheed Martin Company

Advanced Engineering and
Technology Division

Summary

- Barium Titanate single crystals were grown by the TSSG technique

- New refractive index measurements revealed insufficient birefringence for phase-matching, allowed determination of QPM grating spacings

- Periodic poling of bulk $BaTiO_3$ successfully demonstrated for the first time
  - Wafers survived photoresist patterning and bake-out
  - Domain reversal achieved at low E-fields (200X lower than for PPLN)
  - Mask grating pattern reproduced on wafer (no spreading of domains under photoresist unless overpoled)
  - Large thickness (1.4 mm) poled in first trial

- Quasi-phase-matched SHG demonstrated in PPBT
  - 10W of 2.05um input (10kHz, 10ns) produced ~~300~~ 345mW at 1.025um from an uncoated, 8mm-long sample at ~55˚C (4% conv. eff. after refl. loss)
  - No evidence of photorefractive damage or thermal lensing was observed